Remodelling of Spinal and Supraspinal Axonal Tracts following Spinal Cord Injury: Effects of Rehabilitation and Molecular Factors

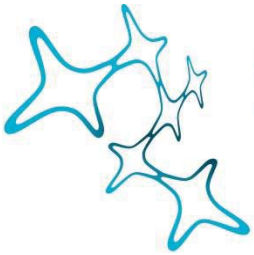

Graduate School of Systemic Neurosciences
LMU Munich

Dissertation der Graduate School of Systemic Neurosciences der Ludwig-Maximilians-Universität München

Submitted by
Kristina Loy
18th January 2018

Date of submission: 18.01.2018
Supervisor: PD Dr. Florence Bareyre
2nd reviewer: Prof. Dr. Leda Dimou
External 3rd reviewer: Jean Livet, PhD

Date of oral defense: 11.05.2018

„Das Studium und allgemein das Streben nach Wahrheit und Schönheit ist ein Gebiet, auf dem wir das ganze Leben lang Kinder bleiben dürfen.“
„Study and in general the pursuit of truth and beauty is a sphere of activity in which we are permitted to remain children all our lives.”
Albert Einstein

"Alles, was man zum Leben braucht, ist Unwissenheit und Selbstvertrauen, dann ist der Erfolg sicher."
"All you need in life is ignorance and confidence, then success is sure."
Mark Twain

Table of Contents

I List of Abbreviations

5HT, 5HTR	serotonin/5-Hydroxytryptamin , serotonin receptor
AAV	adeno associated virus
AC	adenylyl cyclase
ASIA	American Spinal Injury Association
BBB	blood brain barrier
BDNF	brain derived neurotrophic factor
C, C1	cervical, cervical vertebrae 1
CA	cornu ammonis
cAMP	cyclic adenosine monophosphat
ChAT	choline acetyltransferase
CMV	cytomegalovirus
CNS	central nervous system
CP	cerebral palsy
CPG	central pattern generator
CSPG	chondroitin sulfate proteoglycans
CST, dCST	corticospinal tract, dorsal corticospinal tract
DCC	deleted in colorectal cancer
DRG	dorsal root ganglion
EAE	experimental autoimmune encephalomyelitis
EMG	electromyography
FGF, FGFR	fibroblast growth factor, fibroblast growth factor receptor
GFAP	glial fibrillary acidic protein
GFP	green fluorescent protein
GPCR	G-protein coupled receptor
GPI	glycophosphatidylinositol
HET	heterozygous
hSyn	human synapsin promotor
IGF	insulin like growth factor
IGF1	Insulin like growth factor 1
IP3	inositol trisphosphate
KO	knock out
L, L1	lumbar, lumbar vertebrae 1
LOT	lateral olfactory tract
LPSN	long propriospinal neuron
MASCIS	Multicenter Animal Spinal Cord Injury Study
mDA	mesodiencephalic dopamine neurons
MS	multiple sclerosis
mTor	mechanistic target of rapamycin
NG2	neuroglial2proteoglycan
NMJ	neuromuscular junction
NRO	nucleus raphe obscurus
OPN	osteopontin
PLC	phospholipase C
PNS	peripheral nervous system
PTEN	phosphatase and tensin homolog
-R or R	receptor
ROM	range of motion
SCI	spinal cord injury
Sema7A	Semaphorin 7A

SOCS3	suppressor of cytokine signaling 3
SPSN	short propriospinal neuron
STAT3	signal transducer and activator of transcription 3
SynCam	synaptic cell adhesion molecule
T, T1	thoracic, thoracic vertebrae 1
TrkB	tropomyosin receptor kinase B
USA	United States of America
VEGF	vascular endothelial growth factor
VLM	ventral lateral medulla oblongata
VTA	ventral tegmental area
WT	wild type

II Abstract

Spinal cord injury is a devastating disease with limited therapeutic options today. Affected individuals loose sensory and motor function below the level of the injury and remain impaired throughout their life, in particular in case of anatomically complete lesions. Incomplete lesions have a better prognosis and it has been shown that in case of incomplete spinal cord injuries remodelling of cut axonal pathways contributes significantly to functional recovery, by forming new connections to relay central information from the brain to the right synaptic partners in the lumbar spinal cord. One well studied example is the detour circuit between the corticospinal tract and long propriospinal relay neurons that re-connect the severed central tract via interneurons to the lumbar motor neurons. This process has different stages and prerequisites: (i) the severed axon has to initiate some form of growth, then (ii) it has to find a suitable synaptic partner and (iii) a working synaptic contact has to be established. My thesis aimed at understanding several aspects of this remodelling process as we believe that only combinatorial therapies that target the different remodelling phases will trigger most significant functional recovery. I focussed on the corticospinal and raphespinal pathways as central motor inputs onto hindlimb motor neurons.

As the only therapy that is beneficial in clinical settings is rehabilitative training, I first asked myself whether and how rehabilitation in the form of voluntary exercise can trigger functional recovery. During this study I have demonstrated that voluntary exercise improves functional recovery and accelerates the remodelling process of the corticospinal pathway. Moreover, it potentiates the correct targeting of serotonergic and corticospinal fibers onto inter- and motorneurons thereby strengthening the newly formed circuitry.

Secondly, I studied the role of Sema7A, a potential guidance cue, following spinal cord injury. Sema7A can act as an attractive and repulsive signal on growing axons in development and is needed for the correct outgrowth and targeting of central nervous system tracts. I discovered that loss of Sema7A impairs functional motor recovery after spinal cord injury and leads to loss of targeting of two major supraspinal pathways, the cortico- and the raphespinal tract. In addition, I showed that loss of Sema7A signalling enhanced axonal growth of these axons without the formation of more needed synapses onto target neurons, outlining the importance of correct axonal targeting and the role of Sema7A in restricting patterning of supraspinal axonal tracts following injury.

Finally, we investigated the role of FGF22 and its receptors FGFR1 and R2 on adult de-novo synapse formation after spinal cord injury. We found that deletion of FGF22 or its two receptors impairs axonal remodelling as well as the de novo formation of new synapses in general and onto relevant relay

neurons. Mice deficient for FGF22 signalling also show deficits in functional motor recovery after spinal cord injury emphasizing the crucial importance of synapse formation in this remodelling process. Studying the overexpression of FGF22 as a potential therapeutic target is currently underway.

In summary my thesis aims at better understanding various underlying mechanisms of successful remodelling of supraspinal pathways following spinal cord injury. In particular we have now identified factors involved in axonal guidance and synapse formation, two key mechanisms of successful axonal remodelling. As we have also evidence that rehabilitation can help functional recovery following spinal cord injury and therefore can potentially be combined to create synergistic effects on motor improvements. Follow up work should now aim at synergistically enhancing synapse formation, promoting correct axonal targeting with gene therapies and rehabilitative training. Therefore my thesis paves the way to combinatorial treatments to promote axonal plasticity following central nervous system trauma.

III Zusammenfassung

Bis heute ist eine Rückenmarksverletzung ein verheerendes Trauma für Betroffene mit sehr eingeschränkten Therapiemöglichkeiten. Betroffene verlieren sensorische und motorische Fähigkeiten Unterhalb des verletzten Rückenmarkssegments und sind lebenslang beeinträchtigt, vor allem wenn der Rückenmarksquerschnitt vollständig ist. Verletzungen in denen nur ein Teil des Rückenmarks geschädigt ist haben eine bessere Prognose, da sich unverletzte und zerstörte Fasern reorganisieren können und signifikant zu einer Wiedererlangung von Funktionen beitragen können. Dies geschieht durch neue neuronale Verknüpfungen, die die Signale des Gehirns wieder an die lumbal gelegenen Motorneuronen weiterleiten. Die Neuentstehung einer solchen neuronalen Umgehung einer Rückenmarksverletzung zwischen der kortikospinalen Bahn und langen propriospinalen Neuronen ist gut beschrieben. Hierbei reorganisieren sich die beschädigten Fasern des Kortikospinaltrakts und kontaktieren rostral von der Läsion Interneurone, über die dann das Signal wieder an die lumbalen Motorneurone weitergegeben werden kann. Dieser Prozess verläuft über mehrere Stadien und unterliegt gewissen Voraussetzungen: Erstens muss das unterbrochene Axon wieder auswachsen, zweitens muss es wieder einen adäquaten synaptischen Partner finden und drittens muss es mit diesem Partner einen synaptischen Kontakt bilden. Meine Dissertation zielt darauf ab, die verschiedenen Prozesse dieses axonalen Umgehungskreislaufs besser zu verstehen, weil in meinen Augen nur die Kombination aus verschiedenen Therapien, die alle diese Prozesse optimieren den größten Erfolg in der Behandlung von Rückenmarksverletzungen haben kann. Mein Fokus lag auf dem kortikospinalen und dem raphespinalen Trakt als zentrale neuronale Bahnen mit Projektionen auf Motorneurone im lumbalen Rückenmark.

In der Klinik der Rückenmarksverletzung ist bis heute nur eine Therapiemöglichkeit bekannt, die einen Nutzen für den Patienten hat: Rehabilitation und Physiotherapie. Auf dieser Grundlage stellte sich mir die Frage ob und wie Rehabilitation in Form von freiwilligem Training zur Wiedergewinnung von motorischen Fähigkeiten beiträgt. In dieser Studie konnte ich zeigen, dass im Mausmodel freiwilliges Training nach einer Rückenmarksverletzung die motorischen Fähigkeiten verbessert und die Reorganisation der kortikospinalen Kontakte beschleunigt. Darüber hinaus konnte durch Training die korrekte neu-Verknüpfung der raphe- und kortikospinalen Fasern auf Inter- und Motorneurone verstärkt und damit die neue Verschaltung der Neuronen gefördert werden.

Als zweites widmete ich mich der Rolle von Sema7A im Maus Model einer Rückenmarksverletzung. Sema7A ist ein Signalmolekül, das in der embryonalen Entwicklung auf neu wachsende neuronale Fasern entweder anziehend oder abstoßend wirken kann und für die korrekte topographische Etablierung und das richtige Wachstum mehrerer zentraler Faserbahnen im Zentralnervensystem notwendig ist. In meiner Arbeit konnte ich zeigen, dass sich in Abwesenheit von Sema7A die motorischen Fähigkeiten

nach einer Rückenmarksverletzung schlechter erholen und dass zwei wichtige zentrale Nervenbahnsysteme nicht mehr im richtigen Maß und an die korrekte Stelle wachsen, der raphe- und der kortikospinale Trakt im Rückenmark. Darüber hinaus konnte ich zeigen, dass die Axone in Sema7A defizienten Mäusen verstärkt wachsen ohne mehr Kontakte mit den notwendigen Neuronen einzugehen, um eine neue Verschaltung zu etablieren. Das unterstreicht die Wichtigkeit von begrenztem axonalen Wachstum in die richtigen Areale im Rückenmark, um sinnvolle Verbindungen zu schaffen.

Zu Letzt beschäftigte ich mich noch mit der Rolle von FGF22 und den zwei passenden Rezeptoren FGFR1 und R2 in der de novo Entstehung von adulten Synapsen nach Rückenmarkstrauma. Fehlt einem Organismus entweder FGF22 oder beide Rezeptoren, dann ist die Reorganisation von kortikospinalen Verbindungen nach der Läsion gestört. Es werden auch generell weniger Synapsen gebildet und ins Besondere weniger Kontakte auf lange propriospinale Neuronen, um die Umgehung der Läsion über Interneurone zu bilden. Das Wiedererlangen von motorischen Fähigkeiten ist dadurch ebenfalls gestört und Mäuse, die entweder kein FGF22 produzieren oder beide Rezeptoren nicht haben, können nach Rückenmarkstrauma motorische Aufgaben schlechter durchführen. Dieser Teil meiner Arbeit zeigt die Unabdingbarkeit relevanten synaptischen Verbindungen für die Wiedererlangung der motorischen Fähigkeiten. Eine zweite Studie, die FGF22 als potentielle virale Therapieoption beleuchten soll wird gerade durchgeführt.

Meine Dissertation zielt auf ein besseres Verständnis der verschiedenen Schritte bei der Reorganisation neuronaler Verbindungen zur Wiedergewinnung von motorischen Funktionen nach Verletzungen des Rückenmarkes ab. Ich konnte im Zuge meiner Arbeit die anatomischen Grundlagen für verbesserte motorische Fähigkeiten mit rehabilitativem Training zeigen und molekulare Faktoren identifizieren, die wichtig für das korrekte Wachstum, die Zielfindung und die Ausbildung neuer Synapsen sind. All dieses Wissen kann kombiniert werden und zur Entwicklung von Therapien beitragen, die nicht nur einen Teil des Prozesses adressieren, dass zu motorischen Verbesserungen führt, sondern mehrere, um so die maximale Wirkung für den Patienten zu erzielen. Kombinationstherapien sind, in meinen Augen, die Zukunft der Therapie des Rückenmarksquerschnitts. Die Arbeit in meiner Dissertation trägt durch den Wissensgewinn zur Entwicklung von Kombinationstherapien bei und wird vielleicht einmal die Grundlage einer effektiven Therapie für Patienten sein.

1. Introduction

1.1. Epidemiology of Spinal Cord Injury

According to the Christopher & Dana Reeve Foundation nearly 1,7% of the population of the United States of America (USA) live with a form of paralysis, which is defined as a central nervous system (CNS) disorder that results in disability or difficulty to move the upper or lower extremities. Leading causes of paralysis are stroke (33,7%), spinal cord injury (SCI, 27,3%), Multiple Sclerosis (MS, 18,6%) and Cerebral Palsy (CP, 8,3%, Figure 1).

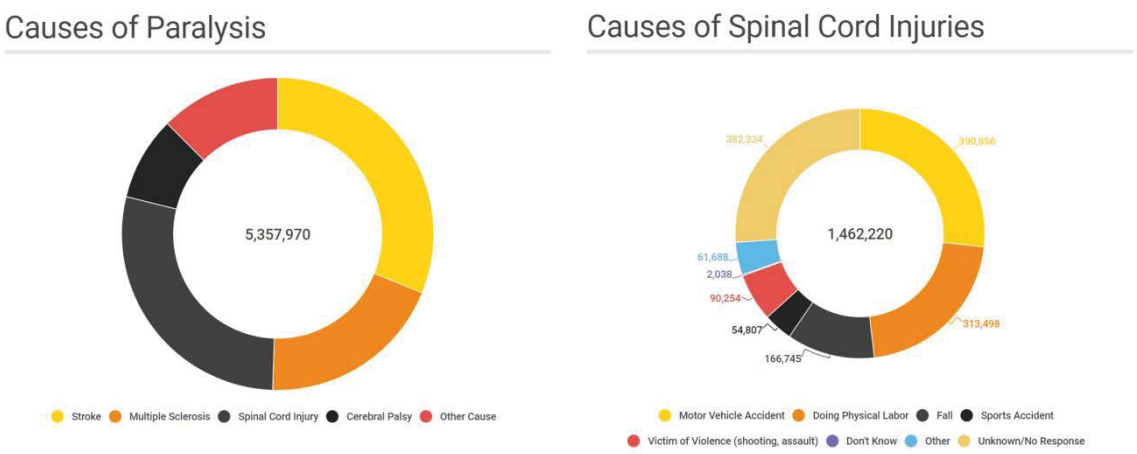

***Figure 1**: Causes of Paralysis and Spinal Cord Injuries in the USA (https://www.christopherreeve.org/)*

While stroke occurs mostly in the elderly population (65+), individuals with SCI are mostly young adults with an average age of 42 (www.nscisc.uab.edu, National Spinal Cord Injury Statistical Center) at occurrence. SCI is almost always caused by trauma due to, for example, motor vehicle accident, accident during physical labor or fall ((Armour et al., 2016), Figure 1). 25000 new cases are reported annually worldwide (http://www.wingsforlife.com, Wings for Life), 17000 in the USA (www.nscisc.uab.edu, National Spinal Cord Injury Statistical Center) and 1800 in Germany (www.dsq.de, Deutsche Stiftung Querschnittslähmung). A total of 17031 people live with paralysis due to spinal cord injury in Germany, amounting to 0.2% of all disabilities and an incidence rate of 10.7 per million (https://www.destatis.de/DE/Publikationen/Thematisch/Gesundheit/BehinderteMenschen/SozialSchwerbehinderteKB5227101139004.pdf?__blob=publicationFile; (Lee et al., 2014)). The survivors of a traumatic SCI usually suffer from disabilities or impairments, which depend on the level and the severity of the injury. This is evaluated and classified according to the ASIA score which assesses the level as well as completeness of the injury (Figure 2). The level of the injury determines also the body-level with impaired sensory and motor function. The ASIA score determines the lowest level of sensation following

injury thereby defining the injured spinal segment. An injury to the levels C1 to T1 leaves the affected individual tetraplegic meaning that both upper and lower body extremities are affected and sensorimotor function is lost or impaired. If the damage is below the T1 level, the individual is classified as paraplegic with upper body, hand and arm function but without sensation or movements in the legs.

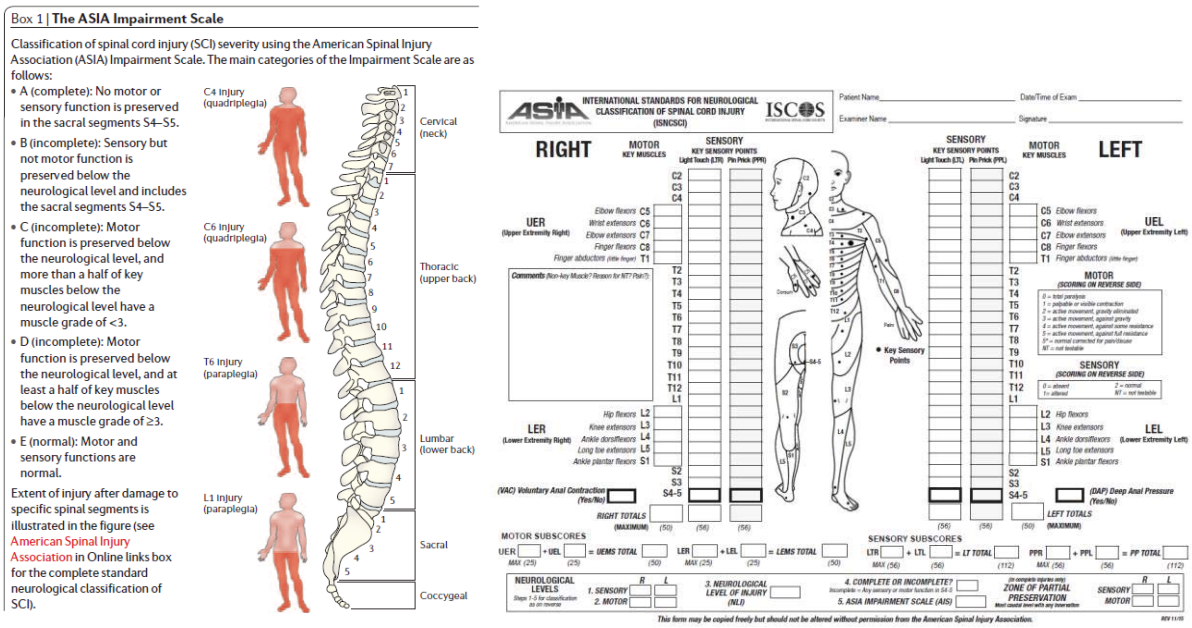

***Figure 2**: The ASIA Impairment Scale (from (Thuret et al., 2006)) and ASIA Score Sheet (http://asia-spinalinjury.org/wp-content/uploads/2016/02/International_Stds_Diagram_Worksheet.pdf)*

Another parameter assessed by the ASIA score is the completeness of the injury. Over 60% of all recorded spinal cord injuries in the USA are incomplete (www.nscisc.uab.edu), meaning that only part of the cord is transected with some extent of spared tissue. Whereas a complete transection of the spinal cord leaves no potential for recovery or functional improvement, the prognosis of an incomplete injury is sensibly superior. The ASIA scores for functional completeness, e.g. no sensory or motor function below a certain body level has to be differentiated from anatomical completeness, e.g. a full anatomical transection of the cord. One post mortem study reported 90% of SCIs as anatomically incomplete although they were functionally classified as complete leaving anatomically more recovery potential than originally estimated (Bunge et al., 1993).

For most patients, spinal cord injury is a devastating and life changing condition. Dependence on a wheelchair is common as well as a lifelong dependency on care, medical treatment and special equipment in their daily lives. Varying with the level of the injury the life expectancy ranges between 4 to 45 years which has not improved since 1980 and secondary complications such as infections are very common (www.nscisc.uab.edu). The Christopher & Dana Reeve Foundation estimates annual health costs for spinal cord injury treatment at about 40,5 billion US dollars in the United States. Concrete

numbers for Germany are not published, but health costs per patient in Germany are estimated to be higher due to longer hospital stay after injury and coverage of rehabilitation and longtime care by the German health insurance system (Becker, 2002). All this is driving the need for new therapies and a better understanding of the pathophysiology of SCI.

1.2. Pathophysiology of Spinal Cord Injury

The pathophysiology of SCI consists of an acute, a subacute and a late stage after injury. The injury is usually caused by compression or blunt trauma to the spinal column leading to the entrance of bones, bone fragments or cartilage discs into the soft neural tissue of the cord thereby causing irreversible primary damage to neuronal tissue and oligodendrocytes. The primary damage includes among other complications hemorrhage with shortage in blood flow and perfusion, edema and cell death. If there is intense swelling of the spinal cord secondary compression can worsen the primary trauma to the cord. In the subacute phase the secondary damage occurs that is mainly a long term effect of the primary damage to the neurons, the vasculature and the surrounding cells. Excitotoxicity and demyelination of neuronal connections further impair connectivity and transmission**.** The subacute phase is characterized by the entrance of immune cells to the spinal cord to clear tissue debris and induce inflammation which is thought to be inhibitory to regeneration and decrease tissue sparing thereby increasing the lesion ((Thuret et al., 2006), Figure 3). Action potential propagation is inhibited in spared neurons and fibers by a process called spinal shock due to the previous hypoperfusion of the neuronal tissue. In this phase the injury may seem worse than it really is because spared fibers and neurons also fail to propagate signals, which is why the first functional assessment is done after reflexes return (Atkinson and Atkinson, 1996). The chronic phase lasts basically a lifetime and is characterized by astrocyte proliferation and glia scar formation to encapsulate or fill the lesioned area. This barrier is known to be a major extrinsic factor that hinders intrinsic neuronal regeneration across the lesion site (Dumont et al., 2001a, Dumont et al., 2001b, Kakulas, 1999, McDonald and Sadowsky, 2002).

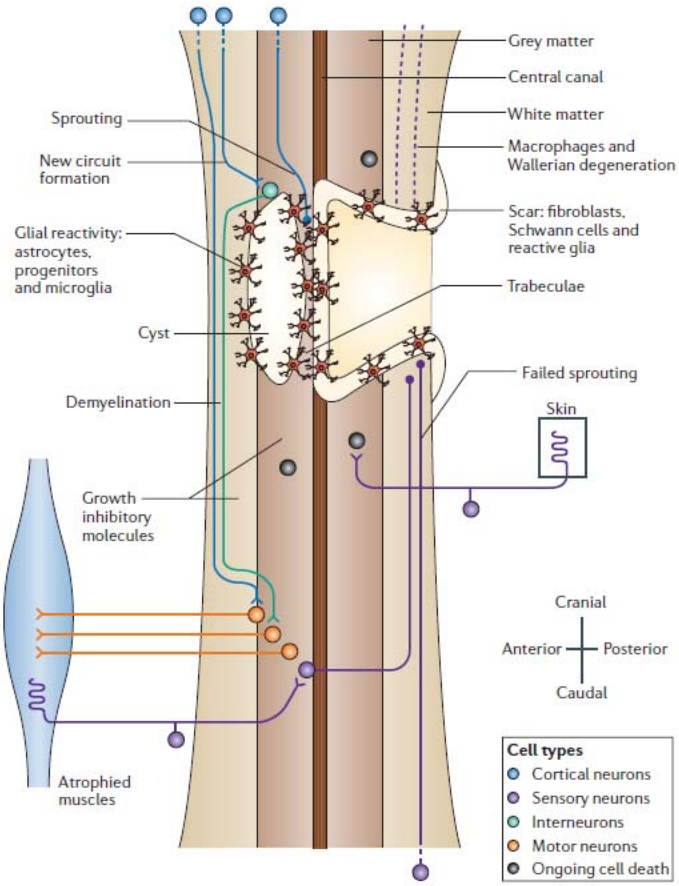

***Figure 3**: Schematic of pathophysiology of spinal cord injury (Thuret et al., 2006).*

1.3. Treatment of spinal cord injury

Treatment of SCI first aims to keep the patient alive as 9% of patients do not survive the first 24 hours (Yeo et al., 1998). After the patient is stabilized the degree of injury is assessed by the ASIA score sheet and the patient is then transferred to a rehabilitation facility to regain motor function and decrease secondary complications.

1.3.1. Acute treatment

Immediately after the accident the patient's spine is stabilized surgically to avoid more damage to the cord due to an instable spinal column or fractured bone pieces. In case of swelling decompression surgery might be needed in which a laminectomy is performed to avoid secondary damage by compression (McDonald et al., 2002). For high cervical injuries above C3-C5 that de-innervate the diaphragm a ventilator might be needed to breathe (Berlly and Shem, 2007). Steroid treatment with methylprednisolone was standard of care for many years in order to reduce post injury inflammation, but was found to be of no benefit to the patient and trigger potentially severe side effects such as hospital-acquired pneumonia, urinary tract infections, abdominal bleeding and respiratory failure that

could in some cases be fatal. This is therefore not a standard treatment today (Hurlbert, 2000). After the patient leaves intensive care and the hospital he or she is usually admitted to a rehabilitation center.

1.3.2. Long term management and treatment – rehabilitation

The aim of rehabilitation is to reduce secondary medical issues which lead to re-admission to a hospital and improve functional recovery in patients with spinal cord injury. Long term rehabilitation of spinal cord injury is very tiring to the patient and the care takers and remains expensive, but is to date the only intervention with benefit for the patient. With an estimated average cost of 68543$ per patient and an average of 47,7 days per year rehabilitation is one of the main cost factors after spinal cord injury (DeVivo et al., 2011). After initial treatment of the primary injury, passive and active exercise is recommended for the patient in order to prevent muscle atrophy, secondary complications such as urinary and bowel problems as well as spasticity. In the hospital with flaccid paralysis range of motion (ROM) rehabilitation is started. The individual is thereby passively moved in the hospital bed by a care giver in order to mobilize joints and avoid severe muscle atrophy. After hospital discharge the patient is transferred to a rehabilitation center to train further and improve functionality and some level of recovery. Later follow up is then home-based mostly (McDonald et al., 2002, Nas et al., 2015).

In motor complete SCI subjects, passive stepping-like movements do not lead to motor recovery, but reduce muscle spasm and improve cardiovascular functions. In these patients, ROM is continued to avoid joint contractures, stiffness and pain. In complete and early in incomplete paraplegics one main first goal is to strengthen upper extremities for e.g. bed or wheelchair transfer or the use of crutches. The arm and shoulder muscles are trained with weight bearing or resistance exercise with elastic bands. In complete paraplegics strengthening of upper limbs is combined with passive mobilization of lower limbs. Balance exercises are also important to re-learn stable sitting and later wheelchair transfer. Incomplete patients always have a theoretical potential to walk again and are trained to stand and step between parallel bars with the assistance of a care giver and/or weight support if needed (Figure 4). Basically, physiotherapy in these patients is gait training to an extent the patient can manage. More modern techniques include robot assisted stepping and exoskeletons to allow for upright posture and stepping (Miller et al., 2016, Wessels et al., 2010). Orthoses (external cast like fixations) to fix and stabilize de-innervated joints and muscles can be useful for the beginning of stepping. For incomplete thoracic injuries walking is usually re-learnt with walkers, crutches and orthosis until some patients become able to self-train and self-ambulate. Self-ambulation and -management is one of the prime goals of rehabilitation as it gives the individual the chance to participate independently in daily and social life and to return to work (Nas et al., 2015). Most motor recovery occurs in the first 2 month after

injury (Wirz et al., 2005) and a proportion of patients improve one grade on the ASIA impairment scale within this time (Mehrholz et al., 2012).

***Figure 4**: Example picture for rehabilitation after spinal cord injury in humans (www.STEPSforRecovery.com).*

One aim of rehabilitation is to first support gait like movements to initiate a new motor learning in the CNS which then can be further trained to allow the individual to self-ambulate again (Harkema et al., 2012, Hubli and Dietz, 2013). The basis for this motor learning is activity-dependent neuronal plasticity, which means that in development as well as in CNS injury neuronal activity forms and strengthens new connections (Bertrand and Cazalets, 2013, Overman and Carmichael, 2014, Sanes and Lichtman, 1999). An exemplary study with tetra- and paraplegic patients reported improvements in quality of live, depression, pain and motor function after training twice weekly over 9 month compared to controls (Hicks et al., 2003). Another study found significant improvements in gait velocity, endurance and performance after robotic assisted treadmill training (Wirz et al., 2005). Until today the exact mechanisms of exercise induced plasticity and recovery of function after spinal cord injury remain elusive. As there is no cure for spinal injury today, one needs to model the disease in animal research to uncover underlying mechanisms and discover new treatment options for patients.

1.4. Experimental spinal cord injury in research

1.4.1. Experimental Models

1.4.1.1 Animal models of spinal cord injury

Depending on the mechanism that one wants to study after spinal cord injury different model organisms can be chosen. Early work was mostly done on cats which recover spontaneous stepping and walking on a treadmill even with a complete thoracic spinal cord injury. This stepping occurs due to the activity of the central pattern generator (CPG), intraspinal motor networks that are independent of central brain input (Rossignol and Bouyer, 2004). The CPG will be described in detail in the next paragraph. Today the most common model organisms to study spinal cord injury are mice and rats due to their broad availability, possibility to use genetically modified animals and reflecting more closely the human situation in comparison to cats. The almost independent central pattern generator (CPG) of cats is present, but seems to be less pronounced in humans, which does not allow for central input independent unassisted stepping (Sasada et al., 2014). Non-human primates are closest to humans when it comes to SCI recovery, but their use for research remains controversial and limited (Abbott, 2014, Friedli et al., 2015). Nevertheless promising therapeutic approaches are usually validated in non-human primates before transition to clinical studies (e.g. (Capogrosso et al., 2016)).

1.4.1.2. Lesion Models

Clinical lesions to the spinal cord are either due to dislocation, contusion, compression, transection or stretching. To study all these different paradigms, different animal models were developed that mimic the injury mechanism and allow for the study of underlying recovery mechanism and therapeutic advances.

The most common used paradigm is the contusion injury, inflicted with a Multicenter Animal Spinal Cord Injury Study (MASCIS) impactor (Gruner, 1992) because it mimics very well most human injuries. To generate a controlled contusion injury a weight is dropped on the spinal cord after laminectomy with a certain height, weight, duration and velocity. This causes a contusion or compression injury leaving the dura mater intact, depending on the height of the drop causing mild injuries up to complete paralysis and destruction of the cord (Gensel et al., 2006, Gruner, 1992). Occurring problems are ‘bouncing’ of the rod on the spinal cord causing multiple injuries and more difficult reproducibility (Cheriyan et al., 2014). The impactor was first developed and used on rats (Beattie et al., 1997), then on mice (Jakeman et al., 2000, Kuhn and Wrathall, 1998) and marmosets (Iwanami et al., 2005).

Second most common are transection models. The spinal cord is cut with small scissors at different levels and positions and to different extends after laminectomy, creating lesion models from very small injuries to complete transections (Bareyre et al., 2004, Friedli et al., 2015, van den Brand et al., 2012). Section or hemisection models are more controlled and allow for studying remodeling and regeneration better than contusion injuries which cause more secondary complications (Cheriyan et al., 2014). Furthermore hemisection injuries result in a smaller inflammatory response when compared to contusion injuries (David and Kroner, 2011). The thoracic dorsal hemisection model interrupts the dorsal corticospinal tract, one of the most important motor tracts in the mouse, causing hindlimb paralysis in mice which recovers due to remodeling and is well suited for studying the recovery, regenerative and remodeling processes of the dCST ((Bareyre et al., 2004, Lang et al., 2012) Figure 5). A full transection of the spinal cord leaves the animal completely paralyzed, which is suited for neuromodulation experiments (Wenger et al., 2014). Lateral hemisections abolish the tracts in the right or left half of the spinal cord and can be used to study remodeling (van den Brand et al., 2012) or stem cell transplantation (Lu et al., 2014).

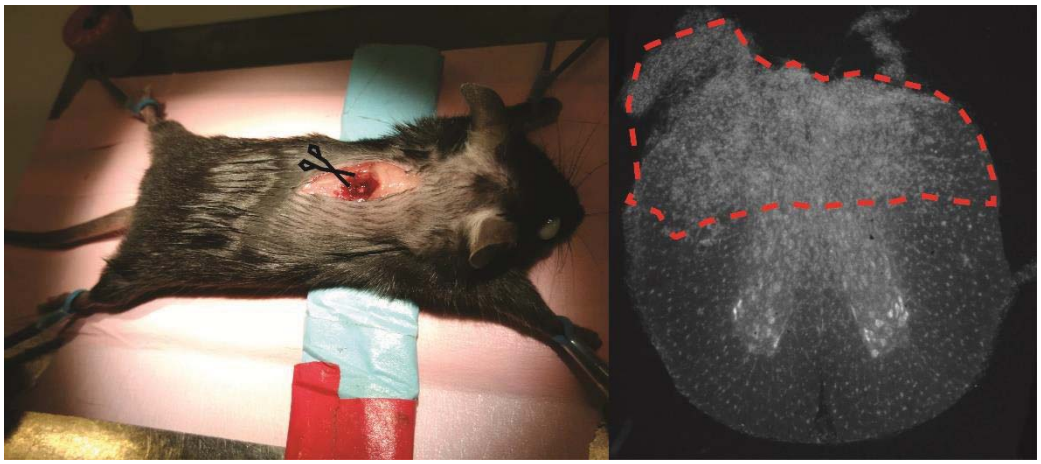

Figure 5*: Dorsal thoracic hemisection with fine scissors as a model for moderate spinal cord injury. Image of mouse surgery after laminectomy (left)and fluorescence image of the transected spinal cord at T8 (right).*

Less common models include forceps compression (Plemel et al., 2008), distraction and dislocation (Choo et al., 2009).

1.4.2. Therapeutic approaches

Experimental treatments on the one hand aim at supporting and re-establishing walking in individuals with body weight supported gait training with or without exoskeletons and functional electrical stimulation. On the other hand, many studies were conducted investigating pharmacological interventions with small molecules ((Thuret et al., 2006), Review). Body weight supported and sometimes robotic assisted gait training remains controversial and does not considerably improve the

patient's outcome when compared to rehabilitative overground gait training (reviewed in (Wessels et al., 2010)). Exoskeletons allow the individual to ambulate freely without additional support for a limited amount of time, but remain expensive and do not yield functional improvements in walking without the exoskeleton (reviewed in (Miller et al., 2016)).

1.5. Intrinsic and extrinsic inhibition of axonal regeneration after SCI

A traumatic event in the CNS is always characterized by cell death. Unlike embryonic neurons or neurons of the peripheral nervous system CNS neurons fail to regenerate. This is thought to be due to both extrinsic and intrinsic factors, meaning factors that concern the environment of the neuron and the neuronal growth response itself. Extrinsic factors that inhibit regeneration can be summarized under physically or molecular barriers that prevent axonal regeneration. Physical barriers include the reactive astrocytes and the glial scar that is formed and fluid-filled cavities that occur if the tissue loss is vast. Molecular barriers include among others the myelin-associated inhibitors secreted by severed or dying oligodendrocytes and chondroitin sulfate proteoglycans (CSPGs). Extrinsic factors were long thought to be the point of application for new therapies to promote regeneration, but so far have not yielded great results (Yiu and He, 2006). Newly born neurons of the CNS and all neurons of the PNS have an intrinsic program for regeneration that seems to fail if a mature neuron is severed. This might be due to the complex network architecture of the CNS and the prevention of harmful re-wiring of wrong connections. Some central neurons show higher potential for intrinsic re-growth than others, the rubro- and reticulospinal tract for example regenerate better after spinal cord injury than the CST. The dorsal root ganglia (DRG) neurons are an exception concerning regenerative growth as they contain neurons of the PNS and CNS alike. If the PNS neurons are lesioned before the CNS ones, the CNS neurons regenerate remarkably better, indicating that this pre-conditioning lesion activates some growth promoting genetic program in the whole DRG (Di Giovanni, 2009).

1.6. Spontaneous remodeling and autonomous spinal cord mechanisms for recovery after SCI

1.6.1. Detour Circuit of the CST

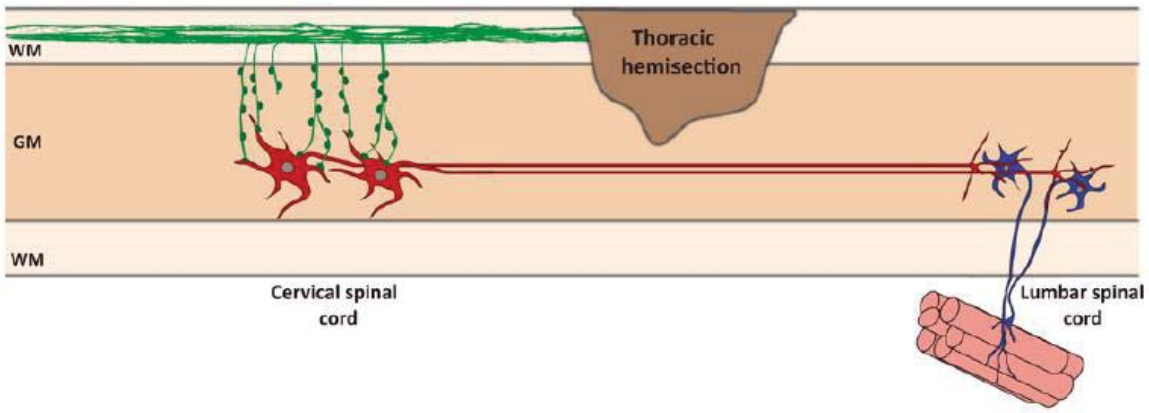

***Figure 6**: Detour circuit formation after spinal cord injury to re-relay the signal of the motor cortex to the lumbar motor neurons (Jacobi and Bareyre, 2015).*

Regrowth of severed axonal fibers e.g. across the lesion is defined as axonal regeneration. The neuron thereby reconnects to its target by re-growing its axon back to the target area after the cut part died. The potential for regenerative recovery in the CNS is limited after the end of development. Remodeling, meaning the formation of new circuits using pre-existing and spared supra- and intraspinal neurons can nevertheless greatly contribute to recovery. After dorsal thoracic hemisection the dorsal CST is interrupted and the animal's hindlimbs are paralyzed. After lesion a detour circuit forms by contacting spinal interneurons cervically, which then re-relay the information from the interrupted tract to the lumbar motor neurons ((Bareyre et al., 2004, Courtine et al., 2008) Figure 6). Preferentially contacts are formed and maintained on long propriospinal neurons (LPSN) which are normally used for the coordination of fore- and hindlimb in the animal (Alstermark et al., 1987). Specifically, the dorsal CST sprouts rostral to the thoracic lesion into the grey matter within the first 10 days after lesion and then contacts first short (SPSN) and long propriospinal neurons within the first 3 weeks. These contacts are then refined and maintained between 3-4 and 12 weeks after injury creating a stable detour circuit consisting of CST fibers and LPSN, connecting the motor cortex with the lumbar motor neuron once again. This re-connection is accompanied by spontaneous functional motor recovery in mice after dorsal thoracic hemisection (Lang et al., 2012). Remodeling and reconnecting of supraspinal pathways was also shown in full, time and segment separated, lesion models (van den Brand et al., 2012), from the ventral corticospinal tract (Weidner et al., 2001) and the reticulospinal tract (Zorner et al., 2014), indicating axonal remodeling as a general concept of central nervous system recovery.

1.6.2. Plasticity of the serotonergic system and the central pattern generator (CPG)

The serotonergic system has many functions in the nervous system. It regulates digestion, sleep-wake and arousal cycles and motor activity among others, but appears to be essential for none of these functions, thus possessing a more enabling or facilitating effect (Jacobs and Azmitia, 1992).

In my thesis, I will focus on the role of 5HT and its receptors in the descending motor system of the mouse as this will be a key topic of this thesis. The major descending serotonergic motor system arises in the nucleus raphe obscurus (NRO), pallidus and magnus (to lesser extend) which are located in the brainstem and the ventral lateral medulla oblongata (VLM Figure 7).

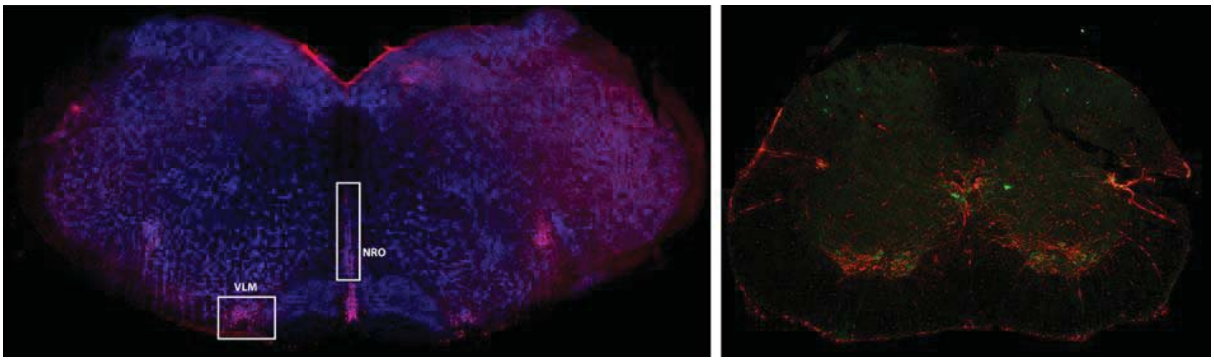

***Figure 7**: Fluorescence image of mice brainstem illustrating the localization of descending serotonergic tract cells in the brainstem (red) with neuronal staining (blue, left). The white boxes outline the area of descending pathways that connect to the lumbar motor centers (nucleus raphe obscurus (NRO) and ventral lateral medulla oblongata (VLM)). Serotonergic wiring (red) around motor neurons (green) in the lumbar spinal cord (right).*

The descending motor tracts run partially in the dorsal white matter (obscurus and pallidus) and partially in the ventral white matter (magnus). Descending serotonergic brainstem projections terminate in all grey matter parts and all levels of the spinal cord and most of the fibers are concentrated around spinal motor neurons (Ballion et al., 2002). The raphe obscurus spinal tract then contacts motor neurons and modulates their activity. In addition to that, spinal 5HT neurons are located directly in the spinal cord, contact and modulate inter- and motor neurons (Cina and Hochman, 2000, Guertin, 2009, Jacobs and Azmitia, 1992, Jacobs and Fornal, 1997). These neurons form the mammalian CPG, which consists of an intraspinal neuronal network that is able to generate motor behavior, e.g. rhythmic stepping, without central brain input (Hayes et al., 2009). After spinal cord injury the reorganization of these spinal networks contributes to recovery of rhythmic stepping, but can also cause system dysfunction up to paralysis (Ghosh and Pearse, 2014). This intraspinal network appears to consist of few cells (Ballion et al., 2002, Cina and Hochman, 2000) and still remains a black box requiring further studies (Guertin, 2009). The locomotor-like movements induced by 5HT are dependent on different 5HT receptors (5HTR). There are 14 known 5HTRs, 13 of which are G protein-coupled receptors (GPCRs) and

one ligand gated ion channel (5HTR3) (Hannon and Hoyer, 2008). They are divided into 7 families as per sequence similarities and the main receptors for locomotion in the spinal cord are from the 5HTR1, 5HTR2 or 5HTR7 family. All but the 5HTR3 modulate neuronal activity of the 3rd neuron by influencing release probabilities of the 2nd neuron. Depending on the signal of the 5HTR and the type of the neuron that carries the receptor 5HT signaling can be inhibitory as well as excitatory on the 3rd neuron. If a second inhibitory neuron is inhibited or an excitatory neuron is facilitated the 3rd neuron would receive and increased signal, whereas if the inhibitory neuron is facilitated or the excitatory inhibited the 3rd neuron would be inhibited ((Fink and Göthert, 2007) Figure 8). 5HT receptors classically signal via the adenylyl cyclase (AC) and Cyclic adenosine monophosphate (cAMP) and then protein kinase A or the phospholipase (PLC), that then produces inositol trisphosphate (IP_3) activating protein kinase C. The kinases then mediate the downstream effectors and inhibit or facilitate ((Ohno et al., 2015) Figure 8).

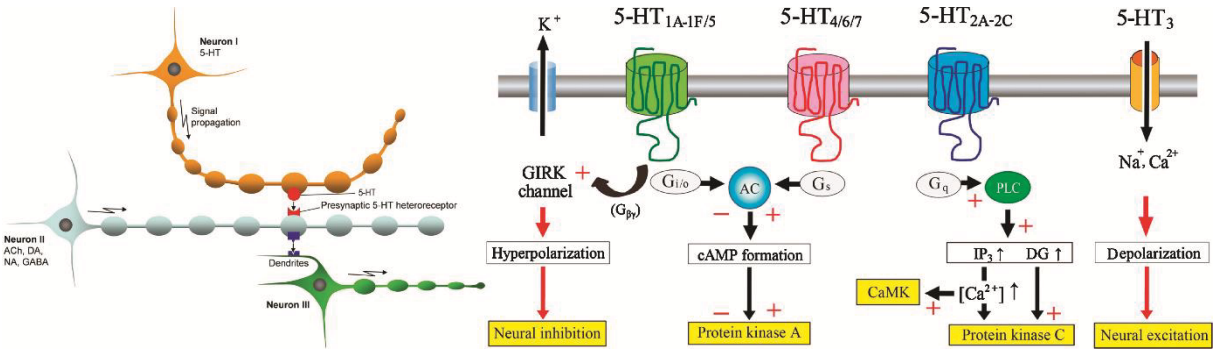

***Figure 8**: Influence of serotonergic signaling on the 2nd and the 3rd neuron (left (Fink and Göthert, 2007)). 5HT receptor subtypes and their mode of action (right, (Ohno et al., 2015))*

After complete spinal cord transection 5HT in the cord drops to 5-10% followed by upregulation of 5HTR2 (Kong et al., 2010, Lee et al., 2007, Murray et al., 2010) and 5HTR1 (Landry et al., 2006, Otoshi et al., 2009) on motor neurons most likely to compensate for the loss of input. Supraspinal independent locomotion is furthermore initiated by 5HTR7 signaling (Cabaj et al., 2017, Landry et al., 2006).

1.7. Rehabilitation

1.7.1. Differences between humans and Animals

Humans and animals recover slightly different from a spinal cord injury. Most animal models engage in quadrupedal stepping whereas humans walk erect on two feet, therefore some of the rhythmic connections between upper and lower extremities and fore and hind paws respectively are different. Moreover corticospinal tract organization, fiber crossings, interneuron populations and in general greater complexity in higher mammals compared to mice has to be taken into account. In the mouse the spinal cord accounts for 30% of CNS volume in comparison to 3% in humans, which suggests a greater

relative autonomous computing power in the spinal cord of rodents. Nevertheless the basic principles of reflexes, stepping, CPG wiring and recovery from central nervous injuries are comparable between mammals. Previous animal model findings in exercise dependent plasticity and rehabilitation paradigms have successfully advanced rehabilitation in humans. Electromyographic (EMG) recordings and reflex responses show comparable results after rehabilitative training in humans and animal models of SCI (Côté et al., 2016).

1.7.2. Exercise and Rehabilitation in Animal Models of Spinal Cord Injury

Depending on the experimental spinal cord injury model and the capabilities of the studied animals, different rehabilitation paradigms can by studied. The most commonly used rehabilitation method is treadmill training, in which a mouse or rat is walking on a treadmill belt, with or without body-weight support. These animals usually undergo an incomplete, complete or near complete transection of the spinal cord (Dominici et al., 2012, Multon et al., 2003) and treadmill training also proved effective in promoting recovery in cats (Martinez et al., 2013). Other rehabilitation paradigms commonly used in rodents are wheel running or bicycle training for the hindlimbs and food pellet reaching and grasping for forelimb use (Dupont-Versteegden et al., 2004, Girgis et al., 2007). Whereas treadmill and bicycle training are forced training paradigms wheel running is a voluntary elective behavior in mice ((Meijer and Robbers, 2014) Figure 9). Many different studies mimicking rehabilitation after SCI have been published over the years with different findings and different outcomes. Most studies rely on forced exercise, but after stroke and spinal cord injury voluntary exercise increases brain derived neurotrophic factor (BDNF) levels more than forced training paradigms resulting in more plasticity in the brain and spinal cord (Ke et al., 2011, Vaynman and Gomez-Pinilla, 2005). A previous study reported a negative effect of wheel running in the recovery from a moderate contusion injury, but reported an improvement in locomotor recover following the use of a flat surface wheel instead of a wheel with regular spaced bars (Engesser-Cesar et al., 2005). The combination of forelimb and hindlimb use that is provided with wheel running improves locomotor function and strengthens neuronal spinal cord wiring (Shah et al., 2013). More recent studies aimed at combining exercise with pharmacological or other stimulatory treatments. Combining for example chondroitinase treatment with different exercise paradigms sometimes did improve functional outcomes, and sometimes it did not. The authors concluded that the timing and form of exercise as well as the timing and duration of chondroitinase treatment determines success or failure of these studies (Jakeman et al., 2011). Cell transplantation after spinal cord injury also showed better functional outcomes and axonal regeneration when combined with exercise (Houle and Cote, 2013). The clear mechanisms underlying the beneficial effect of rehabilitative training remain unclear until today (Fouad and Tetzlaff, 2012). All these studies indicate that the timing, kind and amount of exercise is crucial for the maximum benefit in recovery after spinal cord injury.

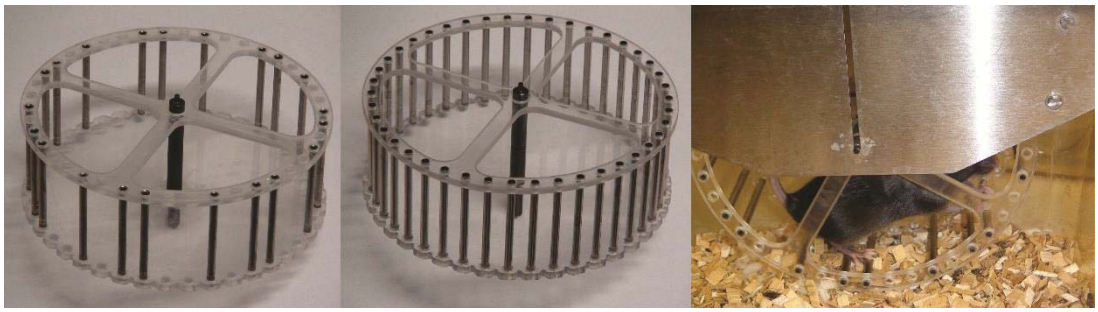

***Figure 9**: Different types of wheels for mice. Left is an irregular or complex wheel, middle a regular wheel and on the right a mouse training on the wheel.*

1.8. Molecular cues involved in axon guidance and synapse formation

As neurons grow out axons during development they are constantly searching for other neurons to form meaningful connections for the organism to function. This process follows steps: 1) the axon growth and migrates along a molecular gradient and is thereby attracted or repelled to grow in the right direction until it stops in the vicinity of a potential synaptic partner and 2) the axon develops a presynaptic specialization and the contacted cell forms a postsynaptic site thereby establishing a chemical synapse that allows for information transmission (Figure 10). Throughout these steps different molecules have been discovered to play a major role in the past decades. Synaptic guidance molecules are secreted by the environment of the growing axon and depending on the receptor set of this axons it can either 'read' this molecular cue or not and if it can, it can be attracted or repelled by the gradient (Figure 10 top). Known signaling molecule/receptor pairs for axonal growth and guidance in development are Netrin1/Unc6 or DCC (deleted in colorectal cancer), BDNF/TrkB (tropomyosin receptor kinase B), Ephrins/EphrinR and Semaphorins/Plexins, to mention a few (Shen and Cowan, 2010). Besides the growth promoting, more environmental, effects of these guidance molecules, some growth promoting molecules are differentially expressed between the CNS and the PNS as response to injury. One of the known molecules is signal transducer and activator of transcription 3 (STAT3) which is upregulated in PNS axons after axotomy and initiates re-growth, which is not the case in the CNS (Bareyre et al., 2011). Overexpression of STAT3 in the CNS leads to increased axonal growth also in this system after injury, indicating a general growth promoting effect of STAT3 after injury in all neurons (Lang et al., 2013). In accordance with this, deletion of SOCS3 (suppressor of cytokine signaling 3), a negative regulator of STAT3 also promotes axonal growth (Sun et al., 2011). Another known player in axonal growth is the mTor (mechanistic target of rapamycin) pathway that is inhibited by PTEN (phosphatase and tensin homolog). If PTEN is deleted and mTOR thereby activated robust regeneration across CNS lesion sites can be seen. Overexpression of growth promoting insulin like growth factor 1 (IGF1) and osteopontin

(OPN) has the same effect (Liu et al., 2010). All these growth promoting and guidance molecules are potential targets for therapeutic molecular approaches in spinal cord injury patients. Nevertheless promoting only growth is not sufficient to establish a functional relevant connection between two neurons and approaches that are only growth promoting do not always result in functional recovery in the animal model (Geoffroy et al., 2015).

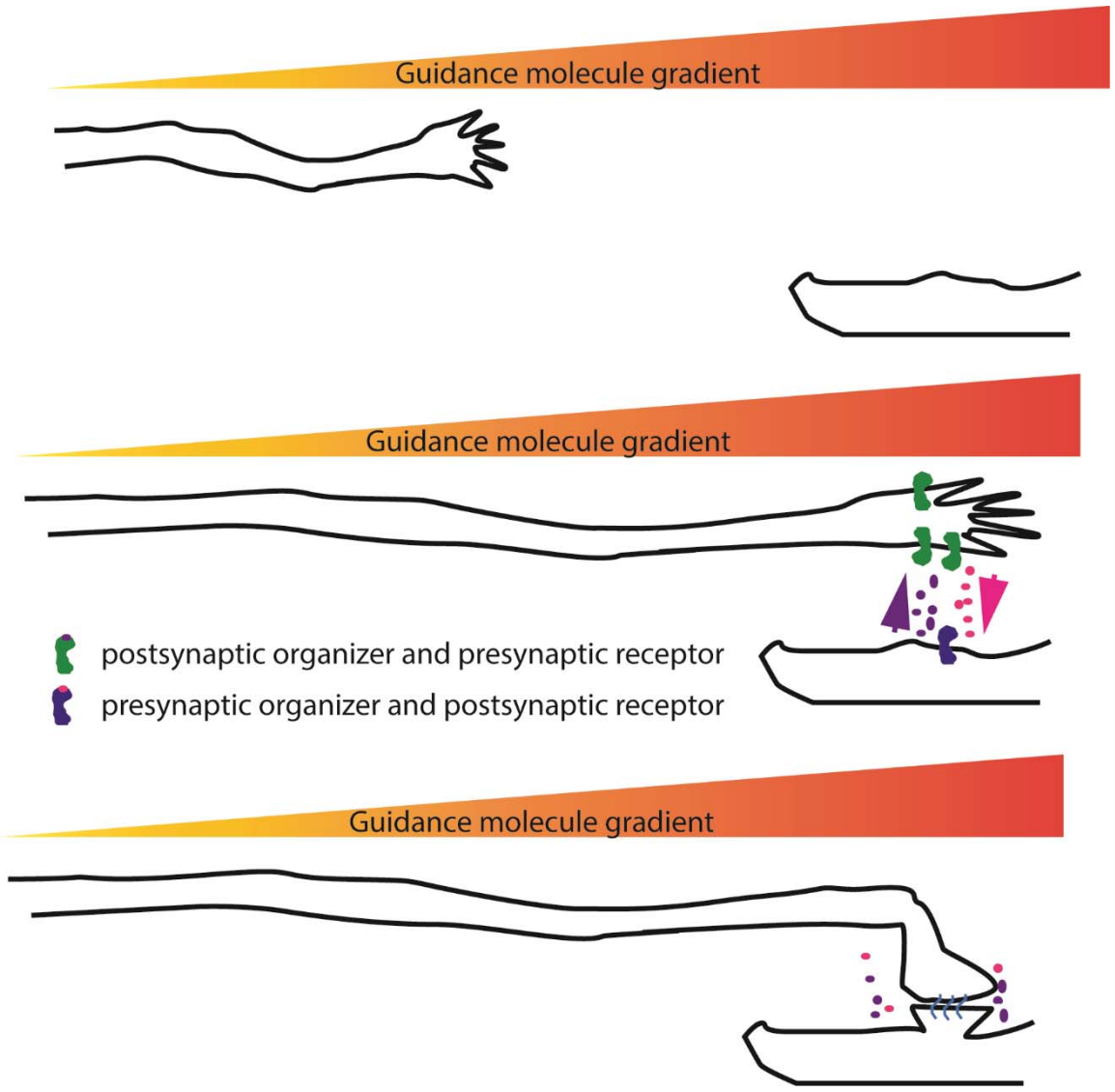

***Figure 10**: Schematic of axonal growth guidance and synapse formation. Depicted is first the attractive gradient that leads the later presynaptic partner to his target region (top). Then secretion of pre- and postsynaptic organizers halts the growth of the axon (middle) and a synapse is formed (bottom).*

The formation of a meaningful synapse is a crucial step for connection or re-connection and function as well as functional regeneration. Synapse formation and molecules involved were first studied at the neuromuscular junction (NMJ). The first molecule to be identified, that triggers synapse formation was laminin β2 at the basal lamina of the NMJ, which induces presynaptic differentiation in motor neurons in close apposition to the motor endplate (Sanes and Hall, 1979). The molecule on the other side that is

expressed in the motor neuron and induces postsynaptic differentiation in the muscle endplate was discovered several years later and called agrin (Magill-Solc and McMahan, 1988). Over time several molecules that establish synaptic connections in the CNS have been identified and they have been divided in postsynaptic organizers (such as agrin) and presynaptic organizers (such as laminin β2). To date the presynaptic organizers that have been identified are WNT-7a, Neuroligin, synaptic cell adhesion molecule (SynCam) and members of the fibroblast growth factor (FGF) family. Postsynaptic organizers in the CNS known to date are Narp, members of the Ephrin family and Neurexins ((Fox and Umemori, 2006), Fig 10 middle and bottom).

1.9. Semaphorin7a in axon outgrowth and guidance

Semaphorins have many different functions in many different systems during development and maintenance of an organism, including the nervous system, the immune system and bone and heart development. They are present in invertebrates and vertebrates and bind to specific receptors. Twenty-seven different Semaphorins have been identified and studied so far, categorized in 8 classes. Semaphorins typically consist of a signaling domain intracellularly, a membrane anchor and a Sema domain. The Sema domain controls receptor binding and dimerization (Pasterkamp, 2012).

Sema7A is a member of this family mainly known for its role in vascularization, the immune system and the nervous system. It acts via two known receptors: PlexinC1 and α1β1 integrin ((Pasterkamp et al., 2003, Zhou et al., 2008) Figure 11).

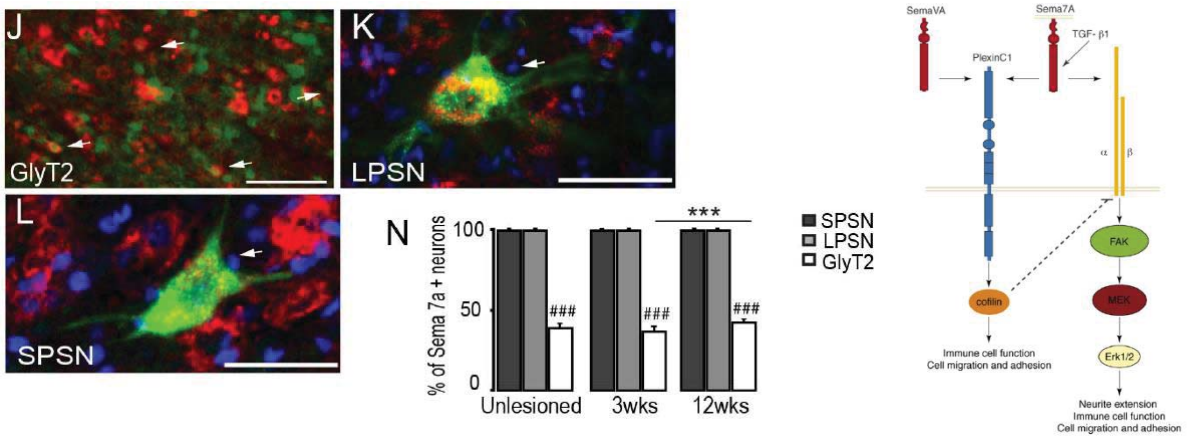

***Figure 11**: Images and quantification of spinal cord interneurons and their Sema7A expression (left (Jacobi et al., 2014)) and the downstream signaling pathway of the PlexinC1 and Integrinα1β1 receptor ((Zhou et al., 2008)).*

It is either GPI (glycophosphatidylinositol) anchored on the cell membrane or shed, making it a secretable signaling molecule (Pasterkamp, 2012). Sema7A promotes tumor growth and has a pro-

angiogenic effect via macrophage activation (Garcia-Areas et al., 2014). In the immune system Sema7A is expressed on T-cells and stimulates cytokine production in monocytes and macrophages via its receptor α1β1 integrin. This macrophage activation contributes to the inflammatory process and induced experimental autoimmune encephalomyelitis (EAE) was reported to be less severe in KO mice (Suzuki et al., 2007). Another study reported a negative effect of Sema7A on T-cell responses and a more severe clinical course in EAE. The knock out (KO) of Sema7A led to hyperresponsiveness of T-cells (Czopik et al., 2006).

In the nervous system Sema7A is expressed in the developing and mature glial scar and acts profibrotic. Its expression seems to also be a marker for astrocyte activation after spinal cord injury (Kopp et al., 2010). Furthermore Sema7A promotes axon outgrowth and is needed for proper formation of the lateral olfactory tract (LOT), suggesting a role in axon guidance and neuronal migration in development in the mouse. Sema7A/PlexinC1 signaling can also function as a repulsive axon guidance cue (Pasterkamp and Kolodkin, 2003, Pasterkamp et al., 2003). It is expressed in the developing brain and spinal cord alongside with one of its receptors PlexinC1 (Pasterkamp et al., 2007). Sema7A KO mice are without gender preference during mating due to the malformation of the LOT (Schellino et al., 2016) and abnormal gonadal development and reduced fertility, which is due to abnormal gonadotropin-releasing hormone- 1 cell migration, neurons that mediate reproductive functions in mammals. This results in smaller litters in KO breeding (Messina et al., 2011). A knockdown of Sema7A in the cerebellum impairs climbing fiber synapse elimination which impairs synaptic refinement (Uesaka et al., 2014). Sema7A is also needed for the proper formation of the barrel cortex, which represents the whiskers in mice and is a somatosensory cortical circuit (Carcea et al., 2014). In the adult mouse Sema7A is a key regulator of hippocampal neurogenesis through the α1β1 integrin receptor (Jongbloets et al., 2017). Sema7A was found to be expressed on excitatory interneurons that are preferentially contacted by remodeling CST fibers after spinal cord injury ((Jacobi et al., 2014) Figure 11). In summary Sema7A has various roles in circuit maturation and refinement, neurogenesis and axonal outgrowth throughout the CNS. The genetic region spanning the SEMA7A gene in humans is affected by the chromosome 15q24 microdeletion syndrome that leads to mental retardation, developmental delay and facial abnormalities among other possible symptoms (Magoulas and El-Hattab, 2012).

1.10. FGF22: A regulator of synapse formation

A key step in neuronal development is the formation of a synapse, a chemical contact that links two neurons and allows for the transmission of information. Some molecules that establish this critical connection in the CNS have been identified so far, among them Wnt-7a, Neuroligin, SynCam and members of the FGF family (Fox and Umemori, 2006). FGF22 is a member of the FGF subfamily 7 which

also includes FGF3, 7 and 10 and binds to two out of four FGF receptors (FGFR), FGFR1 and FGFR2 (Zhang et al., 2006). FGF22 was identified as key presynaptic organizer for the establishment of new synapses between mossy fibers and granule cells in the cerebellum. FGF22 acts as presynaptic signal and interacts with FGFR2 on the postsynaptic cell to induce synapse formation (Umemori et al., 2004). Moreover FGF22 induces excitatory synapse formation in the CA3 region of the hippocampus in contrast to FGF7 which leads to the formation of an inhibitory synapse (Figure 12). FGF22 KO mice are thereby rendered resistant to kindling and the development of epileptic seizures whereas FGF7 KO mice develop earlier seizures due to an imbalance in inhibitory and excitatory synapses (Terauchi et al., 2010). These alterations in the CA3 region of the hippocampus also lead to a depression like phenotype in the FGF22 KO mice without impairments in motor abilities and social interaction and without anxiety (Williams et al., 2016). FGF22 signaling in the brain induces insulin like growth factor 2 (IGF2) which is required for activity dependent synapse stabilization. Overexpression of IGF2 rescues the synapse formation phenotype of the FGF22 deficiency (Terauchi et al., 2016). While the role of FGF22 in synapse formation during development starts to be well understood (Terauchi et al., 2010), whether the molecule is expressed throughout adulthood and its role following injury is currently unknown. It is therefore interesting to study the role of FGF22 and its receptors further in spinal cord injury in adult mice.

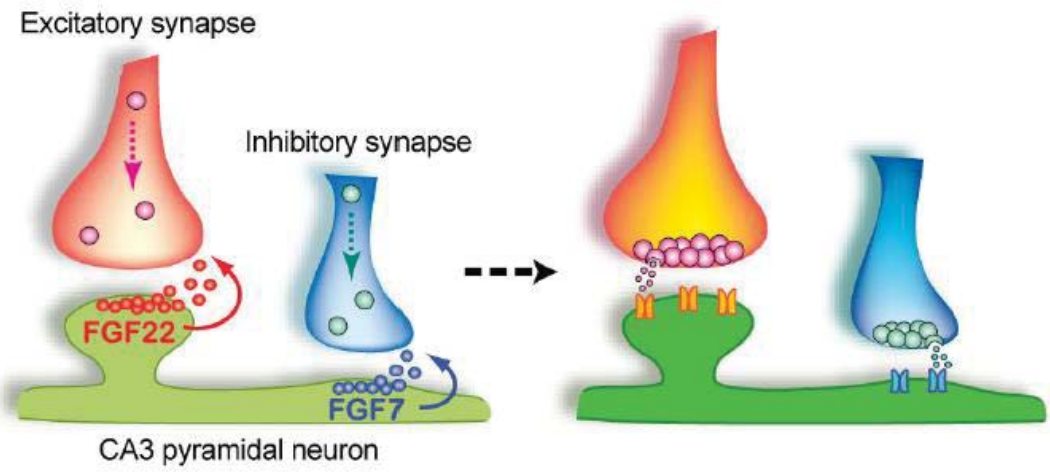

***Figure 12**: Regulation of synapse formation by FGF7 and FGF22 (modified (Terauchi et al., 2010)).*

2. Aims of the Thesis

The aim of this thesis is to better understand the recovery mechanism after an incomplete lesion of the spinal cord in mice. Therefore, I examined different interventions and molecular cues involved in axonal growth, guidance and synapse formation in order to address the following aims.

Aim 1) Determine whether and how wheel running, a form of voluntary exercise, influences recovery after spinal cord injury and understand the underlying anatomical mechanisms that could lead to functional improvements after rehabilitative training.

To achieve this goal, mice were offered unlimited access to running wheels before and after SCI. Exercise and rehabilitation are standard of care in patients after SCI nowadays and improvements in the first two months are common (Wirz et al., 2005). However, the underlying mechanisms of this recovery remain elusive. I wanted to present mice with a less stressful training model in which each animal could choose the amount of training in accordance to its current stepping abilities. My mice were divided into four groups: Mice without SCI with and without running wheels and mice with SCI with and without running wheels. I then examined functional recovery using different behavioral tests to determine hindlimb fine stepping capabilities and general locomotor ability in all groups. For this study I used a complex training wheel to challenge fine stepping and motor control which are mostly related to supraspinal descending motor tracts in particular the corticospinal tract (Metz and Whishaw, 2009) to specifically challenge remodeling of this tract. I traced first order motor neurons from the cortex and looked at CST sprouting in the cervical spinal cord rostral to the lesion and around the lesion. My aim was to determine, among others, the effect of CST-specific training on detour circuit formation, for which we back-traced LPSN and looked at contacts between the CST and the LPSN. To take into account another supraspinal locomotor input, the raphespinal serotonergic tract and interneurons, I furthermore investigated serotoninergic and choline acetyltransferase (ChAT) positive neurons to look at supra-, but also intraspinal input on second order motor neurons in the lumbar spinal cord. Axonal growth in the CNS is not only limited by the capacity of the neuron to grow, but also by the inhibitory environment that is generated by the lesion. Therefore, I also took a closer look at the effect of exercise on myelination, which was found in another model to be improved by exercise (Liebetanz and Merkler, 2006) and glial scar formation.

Aim 2) Determine whether Sema7A signaling is important to mediate functional recovery following spinal cord injury and investigate how this influences the formation and maintenance of supraspinal and spinal networks.

Sema7A is a molecule that regulates many functions in health and development that are important in recovery from SCI: Vascularization, immune response, astrocyte scaring and neuronal growth and guidance (Lang et al., 2013, Li et al., 2017, Schwab et al., 2014). Using SEME7A KO mice, I aimed at investigating whether Sema7A signaling affects functional recovery following SCI to then characterize the underlying mechanisms linking Sema7A signaling to recovery of function. I investigated several functions that could be affected by Semaphorin 7A signaling. In particular I focused on remodeling of the vasculature, cell proliferation and correct motor neuron distribution in the cortex following the lesion. I also focused on neuronal growth potential and rewiring of spinal and supraspinal pathways after spinal cord injury by investigating the corticospinal tract, which is a central direct motor input and the serotonergic raphe-spinal tract, which modulates autonomous and central motor activity in the spinal cord. The dorsal thoracic hemisection model I used is highly suitable for studying adult central neuronal growth and remodeling.

In addition, I thought to subject these mice to immunophenotyping early after SCI to see whether the immunological state of them is altered in any way. Considering that I performed flow cytometry analysis of the lesioned area in the spinal cord.

Aim 3) Determine whether FGF22 plays a role in adult synapse formation and whether it contributes to detour circuit formation and recovery after SCI?

Previous research has shown that FGF22 and its receptors are important inducers of synapse formation in different systems, like the cerebellum or the hippocampus, during development (Terauchi et al., 2010, Umemori et al., 2004). The role of FGF22 in synaptogenesis during adulthood was little understood. As detour circuit formation presents us with a model for adult synapse formation of the CST on LPSN (Bareyre et al., 2004). We were interested whether FGF22 plays a role in this remodeling process, we thus aimed at deleting FGF22 from the relay neurons in the spinal cord by a full knock out and to delete the two receptors, FGFR1 and FGFR2, from the CST by viral Cre expression in floxed mice. We then examined CST sprouting and detour circuit formation after injury, taking a closer look at boutons, contacts and synaptic maturation. We also assessed functional motor recovery after injury to determine the role of synapse maturation and formation in the establishment of the detour circuit and the thereby caused motor recovery. Further work will then determine whether exogenous application of FGF22 could also be a therapeutic option to improve functional recovery following SCI.

The work of this thesis aims at unraveling different regulatory aspects of adult neuronal growth, guidance and synapse formation after CNS injury to lay the groundwork for future combinatorial

therapies. We first have to understand the regenerative failure after spinal cord injury and the different aspects we can modulate, like axonal growth and guidance as well as synaptogenesis and then combine these tools together with rehabilitative strategies to achieve the best possible outcome following CNS injuries and in particular spinal cord injuries.

3. Results

The work of this doctoral thesis has resulted in one already published peer-reviewed publication in the EMBO Journal, one manuscript that is submitted for peer-reviewed publication to the Journal of Neurotrauma and one manuscript that is in preparation for submission. They are included in this thesis and constitute the results part.

1. **Loy K**, Schmalz A, Hoche T, Jacobi A, Kreutzfeld M, Merkler D, Bareyre FM. Voluntary exercise improves functional recovery and strengthens rewiring of supraspinal circuits following spinal cord injury. *(submitted to J Neurotrauma)*

2. **Loy K**, Meng N, Jacobi A, Locatelli G, Bareyre FM. Semaphorin 7A controls the proper targeting of corticospinal and serotonergic fibers following spinal cord injury *(to be submitted)*

3. Jacobi A, **Loy K**, Schmalz AM, Hellsten M, Umemori H, Kerschensteiner M, Bareyre FM. FGF22 signaling regulates synapse formation during post-injury remodeling of the spinal cord. *EMBO J. 2015 May 5;34(9):1231-43.*

3.1. Voluntary exercise improves functional recovery and strengthens rewiring of supraspinal circuits following spinal cord injury.

Loy K, Schmalz A, Hoche T, Jacobi A, Kreutzfeld M, Merkler D, Bareyre FM

The manuscript is currently submitted to the Journal of Neurotrauma for peer-review.

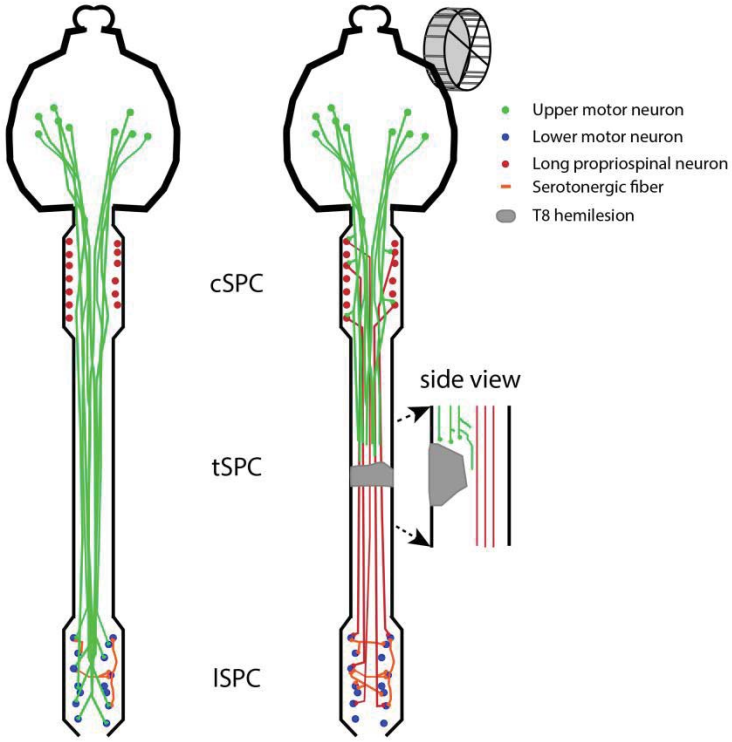

***Figure 13**: Graphic summary of plastic changes in the spinal cord after spinal cord injury with voluntary wheel running. Remodelling was prominent in the dorsal corticospinal tract and the descending serotonergic tract.*

In this study we investigated the effect of voluntary exercise, in the form of wheel running, on recovery after spinal cord injury in mice. We found that trained mice showed improved functional recovery, which correlates with accelerated and partially improved remodelling of supraspinal circuitry. We found transient changes in myelination, sprouting and glial scar formation at the lesion site, which only explained the early steeper recovery, but not the long lasting one. Our focus was on detour circuit formation of the hindlimb corticospinal tract onto long propriospinal neurons and the serotonergic wiring onto lumbar motor neurons. We found that voluntary wheel running accelerates and increases detour circuit formation and accelerates the remodelling of serotonergic input onto lumbar motor neurons, leading to hard wired changes in neuronal circuitry which correlate with improved functional recovery.

Contributions: KL: designed experiments, wrote the manuscript, performed all surgical procedures if not stated otherwise, collected and analysed all data if not stated otherwise; AS: collected and analysed all data concerning the 5HT and ChAT experiments; TH: implemented and analyzed part of the behavioural experiments; AJ: performed part of the brain injections; MK and DM: implemented and helped analyse the quantitative wheel running experiments; FB: designed experiments, wrote the paper, analysed the GFAP and MBP dataset.

Voluntary exercise improves functional recovery and strengthens rewiring of supraspinal circuits following spinal cord injury

Kristina Loy[1,2,3], Anja Schmalz[1,2], Tobias Hoche[1,2], Anne Jacobi, PhD[1,2], Mario Kreutzfeldt, PhD[4], Doron Merkler, MD[4] and Florence M. Bareyre, PhD[1,2,5,*]

1 Institute of Clinical Neuroimmunology, University Hospital, LMU Munich, Marchioninistrasse 15, 81377 Munich, Germany
2 Biomedical Center Munich (BMC), Faculty of Medicine, LMU Munich, Grosshadernerstrasse 9, 82152 Planegg-Martinsried, Germany
3 Graduate School of Systemic Neurosciences, Ludwig-Maximilians-Universitaet Munich, Grosshadernerstrasse 2, 82152 Planegg-Martinsried, Germany
4 Departement of Pathology et Immunology, CMU, University of Geneva, Rue Michel-Servet , 1211 Geneva, Switzerland
5 Munich Cluster of Systems Neurology (SyNergy), Feodor-Lynen-Str. 17, 81377 Munich, Germany

Contact Information
kristina.loy@med.uni-muenchen.de – Phone: +004989218071684 – Fax +4989 218071811
anja.schmalz@med.uni-muenchen.de – Phone: +004989218071658 – Fax +4989 218071811
tobias.hoche@med.uni-muenchen.de – Phone: +004989218071684 – Fax +4989 218071811
anne.jacobi@med.uni-muenchen.de – Phone: +004989218071684 – Fax +4989 218071811
Mario.Kreutzfeldt@unige.ch – Phone: +0041223724966 – Fax +0041223724944
Doron.Merkler@unige.ch - Phone+0041223724943 – Fax +0041223724944

***Correspondence should be addressed to:**
Florence M. Bareyre
florence.bareyre@med.uni-muenchen.de
Phone:+004989218071663 - Fax: +004989218071811

Running Title: Exercise improves recovery and circuit rewiring

Table of Contents Title: Voluntary exercise improves recovery and circuit rewiring after spinal cord injury

Words: 5069 **Abstract: 171** **Introduction: 355** **Discussion: 849**
Pages: 31 **Figures: 6** **Tables: 0**

ABSTRACT

Recent reports suggest that rehabilitation measures that increase physical activity of patients can improve functional outcome following incomplete spinal cord injuries (iSCI). To investigate the structural basis of exercise-induced recovery we examined local and remote consequences of voluntary wheel training in spinal cord injured female mice. We offered free access to running wheels and observed that voluntary exercise resulted in improved recovery of both overground locomotion as well as skilled motor function following iSCI. Exercise-induced changes to the neuronal and glial response at the lesion site were transient and while they might contribute to earlier onset of recovery, they did not correlate with long-lasting functional improvements. In contrast, voluntary exercise led to profound and sustained effects on axonal rewiring processes remote from the lesion that resulted in strengthened supraspinal connections to the injured spinal cord. Voluntary exercise can thus improve the efficiency of circuit rewiring processes that are endogenously initiated after injury. This indicates that increasing physical activity soon after an incomplete CNS insult leads to hard-wired changes of spinal circuitry.

KEYWORDS: Spinal cord injury, Axonal remodeling, Rehabilitation, Corticospinal tract, Voluntary exercise

INTRODUCTION

Despite intensive research efforts, there is still no effective therapy that efficiently promote functional recovery following spinal cord injury.[1] The clinical translation of many experimental approaches based on pharmacological interventions or cell replacement has so far often failed due to side effects or lack of efficacy.[2] In contrast, non-invasive measures to promote physical activity such as treadmill training, bicycling or swimming have all shown promises in improving patient outcome following spinal cord injury. Such measures not only lower the risk of secondary complications[3, 4] but have also shown potential to improve walking ability in particular in patients with incomplete injuries.[5, 6] Likewise, experimental studies have reported that training paradigms improve recovery of stepping movements in mice, rats and cats.[7, 8]

How such increased physical activity can lead to lasting improvements of neurological function is only incompletely understood. Both local changes at the lesion site and remote effects on brain and spinal connectivity are conceivable. Here, we therefore explored how voluntary exercise influences the neuronal and glial response at the lesion site as well as the rewiring of supraspinal tracts after incomplete midthoracic spinal cord injury (iSCI). We chose voluntary exercise initiated by providing mice with free access to running wheels over "forced overuse" paradigms as the latter, at least in some cases can lead to worsening of functional outcomes following spinal cord injury.[9, 10] Our results show that mice extensively use their running wheels not only before but also after injury reaching their pre-lesion exercise levels within 5 days after injury. Running affected both their overall as well as their skilled motor function after injury and exercising mice started to recover earlier and reached better sustained performance levels. Such long-lasting improvements in motor performance are unlikely to be related to local axonal and glial changes at the lesion site that were only transiently affected by exercise. In contrast, we detected marked and sustained improvements of the rewiring of supraspinal connections that resulted in a

strengthening of both indirect and direct inputs to lumbar motoneurons. Lasting strengthening of brain-spinal cord connectivity can thus be induced by increasing physical activity within days after incomplete spinal cord injury.

MATERIAL AND METHODS

Animals

Adult female C57Bl6j mice (Janvier, France; https://www.janvier-labs.com/rodent-research-models-services/research-models/per-species/inbred-mice/product/c57bl6jrj.html) from 6 to 12 weeks of age were used in this study. Mice were separated into four groups: Mice without thoracic dorsal hemisection with or without a running wheel and mice with thoracic dorsal hemisection with or without a running wheel. Animals were housed in a 12-hour night day cycle with food and water ad libitum. All animal procedures were performed according to institutional guidelines and were approved by the local regulatory authorities (Regierung von Oberbayern 55-2-1-54-2532-136-2015136-2015; Cantonal veterinary office Geneva GE/81/16).

Wheel Training

All animals with free access to running wheels were housed individually and introduced to a wheel in their home cage 7 days prior to the first surgery. Animals were given a running wheel with regular spacing (regular wheel) for the first 2 days. After this habituation period the regular wheel was exchanged for one with irregular spaced bars (complex wheel). After each surgical intervention mice were given a regular wheel for 2 days post-surgery which then was exchanged for a complex wheel again. The rationale for using a complex wheel was the following: as rhythmic locomotion is largely controlled at the level of the spinal central pattern generator networks, supraspinal input might be more important for running in wheels with irregularly spaced bars. Wheel running behavior was monitored regularly throughout the entire experiment. Measurements of wheel running velocity, distance and frequency were obtained as previously described.[11] Animals that were provided with a wheel, but didn't run in it during the habituation period were excluded from the study.

Surgical procedures

For all surgical procedures mice were anesthetized with an i.p. injection of midazolam/medetomidin/fentanyl (MMF; midazolam 5.0mg/kg, medetomidin 0.5mg/kg, fentanyl 0.05mg/kg) on a heating pad (38°C). Mice were returned to the heating pad until fully awake. For pain management meloxicam (Metacam®, Boeringer Ingelheim) was administered 6 hours after antagonization and every 12 hours for 72 hours.

Thoracic dorsal hemisection: The skin over the vertebral column was incised and the 8th thoracic vertebra was carefully exposed. A laminectomy was performed, followed by a dorsal hemisection of the spinal cord with fine iridectomy scissors as previously described.[12-14] This lesion bilaterally transects the main dorsal and minor dorsolateral corticospinal tract (CST), leaving the ventral white matter intact.

Stereotactic labeling of the hindlimb motor cortex: In order to label CST fibers we pressure injected 1µl of 10% biotinylated dextran amin (BDA, in 0.1% phosphate buffer (PB), 10000 MW, Life Technologies) in the hindlimb motor cortex of each hemisphere. Stereotactical injections were performed 14 days prior to sacrifice with a finely pulled glass micropipette at the following coordinates: -1.3 mm rostro-caudal, 1 mm lateral from bregma and 0.6 mm depth. The micropipette remained in place 3 min following the injection.

Labeling of long propriospinal neuron: Long propriospinal neurons were labeled by pressure injection of 0.5µl of 2.5% dextran conjugated with Texas Red® (3,000 MW; Life Technologies D-3328) in the first lumbar segment of the spinal cord 9 day prior to sacrifice. In brief the skin was incised and the space between the last thoracic and first lumbar vertebra was exposed. The dura was carefully removed and Texas Red® was injected bilaterally into the spinal cord (coordinates from central vein ±0.6 mm, 0.8 mm depth). The capillary was left in place for 3 minutes after injection.

Tissue processing and histology

Mice were deeply anesthetized and perfused transcardially with 4% paraformaldehyde (PFA) in 0.1% PB. If not stated otherwise the tissue was post-fixed overnight in 4% PFA followed by the dissection of brain and spinal cord and cryoprotection in 30% sucrose (Sigma) for at least 48 hours.

Visualization of CST collaterals: To reveal hindlimb CST collaterals and sprouting we cut 30 sections 50µm thick of the cervical spinal cord (C3-C5) of mice, which had been stereotactically injected with BDA. Sections were incubated in ABC complex (Vector Laboratories) over night at 4°C, then washed and incubated for 30 minutes with tyramide (Biotin-XX, TSA Kit #21; Life Technologies), washed again and stained with streptavidin conjugated to FITC, Alexa488 or Alexa 594 (1:500, Life Technologies). For CST sprouting at the lesion site, longitudinal consecutive sections from the lesion site were cut (40µm) and stained similarly.

Visualisation of synaptic contacts between CST collaterals and propriospinal relay neurons: Synapsin staining was performed using a rabbit-α-synapsin1 (1:500, Merck Millipore AB1543) primary and goat-α-rabbit Abberior STAR 635P (1:200, Abberior) secondary antibody. Collaterals were stained with Streptavidin Alexa594/488. Confocal Images were taken with a 63x Objective with the pinhole closed to 0.5 Airy unit in order to gain better resolution.

Detection of serotonergic fibers and motoneurons in the lumbar spinal cord: We performed sequential staining of motoneurons and serotonergic neurons respectively by incubating sections with goat-α-ChAT primary antibody (1:100, Merck Millipore AB144P; RRID: AB_2079751) overnight. Secondary staining was done with donkey-α-goat Alexa488 (1:500, Thermo Fisher Scientific) antibody before incubation with rabbit-α-5HT (1:10000, Immunostar 20080; RRID: AB_2313880) over the second night. To better visualize serotinergic fibers, sections were then

incubated with donkey-α-rabbit HRP primary antibody (1:100, Thermo Fisher Scientific) for 1 hour, then for 5 hours with Tyramide coupled to Alexa647 (1:500, Thermo Fisher Scientific).

Visualization of the glial response at the lesion site: For immunohistochemical analysis of myelin basic protein and reactive astrocytes every second section of the lesion site was post-fixed for 15 minutes in ice cold methanol, blocked in 10% goat serum (GS) in 0,5% Triton X-100/PBS (TPBS), and incubated over night at 4°C with rabbit-α-human Myelin Basic Protein (1:200, Dako A0623; RRID: AB_2650566) and rat-α-GFAP (1:500, Thermo Fisher Scientific 13-0300; RRID: AB_2532994) primary antibodies. Secondary antibodies were goat-α-rabbit Alexa488 and goat-α-rat Alexa647 (1:500, Thermo Fisher Scientific).

Visualization of oligodendrocyte progenitors and cell proliferation: For Ki67 and NG2 staining spinal cords were immediately dissected and postfixed for one hour before they were transferred into 30% sucrose. Every third section of the lesion area was stained for oligodendrocyte progenitors and cell proliferation. For this purpose, sections were first incubated for two nights with rabbit-α-NG2 primary antibody (1:250, Merck Millipore AB5320; RRID: AB_91789), then stained overnight with goat-α-rabbit Alexa594 secondary antibody and then washed thoroughly. Afterwards sections were incubated over night with rabbit-α-Ki-67 primary antibody (1:100, Thermo Fisher Scientific MA5-14520; RRID: AB_10979488) and stained with goat-α rabbit Alexa488 secondary antibody (1:500, Thermo Fisher Scientific) for 6 hours, followed by a 5 min DAPI (1:10000, Sigma) staining to visualize nuclei.

Imaging

All confocal images were acquired with a Leica TCS SP8 confocal (Leica Microsystems) with 20x, 40x or 63x oil immersion objectives and appropriate laser lines and filter sets (for details of image acquisition see below).

Quantifications

Quantification of hCST sprouting: To analyze exiting hindlimb CST fibers the cervical spinal cord was stained as above. Confocal scans (50µm, 20x, Z-step size: 1.042µm) of 20 sections were taken with a Leica TCS SP8. Images (20) were then processed in Fiji (http://Fiji.nih.gov/ij/) to generate maximum intensity projections. Length tracing and counting of collaterals, exiting collaterals, branchpoints and boutons were also done in Fiji by an investigator blinded to treatment and injury status of the animal. For length quantification NeuronJ[15] was used. To account for different CST labeling in different animals, all labeled fibers in the main white matter corticospinal tract were counted and the length as well as the number of collaterals was normalized to this value. A bouton was deemed as such and counted if a thick varicosity was clearly visible along the CST collateral and boutons were normalized to total length and plotted per µm (as previously established).[12-14, 16]

Quantification of contacts on long propriospinal neurons: To count contacts on LPSN we used a fluorescent microscope (Olympus IX71) with a ×40/0.65 air objective. CST collaterals were visualized by tyramide amplification and FITC or Alexa488 labeling and LPSN were labeled with Texas Red®. We counted the total number of contacts by CST collaterals on LPSN as defined by close apposition between CST collaterals and LPSN at 40X magnification. We normalized the number of contacts to the number of labeled CST fibers in the white matter tract and the number of labeled LPSN. All quantitative analyses were performed by an investigator blinded to treatment and injury status. We also determined the proportion of labeled propriospinal neurons that were contacted by CST collaterals and normalized this value to the number of labeled CST fibers in the white matter tract and expressed it as a relative value compared to the proportion of contacted LPSN in untrained animals.

Collateral sprouting at the lesion site: In order to quantify collateral sprouting at the lesion site, all lesion sites were imaged with a Leica DM4 (Leica microsystems) fluorescence microscope and the Stereo Investigator Software (MBF). All stacks were then projected and stitched in Fiji and a 200µm grid was placed on the stitched image, the 0 line representing the location of the CST stump. The number of sprouts on longitudinal sections (average of 7 sections per animals) crossing each line was counted and normalized to the number of CST fibers labeled in the white matter and the number of sections counted.

Quantification of serotonergic fibers and contacts on motor neurons: We assessed serotonergic rewiring onto motor neurons in coronal lumbar spinal cord sections (3 sections per animals). Stacks (40µm, 20x, Z-step size: 1.042µm) were used to count the number of contacts between 5-HT fibers and motor neurons in 3D reconstructions assembled using Imaris software (Bitplane). Serotonergic innervation in the lumbar grey matter was quantified by using the integrated density function in Fiji and normalizing it to the background intensity (n=6 sections each).

Quantification of Myelin, GFAP, NG2 and Ki-67 immunoreactivity at the lesion site: To assess myelin preservation and astrocyte scaring, lesioned spinal cords were confocal imaged with a 20x objective (15 images in Z per 40µm stack). For GFAP, the region of GFAP immunoreactivity-increase was outlined. Differential integrated densities between the region showing an increased immunoreactivity and the surrounding region corrected to a similar area were calculated in Fiji. For MBP the region of MBP immunoreactivity-decrease was outlined. Differential integrated densities between the region showing a decreased immunoreactivity and the surrounding region was calculated in Fiji. Data were presented as normalized values to non-trained animals (average of 5 sections per animals).

For NG2 and Ki67 quantification, three 40x stacks of each region of interest (lesion, lesion border, outside lesion) were acquired with a Leica TCS SP8 confocal (step size 0.5µm) by an

investigator blinded to timepoints and training paradigms. For each animal three sections were imaged. DAPI- and NG2-positive as well as the DAPI-, NG2- and Ki67-positive cells were counted in the central 20µm part of the stacks (top and bottom 10µm were excluded) and cell density (per 10000µm^2) and percentages per area were calculated. A cell was deemed NG2$^+$ if the DAPI$^+$ nucleus was encased with at least 2/3 of NG2 labeling. A Ki67 positive cell was counted if the Ki67 staining entirely overlapped the DAPI staining of the nucleus. A double positive cell was counted if both criteria were fulfilled.

Lesion Volume: For determination of lesion volume, every second consecutive section (average of 10 sections per animal) was stained with a fluorescent Nissl dye (NT435; Life Technologies N-21479, dilution 1:500). Sections were imaged using an Olympus IX71 microscopes, then processed in Fiji and the lesion area (cavities and surrounding damaged tissue) was outlined and measured. For volume calculation the area was multiplied by the thickness (80µm) between two consecutive sections and the results were summed up.

Image processing

Maximum intensity projections and stitching were done in LasX (Leica microsystems) or in Fiji. For final illustration images were processed in Adobe Photoshop using gamma adjustment to enhance visibility if necessary. 3D-rendering of contacts on ChAT-positive neurons was done using Imaris software (Bitplane).

Behavioral analysis

Mice were habituated on all behavioral tasks three times prior to first testing. One out of 14 wheel-trained animals could not perform the tests at day 2 post-injury due to its lesion and was excluded from the analysis for this timepoint.

Ladder rung: To assess hindlimb motor function and paw placement all mice were tested on the ladder rung test (also called grid walk test) as described previously.[17] Animals crossed a 1 m long horizontal metal-rung runway three times with varying spacing (irregular walk) between the rungs. Sessions were videotaped and footfalls were counted by an investigator blinded to the timepoints and training status of the mice. A footfall was counted each time the hind paw of the animal either completely missed the rung or slipped from it. Recordings were done 2 days prior and 2, 7, 21 and 56 days after dorsal thoracic hemisection of the operated groups. Animals with incomplete lesions or animals that performed poorly prior to the surgery were excluded from the study.

Rotarod: To evaluate locomotor activity, we used a Rotarod test (Ugo Basile, Italy). In brief mice were placed on the device for a maximum of 120 seconds at either a constant speed of 20 rounds per minute (constant Rotarod) or at accelerating speed from 2 to 40 rounds per minute (accelerating Rotarod). The time and velocity was recorded at the point where the animal was unable to hold on and dropped from the rod. Like the ladder rung, the Rotarod test was performed at -2, 2, 7, 21 and 56 days.

Catwalk gait analysis: To perform gait analysis, the Catwalk XT™ ([18]; Noldus) was used. The system was calibrated each day prior to acquisition and minimal requirements for a valid run were duration between 0.5 and 4 seconds with a maximum speed variance of 60%. This ensures that the animal crossed the walkway without stopping and at a normal speed. Three valid runs were recorded for each animal and all parameters were calculated by the software. The regularity index (RI) is calculated by multiplying the normal step sequence patterns (NSSP) with 4 for the amount of paw placements and then dividing it by the number of paw placements (PP).

Statistical evaluation

All results are given in mean±SEM. For statistical analysis we used GraphPad Prism 5.01 for Windows (GraphPad Software, La Jolla, USA). We used one- and two-ways ANOVA with Tukey and Bonferroni pot hoc test to analyze behavioral data. To compare two columns together, we first tested for normality and used appropriate tests e.g. unpaired t-tests for data that distributed normally and Mann-Whitney tests for data that did not distribute normally. Significance levels are indicated as follows: *$p < 0.05$; **$p < 0.01$;***$p < 0.001$.

RESULTS

Mice rapidly recover the ability to exercise and improve their behavioural function following iSCI.

To evaluate the role of voluntary exercise following incomplete spinal cord injury we used two types of wheels in our experiments: a regular wheel with equally spaced bars that should in particular train the intraspinal circuits that form the central patterns generator (CPG) known for its importance for rhythmic locomotion and a complex wheel with irregularly spaced bars that should in particular train supraspinal pathways such as the corticospinal tract that are required for continuous step-length adaptation, bilateral coordination and skilled paw placement.[11] We first pre-trained mice for 10 days on a regular wheel and then following spinal cord injury, mice were again offered the regular wheel for 2 days before they were switched to the complex wheel (**Fig. 1A**). Despite a thoracic hemisection that interrupts major descending motor and ascending sensory tracts, mice started running again on the second day following the lesion although they ran less and much slower than control mice at this time (**Fig. 1B**). However as early as 4 days following the hemisection lesion, mice regained the capacity to run on the running wheels at the same speed and for the same distance and comparable time as unlesioned mice and did so for the remaining period of the study (**Fig. 1B**). We then examined how such voluntary exercise affected the recovery of motor function after the injury. For this purpose, mice were habituated before injury to perform on the ladder rung test, which assesses skilled walking and fine paw placement, and on the rotarod (accelerated and constant speed), which assesses overall locomotion and coordination. We tested motor performance following dorsal thoracic hemisection at 2 days as well as 1, 3 and 8 weeks following lesion (**Fig. 1C**). While motor performance at early time points after the lesion (2 days and 1 week) was not affected by exercise, mice which exercised on the running wheels performed significantly better than untrained mice in all tasks from 3 weeks

after lesion onward. Mice that exercised both started to recover quicker and had recovered more completely at the end of the study period (**Fig. 1D-F**). No effects of voluntary exercise were detected on the performance of unlesioned animals in these test paradigms (**Fig. 1D-F**).

Voluntary exercise promotes transient neuro-glial changes at the lesion site.

We next explored which structural changes to the nervous system underlie the observed improvement of functional recovery. First, we measured the lesion volumes in our mice and found no differences between exercise and control group. Furthermore, in our experiment individual lesion volumes did not correlate with the performance of the respective animals in the behavioral tasks (**Fig. 2**). We next examined the effect of voluntary exercise on reactive astrogliosis and myelin integrity at the lesion site. Using GFAP immunoreactivity to determine the extent of glial reactivity, we observed that voluntary exercise reduces astrogliosis at an early timepoint (at 2 weeks) but not at a late timepoint (at 10 weeks) after spinal cord injury (**Fig. 3A, B**). Similarly, we found that the decrease in MBP immunoreactivity that normally follows a transection to the spinal cord is significantly attenuated by voluntary exercise at early but not at later timepoints following lesion (**Fig. 3A, C**). To determine whether these early myelin changes were due to myelin protection or generation of new myelinating cells, e.g. from oligodendrocyte progenitors, we quantified the total number of $NG2^+$ oligodendrocyte progenitors as well as the number of these cells that are proliferating at different timepoints after lesion. We did not detect any significant increase in either the total number of NG2 positive cells or the number of proliferating NG2 cells suggesting that the initial difference in MBP intensity following wheel running is mostly due to myelin protection (**Fig. 4**). To assess whether the local neuronal response shows similar kinetics, we next analyzed the regeneration of the corticospinal tract, a major supraspinal motor tract that is transected by the dorsal hemisection, at different distances

from the site of the lesion at an early (2 weeks) and late timepoint after injury (10 weeks; **Fig. 3A, D**). For this purpose, we anterogradely traced the hindlimb portion of the corticospinal tract, identified the stump of the CST tract after the lesion and drew lines every 200μm from it. We then evaluated the number of sprouts originating from the corticospinal tract that crossed those lines. In line with our analysis of the glial response our results indicate that voluntary exercise increased CST regeneration early on following the injury. However, this effect is lost at later timepoints of the recovery process when CST sprouting in control animals reached the same levels as the sprouting observed in exercising mice (**Fig. 3D**).

Voluntary exercise leads to improved serotonergic remodelling and sustained strengthening of corticospinal rewiring following iSCI.

We next examined the response of monoaminergic fiber tracts containing serotonin (5-hydroxytryptamine, 5-HT). We revealed serotonergic fibers in the lumbar part (L1 to L2) of the spinal cord below the lesion site and found that while wheel running did not change the density of serotonergic fibers in the spinal cord (17.5±1.1 10^6 vs 19.5±1.3 10^6 AU at 2wks and 17,1±1.9 10^6 vs 17.4±2.1 10^6 AU at 10wks control vs exercise), it did significantly increase the number of serotonergic contacts onto ChAT positive motoneurons (**Fig. 5A, B**) at 2 weeks after injury. By 10 weeks after lesion the number of contacts were equally increased in non-exercising mice (**Fig. 5A, B**). As the serotonergic system is known to regulate and affect the central pattern generator important for rhythmic stepping (Grillner, 2006), we use the catwalk to evaluate several gait parameters, among them rhythmic stepping. In line with the previous finding of the serotonergic patterning, we found that rhythmic stepping was also re-established in both wheel running and control mice at this late timepoint (**Fig. 5B**).

In contrast to rhythmic stepping, skilled aspects of locomotion that require corticospinal input recover slower and often incompletely. To assess whether the sustained improvement of skilled locomotion induced by voluntary exercise results from enhanced rewiring of the corticospinal tract, we analyzed the formation of corticospinal detour circuits that have been shown to mediate functional recovery after spinal cord injury (Bareyre *et al.*, 2004; Courtine *et al.*, 2008). These detour circuits are created via the emergence of new hindlimb CST collaterals into the cervical grey matter where they contact long propriospinal neurons that provide a detour around the thoracic lesion site and contact lumbar motoneurons. We therefore performed a bilateral dorsal hemisection of the spinal cord at T8 in wheel running mice and age-matched non-running mice, traced the hindlimb portion of the corticospinal tract and then analyzed the number and structure of emerging CST collaterals as well as their contacts onto long propriospinal neurons at 2 and 10 weeks following the lesion (**Fig. 5A**). We found that exercise led to a marked increase in both the total number and length of cervical CST collaterals (**Fig. 5C**) that resulted in a more than 3-fold increase in the number of CST contacts onto long propriospinal neurons (**Fig. 5D**). Notably and in contrast to the transient changes observed at the lesion sites, these exercise-induced changes were sustained throughout the study period. Exercise-induced changes to CNS circuitry appear to be specific for injured mice as wheel running did not alter the number of grey matter CST collaterals, their length, the number of contacts onto propriospinal relay neurons or the number of relay neurons contacted by CST collaterals in unlesioned animals (**Fig. 6**).

DISCUSSION

To determine the role of voluntary exercise following incomplete spinal cord injury we made use of the fact that running is an elective voluntary behavior in mice[19] and offered some of them free access to a running wheel in the cage. Notably, mice which underwent an incomplete spinal cord injury (iSCI) retained the motivation to run quickly following the injury and reached running abilities similar to unlesioned mice few days following injury. In addition, mice that exercised both started to recover quicker and had recovered more completely at the end of the study period. It is interesting to note that improved recovery was seen both in tests of overground locomotion such as the accelerated and constant speed rotarod that primarily rely on local spinal circuits[20] as well as in the irregular ladder rung test that requires input from supraspinal tract systems.[21] Overall the sustained effects on different aspects of locomotor recovery we observed here support the notion that voluntary exercise that enforces physiological movement patterns can be initiated timely following injury and lead to lasting improvements of functional recovery.

We wanted to understand the mechanisms at play that can explain this early and sustained recovery triggered by voluntary exercise. We thus first investigated local changes at the lesion site as previous reports have suggested that increased physical activity can affect glial reactivity and increase axon sprouting at the site of injury.[22-24] As the local response of glial cells and in particular of astrocytes and oligodendrocytes is a critical determinant of recovery from spinal cord injury[25], we examined the effect of voluntary exercise on reactive astrogliosis and myelin integrity at the lesion site. In our study, we observe changes to the initial injury response of both astrocytes and oligodendrocytes that are however not maintained over the entire recovery period. These transient changes are paralleled by the local neuronal response as voluntary exercise increased CST regenerative sprouting at the lesion site only at early timepoints following the injury. Thus, exercise-induced local changes to either the neuronal or glial response at the lesion

site can contribute to the earlier onset of functional recovery induced by wheel running. However, they are unlikely to explain the sustained improvements that remained significantly different from the non-exercising control group throughout the entire study period. We therefore explored whether voluntary exercise induces more permanent changes in the central nervous system remote from the lesion site. This line of investigation is supported by recent studies highlighting the importance of supraspinal neuronal rewiring processes that often occur at a distance from the original lesion site for both endogenous and therapeutically-supported recovery of neuronal function after spinal cord injury.[12, 26-28] We focused our analysis on two axonal tract systems, the serotonergic and corticospinal pathways that play a crucial role for rhythmic stepping and skilled movements respectively. First we examined the response of the serotonergic tract system that provides a tonic input from the brainstem, influence neuronal networks of the central pattern generator responsible for rhythmic stepping and contribute to the reorganization of lumbar motor networks following SCI.[22, 29, 30] Wheel running significantly increased the rewiring of serotonergic fibers early following exercise training but again non-exercising mice reached similar levels at later timepoints of the recovery process. As rhythmic stepping (analyzed using the catwalk) was also re-established in both groups at this timepoint, this indicates that rhythmic stepping can be regained without additional training at least in our incomplete spinal cord injury paradigm. In contrast, our behavioral analysis indicates that skilled movements such as the paw placement measured by the gridwalk task only recovered in exercising mice. As skilled movements critically depend on supraspinal input provided by the CST, we next assessed the effects of voluntary exercise on CST remodeling. We and other have previously shown that the CST responds to a lesion by the spontaneous formation of intraspinal detour circuits that re-establish corticospinal input to lumbar motor circuits after injury.[12-14, 26, 27] These detour circuits are shaped by the formation of new CST collaterals that emerge from transected hindlimb CST fibers and enter the gray matter of the cervical spinal cord where they

contact long propriospinal neurons that in turn provide a detour around the thoracic lesion site and contact lumbar motoneurons. We found that exercise led to a marked - more than 3-fold - increase in the formation of these corticospinal detour circuits. Notably and in contrast to the changes observed at the lesion sites, these exercise-induced detour circuits were detected at both 2 and 10 weeks and thus maintained throughout the critical time period during which novel circuits are formed and refined.[12, 14] Interestingly, exercise-induced changes to CNS circuitry were only found following injury indicating that stable circuits in uninjured animals are not modified by exercise training.

Taken together our study provides evidence that voluntary exercise initiated within days after incomplete injury leads to the sustained improvement of functional recovery that are encoded in hard-wired changes to CNS circuitry and can thus be maintained long-term. Our study thus argues for the timely introduction of rehabilitative measures in patients suffering incomplete CNS injuries of traumatic, ischemic or other origin.

Acknowledgements: The authors would like to thank Martin Adrian, Bernadette Fiedler and Lena Schödel for excellent technical assistance as well as Dana Matzek and Bianca Stahr for animal husbandry. We would like to thank Martin Kerschensteiner for critically reading the manuscript. Work in F.M.B.'s lab is supported by grants from the Deutsche Forschungsgemeinschaft (DFG, SFB 870), by the Munich Center for Neurosciences (MCN) and the Wings for Life foundation. F.M.B. is also supported by the Munich Center for Systems Neurology (DFG, SyNergy; EXC 1010). The authors declare no competing financial interests.

Author contributions: KL and FB designed the experiments. KL performed all surgical procedures. KL, AS, TH, FB, collected and analyzed data. AJ contributed to surgical procedures and injections. MK, DM contributed to the analysis of the wheel running parameters. KL and FB wrote the manuscript. All authors approved the final version of the paper.

Author Disclosure Statement: No competing financial interests exist.

REFERENCES

1. Wessels, M., Lucas, C., Eriks, I. and de Groot, S. (2010). Body weight-supported gait training for restoration of walking in people with an incomplete spinal cord injury: a systematic review. Journal of rehabilitation medicine 42, 513-519.

2. Cote, M.P., Murray, M. and Lemay, M.A. (2017). Rehabilitation Strategies after Spinal Cord Injury: Inquiry into the Mechanisms of Success and Failure. Journal of neurotrauma 34, 1841-1857.

3. McDonald, J.W. and Sadowsky, C. (2002). Spinal-cord injury. Lancet (London, England) 359, 417-425.

4. Hicks, A.L., Martin, K.A., Ditor, D.S., Latimer, A.E., Craven, C., Bugaresti, J. and McCartney, N. (2003). Long-term exercise training in persons with spinal cord injury: effects on strength, arm ergometry performance and psychological well-being. Spinal cord 41, 34-43.

5. Harkema, S.J., Hillyer, J., Schmidt-Read, M., Ardolino, E., Sisto, S.A. and Behrman, A.L. (2012). Locomotor training: as a treatment of spinal cord injury and in the progression of neurologic rehabilitation. Archives of physical medicine and rehabilitation 93, 1588-1597.

6. Edgerton, V.R. and Roy, R.R. (2012). A new age for rehabilitation. European journal of physical and rehabilitation medicine 48, 99-109.

7. Battistuzzo, C.R., Callister, R.J., Callister, R. and Galea, M.P. (2012). A systematic review of exercise training to promote locomotor recovery in animal models of spinal cord injury. Journal of neurotrauma 29, 1600-1613.

8. Fouad, K. and Tetzlaff, W. (2012). Rehabilitative training and plasticity following spinal cord injury. Experimental neurology 235, 91-99.

9. Smith, R.R., Brown, E.H., Shum-Siu, A., Whelan, A., Burke, D.A., Benton, R.L. and Magnuson, D.S. (2009). Swim training initiated acutely after spinal cord injury is ineffective and induces extravasation in and around the epicenter. Journal of neurotrauma 26, 1017-1027.

10. Krajacic, A., Ghosh, M., Puentes, R., Pearse, D.D. and Fouad, K. (2009). Advantages of delaying the onset of rehabilitative reaching training in rats with incomplete spinal cord injury. The European journal of neuroscience 29, 641-651.

11. Liebetanz, D. and Merkler, D. (2006). Effects of commissural de- and remyelination on motor skill behaviour in the cuprizone mouse model of multiple sclerosis. Experimental neurology 202, 217-224.

12. Bareyre, F.M., Kerschensteiner, M., Raineteau, O., Mettenleiter, T.C., Weinmann, O. and Schwab, M.E. (2004). The injured spinal cord spontaneously forms a new intraspinal circuit in adult rats. Nat Neurosci 7, 269-277.

13. Lang, C., Bradley, P.M., Jacobi, A., Kerschensteiner, M. and Bareyre, F.M. (2013). STAT3 promotes corticospinal remodelling and functional recovery after spinal cord injury. EMBO reports 14, 931-937.

14. Jacobi, A., Loy, K., Schmalz, A.M., Hellsten, M., Umemori, H., Kerschensteiner, M. and Bareyre, F.M. (2015). FGF22 signaling regulates synapse formation during post-injury remodeling of the spinal cord. The EMBO journal 34, 1231-1243.

15. Meijering, E., Jacob, M., Sarria, J.C., Steiner, P., Hirling, H. and Unser, M. (2004). Design and validation of a tool for neurite tracing and analysis in fluorescence microscopy images. Cytometry. Part A : the journal of the International Society for Analytical Cytology 58, 167-176.

16. Lang, C., Guo, X., Kerschensteiner, M. and Bareyre, F.M. (2012). Single collateral reconstructions reveal distinct phases of corticospinal remodeling after spinal cord injury. PloS one 7, e30461.

17. Metz, G.A. and Whishaw, I.Q. (2002). Cortical and subcortical lesions impair skilled walking in the ladder rung walking test: a new task to evaluate fore- and hindlimb stepping, placing, and co-ordination. Journal of neuroscience methods 115, 169-179.

18. Hamers, F.P., Koopmans, G.C. and Joosten, E.A. (2006). CatWalk-assisted gait analysis in the assessment of spinal cord injury. Journal of neurotrauma 23, 537-548.

19. Meijer, J.H. and Robbers, Y. (2014). Wheel running in the wild. Proceedings. Biological sciences 281.

20. Marder, E. and Bucher, D. (2001). Central pattern generators and the control of rhythmic movements. Current biology : CB 11, R986-996.

21. Escalona, M., Delivet-Mongrain, H., Kundu, A., Gossard, J.P. and Rossignol, S. (2017). Ladder Treadmill: A Method to Assess Locomotion in Cats with an Intact or Lesioned Spinal Cord. The Journal of neuroscience : the official journal of the Society for Neuroscience 37, 5429-5446.

22. Engesser-Cesar, C., Ichiyama, R.M., Nefas, A.L., Hill, M.A., Edgerton, V.R., Cotman, C.W. and Anderson, A.J. (2007). Wheel running following spinal cord injury improves locomotor recovery and stimulates serotonergic fiber growth. The European journal of neuroscience 25, 1931-1939.

23. Goldshmit, Y., Lythgo, N., Galea, M.P. and Turnley, A.M. (2008). Treadmill training after spinal cord hemisection in mice promotes axonal sprouting and synapse formation and improves motor recovery. Journal of neurotrauma 25, 449-465.

24. Almeida, C., DeMaman, A., Kusuda, R., Cadetti, F., Ravanelli, M.I., Queiroz, A.L., Sousa, T.A., Zanon, S., Silveira, L.R. and Lucas, G. (2015). Exercise therapy normalizes BDNF upregulation and glial hyperactivity in a mouse model of neuropathic pain. Pain 156, 504-513.

25. Silver, J., Schwab, M.E. and Popovich, P.G. (2014). Central nervous system regenerative failure: role of oligodendrocytes, astrocytes, and microglia. Cold Spring Harbor perspectives in biology 7, a020602.

26. Courtine, G., Song, B., Roy, R.R., Zhong, H., Herrmann, J.E., Ao, Y., Qi, J., Edgerton, V.R. and Sofroniew, M.V. (2008). Recovery of supraspinal control of stepping via indirect propriospinal relay connections after spinal cord injury. Nature medicine 14, 69-74.

27. van den Brand, R., Heutschi, J., Barraud, Q., DiGiovanna, J., Bartholdi, K., Huerlimann, M., Friedli, L., Vollenweider, I., Moraud, E.M., Duis, S., Dominici, N., Micera, S., Musienko, P. and Courtine, G. (2012). Restoring voluntary control of locomotion after paralyzing spinal cord injury. Science 336, 1182-1185.

28. Zorner, B., Bachmann, L.C., Filli, L., Kapitza, S., Gullo, M., Bolliger, M., Starkey, M.L., Rothlisberger, M., Gonzenbach, R.R. and Schwab, M.E. (2014). Chasing central nervous system plasticity: the brainstem's contribution to locomotor recovery in rats with spinal cord injury. Brain 137, 1716-1732.

29. Grillner, S. (2006). Biological pattern generation: the cellular and computational logic of networks in motion. Neuron 52, 751-766.

30. Ghosh, M. and Pearse, D.D. (2014). The role of the serotonergic system in locomotor recovery after spinal cord injury. Frontiers in neural circuits 8, 151.

Figure 1: Mice rapidly recover the ability to exercise and improve their behavioural function following iSCI. (**A**) Timeline of the experiment to evaluate the performance of injured mice on a running wheel. (**B**) Measurement of wheel running parameters: number of runs per day (top panel), covered distance in the wheel (middle panel) and average velocity (bottom panel); (n=8- 10). (**C**) Timeline of the experiments evaluating behavioral recovery following SCI with and without voluntary exercise. (**D**) Image of a mouse performing the rotarod test (left) and quantification of the "time at fall" at a constant speed of 20 rounds per minute (middle). Quantification of the "time at fall" averaged at 7d, 21d and 56d post-injury (right); n=8-15 mice per group; data analysed with a two-way ANOVA; *: indicate improvement compared to the 2d timepoint. (**E**) Schematic representation of the time/velocity curve of the accelerating rotarod (left) and quantification of the "time at fall" on the accelerating rotarod. Quantification of the average "time at fall" averaged at 7d, 21d and 56d post-injury (right). n=8-15 mice per group; data analysed with a two-way ANOVA; *: indicate significant improvement compared to the 2d timepoint. (**F**) Scheme of the irregular rung spacing of the irregular ladder rung test (left) and quantification of the number of footfalls in the irregular ladder rung test over 56 days post-injury (middle panel). Quantification of the average number of mistakes made by the injured mice averaged at 21 and 56d post-injury (right panel). n=8-15 mice per group; data analysed with a two-way ANOVA and Bonferroni post-hoc test; *: indicate significant improvement compared to the 2d timepoint.

Figure 2: Low correlation between behavioural performance and lesion volume at 10 weeks following iSCI. (**A**) Representative fluorescence image of a spinal lesion site 10 weeks after injury stained with Neurotrace 435 and quantification of lesion volume in exercise and control mice at 10 weeks after spinal cord injury (n=11-12 mice per group) Dashed lines indicate the lesion area. (**B**) Correlation of the motor scores obtained 56d post-injury with lesion volume. Motor performance does not (or only weakly) correlate with the irregular Ladder Rung (top), or the constant (middle) or the accelerating (bottom) Rotarod (n=10-11; Pearson's R^2). Scale bar represents 200μm in (**A**).

Figure 3: Voluntary exercise promotes transient neuro-glial changes at the lesion site. (**A**) Schematic timeline of the experiment aiming at evaluating corticospinal tract (CST) sprouting. (**B**) Representative confocal images of glial fibrillary acidic protein (GFAP) at lesion sites of control and exercise animals 2 weeks post midthoracic dorsal hemisection and quantification of the increased GFAP intensity around the lesion site (normalized to the untrained group) at 2 and 10 weeks after midthoracic dorsal hemisection (n= 7 at 2wks, n=6-7 at 10 wks; unpaired t-test; p=0,0404). (**C**) Representative confocal images of myelin basic protein (MBP) stainings at the lesion sites of control and exercise animals 2 weeks post midthoracic dorsal hemisection and quantification of the decreased MBP intensity at the lesion site (normalized to the untrained group) at 2 and 10 weeks after midthoracic dorsal hemisection. (n= 7 at 2 wks and n=6-7 at 10wks; unpaired t-test; p=0,0264). (**D**) Confocal images of corticospinal tract 2 weeks after spinal cord lesion (CST: green, NT435: blue). Dotted line indicates the level of retraction bulbs and the 0 line. Arrowheads indicate sprouting collaterals in the grey matter below the lesion. Higher magnification insets (2X) are outlined by a white dotted box. Quantification of the normalized number of sprouts at different distances from the 0 line defined from the level of retraction bulbs (left panel, p<0,001 two-way ANOVA followed by Bonferroni test) and the cumulative normalized number of sprouts at 2 weeks (top panel, p=0,043; unpaired t-test; p=0,0468) after lesion (n=5-6) and 10weeks (bottom panel) after lesion (n=6-8). Scale bar in (**B, C, D**) represents 200μm.

Figure 4: Wheel running does not trigger proliferation of oligodendrocyte precursors (**A**) Confocal images of lesion site (coronal sections) stained for NG2, Ki67 and DAPI in untrained animals (top) and wheel trained animals (bottom). (**B**) Higher magnification image of NG2 and Ki67 double positive cells boxed in (**B**). (**C**) Quantification of the number of NG2 glia in the lesion area, lesion border and outside the lesion at 2 and 10 wks post-injury and quantification of the percentage of Ki67+ NG2 glia 2 and 10wks post-injury (n= 7 at 2wks and n=3 at 10wks). Scale bar equals 200µm in (**A**), and scale bar equals 20µm in (**B**).

Figure 5: Voluntary exercise leads to improved serotonergic remodelling and sustained strengthening of corticospinal rewiring following iSCI. (A) Timeline of the experiments aiming at evaluating the rewiring of axonal tracts at 2 weeks (left) and 10 weeks (right) following iSCI. (**B**) Confocal images of lumbar spinal cord sections stained for serotonin and choline acetyl transferase (Left; ChAT+ motoneurons: green, Serotonergic fibers: red). 3D-reconstructions (middle) and single confocal image planes (right) used to quantify contacts between serotonergic fibers and ChAT+ motoneurons. Quantification of the total number of contacts (top) and the number of contacts per motoneurons (bottom) at 2 and 10 weeks after injury (n=7 mice per group, unpaired t-test, $p_{contacts}$=0,0236; $p_{contacts\ per\ neuron}$=0,0208 at 2wks). Quantification of the regularity index determined by gait analysis on the Catwalk system (n=6-10 mice per group, One-way ANOVA and Tukey post-hoc test). (**C**) Confocal images of cervical spinal cord cross sections showing hindlimb CST collateral sprouting in control (left) and exercise (right) animals at 2 (top) and 10 weeks (bottom) after spinal cord injury. Quantification of the number and length of collaterals into the cervical spinal cord of lesioned mice 2 weeks (top) and 10 weeks (bottom) after spinal cord injury (top). (n=7-9 mice per group, unpaired t-test, p_{length}=0,0154, $p_{collateral=}$0,0185 for 2wks; n=13-14, Mann Whitney t-test, p_{length}=0,024, $p_{collateral=}$0,0143 for 10wks; Mean ±SEM). (**D**) Confocal image of a synapsin-positive contact (arrowhead) between a CST collateral and a long propriospinal neuron (higher magnification shown in inserts below). Quantification of number of contacts on long propriospinal neurons 2 and 10 weeks after spinal cord injury and normalized number of LPSN neurons contacted by CST collaterals (n=6-7, Mann-Whitney test $p_{contacts2wks}$=0,0152; $p_{contacts10wks}$=0,0256; $p_{contacted2wks}$=0,0152; $p_{contacted10wks}$=0,0324; Mean ±SEM). Scale bar represents 100µm in (**B, left image**) and (**C**), 10 µm in (**D**). Scale bar represents 20µm in (**B, right images**).

Figure 6: Wheel training does not affect mature corticospinal circuits in unlesioned mice. **(A**) Quantification of the number of CST collaterals, collateral length, contacts on LPSN and number of LPSN contacted in uninjured mice 2 weeks after injury (n=4-6 mice per group). (**B**) Quantification of the number of CST collaterals, collateral length, contacts on LPSN and number of LPSN contacted in uninjured mice 10 weeks after injury (n=5-9).

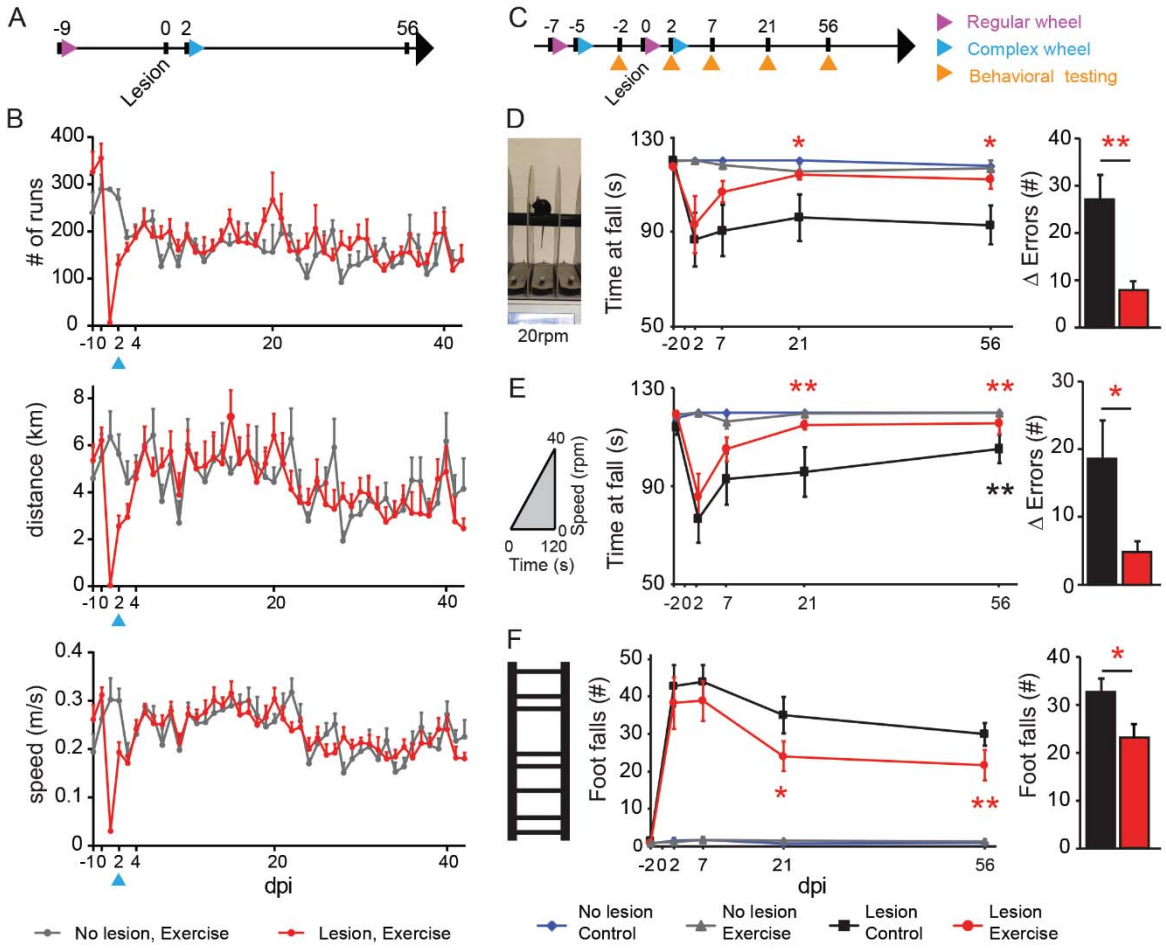

Loy et al., Figure 1

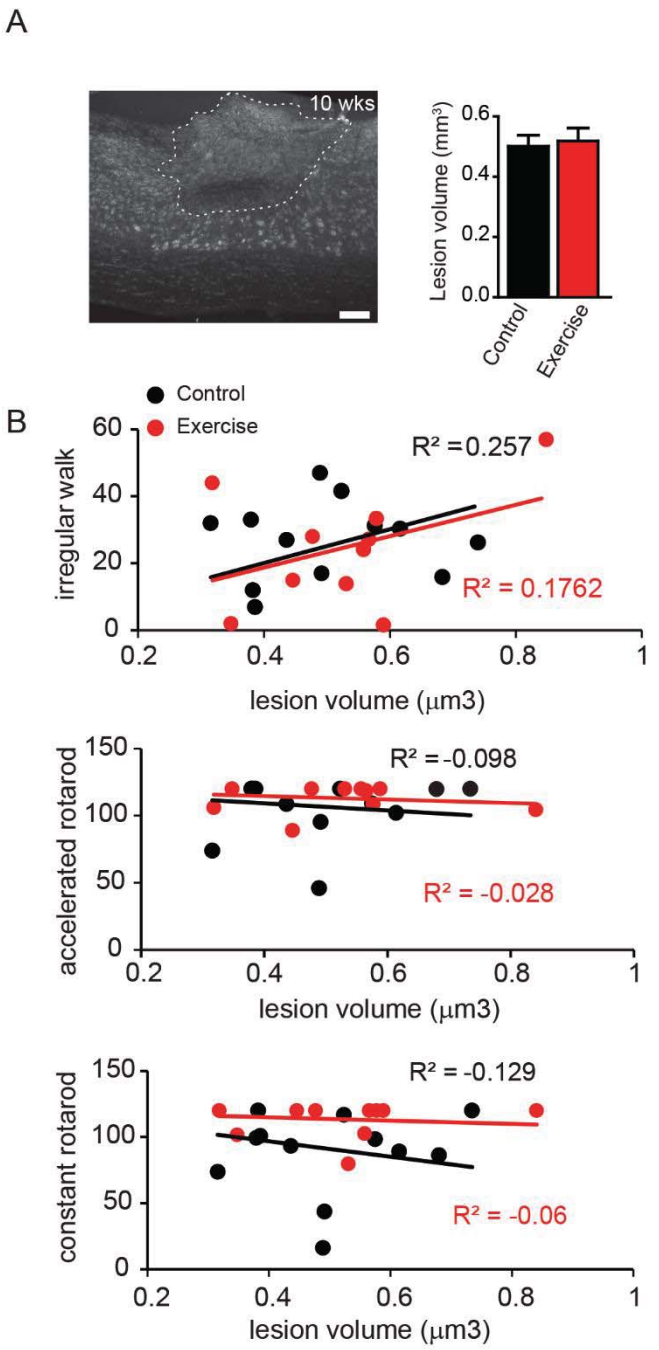

Loy et al., Figure 2

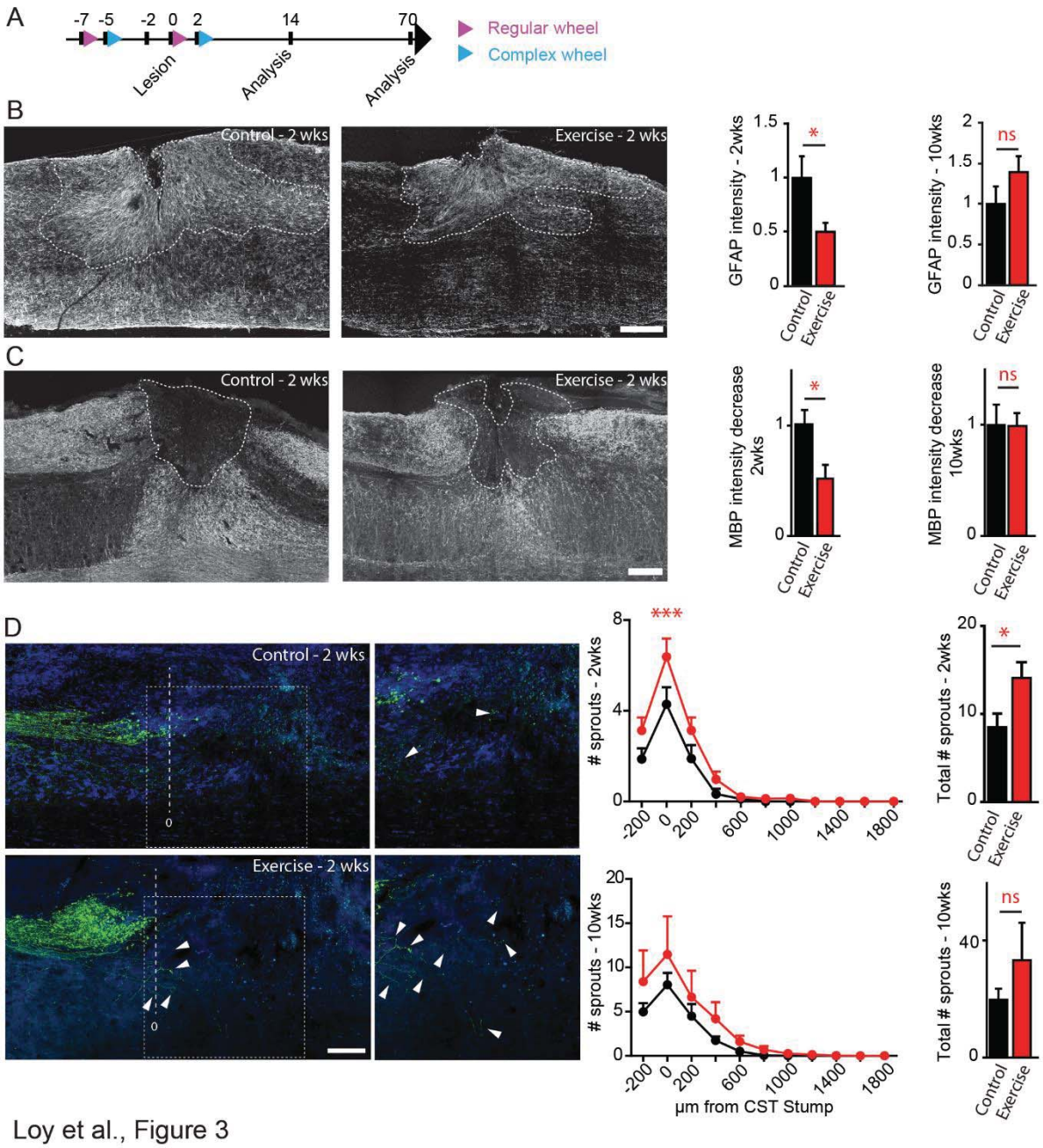

Loy et al., Figure 3

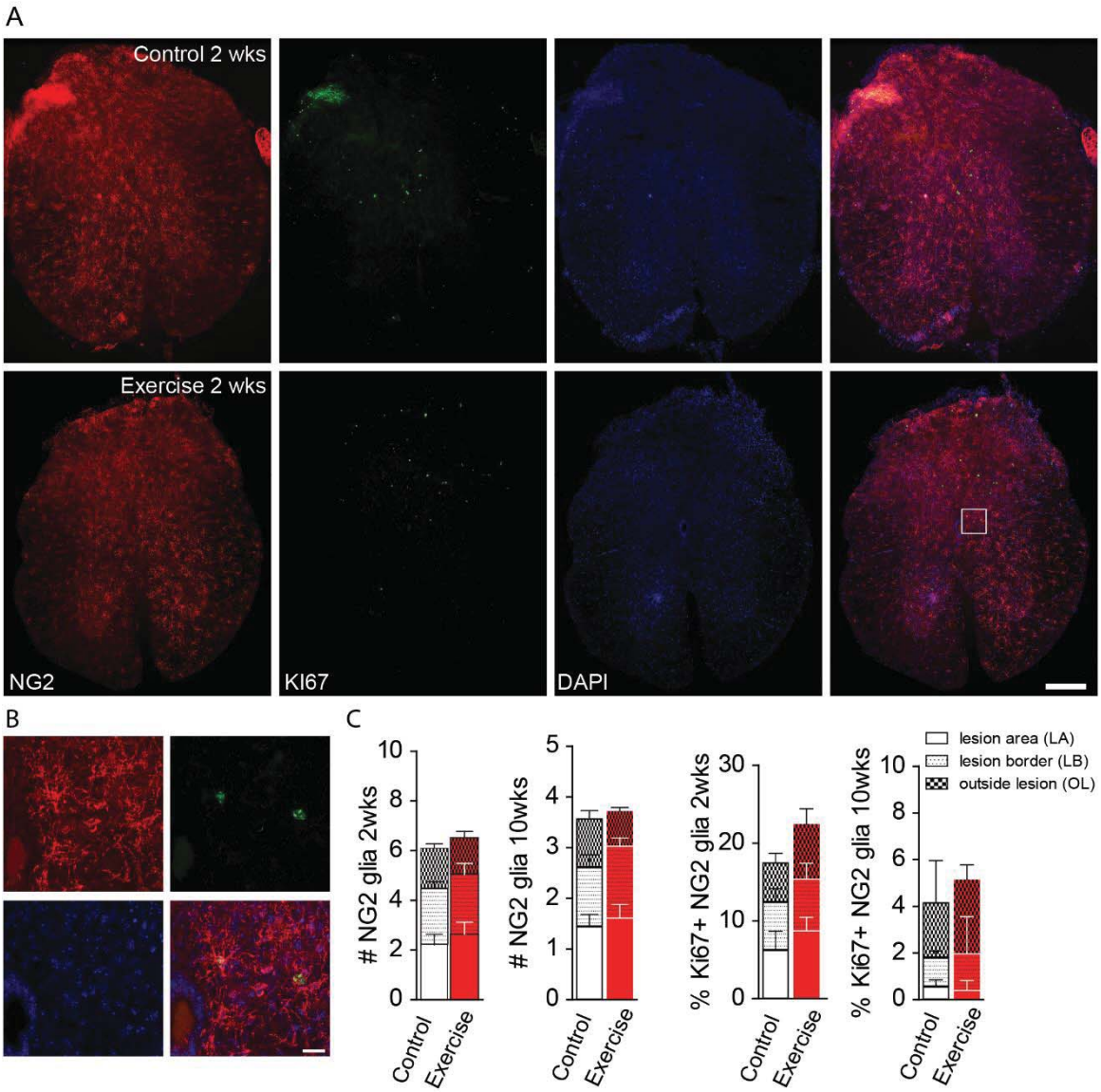

Loy et al., Figure 4

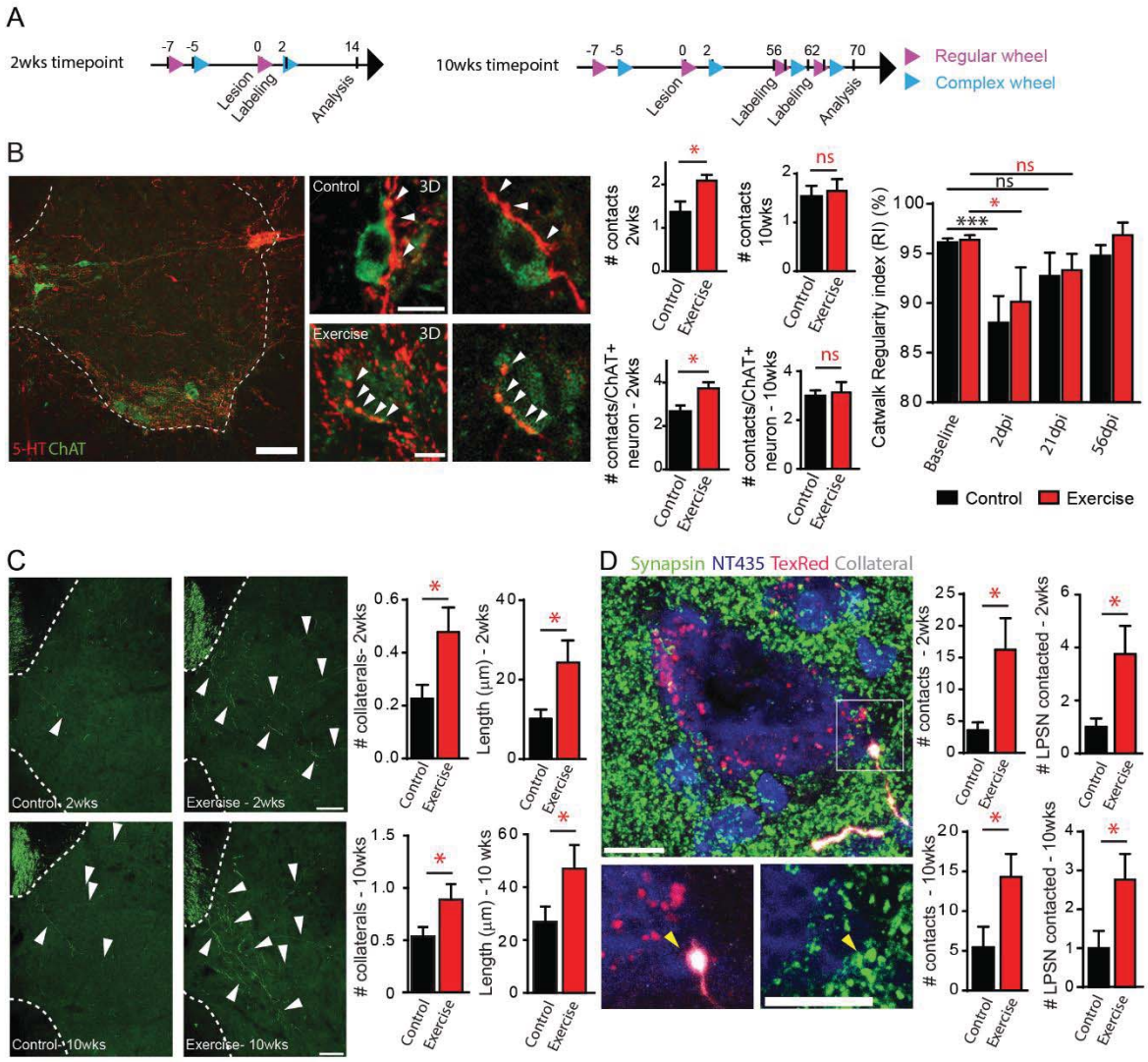

Loy et al ., Figure 5

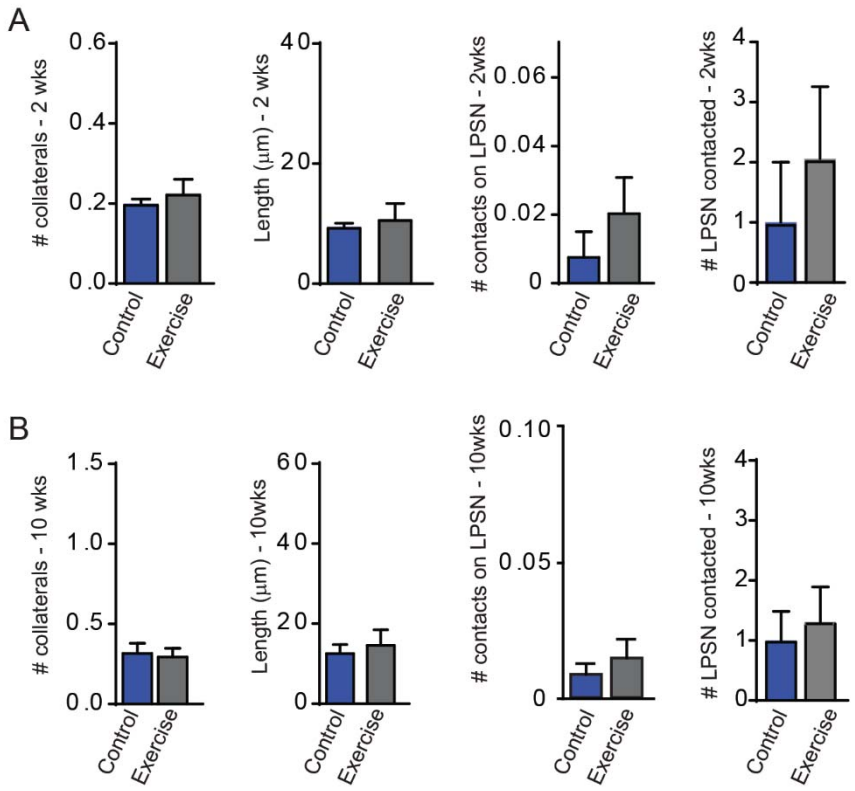

Loy et al., Figure 6

3.2. Semaphorin 7A controls the proper targeting of corticospinal and serotonergic fibers following spinal cord injury

Loy K, Meng N, Jacobi A, Locatelli G, Bareyre FM.

The manuscript is in preparation to be submitted for peer-review.

This study focussed on the contribution of Sema7A signalling in the recovery from incomplete spinal cord injury. We found that mice lacking Sema7A showed impaired functional recovery after SCI in tests that addressed fine paw placement as well as in others that test for rhythmic, regular locomotion. Anatomically we found an increase in the number, length and complexity of corticospinal collaterals in the cervical spinal cord that was not accompanied by an increase in boutons or contacts on LPSN in the deficient animals. We next focused on the lumbar spinal cord and the serotonergic projections that are thought to be part of the central pattern generator. We found no difference in brainstem serotonergic neurons, but a robust increase in fiber density in the KO. Our data indicates a release of tight patterning of the corticospinal and serotonergic connections in absence of Semaphorin7A signalling.

Contributions: KL: designed experiments, wrote the manuscript, performed all surgical procedures if not stated otherwise, collected and analysed all data if not stated otherwise; NM: collected and analysed all data concerning the 5HT and ChAT experiments; AJ: performed part of the brain injections; GL: implemented and analysed the FACS experiment; FB: designed experiments, wrote the paper

Semaphorin 7A controls the proper targeting of corticospinal and serotonergic fibers following spinal cord injury

Kristina Loy[1,2,3], Ning Meng[1,2], Anne Jacobi[1,2], Giuseppe Locatelli[1,2] and Florence M Bareyre[1,2,4]

1 Institute of Clinical Neuroimmunology, University Hospital, LMU Munich, 81377 Munich, Germany
2 Biomedical Center Munich (BMC), Faculty of Medicine, LMU Munich, 82152 Planegg-Martinsried, Germany
3 Graduate School of Systemic Neurosciences, Ludwig-Maximilians-Universitaet Munich, 82152 Planegg-Martinsried, Germany
4 Munich Cluster of Systems Neurology (SyNergy), 81377 Munich, Germany

Correspondence should be addressed to:
Florence M. Bareyre
florence.bareyre@med.uni-muenchen.de

Abbreviated Title: Axonal networks in Semaphorin 7A deficient mice

Acknowledgements: The authors would like to thank Martin Adrian, Bernadette Fiedler and Lena Schödel for excellent technical assistance as well as Dana Matzek and Bianca Stahr for animal husbandry. We would like to thank Martin Kerschensteiner for critically reading the manuscript. Work in F.M.B.'s lab is supported by grants from the Deutsche Forschungsgemeinschaft (DFG, SFB 870), by the Munich Center for Neurosciences (MCN) and the Wings for Life foundation. F.M.B. is also supported by the Munich Center for Systems Neurology (DFG, SyNergy; EXC 1010). The authors declare no competing financial interests.

Author contributions: KL and FB designed the experiments. KL performed surgical procedures. KL, NM, GL collected and analyzed data. AJ helped with surgical procedures. KL and FB wrote the manuscript. All authors approved the final version of the paper.

Words: 6845 **Abstract: 302** **Introduction: 688** **Discussion: 1050**

Pages: 26 **Figures: 6 (+2 supplementary)**

Abstract

While basic rhythmic locomotion is controlled by intraspinal circuits, supraspinal pathways are also necessary for gait adaptations and precise control of complex movements. An efficient wiring of these axonal tracts is therefore paramount to the appropriate control or rhythmic and complex motion. Several molecules have been shown to control a tight and targeted wiring during development. Among those, Semaphorin7A was recently shown to be important for axonal growth, axon guidance and synapse refinement. Here we ask whether Semaphorin7A, which also plays an important role in immune response, cell proliferation and revascularization, is important for the rewiring of supraspinal tracts following spinal cord injury. We therefore performed a Th8 hemisection in Sema7A-competent and Sema7A-deficient mice and evaluated rhythmic and complex functional recovery, immune response, revascularization, cell proliferation and the rewiring of two supraspinal axonal pathways, the corticospinal and serotonergic tracts. We found that mice in which Semaphorin7A signaling was deleted showed exacerbated functional deficits following the injury and a poorer recovery compared to control mice. While no difference in cell proliferation, revascularization, immune response or lesion volume could explain these functional data, we found that the rewiring of the corticospinal tract and of serotonergic tracts were profoundly affected in Sema7A-deficient mice. When we mapped axon pathfinding of CST and 5-HT profiles, we found that the lack of Semaphorin7A signaling released the patterning of the corticospinal and serotonergic pathways that sprouted more ectopically following injury. In particular 5-HT profiles were strongly present in the intermediate horn in Sema7A-deficient mice and upper laminae of the dorsal horn while normally absent following spinal cord injury. Similarly the CST profiles showed increase innervation in the cervical spinal cord without increasing the potential for detour circuit pathways. Our data shed light on possible targeting defects of supraspinal axonal pathways in Sema7A-deficient mice following spinal cord injury.

Introduction

In order to control locomotion, the maturation of supraspinal and intraspinal networks need to be tightly regulated. During development, several molecules tighten and precisely control the organization, the growth and navigation of axons along what will become their final path. Such molecules are for example the pair Netrin1/Unc6 or DCC (deleted in colorectal cancer), BDNF/TrkB (tropomyosin receptor kinase B), Ephrins/EphrinR, and Semaphorins/Plexins (Shen and Cowan, 2010). Among those molecules Semaphorins play a particular role in health and development. They are a class of membrane bound or secreted molecules with many different functions in various processes in the development and maintenance of the nervous system, the immune system, bones and heart (Pasterkamp, 2012). Semaphorin 7A (John Milton Hagen Blood Group antigen, Sema7A), is particularly involved in vascularization, glial scar formation, the immune and nervous system. Sema7A is GPI-anchored to the plasma membrane and can be shed thereby also acting as a secreted molecule on its two known receptors, plexinC1 (PLXNC1) and α1β1 integrin (very late antigen-1; VLA-1) (Pasterkamp et al., 2003; Zhou et al., 2008; Pasterkamp, 2012), depending of its role either on axonal growth or axonal pathfinding and targeting. In the nervous system Sema7A plays a crucial role during development and was first identified to promote axon outgrowth in the lateral olfactory tract (LOT) (Pasterkamp et al., 2003). Loss of Sema7A in mice also results in aberrant architecture of the barrel cortex (Carcea et al., 2014) and impaired climbing fiber elimination in the cerebellum resulting in impaired synaptic refinement (Uesaka et al., 2014). In the adult mouse Sema7A is a key regulator of hippocampal neurogenesis through VLA-1 (Jongbloets et al., 2017). Sema7A and PLXNC1 are expressed in the developing brain and spinal cord suggesting more involvement in axonal growth, guidance and targeting there (Pasterkamp et al., 2007). In contrast to SEMA3A, which was already studied in spinal cord injury (Kaneko et al., 2006), the role of Sema7A in the recovery process following spinal cord injury is, to date, unknown. Due to the various roles of Sema7A in circuit maturation and refinement, neurogenesis and axonal outgrowth throughout the CNS, the molecule is a multifaceted target

in neuronal remodeling and regrowth after spinal cord injury. As spinal cord trauma challenges many systems throughout the organism in the acute and sub-acute phases that follow (Schwab et al., 2014; Li et al., 2017), we therefore studied the influence of Sema7A on functional recovery, supraspinal axonal remodeling, immune response and vascularization following incomplete spinal cord injury.

Incomplete spinal cord lesions, have a substantial potential for recovery due to reorganization of injured and spared fiber tracts. Recent studies have demonstrated th reorganization of, not only, supraspinal tracts (Weidner et al., 2001; Bareyre et al., 2004; van den Brand et al., 2012; Zorner et al., 2014) but also intraspinal circuitry/ networks (Cina and Hochman, 2000; Guertin, 2009; Ghosh and Pearse, 2014) and have shown their contribution to post-injury functional recovery. Remodeling of intraspinal circuits is largely attributed to the central pattern generator (CPG) which consists of few serotonergic fibers and other interneurons that wire motor neurons to generate rhythmic movement without central input (Cina and Hochman, 2000). After spinal cord injury the reorganization of these spinal networks contributes to recovery of rhythmic stepping, but can also cause system dysfunction such as spasticity and up to paralysis (Ghosh and Pearse, 2014). Supraspinal reorganization also plays a crucial role for the recovery of gross and fine motor behavior after partial spinal cord injury in mice (Bareyre et al., 2004; Lang et al., 2012). In this paper, we demonstrate that Sema7A deficient mice show strongly impaired functional recovery after spinal cord injury in both gross rhythmic stepping as well as fine paw placement. We then wanted to determine the underlying reasons of this impaired recovery, and found that Sema7A deficient mice did not show changes in lesion volume, immune response or increased cell proliferation but rather that the targeting of supraspinal networks was strongly altered. In clear our data indicated that following spinal cord injury, the lack of Sema7A expression triggered aberrant and profuse sprouting of corticospinal and serotonergic fibers. This indicates that in competent mice Sema7A restricts the patterning of rewiring axonal pathways following spinal cord injury.

Materials and Methods

Animals

Adult female and male Sema7A knock-out mice (Sema7A$^{-/-}$, The Jackson Laboratory Sema7A^{tm1Alk}/J #005128, (Pasterkamp et al., 2003) from 6 to 12 weeks of age at onset of experiment were used in this study. All animals were housed in a 12 hour night day cycle and received food and water ad libitum. All animal procedures were performed according to institutional guidelines and were approved by the local authority (Regierung von Oberbayern #55-2-1-54-2532-140-2013).

Surgical procedures

For all surgical procedures mice were anesthetized using an intraperitoneal injection of a midazolam/medetomidine/fentanyl mix (MMF; midazolam 5.0mg/kg, medetomidine 0.5mg/kg, fentanyl 0.05mg/kg) and kept on a 38°C heating pad until fully asleep. After surgery, all mice were returned to the heating pad and kept there until fully awake. For pain management meloxicam (Metacam®, Boehringer Ingelheim) was administered before and every 12 hours after surgery.

Dorsal thoracic hemisection: Dorsal thoracic hemisection was done as previously described (Bareyre et al., 2004; Lang et al., 2013; Jacobi et al., 2015). In brief, the skin above the 8th thoracic vertebrae was incised and the bone was carefully exposed. A laminectomy was performed, followed by a dorsal hemisection with small iridectomy scissors, thereby transecting the main dorsal and minor dorsolateral part of the corticospinal tract (CST) while leaving the ventral grey and white matter intact.

Stereotactic labelling of the hindlimb motor cortex: In brief, the skin above the scull was incised and a hole was drilled at the right coordinates. 1µl of 10% biotinylated dextran amine (BDA, in

0.1% phosphate buffer (PB), 10000 MW, Thermo Fisher Scientific) was pressure injected in both hindlimb motor cortices 14 days prior to sacrifice with a finely pulled glass micropipette. Coordinates were -1.3mm rostro-caudal, 1.1mm lateral from bregma and 0.6mm depth. The micropipette remained in place for 3 min following the injection.

Labelling of long propriospinal neurons: Long propriospinal neurons (LPSN) were labelled using 0,5µl of 2.5% dextran tracer conjugated with TexasRed® (3000MW, Thermo Fisher ScientificD-3328) in both sides of the cord between the last thoracic and the first lumbar vertebrae. First the skin was opened and the gap between the two vertebrae was exposed. The dura was carefully removed and the TexasRed® pressure injected with a fine glass micropipette (lateral from the central vein: ±0.6mm, 0.8mm depth) which was kept in place 3 min after the injection. Animals were sacrificed 9 days after surgery.

Backtracing of the hindlimb motor neurons in the cortex: Hindlimb motor cortex neurons were backtraced from the 8th segment of the spinal cord using 2.5% TexasRed®. After a dorsal hemisection as described above a finely pulled glass micropipette was inserted rostral to the lesion and ±0.2mm lateral from the central vein and at 0.2-0.3mm depth, thereby labelling the cut dorsal CST. The micropipette remained in place 3 min after the end of injection. Animals were sacrificed 10 days after injection.

Behavioural evaluation of hindlimb stepping and coordination

All animals were habituated three times to all the behaviour equipment prior to beginning of the study. Animal with incomplete lesions or poor performance prior to dorsal hemisection were excluded from the study. All behaviour testing was performed 2 days prior to surgery (baseline) and 2, 7, 21 and 56 days after surgery.

Ladder rung test: For assessment of regular walking and fine paw placement the ladder rung test (aslo called gridwalk test) was used (Metz and Whishaw, 2009). Therefore, the animals had

to cross a 1m horizontal grid ladder and footfalls were counted in three consecutive crossings by videotaping by an investigator blinded to genotype and timepoint. We evaluated regular and rather rhythmic paw placements in the regular walk with evenly distributed spacing between the rungs and irregular spacing of the rungs aiming at judging the animal's ability for fine coordinated paw placements.

Rotarod test: To evaluate motor ability, we used the RotaRod test (Ugo Basile, Italy). Mice were placed on the apparatus that either kept a constant speed 20 rounds per minute (constant RotaRod) or accelerated from 2 to 40 rounds per minute (accelerated Rotarod). Maximum score was 120 seconds,the device automatically recorded the time and velocity at fall from the rod when the animal was unable to hold on any longer.

Tissue processing and histology

Mice were deeply anesthetized and perfused transcardially with PBS/Heparin (Braun) followed by 4% paraformaldehyde (PFA) in 0.1%PB. The tissue was postfixed overnight in 4% PFA followed by dissection of brain and spinal cord and cryoprotection in 30% sucrose (Sigma) for at least 48 hours.

Visualization of CST collaterals and contacts on LPSN: To stain hindlimb CST collaterals and sprouting we cut 30 50µm sections of the cervical spinal cord (C3-C5) of mice that had a dorsal thoracic hemisection, LPSN labelling and BDA injected in the motor cortex. All sections were first incubated in ABC complex (Vector Laboratories) over night at 4°C, then washed and incubated with tyramide (Biotin-XX, TSA kit #21, Thermo Fisher Scientific) for 30 minutes, washed again and incubated with Streptavidin-FITC or -Alexa488 (1:500, Thermo Fisher Scientific).

Visualization of first order motor neurons and cortical layering: Brains with backtraced motor neurons were sectioned consecutively at 40µm and stained with mouse-α-NeuN (1:500, neuronal nuclei antibody, Merck Millipore MAB377). For antibody detection goat-α-mouse

Alexa488 (1:500, Thermo Fisher Scientific) was used and nuclei were counterstained with Neurotrace 435 (1:500, NT435, Thermo Fisher Scientific).

Lesion site staining: To visualize the lesion site 40µm sections approximately from T6-L2 were stained with NT435.

Visualization of cell proliferation and vascularization: To reveal proliferating cells and vascularization, lesion sites were cut in 50µm coronal sections and incubated free floating with rabbit-α-Ki67 (1:100, Thermo Fisher Scientific MA5-14520) and rat-α-CD31 (1:50, BD Biosciences 550274), a marker of endothelial cells that line the vasculature. For secondary staining sections were incubated in goat-α-rabbit Alexa488 (1:500) and goat-α-rat Alexa594 (1:200, both Thermo Fisher Scientific) for 2 hours at room temperature. Nuclei were counterstained with NT435.

Visualization of cholin acetyltransferase$^+$ (ChAT$^+$) motorneurons, serotonergic fibers and cells (5HT) and serotonin receptors (5HTR): Staining for motorneurons and serotonergic fibers was done sequentially. First 40µm sections were incubated with goat-α-ChAT (1:100, Merck Millipore AB144P) primary antibody and secondary staining with donkey-α-goat Alexa488 (1:500, Thermo Fisher Scientific). Consecutively sections were stained with rabbit-α-5HT (1:10000, Immunostar 20080) followed by incubation with donkey-α-rabbit HRP (1:100, Thermo Fisher Scientific) for 1 hour and then for 5 hours with tyramide coupled to Alexa594 (1:100, Thermo Fisher Scientific Tyramide kit #15). For 5HTR staining sections were incubated with either rabbit-α-5HTR1a (1:500, Immunostar 24504), rabbit-α-5HTR2a (1:333, Immunostar 24288) or rabbit-α-5HTR7 (1:500, Immunostar 24439) for 2 nights at 4°C followed by tyramide amplification exactly like described for the 5HT antibody. For the 5HTR1a and 5HTR7 no triton was used in accordance with the manufacturers suggestions.

Imaging

All confocal images were acquired with a Leica TCS SP8 confocal (Leica Microsystems) with 20x, 40x or 63x oil immersion objectives and appropriate laser lines and filter sets and no zoom if not otherwise stated.

Quantifications

All quantifications were done by an investigator blind to genotype of the animal.

Quantification of CST sprouting: To analyse sprouting in the cervical spinal cord, fibers were stained as described above and confocal scans (50µm, Z-step size 1.042µm) of 20 sections were acquired. All images were then processed in Fiji (https://fiji.sc/) to generate maximum intensity projections. Length tracing, counting of total collaterals and exiting collaterals, branchpoints and boutons were also done in Fiji and the NeuronJ plugin (Meijering 2004) was used for length quantification of the total CST grey matter collaterals. To account for differences in CST labelling between the animals all fibers in the tract were counted in the dorsal funiculus and the length as well as the number of collaterals was normalized to this number. A bouton was counted if a thick varicosity was clearly visible along an axon. All boutons were normalized to the total length of each animal and plotted per µm (as previously established in (Bareyre et al., 2004; Lang et al., 2012; Lang et al., 2013; Jacobi et al., 2015).

Quantification of contacts on LPSN: Contacts on between the CST and LPSN were counted using a fluorescent microscope (Olympus IX71) with a 40x/0.65 air objective. We counted the total number of contacts and the total number of LPSN contacted by labelled CST collaterals. A contact was defined as a close apposition between a CST bouton and a LPSN. All numbers were normalized to the number of TexasRed® labelled neurons and the number of labelled CST fibers in the white matter tract.

Quantification of the number of traced motor neurons in the brain and brain layering: For quantification of TexasRed®$^{+}$ motor neurons in the brain we counted all labelled cells in every

second section of the brain from the first section to the last section with labelling on an Olympus IX70 with a 10x air objective. All results are plotted as mean per section counted.

Quantification of lesion volume: For lesion volume every second section of the lesion area stained with NT435 was imaged with an Olympus IX71 with a 4x objective. The lesion was outlined and measured in Fiji and values were multiplied by 80µm and summed up to calculate the total lesion volume.

Quantification of proliferating cells and vascularization: To quantify $Ki67^+$ cells and $CD31^+$ vessels lesion site sections were imaged using a Leica DM4 fluorescent microscope with a 10x air objective and an 2µm Z-step size with the Stereo Investigator software (SI, MBF). All images were stitched and Z-projected in Fiji and the lesion area was outlined. For Ki67 an automated approach was used. First the background was removed using the rolling background function in Fiji with a setting of 10, then all Images were thresholded using the triangle method creating a mostly black and white picture of nuclei and background. Then the analyse particle function of Fiji was used to count all particles of at least 25µm size and a circularity between 0.3 and 1.0 to ensure only nuclei were counted. This procedure was done for the lesion area and the area outside of the lesion. We analysed 6 sections where the lesion was clearly visible. Vascularization was traced and measured using the NeuronJ plugin in Fiji and branchpoints were counted with the cell counter. All values are displayed as average per section.

Quantification of serotonergic fibers, cells and contacts on motor neurons: For quantification of 5HT intensity around the lesion site we used the integrated density function in Fiji and normalized to a clearly negative region of the cord. To generate heat maps of the L1/2, L3/4 and L5/6 area in Fiji a custom written script was used. In brief, we maximum projected all confocal scans taken with identical scan settings and aligned them to the central canal for all animals of one genotype (3 sections per animal, 2-3 animals per genotype and timepoint). Then an average intensity projection was done and a heatmap was generated by averaging the intensity within 200 squares over the images. The intensity was normalized to the intensity within the

dorsal funiculus that does not contain $5HT^+$ fibers. To quantify the number of serotonergic cells that project to the spinal cord we imaged 5HT stained brainstems at -6.36mm, -6.96mm, -7.48mm and -8.00mm from bregma with a Leica DM4 and the SI software (1 plane in Z). Images were then stitched and cells in the raphe obscurus nucleus (Rob) and ventrolateral medulla (VLM) that project to the spinal cord ventral horn and intermediate grey matter respectively were counted. To quantify contacts of 5HT fibers on $ChAT^+$ cells in the lumbar spinal cord we used 3D reconstruction in Imaris (Bitplane) on confocal scans (40µm, 20x, Z-step size: 1.042µm).

Image processing

All images were stitched and maximum projected either in LasX (Leica microsystems) or Fiji. For illustration images were processed in Adobe Photoshop using gamma adjustment to enhance visibility if necessary.

Flow cytometry (FACS)

For analysis of cell populations around the lesion site, mice were sacrificed, spinal cord from approximately T6-L2 isolated and transferred to ice-cold PBS (Sigma-Aldrich). Tissue was cut in small pieces and digested in RPMI containing 2% fetal calf serum (Sigma-Aldrich), 25mM HEPES (Sigma-Aldrich), DNase I (10ng/ml, StemCell Technologies) and Collagenase D (0.8mg/ml, Roche) for 30' at 37°C. Reaction was stopped by adding 1:100 dilution of a 0.5M EDTA (Sigma-Aldrich) solution. Suspension was filtered through 70µm cell strainers (Falcon) and re-suspended in a 30% solution of Percoll (Sigma-Aldrich). After 30' of gradient centrifugation at 10.800 r.p.m., the top (myelin) and lower (red cells) layers were removed and the remaining solution was filtered through 70µm cell strainers (Falcon). For analysis of cell populations in lymph nodes, mice were sacrificed and the inguinal and axillary lymph nodes

isolated and mechanically dissociated in ice-cold PBS (Sigma-Aldrich) using glass slides. The suspension was filtered through 70µm cell strainers (Falcon). Stainings were performed in ice-cold PBS after Fc-receptor blockade (CD16/32, 1µl/million cells, clone 2.4G2, BD Biosciences) using LIVE/DEAD staining (Invitrogen) and the following antibodies: CD45 (clone 30-F11, BioLegend), CD11b (clone M1/70, BD Biosciences), Ly6C (clone AL21, BD Biosciences), Ly6G (clone 1A8, Biolegend). Samples were acquired on a LSR-Fortessa cytometer (BD Biosciences) and results analyzed by FlowJo software.

Statistical evaluation

All results are given in mean±SEM. For statistical evaluation, we used GraphPad Prism 5.01 (GraphPad, USA). We used one- and two-ways ANOVA with Tukey and Bonferroni post-hoc to test for significance in the behaviour data. For two column comparison between the genotypes we fist tested for normality and then used the appropriate t-Test, e.g. unpaired for normal distribution and Mann-Whitney for data that did not distribute normally. Significance levels are indicated as follows: *$p < 0.05$; **$p < 0.01$; ***$p < 0.001$.

Results

Loss of Semaphorin7A signalling limits recovery of function after spinal cord injury.

First, we tried to understand whether the loss of Semaphorin7A signalling would influence the functional recovery of the mice following an incomplete spinal cord injury (Bareyre et al., 2004; Jacobi et al., 2015). To assess this, we performed thoracic dorsal bilateral hemisections of the spinal cord and followed the recovery of CST function using behavioural testing paradigms such as the 'ladder rung test' (Metz and Whishaw, 2009), the rotarod test (Whishaw et al., 2008) and the 'catwalk analysis' (Hamers et al., 2006) in Semaphorin7A-deficient mice and Semaphorin7A -competent control mice. While neither of these genetic manipulations altered the size of the thoracic lesions (Fig.2; n = 13–15 mice per group), deletion of Semaphorin7A decreased functional recovery after injury. We followed the mice over 56d following the injury and observed that more pronounced deficits remained in mice with impaired Semaphorin7A signaling for at least 8 weeks after injury in both the constant and accelerated rotarod test that evaluates locomotion and rhythmic behavior (Fig. 1A, B) as in the ladder rung test 'regular walk' that also evaluates rhythmic stepping and the ladder rung 'irregular walk' paradigm that is more reflective of a CST dependent rhythmic behaviour (Fig. 1C,D). Interestingly, the motor performance of uninjured Semaphorin7A deficient mice was not different from the motor performance of Semaphorin7A competent mice (Supplementary Fig. 2). Taken together, our results of the behavioral analysis indicate that intact Semaphorin7A signaling is required for the timely recovery of motor function after spinal cord injury.

Semaphorin 7A does not affect lesion size, immune response, cell proliferation or vascular resealing following spinal cord injury.

As early functional deficit and recovery are likely to be dependant of the lesion extent which itself might be influences by the development of inflammation, vascular resealing and cell

proliferation we examined first all those parameters. We performed lesion volume at the end of the behavioural experiment and found that lesion volume was not significantly different between the Semaphorin7A deficient animals and the wild type control mice (Fig.2A). Likewise, when we analysed inflammation at the lesion site at acute and sub-acute timepoints, we found that neither leucocytes, macrophages and granulocytes were changed during the post-injury inflammatory response between the deficient and competent mice in the spinal cord (Fig. 2B). We next focussed on vascular resealing and cell proliferation and found, also there, no differences between the Semaphorin7A deficient and competent mice (Fig. 2C, D). As none of these parameters showed any differences we concluded that they were unlikely to explain the behavioural differences seen in Semaphorin7A deficient mice. Therefore we focussed on the remodelling of supraspinal tract following injury.

Semaphorin7A signaling restricts the growth of corticospinal connections during circuit remodelling following spinal cord injury.

To determine whether Semaphorin7A signaling regulates sprouting of corticospinal connections following spinal cord injury, we performed a bilateral dorsal hemisection of the spinal cord at T8 in Sema7A-deficient mice (Pasterkamp et al., 2003) and age-matched Sema7A-competent wild-type mice and traced the hindlimb portion of the corticospinal tract by stereotactic injection of the anterograde tracer biotinylated dextran amine (BDA). Sema7A-deficient mice showed a normal density and distribution of cortical layer V neurons of the hindlimb CST (Supplementary Fig.2). At 3 weeks after spinal cord injury, however, Sema7A deficiency increased the number of newly formed CST collaterals that enter the gray matter of the cervical spinal cord as part of the detour circuit formation process (Fig. 3A,B) as well as the length of these collaterals (Fig. 3B). Along this line, the complexity of the collaterals evaluated as the number of branches originating from the main collaterals was also significantly increased (Fig. 3C, D). However, when we evaluated the number of boutons per length on exiting collaterals we could find no

differences (Fig. 3E, F) indicating that Sema7A deficiency primarily affect the number, length and complexity of newly generated corticospinal collaterals participating to the process of axonal remodelling following spinal cord injury. We then investigated whether the increased number of collaterals and their overall increased length and complexity could play a modulatory role during targeting onto cervical relay neurons. We thus investigated the proportion of long propriospinal relay neurons in the cervical spinal cord that are contacted by these CST collaterals and found that despite the increased number of collaterals the number of contacts onto long propriospinal neurons was not significantly changed (Fig. 4A-C). These data indicate that Semaphorin 7A signaling is not involved in correct corticospinal targeting onto cervical relay neurons following spinal cord injury.

Semaphorin 7A signalling restricts patterning of serotoninergic fibers following spinal cord injury.

We then turned our attention to another supraspinal tract that contributes to locomotion by its output onto spinal networks, the serotonergic system. We mapped out the innervation of the serotonergic system at the lumbar level L1 acutely following the injury (2d) and sub-acutely (7d and 21d). We generated heatmaps representing the innervation and intensity of the lumbar spinal cord before and after injury. We mapped regional intensities of 5-HT profiles by creating heatmaps and found that acutely following the injury the innervation of the spinal cord was very segregated in three main regions in Semaphorin competent and deficient mice (Fig.5A-B). When we compared the expression pattern of Semaphorin7A-competent mice against that of Semaphorin7A-deficient mice we observed that the intensity was significantly lower in deficient animals in the three regions observed (Fig.5C). However the regions showing the distribution of 5HT fibers was similar at this point between the two groups of mice and we could not see changes in patterning of 5-HT profiles. When we performed the same analysis in the sub-acute phase we observed a post-injury adaptation of 5HT fibers (Fig.6). Indeed both at 7 and 21d the

intensity of 5HT fibers increased significantly more in Sema7A deficient mice compared to Sema7A competent mice (Fig. 6A-D). Not only intensity was increased in Sema7A deficient mice but also the localisation of 5HT fibers was different in those mice with central regions of the lumbar cord significantly more innervated in those mice compared to control mice (Fig. 6E). In particular specific areas of the intermediate spinal cord showed ectopic sprouting with 5-HT profiles (Fig. 6E) These data indicated a bi-phasic response of the serotonergic tract to spinal cord injury in Sema7A deficient mice with an early phase of intensity decrease and a later phase of over innervation of the regions normally innervated but also non-innervated regions (Fig. 6B, D).

DISCUSSION

The proper wiring of supraspinal pathways is critical to efficient locomotion. Similarly, following incomplete spinal cord injury the correct and targeted re-wiring of those circuits is critical to a possible recovery of some motor or sensory function. In this paper we show that global deletion of Semaphorin7A not only significantly worsen the acute functional outcome following spinal cord injury but also delays or impairs functional recovery of rhythmic and complex locomotion. could the acute worsening of locomotion in Sema7A –deficient animals could be due to several factors, e.g. default of revascularization, modified immune response following injury or default in glial scar formation (Kopp et al., 2010; Schwab et al., 2014; Silver et al., 2014; Li et al., 2017). Indeed, following SCI the neuronal tissue must be re-vascularized to ensure proper sustenance of the regenerating tissue, with grey matter vascularization being especially susceptible to damage (Figley et al., 2013). The absence of Sema7A signalling could there be key as a growing knowledge suggests the involvement of Sema7A in tumour progression through its pro-angiogenic mode of action (Pasterkamp et al., 2007; Garcia-Areas et al., 2013; Garcia-Areas et al., 2014; Li et al., 2017). We investigated re-vascularization and cell proliferation after spinal cord injury in Sema7A-competent and deficient mice and found no differences in the number of vessels, the branchpoints of those vessels - a measure of vascular network complexity - or length of the vasculature after SCI. Similarly we found no differences in proliferating cells, measured by the number of KI67 positive cells. In this post-injury model, Sema7A does not seem to play a role in vascular remodelling and tissue re-perfusion, which is also in accordance with identical lesion volumes in both groups. This is not completely surprising as the pro-angiogenic activity has thus far only be reported in cancer progression but not in development (Ghanem et al., 2011; Saito et al., 2015). In the vascular system, developmental programs seem to be re-activated following injury (Jeansson et al., 2011) and therefore our data showing an absence of difference in vascular regeneration are in line with the role of Sema7A in angiogenesis during development.

Recovery from spinal cord injury also triggers a complex cascade of immune responses whose beneficial or detrimental role for recovery remains controversial (Schwab 2014). Sema7A was reported to be expressed on T-cells, thereby stimulating and activating monocytes and macrophages via α1β1 Integrin leading to a more severe immune response. In the absence of Sema7A, and thereby the absence of this activation, a less severe disease course in experimental autoimmune encephalomyelitis (EAE) was reported (Suzuki et al., 2007). Conflicting evidence showed impairment of T-cell response in the absence of Sema7A and more severe EAE (Czopik et al., 2006). We did not see any difference in the invasion of lymphocytes, macrophages or CD4+-T cells into the spinal cord of Sema7A-deficient and competent mice. In comparison to the immune response in EAE, an autoimmune disease, the activation and recruitment of immune cells in the injured spinal cord is considered much lower. Sema7A deletion might therefore trigger differences that are minor and could not be observed by flow cytometry.

We then focussed on the wiring and re-wiring of supraspinal pathways following incomplete spinal cord injury. As gross rhythmic motor function and balance (investigated using the rotarod and the regular ladder rung) and more complex movements and fine stepping, (investigated with the irregular ladder rung) are impaired in Sema7A-deficient mice, we focussed our attention on two specific supraspinal tracts, the CST known for its control of fine paw placement and the serotonergic system whose input on spinally generated networks (Marder and Bucher, 2001) is important for rhythmic locomotion. Interestingly we found that the re-wiring of both tracts was altered in Sema7A-deficient mice. The corticospinal tract sprouted more and longer collaterals that were significantly more complex and innervated significant larger portion of the cervical spinal cord. Similarly the targeting of the serotonergic system was altered in Sema7A-deficient mice. There we observed a significantly lower innervation of the lumbar cord acutely following the injury and a significantly increased re-wiring in the sub-acute phase as more fibers started to emerge and ectopically innervate regions of the intermediate spinal grey matter that previously showed no innervation. There is currently no knowledge of the role of Sema7A following injury.

However this molecule has been already implicated in neuronal outgrowth, guidance and repulsion during development (Pasterkamp et al., 2003; Chabrat et al., 2017). Recent studies have demonstrated that Sema7A has growth promoting properties and is involved in repulsive and attractive axon guidance in the lateral olfactory tract and the brain dopaminergic system (Pasterkamp and Kolodkin, 2003; Pasterkamp et al., 2003; Chabrat et al., 2017). Our data on the CST and 5-HT tract systems argues for a role of Sema7A as a repulsive cue during circuit re-wiring following spinal cord injury. Indeed the CST fibers appear more complex and numerous and as for the 5-HT pathways innervate ectopic areas in Sema7A-deficient mice. Because of the over abundant innervation of the spinal cord by the CST, we investigated the formation of detour pathways e.g targeting onto and contacts with long propriospinal relay neurons that have been involved in the functional recovery following spinal cord injury (Bareyre et al., 2004; Lang et al., 2012; Jacobi and Bareyre, 2015). The fact that detour circuit did not increase and that proportionally lower units of collaterals were engaged into contacts with relay neurons argues that Sema7A does not play an important role in the CST-LPSN targeting. Conversely our data speak for a role of Sema7A signaling in precise targeting and accurate topographic organization of supraspinal tracts. Those finding are supporting recent conclusions that reported a Sema7A/PlexinC1 interaction crucial for the correct targeting of the mesodiencephalic dopaminergic tracts (mDA) of the brain. This repulsive interaction was responsible for the correct outgrowth and tight organization of mDA neurons. If Sema7A is absent, the mDA neurons are no longer repelled from the ventral tegmental area (VTA) and overgrow their target area into the striatum (Chabrat et al., 2017). Similarly, our data argue for a similar repellent effect of Sema7A during re-wiring of the CST and 5-HT pathways following spinal cord injury. As deficits and recovery in gross locomotor performance and fine movement tuning following incomplete spinal cord injury are primarily dependent on the proper and efficient re-wiring of supraspinal input, it is therefore likely that the perturbation and lack of repulsive interaction via Sema7A is paramount to those deficits.

REFERENCES

Bareyre FM, Kerschensteiner M, Raineteau O, Mettenleiter TC, Weinmann O, Schwab ME (2004) The injured spinal cord spontaneously forms a new intraspinal circuit in adult rats. Nat Neurosci 7:269-277.

Carcea I, Patil SB, Robison AJ, Mesias R, Huntsman MM, Froemke RC, Buxbaum JD, Huntley GW, Benson DL (2014) Maturation of cortical circuits requires Semaphorin 7A. Proceedings of the National Academy of Sciences of the United States of America 111:13978-13983.

Chabrat A, Brisson G, Doucet-Beaupre H, Salesse C, Schaan Profes M, Dovonou A, Akitegetse C, Charest J, Lemstra S, Cote D, Pasterkamp RJ, Abrudan MI, Metzakopian E, Ang SL, Levesque M (2017) Transcriptional repression of Plxnc1 by Lmx1a and Lmx1b directs topographic dopaminergic circuit formation. Nature communications 8:933.

Cina C, Hochman S (2000) Diffuse distribution of sulforhodamine-labeled neurons during serotonin-evoked locomotion in the neonatal rat thoracolumbar spinal cord. J Comp Neurol 423:590-602.

Czopik AK, Bynoe MS, Palm N, Raine CS, Medzhitov R (2006) Semaphorin 7A is a negative regulator of T cell responses. Immunity 24:591-600.

Figley SA, Khosravi R, Legasto JM, Tseng Y-F, Fehlings MG (2013) Characterization of Vascular Disruption and Blood–Spinal Cord Barrier Permeability following Traumatic Spinal Cord Injury. Journal of Neurotrauma 31:541-552.

Garcia-Areas R, Libreros S, Iragavarapu-Charyulu V (2013) Semaphorin7A: branching beyond axonal guidance and into immunity. Immunologic research 57:81-85.

Garcia-Areas R, Libreros S, Amat S, Keating P, Carrio R, Robinson P, Blieden C, Iragavarapu-Charyulu V (2014) Semaphorin7A promotes tumor growth and exerts a pro-angiogenic effect in macrophages of mammary tumor-bearing mice. Frontiers in physiology 5:17.

Ghanem RC, Han KY, Rojas J, Ozturk O, Kim DJ, Jain S, Chang JH, Azar DT (2011) Semaphorin 7A promotes angiogenesis in an experimental corneal neovascularization model. Current eye research 36:989-996.

Ghosh M, Pearse DD (2014) The role of the serotonergic system in locomotor recovery after spinal cord injury. Frontiers in Neural Circuits 8:151.

Guertin PA (2009) The mammalian central pattern generator for locomotion. Brain Res Rev 62:45-56.

Hamers FP, Koopmans GC, Joosten EA (2006) CatWalk-assisted gait analysis in the assessment of spinal cord injury. J Neurotrauma 23:537-548.

Jacobi A, Bareyre FM (2015) Regulation of axonal remodeling following spinal cord injury. Neural regeneration research 10:1555-1557.

Jacobi A, Loy K, Schmalz AM, Hellsten M, Umemori H, Kerschensteiner M, Bareyre FM (2015) FGF22 signaling regulates synapse formation during post-injury remodeling of the spinal cord. The EMBO journal 34:1231-1243.

Jeansson M, Gawlik A, Anderson G, Li C, Kerjaschki D, Henkelman M, Quaggin SE (2011) Angiopoietin-1 is essential in mouse vasculature during development and in response to injury. The Journal of clinical investigation 121:2278-2289.

Jongbloets BC, Lemstra S, Schellino R, Broekhoven MH, Parkash J, Hellemons AJ, Mao T, Giacobini P, van Praag H, De Marchis S, Ramakers GM, Pasterkamp RJ (2017) Stage-specific functions of Semaphorin7A during adult hippocampal neurogenesis rely on distinct receptors. Nature communications 8:14666.

Kaneko S, Iwanami A, Nakamura M, Kishino A, Kikuchi K, Shibata S, Okano HJ, Ikegami T, Moriya A, Konishi O, Nakayama C, Kumagai K, Kimura T, Sato Y, Goshima Y, Taniguchi M, Ito M, He Z, Toyama Y, Okano H (2006) A selective Sema3A inhibitor enhances regenerative responses and functional recovery of the injured spinal cord. Nature medicine 12:1380-1389.

Kopp MA, Brommer B, Gatzemeier N, Schwab JM, Pruss H (2010) Spinal cord injury induces differential expression of the profibrotic semaphorin 7A in the developing and mature glial scar. Glia 58:1748-1756.

Lang C, Guo X, Kerschensteiner M, Bareyre FM (2012) Single collateral reconstructions reveal distinct phases of corticospinal remodeling after spinal cord injury. PloS one 7:e30461.

Lang C, Bradley PM, Jacobi A, Kerschensteiner M, Bareyre FM (2013) STAT3 promotes corticospinal remodelling and functional recovery after spinal cord injury. EMBO reports 14:931-937.

Li Y, Lucas-Osma AM, Black S, Bandet MV, Stephens MJ, Vavrek R, Sanelli L, Fenrich KK, Di Narzo AF, Dracheva S, Winship IR, Fouad K, Bennett DJ (2017) Pericytes impair capillary blood flow and motor function after chronic spinal cord injury. Nature medicine 23:733-741.

Marder E, Bucher D (2001) Central pattern generators and the control of rhythmic movements. Current Biology 11:R986-R996.

Metz GA, Whishaw IQ (2009) The ladder rung walking task: a scoring system and its practical application. Journal of visualized experiments : JoVE.

Pasterkamp RJ (2012) Getting neural circuits into shape with semaphorins. Nature reviews Neuroscience 13:605-618.

Pasterkamp RJ, Kolodkin AL (2003) Semaphorin junction: making tracks toward neural connectivity. Current opinion in neurobiology 13:79-89.

Pasterkamp RJ, Peschon JJ, Spriggs MK, Kolodkin AL (2003) Semaphorin 7A promotes axon outgrowth through integrins and MAPKs. Nature 424:398-405.

Pasterkamp RJ, Kolk SM, Hellemons AJ, Kolodkin AL (2007) Expression patterns of semaphorin7A and plexinC1 during rat neural development suggest roles in axon guidance and neuronal migration. BMC developmental biology 7:98.

Saito T, Kasamatsu A, Ogawara K, Miyamoto I, Saito K, Iyoda M, Suzuki T, Endo-Sakamoto Y, Shiiba M, Tanzawa H, Uzawa K (2015) Semaphorin7A Promotion of Tumoral Growth and Metastasis in Human Oral Cancer by Regulation of G1 Cell Cycle and Matrix Metalloproteases: Possible Contribution to Tumoral Angiogenesis. PloS one 10:e0137923.

Schwab JM, Zhang Y, Kopp MA, Brommer B, Popovich PG (2014) The paradox of chronic neuroinflammation, systemic immune suppression and autoimmunity after traumatic chronic spinal cord injury. Experimental neurology 0:121-129.

Shen K, Cowan CW (2010) Guidance Molecules in Synapse Formation and Plasticity. Cold Spring Harbor Perspectives in Biology 2:a001842.

Silver J, Schwab ME, Popovich PG (2014) Central nervous system regenerative failure: role of oligodendrocytes, astrocytes, and microglia. Cold Spring Harb Perspect Biol 7:a020602.

Suzuki K, Okuno T, Yamamoto M, Pasterkamp RJ, Takegahara N, Takamatsu H, Kitao T, Takagi J, Rennert PD, Kolodkin AL, Kumanogoh A, Kikutani H (2007) Semaphorin 7A initiates T-cell-mediated inflammatory responses through alpha1beta1 integrin. Nature 446:680-684.

Uesaka N, Uchigashima M, Mikuni T, Nakazawa T, Nakao H, Hirai H, Aiba A, Watanabe M, Kano M (2014) Retrograde semaphorin signaling regulates synapse elimination in the developing mouse brain. Science 344:1020-1023.

van den Brand R, Heutschi J, Barraud Q, DiGiovanna J, Bartholdi K, Huerlimann M, Friedli L, Vollenweider I, Moraud EM, Duis S, Dominici N, Micera S, Musienko P, Courtine G (2012) Restoring voluntary control of locomotion after paralyzing spinal cord injury. Science 336:1182-1185.

Weidner N, Ner A, Salimi N, Tuszynski MH (2001) Spontaneous corticospinal axonal plasticity and functional recovery after adult central nervous system injury. Proceedings of the National Academy of Sciences of the United States of America 98:3513-3518.

Whishaw IQ, Li K, Whishaw PA, Gorny B, Metz GA (2008) Use of rotorod as a method for the qualitative analysis of walking in rat. Journal of visualized experiments : JoVE.

Zhou Y, Gunput R-A, Pasterkamp J (2008) Semaphorin signaling: Progress made and promises ahead.

Zorner B, Bachmann LC, Filli L, Kapitza S, Gullo M, Bolliger M, Starkey ML, Rothlisberger M, Gonzenbach RR, Schwab ME (2014) Chasing central nervous system plasticity: the brainstem's contribution to locomotor recovery in rats with spinal cord injury. Brain 137:1716-1732.

FIGURE LEGENDS

Figure 1: Genetic disruption of Sema7A signaling impedes functional recovery following spinal cord injury. (**A**) Quantification of the functional recovery in the rotarod test (constant speed) in Sema7A-deficient (pink lines, n=15), and Sema7A-competent control mice (blue lines; n=14) before (-2d) and 2 days, 7 days, 21days and 56 days following spinal cord injury. *P < 0.05. (**B**) Quantification of the functional recovery in the rotarod test (accelerated speed) in Sema7A-deficient (pink lines; n=15), and Sema7A-competent control mice (blue lines; n=14) before (-2d) and 2 days, 7 days, 21days and 56 days following spinal cord injury. *P < 0.05. (**C**) Quantification of the functional recovery in the ladder rung test (regular walk) in Sema7A-deficient (pink lines; n=15), Sema7A-competent control mice (blue lines; n=14) before (-2) and 2 days, 7 days, 21days and 56 days following spinal cord injury. *P < 0.05. (**D**) Quantification of the functional recovery in the ladder rung test (irregular walk) in Sema7A-deficient (pink lines; n=15), Sema7A-competent control mice (blue lines; n=14) before (-2) and 2 days, 7 days, 21days and 56 days following spinal cord injury. *P < 0.05.

Figure 2. Genetic disruption of Sema7A signaling does not result in increased lesion volume, changes in inflammation, revascularization or cell proliferation following spinal cord injury. (**A**) Fluorescence image of a longitudinal image of a spinal cord lesion (dashed lines outline the lesion border) and quantification of lesion volume between Sema7A-deficient (pink bars; n=15) and Sema7A-competent mice (blue bars; n=13). (**B**) Characterization of the immune response following spinal cord injury between sema7-deficient (pink bars) and Sema7A-competent (blue bars) showing no differences for leucocytes (left panel), granulocytes (middle panel) and macrophages (right panel) (n=3 both groups). (**C**) Confocal pictures of re-vascularization using the CD31 marker in Sema7A deficient (right; n=3) and Sema7A-competent (left; n=2) mice and quantification of the length of vessels and mean number of vessels. (**D**) Confocal pictures of cell proliferation using the KI67 marker in Sema7A deficient (right, n=3) and Sema7A-competent (left; n=2) mice and quantification of the mean number of proliferative cells outside of the lesion and inside the lesion. All scale bars represent 100µm.

Figure 3. Deletion of Sema7A triggers a loss of patterning of corticospinal growth following spinal cord injury. (**A**) Confocal images of hindlimb CST collaterals from the main CST tract in the cervical spinal cord (arrowheads) 3 weeks following T8 dorsal bilateral hemisection in Sema7A-competent (left panel) and Sema7A-deficient (right panel) mice. Scale bar equals 100 μm. (**B**) Quantification of the number of exiting hindlimb CST collaterals (left panel), collateral length (middle panel) and length/exiting collaterals(right panel) at 3 weeks following T8 dorsal bilateral hemisection in Sema7A-deficient and competent mice (n=10 animals per group). Mean ± SEM. *P < 0.05; ***P < 0.001 (ANOVA followed by Tukey tests for Sema7A-competent versus Sema7A-deficient mice). (**C**) Confocal images of representative branches (arrows) of hindlimb CST collaterals from the main CST tract in the cervical spinal cord 3 weeks following T8 dorsal bilateral hemisection in Sema7A- competent (left panel) and Sema7A-deficient (right panel) mice. Scale bar equals 100 μm. (**D**) Quantification of the number of branchpoints on hindlimb CST collaterals at 3 weeks following T8 dorsal bilateral hemisection in Sema7A-deficient and competent mice (n=10 animals per group). Mean ± SEM. *P < 0.05; ***P < 0.001 (ANOVA followed by Tukey tests for Sema7A-competent versus Sema7A-deficient mice). (**E**) Representative confocal images showing putative synaptic boutons (asterisks) on newly formed cervical hindlimb CST collaterals at 3 weeks following spinal cord injury in Sema7A-competent (left panel), Sema7A-deficient (right panel). Scale bar equals 10 μm. (**F**) Quantification of the bouton density on newly formed cervical hindlimb CST collaterals in Sema7A-competent and Sema7A-deficient mice (n=10 animals per group). Mean ± SEM. *P < 0.05, **P < 0.01 (ANOVA followed by Tukey tests in case of multiple group comparisons, e.g. Sema7A-competent versus Sema7A-deficient mice). **P = 0.0028 (unpaired two-tailed t-tests for comparisons of Sema7A-competent versus Sema7A-deficient mice).

Figure 4. Deletion of Sema7A decreases the contact formation rate onto relay neurons

(**A**) Confocal images of putative contacts between CST collaterals in the cervical spinal cord and long propriospinal neurons in Sema7A-competent mice. (**B**). Confocal images of putative contacts between CST collaterals in the cervical spinal cord and long propriospinal neurons in Sema7A-deficient mice. Scale bars represent 100µm. (**C**) Quantification of the number of contact per CST length (left panel), number of contacts onto LPSN (middle panel) and number of contacts per LPSN (right panel) in Sema7A-competent and Sema7A-deficient mice (n = 6 animals per group). *P < 0.01 (unpaired two-tailed t-tests for comparisons Sema7A-competent and Sema7A-deficient mice). No significant differences were found between Sema7A-competent and Sema7A-deficient mice (ANOVA followed by Tukey tests).

Figure 5. Deletion of Sema7A triggers a loss of serotonergic expression acutely following spinal cord injury.

(A) Representative confocal images of serotonergic staining in the segment L1 of the spinal cord 2 days following spinal cord injury in Sema7A-competent (left) and Sema7A-deficient mice. Scale bar equals 100µm (**B**) Heatmaps of 5HT fibers intensity in the different regions of the lumbar cord at L1 in Sema7A-competent (left) and Sema7A-deficient mice. Heatmaps go from dark blue (very low fiber intensity) to bright white (very high fiber intensity). Boxed areas represent the 3 regions of the spinal cord chosen for quantifications. (**C**) Quantification of relative 5-HT intensity in the different areas boxed in (**A**) at 2 days post-injury. Blue bars: Sema7A-competent mice; n=3. Pink bars: Sema7A-deficient mice; n=2.

Figure 6. Deletion of Sema7A changes the patterning of serotonergic fiber growth sub-acutely following spinal cord injury.

(A) Representative confocal images (top) of serotonergic staining in the segment L1 of the spinal cord 7 days following spinal cord injury in Sema7A-competent (left) and Sema7A-deficient mice and heatmaps (bottom) of 5-HT fibers intensity in the different regions of the lumbar cord at L1 in Sema7A-competent (left) and Sema7A-deficient mice. Heatmaps go from dark blue (very low fiber intensity) to bright white (very high fiber intensity). Boxed areas represent the 3 regions of the spinal cord chosen for quantifications. (**B**) Quantification of relative 5-HT intensity at 7 days post-injury in the different areas boxed in (**A**) at 7 days post-injury. Blue bars: Sema7A-competent mice. Pink bars: Sema7A-deficient mice (n=3 animals per group). (**C**) Representative confocal images (top) of serotonergic staining in the segment L1 of the spinal cord 21 days following spinal cord injury in Sema7A-competent (left) and Sema7A-deficient mice and heatmaps (bottom) of 5-HT fibers intensity at 21 days post-injury in the different regions of the lumbar cord at L1 in Sema7A-competent (left) and Sema7A-deficient mice. Heatmaps go from dark blue (very low fiber intensity) to bright white (very high fiber intensity). Boxed areas represent the 3 regions of the spinal cord chosen for quantifications. (**D**) Quantification of relative 5-HT intensity at 7 days post-injury in the different areas boxed in (**A**) at 21 days post-injury. Blue bars: Sema7A-competent mice. Pink bars: Sema7A-deficient mice (n=3 animals per group). (**E**) Confocal image of 5-HT profiles in a spinal cord at L1 to indicate the site of ectopic sprouting (boxed area, left image). Confocal images of the boxed in Sema7A-competent (middle) and Sema7A-deficient (right) mice 7days following injury. Quantification of the ectopic sprouting in area boxed in (**E**; left panel).

Supplemental Figure 1. Sema7A heterozygote mice perform similar to sema7A-competent mice in motor test following spinal cord injury.

(A) Quantification of the functional recovery in the rotarod test (constant speed) in Sema7A-competent (blue lines, n=14), and Sema7A-heterozygote mice (green lines; n=10) before (-2d) and 2 days, 7 days, 21days and 56 days following spinal cord injury. (**B**) Quantification of the functional recovery in the rotarod test (accelerated speed) in Sema7A-competent (blue lines, n=14), and Sema7A-heterozygote mice (green lines; n=10) before (-2d) and 2 days, 7 days, 21days and 56 days following spinal cord injury. (**C**) Quantification of the functional recovery in the ladder rung test (regular walk) in Sema7A-competent (blue lines, n=14), and Sema7A-heterozygote mice (green lines; n=10) before (-2) and 2 days, 7 days, 21days and 56 days following spinal cord injury. (**D**) Quantification of the functional recovery in the ladder rung test (irregular walk) in Sema7A-competent (blue lines, n=14), and Sema7A-heterozygote mice (green lines; n=10)before (-2) and 2 days, 7 days, 21days and 56 days following spinal cord injury. Data analyzed using repeated-measure ANOVA followed by Bonferroni tests.

Supplemental Figure 2. The density and distribution of hindlimb cortical layer V neurons is unaltered in Sema7A deficient mice.

(**A**) The distribution of layer V neurons of the hindlimb CST relative to bregma is unaltered in Sema7A-deficient mice. Blue lines: Sema7A-competent mice; n=5. Pink lines: Sema7A-deficient mice; n=4. (**B**) Representative confocal scans of the brain of Sema7A-deficient and -competent mice. Red: TexasRed positive backtraced first order motor neurons; green: NeuN staining. Scale bar represents 200µm. (**C**) Quantification of the average number of $TexasRed^{+}$ motor neuron per section. Sema7A-competent mice; n=5. Pink bars: Sema7A-deficient mice; n=4.

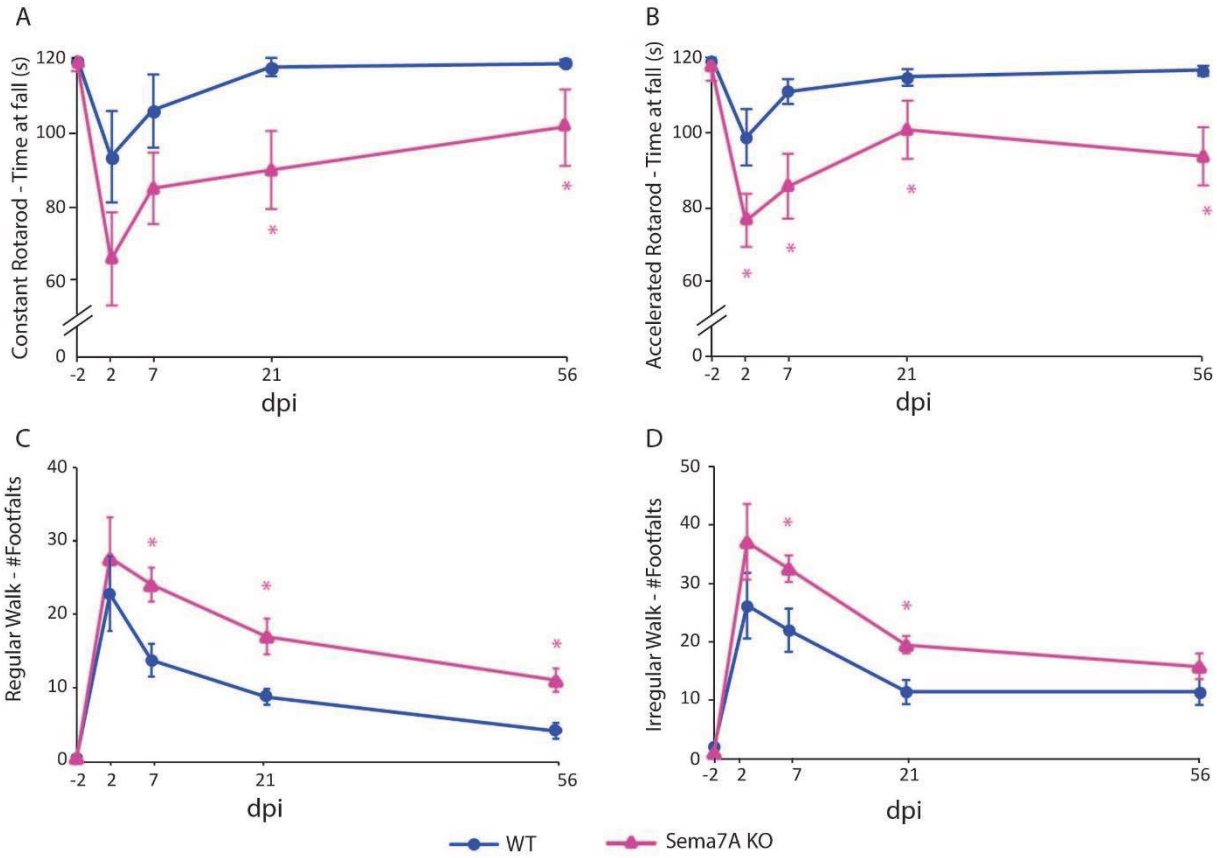

Loy et al., Figure 1

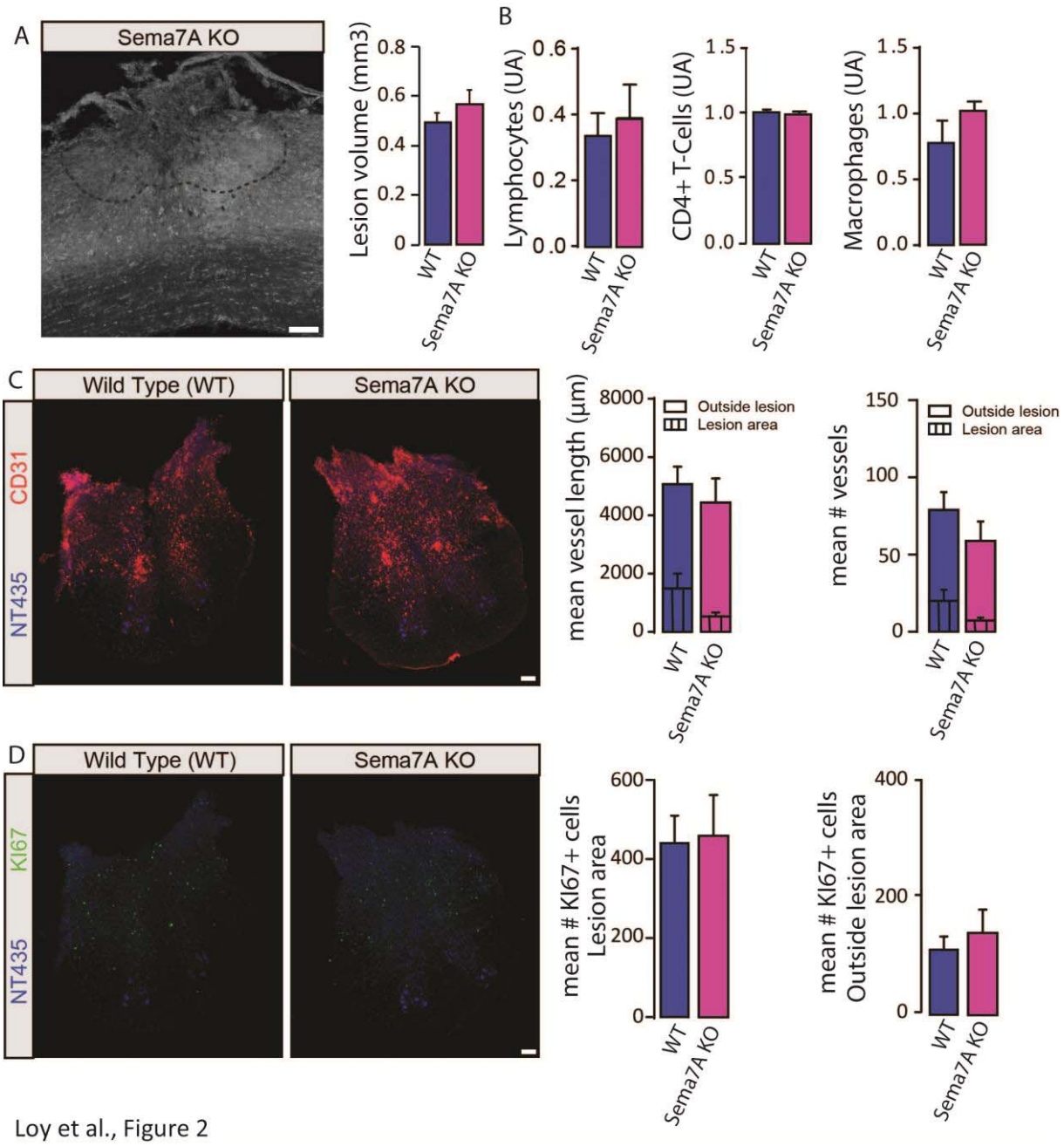

Loy et al., Figure 2

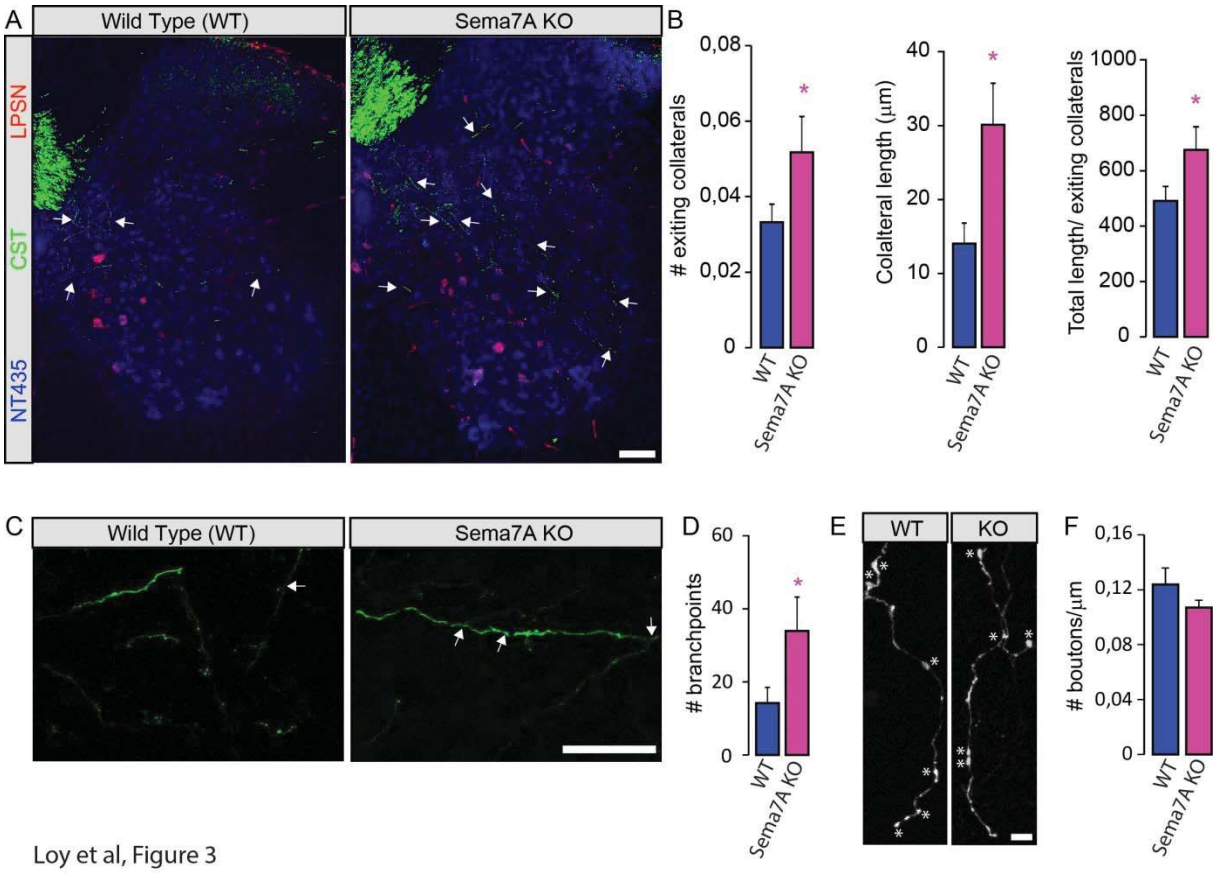

Loy et al, Figure 3

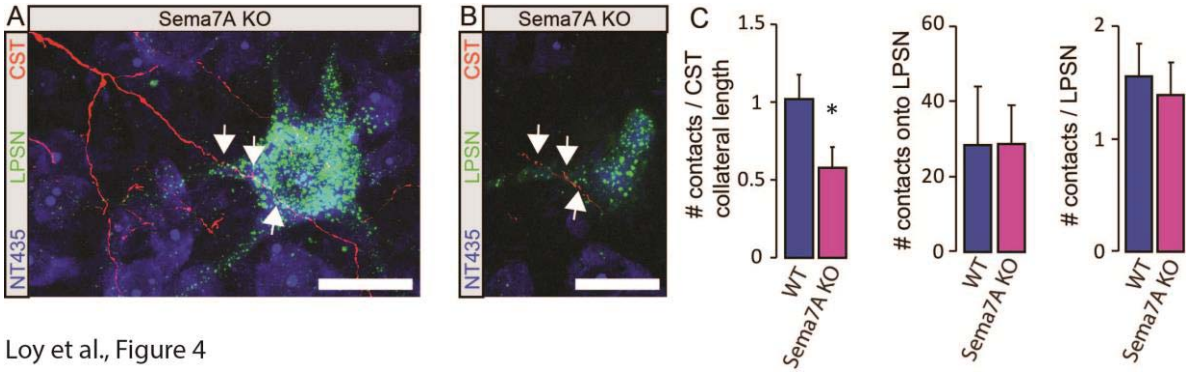

Loy et al., Figure 4

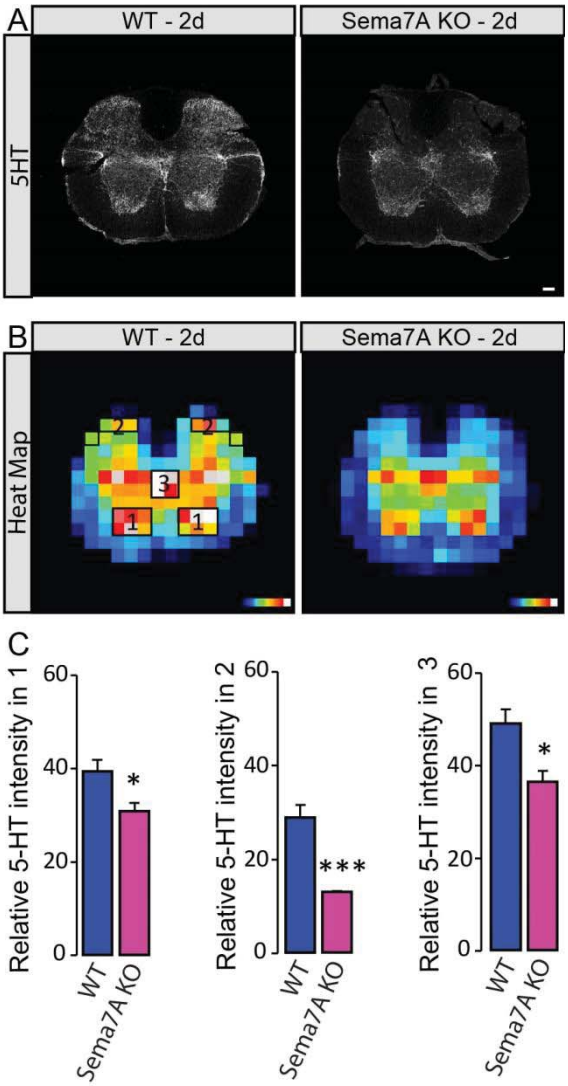

Loy et al., Figure 5

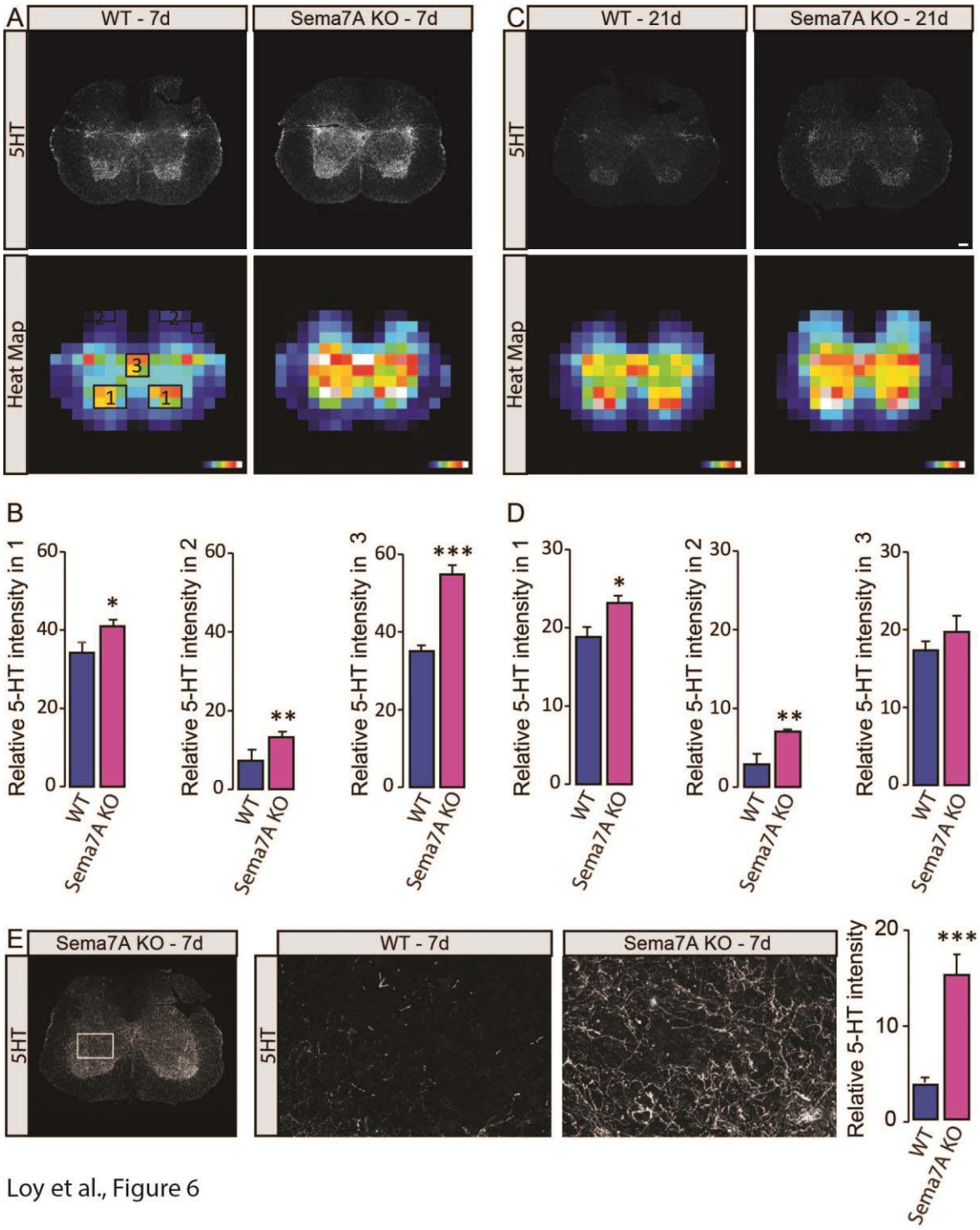

Loy et al., Figure 6

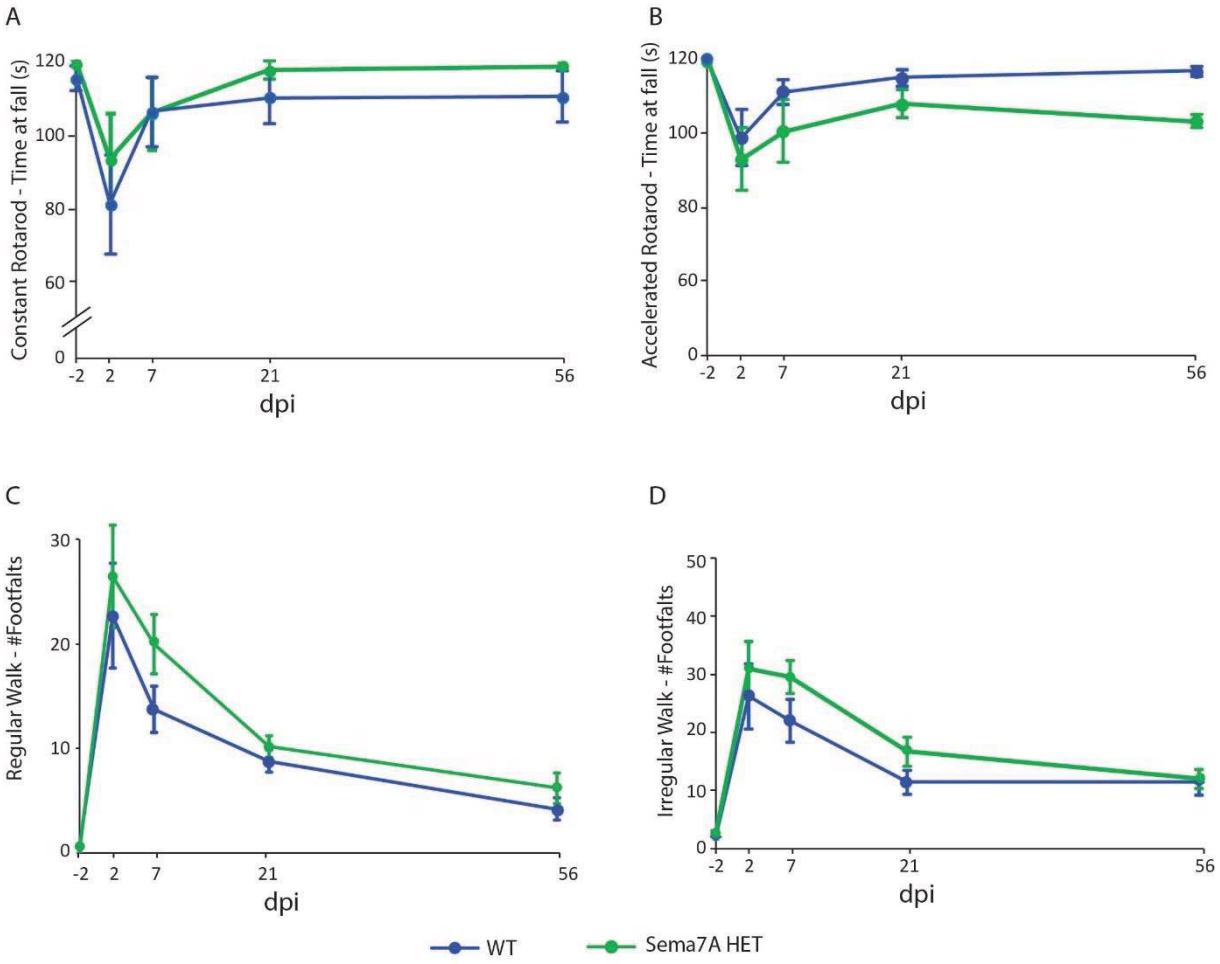

Loy et al., Supplementary Fig.1

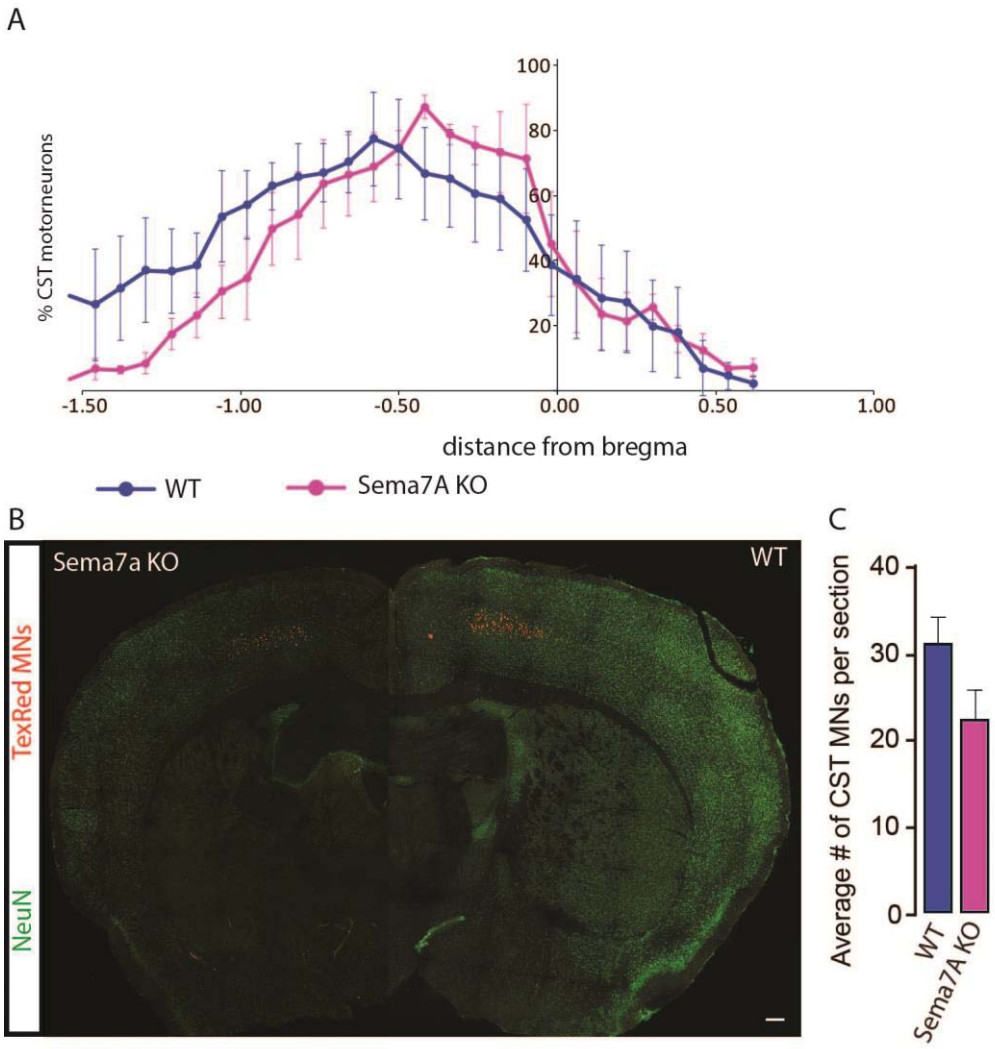

Loy et al., Supplementary Fig.2

3.3. FGF22 signaling regulates synapse formation during post-injury remodeling of the spinal cord.

Jacobi A, **Loy K**, Schmalz AM, Hellsten M, Umemori H, Kerschensteiner M, Bareyre FM.

The study is published in the EMBO Journal (2015 May 5;34(9):1231-43).

This study focussed on the role of FGF22 and its receptors FGFR1 and R2 in remodelling after spinal cord injury in the adult mouse. We found that deletion of FGF22 or its two receptors together lead to no reduction in corticospinal sprouting, but to a significant reduction in boutons along these newly formed collaterals and contacts onto LPSN. Deletion of only one of the receptors leads to increased corticospinal sprouting without impaired bouton and detour circuit formation arguing for a compensatory mechanism. Absence of FGF22 signalling also impaired synapse maturation, reflected in a significant reduction in synapsin and bassoon positivity of these newly formed boutons. FGF22 deficient animals also show a significant reduction in functional recovery after spinal cord injury further confirming the reduced and most likely insufficient detour circuit formation.

Contributions: AJ: wrote the manuscript, performed all surgical procedures, collected and analysed data; KL: performed anatomical and immunohistochemical analysis, performed and analysed part of the behaviour; AS: performed anatomical and immunohistochemical analysis, performed and analysed single cell PCR and in-situ data; MH: performed anatomical and immunohistochemical analysis; HU: characterized mouse strains, designed experiments; MK: designed experiments, wrote the paper; FB: designed experiments, wrote the paper.

Article

TRANSPARENT PROCESS

THE EMBO JOURNAL

FGF22 signaling regulates synapse formation during post-injury remodeling of the spinal cord

Anne Jacobi[1], Kristina Loy[1], Anja M Schmalz[1], Mikael Hellsten[1], Hisashi Umemori[2,3], Martin Kerschensteiner[1,4] & Florence M Bareyre[1,4,*]

Abstract

The remodeling of axonal circuits after injury requires the formation of new synaptic contacts to enable functional recovery. Which molecular signals initiate such axonal and synaptic reorganisation in the adult central nervous system is currently unknown. Here, we identify FGF22 as a key regulator of circuit remodeling in the injured spinal cord. We show that FGF22 is produced by spinal relay neurons, while its main receptors FGFR1 and FGFR2 are expressed by cortical projection neurons. FGF22 deficiency or the targeted deletion of FGFR1 and FGFR2 in the hindlimb motor cortex limits the formation of new synapses between corticospinal collaterals and relay neurons, delays their molecular maturation, and impedes functional recovery in a mouse model of spinal cord injury. These results establish FGF22 as a synaptogenic mediator in the adult nervous system and a crucial regulator of synapse formation and maturation during post-injury remodeling in the spinal cord.

Keywords axonal remodeling; fibroblast growth factor; functional recovery; spinal cord injury; synapse formation

Subject Categories Neuroscience

DOI 10.15252/embj.201490578 | Received 17 November 2014 | Revised 11 February 2015 | Accepted 16 February 2015 | Published online 12 March 2015

The EMBO Journal (2015) 34: 1231–1243

Introduction

Incomplete lesions of the spinal cord can be followed by substantial functional recovery in both human patients and rodent models. This recovery is mediated by the remodeling of spinal and supraspinal axonal circuits (Weidner *et al*, 2001; Bareyre *et al*, 2004; Girgis *et al*, 2007; Courtine *et al*, 2008; van den Brand *et al*, 2012; Shah *et al*, 2013; Zörner *et al*, 2014). The hindlimb corticospinal tract (CST), for example, responds to a thoracic transection with the *de novo* formation of intraspinal detour circuits that circumvent the lesion site and re-establish a functional connection between the motor cortex and the lumbar spinal cord (Bareyre *et al*, 2004; Lang *et al*, 2012). A key step in the formation of these detour circuits is the establishment of synaptic contacts between newly formed CST collaterals that enter the cervical gray matter and long propriospinal neurons (LPSN) that are located in the cervical spinal cord and act as relays to lumbar motor circuits. Although the functional importance of this and similar detour circuits has been well established over the recent years (Bareyre *et al*, 2004; Courtine *et al*, 2008; van den Brand *et al*, 2012), it is currently unclear how the formation of these circuits is regulated and which molecular signals initiate the establishment of new synaptic contacts in the injured adult central nervous system (CNS).

In the developing nervous system, a number of molecules that can promote synapse formation have been identified (Sanes & Lichtman, 2001; Williams *et al*, 2010; Siddiqui & Craig, 2011). Among these, the family of the fibroblast growth factors and their receptors has emerged as important regulators of presynaptic differentiation (Umemori *et al*, 2004; Stevens *et al*, 2010; Terauchi *et al*, 2010). One member in particular, FGF22—a target-derived secreted factor that can act as a presynaptic organizer—is crucial for the establishment of excitatory synapses as shown for CA3 pyramidal cells in the developing hippocampus (Terauchi *et al*, 2010). Whether such developmental signaling pathways remain operational in adulthood is currently not fully understood.

Here, we now show that FGF22 and its receptors FGFR1 and FGFR2 are constitutively expressed in the adult CNS. Genetic interference with FGF22 signaling either on the level of the ligand or its receptors limits the formation and maturation of new synapses in the injured spinal cord and results in deficient detour circuit formation and attenuated functional recovery. These findings establish FGF22 as an important endogenous regulator of synaptic plasticity and circuit remodeling in the adult nervous system.

Results

Impaired post-injury synapse formation and circuit remodeling in FGF22-deficient mice

To investigate whether FGF22 signaling can regulate synapse formation during axonal remodeling after spinal cord injury, we

1 Institute of Clinical Neuroimmunology, Ludwig-Maximilians Universität München, Munich, Germany
2 Department of Neurology, F.M. Kirby Neurobiology Center, Boston Children's Hospital, Harvard Medical School, Boston, MA, USA
3 Molecular & Behavioral Neuroscience Institute and Department of Biological Chemistry, University of Michigan Medical School, Ann Arbor, MI, USA
4 Munich Cluster of Systems Neurology (SyNergy), Munich, Germany
*Corresponding author. Tel: +49 89 218078283; E-mail: Florence.Bareyre@med.uni-muenchen.de

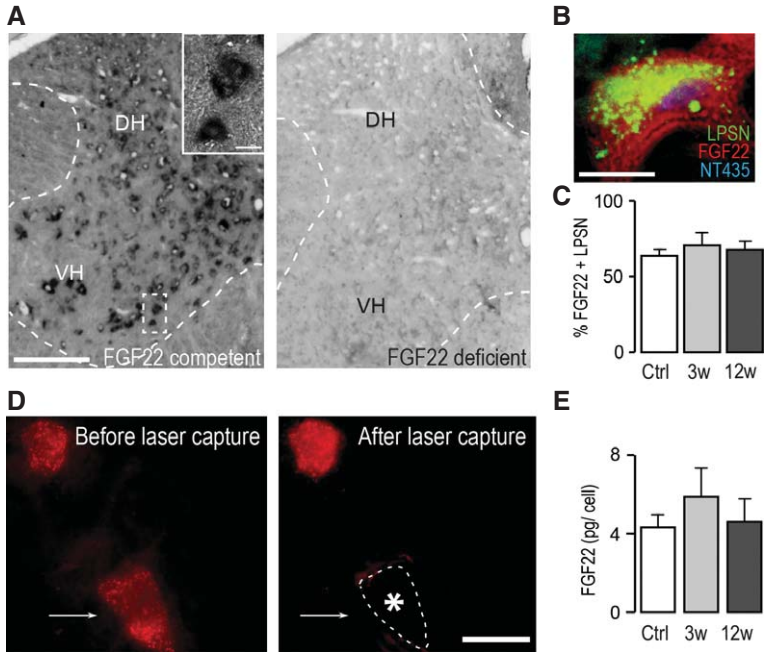

Figure 1. FGF22 is expressed by interneurons in the healthy and injured adult spinal cord.

A *In situ* hybridization of FGF22 mRNA in the spinal cord of FGF22-competent (left panel) and FGF22-deficient (right panel) mice (DH: dorsal horn; VH: ventral horn). Scale bar equals 200 μm (10 μm in inset).

B *In situ* hybridization of a section of the cervical spinal cord at level C4/C5 showing presence of FGF22 mRNA in a long propriospinal neuron (LPSN) retrogradely traced from T12 (LPSN: green; FGF22 mRNA: red; NeuroTrace 435/455: blue). Scale bar equals 20 μm.

C Quantification of the percentage of LPSN showing a FGF22 *in situ* signal in unlesioned mice ('Ctrl') and in mice at 3 ('3w') and 12 ('12w') weeks after spinal cord injury ($n > 30$ LPSN from 2 to 3 animals per group). Mean ± SEM. No significant differences between the groups were detected (ANOVA followed by Tukey tests).

D Images of LPSN (red) before (left panel) and after (right panel) laser microdissection of a single neuron (arrow, asterisk and dotted line in right panel indicate previous location of the microdissected neuron). Scale bar equals 40 μm.

E Quantification of the single-cell PCR analysis of FGF22 mRNA expression in LPSN dissected from unlesioned mice ('Ctrl') and from mice at 3 ('3w') and 12 ('12w') weeks after spinal cord injury (n = 7–8 LPSN per group). Mean ± SEM. No significant differences between the groups were detected (ANOVA followed by Tukey tests).

first assessed whether and where FGF22 is expressed in the spinal cord of adult mice using *in situ* hybridization and single-cell laser microdissection followed by quantitative PCR analysis. Our results showed that FGF22 mRNA is present in spinal interneurons including in a large proportion of long propriospinal neurons both constitutively and at different timepoints after a mid-thoracic spinal cord injury (Fig 1A–E). To investigate the role of spinal FGF22 expression during post-injury remodeling (Fig 2A), we performed a bilateral dorsal hemisection of the spinal cord at T8 in FGF22-deficient mice (Terauchi *et al*, 2010) and age-matched FGF22-competent wild-type mice and traced the hindlimb portion of the corticospinal tract by stereotactic injection of the anterograde tracer biotinylated dextran amine (BDA). Unlesioned FGF22-deficient mice showed a normal density of cortical layer V neurons and an unaltered lumbar and cervical projection pattern of the hindlimb CST (Supplementary Fig S1). At 3 weeks after spinal cord injury, however, FGF22 deficiency diminished the density of boutons on newly formed CST collaterals that enter the gray matter of the cervical spinal cord as part of the detour circuit formation process (Fig 2D and E). As a result, the proportion of long propriospinal relay neurons in the cervical spinal cord that are contacted by these CST collaterals was significantly reduced (Fig 2F and G). In contrast, neither the overall number of CST collaterals that exited the main CST in the cervical spinal cord nor the length of these collaterals was altered in FGF22-deficient mice (Fig 2B and C and Supplementary Fig S2).

FGFR1 and FGFR2 mediate the effects of FGF22 on synapse formation in the injured spinal cord

To better understand which receptors communicate FGF22 signaling to CST collaterals, we first established that the two main receptors of FGF22, FGFR1 and FGFR2 (Singh *et al*, 2012; Umemori *et al*, 2004; Zhang *et al*, 2006), were expressed by cortical projection neurons in adult mice (Fig 3A and B). For this purpose, we performed *in situ* hybridization for FGFR1 and FGFR2 mRNA and retrogradely traced the cortical neurons projecting to the thoracic spinal cord (Fig 3C). Our results showed that more than half of these cortical projection neurons express mRNA for FGFR1 and FGFR2 (Fig 3D). We then conditionally deleted expression of the FGF22 receptors in the forebrain by crossing floxed FGFR1 and FGFR2 mouse strains (Umemori *et al*, 2004; Terauchi *et al*, 2010) to EMX1-Cre mice (Gorski *et al*, 2002; Bareyre *et al*, 2005). Deletion of either receptor did not affect mRNA expression of the other (Fig 3E). Furthermore, forebrain deletion of FGFR1 or FGFR2 did not alter the density of layer V neurons in the cortex or the development of a mature hindlimb CST projection pattern in unlesioned mice (Supplementary Figs S3 and S4). However, when we

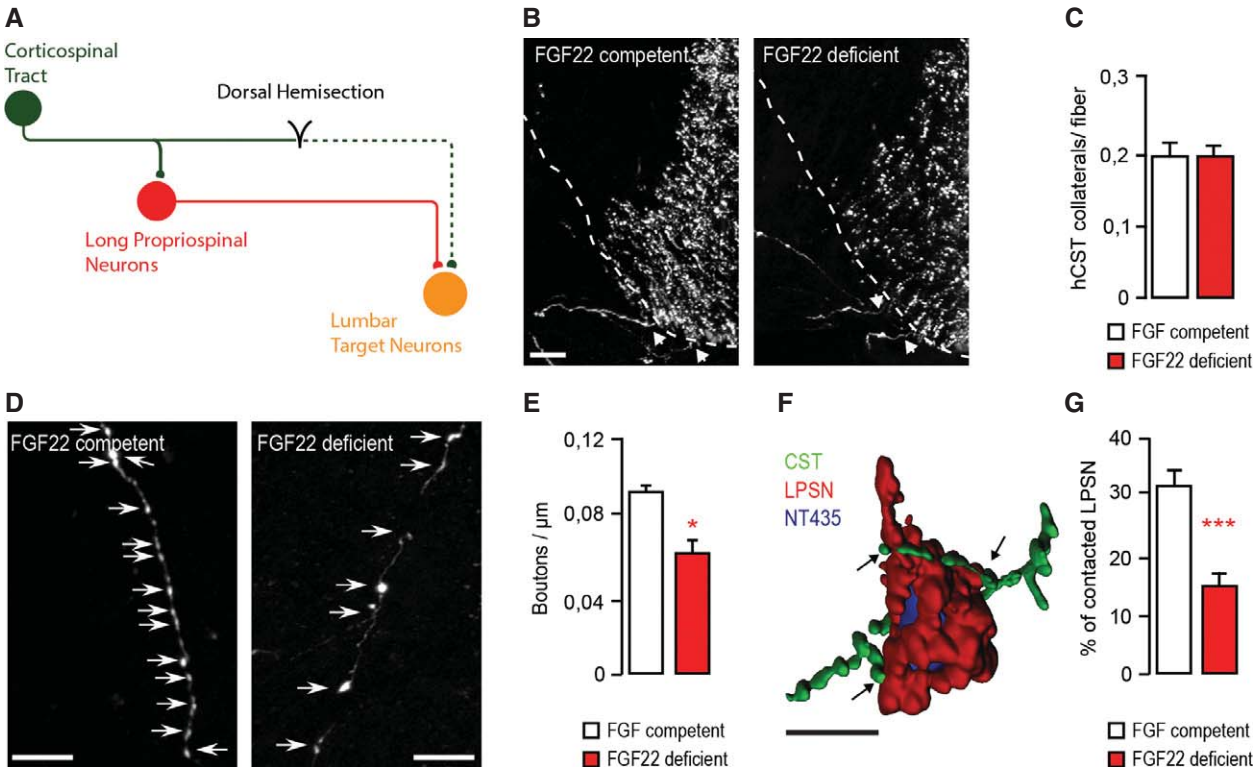

Figure 2. FGF22 deficiency impairs bouton formation and circuit remodeling after spinal cord injury.

A Schematic representation of CST detour circuit formation following a mid-thoracic dorsal bilateral hemisection of the spinal cord.

B Confocal images of hindlimb CST collaterals exiting the main CST tract (arrows) in the cervical spinal cord 3 weeks following a T8 dorsal bilateral hemisection in FGF22-competent (left panel) and FGF22-deficient (right panel) mice. Scale bar equals 40 µm.

C Quantification of the number of exiting hindlimb CST collaterals per labeled hindlimb CST fiber at 3 weeks following T8 dorsal bilateral hemisection in FGF22-competent and FGF22-deficient mice (n = 8 animals per group). Mean ± SEM. No significant differences between the groups were detected (unpaired two-tailed t-test).

D Confocal images showing putative synaptic boutons (arrows) on newly formed cervical hindlimb CST collaterals at 3 weeks following spinal cord injury in FGF22-competent (left panel) and FGF22-deficient (right panel) mice. Scale bar equals 20 µm.

E Quantification of bouton density on newly formed cervical hindlimb CST collaterals in FGF22-competent and FGF22-deficient mice (n = 8 animals per group) at 3 weeks after injury. Mean ± SEM. *P = 0.0244 (unpaired two-tailed t-test).

F 3D Rendering of a confocal image stack that illustrates putative synaptic contacts between CST collaterals (green) and LPSN (red) counterstained with NeuroTrace 435/455 (blue). Scale bar equals 30 µm.

G Quantification of the percentage of LPSN contacted by cervical hindlimb CST collaterals in FGF22-competent and FGF22-deficient mice at 3 weeks after injury (n = 8 animals per group). Mean ± SEM. ***P = 0.0001 (unpaired two-tailed t-test).

performed a thoracic dorsal bilateral hemisection of the spinal cord in these mice, we observed that the deletion of either FGFR1 or FGFR2 reduced the density of boutons on newly formed CST collaterals in the cervical spinal cord at 3 weeks after injury (Fig 4D and E). A similar reduction of CST bouton density in the cervical spinal cord was observed in double-floxed mice, in which both FGFR1 and FGFR2 were depleted in the hindlimb motor cortex by stereotactic injection of a recombinant adeno-associated virus expressing the Cre recombinase (rAAV-GFP-Ires-Cre, Fig 4D and E). Notably, while the length of individual cervical CST collaterals was similar in all groups (Supplementary Fig S2), reduced synapse formation after injury was compensated by sprouting of additional CST collaterals, if either FGFR1 or FGFR2 alone was depleted but not if both receptors were missing (Fig 4A–C). As a result, only mice, in which both FGFR1 and FGFR2 were co-deleted, showed an impaired formation of intraspinal detour circuits (Fig 4F), similar to the one observed in FGF22-deficient mice (Fig 2G).

Genetic disruption of FGF22 signaling delays molecular maturation of synapses after spinal cord injury

To determine whether FGF22 signaling regulates not only the number of new boutons that can be formed but also their molecular composition, we studied the expression of an active zone protein—bassoon—and a synaptic vesicle-associated protein—synapsin—as indicators of synapse maturation (Zhai *et al*, 2001; Shapira *et al*, 2003; Micheva *et al*, 2010; Lang *et al*, 2012). For this purpose, we used confocal microscopy to determine the proportion of boutons on newly formed cervical CST collaterals that were immunoreactive for synapsin and bassoon at different timepoints after a thoracic dorsal bilateral hemisection of the spinal cord. Our results showed that forebrain deletion of either FGFR1 or FGFR2 alone led to a moderate delay in synapse maturation that was most obvious at 3 weeks after injury and primarily altered the presence of synapsin (Fig 5A–D). Furthermore, complete interruption of FGF22 signaling either by conditional deletion of both

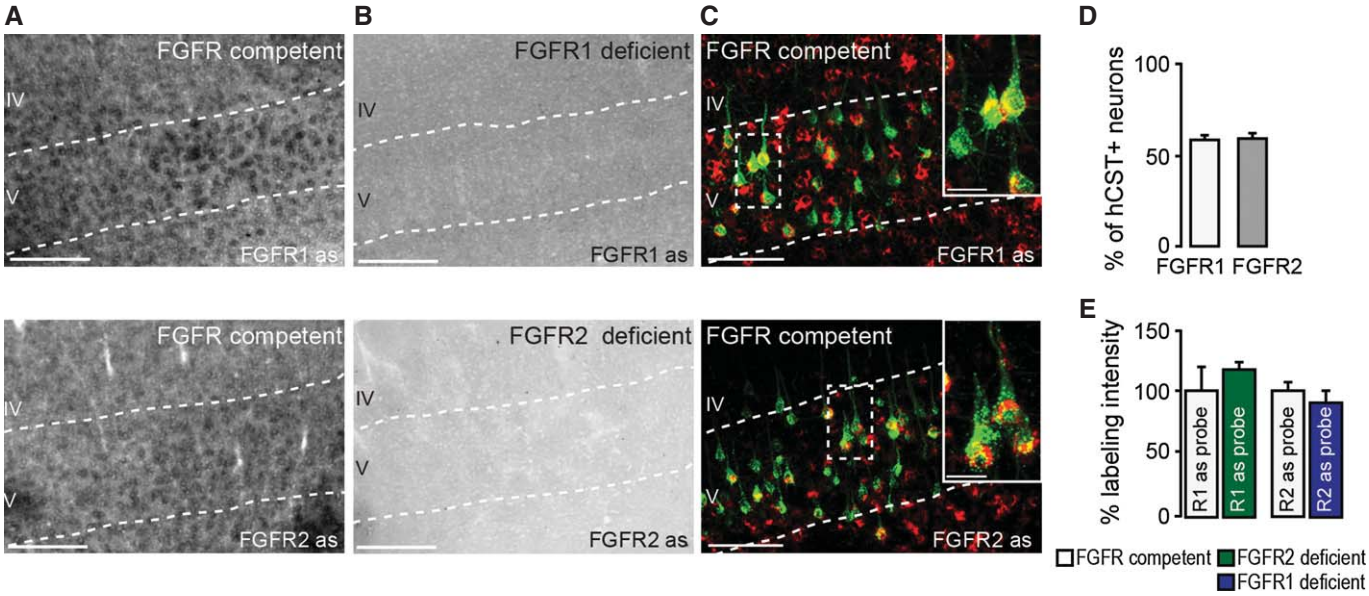

Figure 3. FGFR1 and FGFR2 are expressed in adult cortical projection neurons.

A *In situ* hybridization of FGFR1 (top) and FGFR2 (bottom) mRNA in FGFR-competent mice. Scale bar equals 200 μm.

B *In situ* hybridization of FGFR1 (top) and FGFR2 (bottom) mRNA in forebrain FGFR1 (top)- and FGFR2 (bottom)-deficient mice. Scale bar equals 200 μm.

C Retrograde labeling of CST projection neurons with dextran conjugated with Texas Red® (green) shows that many of these neurons express FGFR1 (red, top) and FGFR2 mRNA (red, bottom; insets in top and bottom panels are twofold magnification of boxed areas). Scale bar equals 100 μm (20 μm in insets).

D Quantification of the percentage of CST projection neurons in layer V of the cortex expressing FGFR1 (white bar) and FGFR2 mRNA (gray bar; n = 5 animals per group). Mean ± SEM.

E Quantification of the intensity of the *in situ* signal for FGFR1 mRNA in FGFR2-deficient mice (green bar) and FGFR2 mRNA in FGFR1-deficient mice (blue bar) normalized to the signal intensity measured in the respective FGFR-competent control group (white bars; n = 3 animals per group). Mean ± SEM. No significant differences between the groups were detected (unpaired two-tailed t-tests).

receptors in the hindlimb motor cortex or by constitutive FGF22 deficiency induced protracted synapse maturation defects that affected the recruitment of both active zone and synaptic vesicle-associated proteins and persisted for at least 12 weeks after injury (Fig 5A–D).

Disturbed FGF22 signaling limits recovery of function after spinal cord injury

Finally, we wanted to understand whether the impaired formation and maturation of new synapses would interfere with the spontaneous recovery of CST function that follows an incomplete spinal cord injury (Bareyre *et al*, 2004). To assess this, we performed thoracic dorsal bilateral hemisections of the spinal cord and followed the recovery of CST function using behavioral testing paradigms such as the 'ladder rung test' (Metz & Whishaw, 2002) and the 'catwalk analysis' (Hamers *et al*, 2006) in FGF22-deficient mice and in mice in which FGFR1 and FGFR2 were conditionally deleted in the hindlimb motor cortex as well as in the respective FGF- and FGFR-competent control mice. While neither of these genetic manipulations altered the size of the thoracic lesions (0.37 ±0.047 mm^3 in FGF22-deficient versus 0.37 ± 0.055 mm^3 in FGF22-competent control mice and 0.35 ± 0.03 mm^3 in hindlimb motor cortex FGFR1/FGFR2-deficient mice versus 0.32 ± 0.054 mm^3 in the FGFR-competent controls; n = 5–7 mice per group), both deletion of FGF22 or co-deletion of FGFR1 and FGFR2 in the hindlimb motor cortex impeded functional recovery after injury. More pronounced deficits remained in mice with impaired FGF22 signaling for at least 3 weeks after injury in both the 'regular walk' and 'irregular walk' paradigms of the ladder rung test as well as measured by the 'paw angle body axis' parameter in the catwalk analysis (Fig 6A–D). In contrast, deletion of either FGFR1 or FGFR2 alone did not alter functional recovery likely due to the compensatory increase in CST sprouting that prevented deficits in detour circuit formation under these conditions (Supplementary Fig S5). Taken together, the results of our behavioral analysis indicate that intact FGF22 signaling is required for the timely recovery of motor function after spinal cord injury.

Discussion

Our study identifies FGF22 as an important contributor to circuit remodeling in the injured adult spinal cord. We show that FGF22 is constitutively expressed by a large proportion of spinal interneurons including those that can function as relays to lumbar motor circuits. FGF22 that is locally released in the spinal gray matter can then come into contact with growing axon collaterals, for example, those emerging from the transected corticospinal tract. The corresponding projection neurons located in layer V of the motor cortex express the mRNA for the main receptors of FGF22, FGFR1 and FGFR2, and the receptor proteins appear to be present along the CST axons as well as in the CST boutons (as we can show for FGFR2, Supplementary Fig S6). Presence of both of

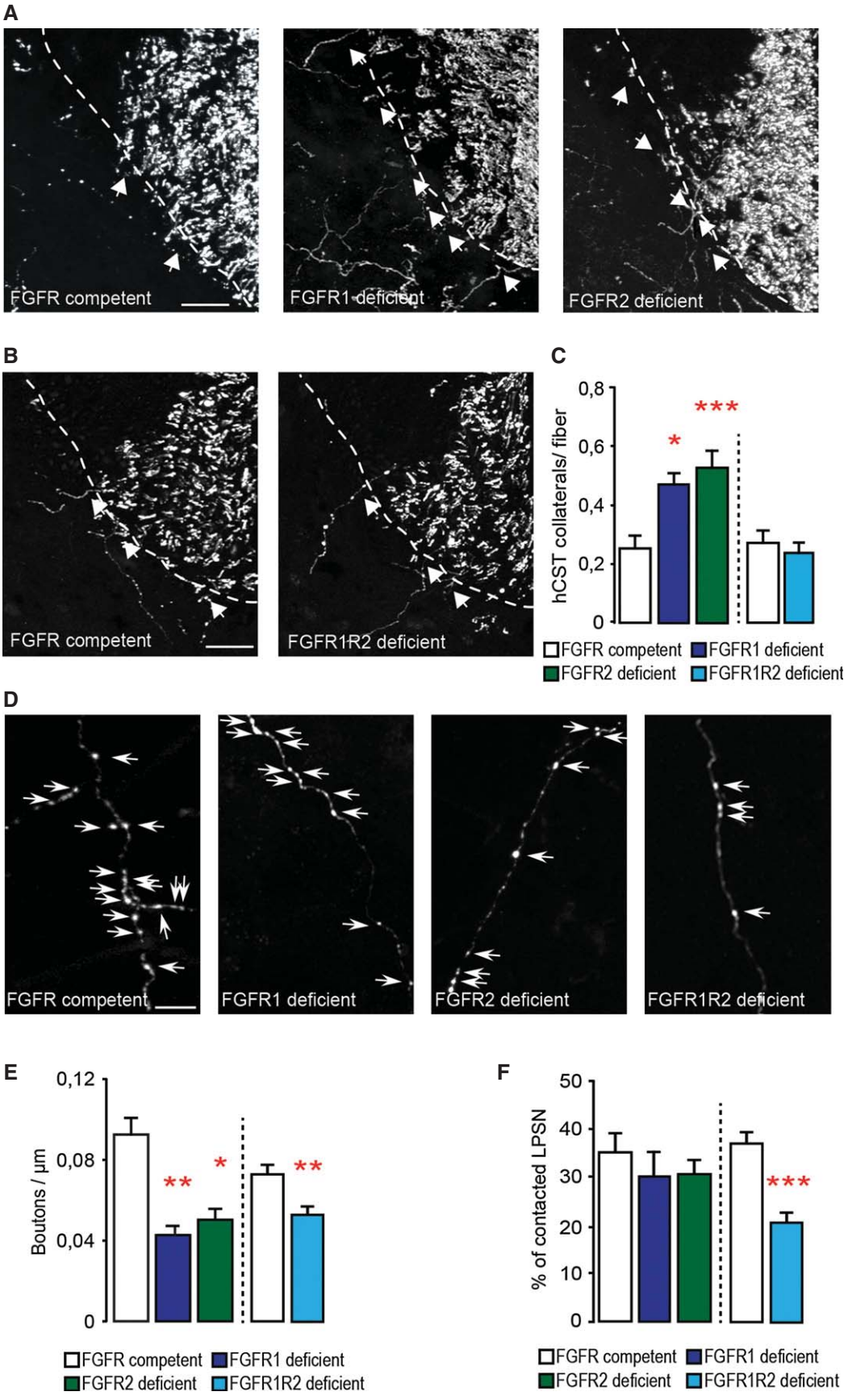

Figure 4.

Figure 4. Deletion of forebrain FGFR1 and FGFR2 expression impairs bouton formation and circuit remodeling after spinal cord injury.

A Confocal images of hindlimb CST collaterals exiting the main CST tract (arrows) in the cervical spinal cord 3 weeks following T8 dorsal bilateral hemisection in FGFR-competent (left panel), forebrain FGFR1-deficient (middle panel), and forebrain FGFR2-deficient (right panel) mice. Scale bar equals 40 μm.

B Confocal images of hindlimb CST collaterals exiting the main CST tract (arrows) in the cervical spinal cord 3 weeks following T8 dorsal bilateral hemisection in FGFR-competent (left panel) and hindlimb motor cortex FGFR1/FGFR2 double-deficient (right panel) mice. Scale bar equals 40 μm.

C Quantification of the number of exiting hindlimb CST collaterals at 3 weeks following T8 dorsal bilateral hemisection in forebrain FGFR single-deficient mice, hindlimb motor cortex FGFR1/FGFR2 double-deficient mice, and the corresponding FGFR-competent control mice (n = 6–15 animals per group). Mean ± SEM. *$P < 0.05$; ***$P < 0.001$ (ANOVA followed by Tukey tests for FGFR-competent versus FGFR single-deficient mice). No significant differences were found between FGFR-competent and FGFR1/FGFR2 double-deficient mice (unpaired two-tailed t-tests).

D Confocal images showing putative synaptic boutons (arrows) on newly formed cervical hindlimb CST collaterals at 3 weeks following spinal cord injury in FGFR-competent (left panel), forebrain FGFR1-deficient (second panel from left), forebrain FGFR2-deficient (second panel from right), and hindlimb motor cortex FGFR1/FGFR2 double-deficient (right panel) mice. Scale bar equals 20 μm.

E Quantification of the bouton density on newly formed cervical hindlimb CST collaterals in FGFR-competent, forebrain single FGFR-deficient, and hindlimb motor cortex FGFR1/FGFR2 double-deficient mice (n = 6–16 animals per group). Mean ± SEM. *$P < 0.05$, **$P < 0.01$ (ANOVA followed by Tukey tests in case of multiple group comparisons, e.g. FGFR-competent versus FGFR single-deficient mice). **$P = 0.0028$ (unpaired two-tailed t-tests for comparisons of FGFR-competent versus FGFR1/FGFR2 double-deficient mice).

F Quantification of the percentage of LPSN contacted by hindlimb CST collaterals in FGFR-competent, forebrain single FGFR-deficient, and hindlimb motor cortex FGFR1/FGFR2 double-deficient mice (n = 6–16 animals per group). ***$P < 0.0001$ (unpaired two-tailed t-tests for comparisons of controls versus FGFR1/FGFR2 double-deficient mice). No significant differences were found between FGFR-competent and FGFR single-deficient mice (ANOVA followed by Tukey tests).

these receptors appears to be required for intact FGF22 signaling to cortical projection neurons as deletion of either one of them results in a decreased density of new CST synapses. However, the alterations induced by the loss of one receptor are mostly temporary and deficits of detour circuit formation and functional recovery can be prevented by compensatory CST sprouting. In contrast, the deletion of both receptors leads to a protracted impairment of synapse formation and maturation after injury that is not compensated by CST sprouting and results in deficient circuit remodeling and attenuated recovery of function. The finding that compensatory sprouting is only observed if either one of the FGF receptors is still present might indicate that FGF22 by itself can promote the formation of additional CST collaterals through either FGFR1 or FGFR2. Alternatively, it is also possible that the induction of this compensatory response requires the presence of at least some mature synapses that are mainly present on the corresponding CST collaterals in the single receptor-deficient mice but not on collaterals that lack both receptors or emerge in FGF22-deficient mice. Taken together, our observations after spinal cord injury indicate that while both FGFR1 and FGFR2 are required for normal FGF22 signaling, loss of one receptor can at least be partially compensated by the presence of its remaining partner. Finally, the finding that FGF22 deficiency and co-deletion of FGFR1 and FGFR2 result in essentially similar changes of synapse formation, circuit remodeling, and functional recovery supports the view that these are indeed the major receptors and ligands involved in this interaction.

It is interesting to note that genetic disruption of FGF22 signaling not only reduces the number of new synapses that can be formed in the injured spinal cord but also alters the molecular composition of those synapses that are formed. These findings are consistent with previous reports that analyzed the role of FGF22 signaling in the developing nervous system. For example, it was shown that genetic inactivation of FGFR2 or FGF22 inhibited presynaptic differentiation in the granule layer of the developing cerebellum as indicated by the reduced immunoreactivity for the vesicle-associated proteins, synapsin and synaptophysin, and the active zone protein, bassoon (Umemori *et al*, 2004). Likewise, the clustering of synaptic vesicles is significantly decreased in the developing hippocampus of FGF22-deficient mice (Terauchi *et al*, 2010). Similar deficits of developmental synapse formation have also been described as the result of impaired FGF22 signaling in the dorsal lateral geniculate nucleus (Singh *et al*, 2012) and at the neuromuscular junction (Fox *et al*, 2007). It is interesting to note that in contrast to these studies, we did not detect abnormalities of CST development in our analysis. This might indicate that the developmental effects of deficient FGF22 signaling are cell type-specific and thus not observed in CST projection neurons or that initial developmental alterations of CST projections are compensated over time and thus no longer apparent in adult mice that we investigate here. The latter seems to be the more plausible explanation as FGF22 signaling can clearly affect CST projection neurons in the injured adult nervous system as we show here, and our analysis of synapse maturation further suggests that FGF22-related synaptic defects can at least partially recover over time. Finally, it is of course possible that more subtle defects, for example, in the number of vesicles per synapse (Terauchi *et al*, 2010) still persist but are not captured by our morphological analysis of the CST projection pattern.

While the role of FGF22-FGFR signaling has thus been well characterized in the developing nervous system, we now show that neuronal expression of FGF22 and its receptors FGFR1 and FGFR2 persists into adulthood. This constitutive expression of FGF22 and its receptors in the adult CNS is in line with the findings of a recent more systematic analysis that shows that many developmental signals that regulate axon guidance and synapse formation are still present in the mature brain and spinal cord (Jacobi *et al*, 2014). Indeed, important roles in the injured adult nervous system are emerging for a number of these molecules. For example, molecules such as EphA4, Sema3A, and Sema6A have all been shown to limit axonal regeneration following adult spinal cord injury (Kaneko *et al*, 2006; Goldshmit *et al*, 2011; Shim *et al*, 2012), while Sema3A and Sema3F influence remyelination (Piaton *et al*, 2011). Taken together, the persistence of these developmental signaling pathways suggests that the molecular machinery that allows the initial formation of neuronal circuits

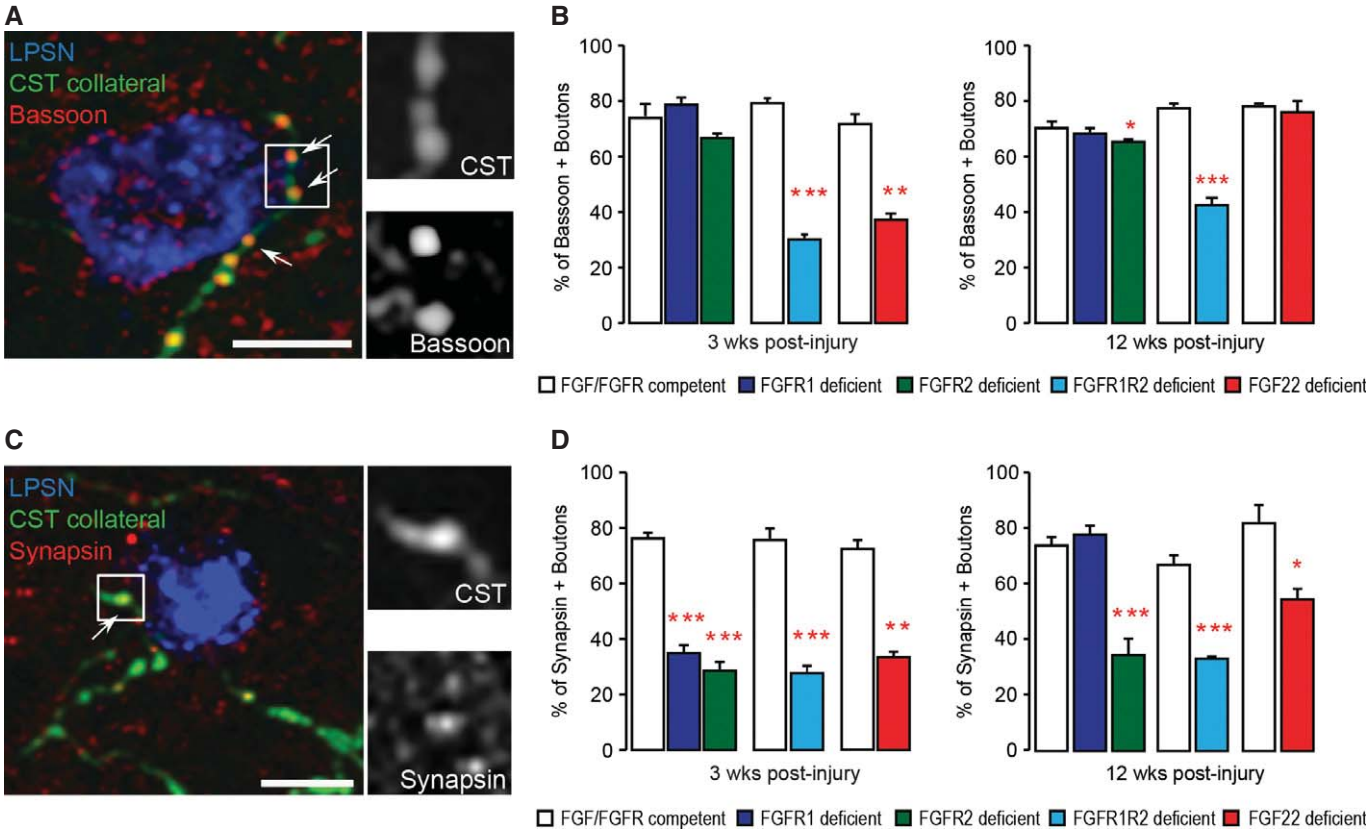

Figure 5. Deletion of FGF22 or its receptors delays synapse maturation following spinal cord injury.

A Confocal image of synaptic contacts (arrows) between a CST collateral (green) and a LPSN (blue) that show bassoon immunoreactivity (red). Right images are magnification (two and a half-fold) of the area boxed on the left. Scale bar equals 25 μm.

B Quantification of the percentage of boutons on cervical hindlimb CST collaterals that are immunoreactive for bassoon at 3 weeks (left) and 12 weeks (right) after spinal cord injury in FGF22-deficient, forebrain FGFR1-deficient, forebrain FGFR2-deficient and hindlimb motor cortex FGFR1/FGFR2 double-deficient mice compared to the respective FGF22- and FGFR-competent control mice. A minimum of 100 boutons per mouse were evaluated for 3 mice per group. ***$P < 0.0001$ FGFR-competent versus FGFR1/FGFR2 double-deficient mice at 3 weeks (unpaired two-tailed *t*-tests), **$P = 0.002$ FGF-competent versus FGF22 deficient at 3 weeks (unpaired two-tailed *t*-tests), *$P < 0.05$ FGFR-competent versus FGFR2 single-deficient mice at 12 weeks (one-way ANOVA followed by Tukey tests), ***$P = 0.001$ FGFR-competent versus FGFR1/FGFR2 double-deficient mice at 12 weeks (unpaired two-tailed *t*-tests).

C Confocal image of synaptic contacts (arrows) between a CST collateral (green) and a LPSN (blue) that show synapsin I immunoreactivity (red). Right images are magnification (two and a half-fold) of the area boxed on the left. Scale bar equals 25 μm.

D Quantification of the percentage of boutons on cervical hindlimb CST collaterals that are immunoreactive for synapsin I at 3 weeks (left) and 12 weeks (right) after spinal cord injury in FGF22-deficient, forebrain FGFR1-deficient, forebrain FGFR2-deficient and hindlimb motor cortex FGFR1/FGFR2 double-deficient mice compared to the respective FGF22 and FGFR-competent control mice. A minimum of 100 boutons per mouse were evaluated for 3 mice per group. ***$P < 0.001$ FGFR-competent versus FGFR1 and FGFR2 single-deficient mice at 3 weeks (one-way ANOVA followed by Tukey tests). ***$P = 0.0001$ FGFR-competent mice versus FGFR1/FGFR2 double-deficient mice at 3 weeks (unpaired two-tailed *t*-tests), $P = 0.00004$ FGF-competent mice versus FGF22-deficient mice at 3 weeks (unpaired two-tailed *t*-tests). ***$P < 0.001$ FGFR-competent versus FGFR2 single-deficient mice (one-way ANOVA followed by Tukey tests). ***$P = 0.0006$ FGFR-competent mice versus FGFR1/FGFR2 double-deficient mice at 12 weeks (unpaired two-tailed *t*-tests), *$P = 0.027$ FGF-competent mice versus FGF22-deficient mice at 12 weeks (unpaired two-tailed *t*-tests).

stays in place in the adult nervous system and provides the blueprint for ongoing nervous system plasticity. Indeed, it is increasingly appreciated that axonal remodeling processes both at the lesion site but also involving distant spinal and supraspinal circuits take place in the injured adult CNS, where they enable functional recovery (Weidner *et al*, 2001; Bareyre *et al*, 2004; Girgis *et al*, 2007; Courtine *et al*, 2008; van den Brand *et al*, 2012; Zörner *et al*, 2014). While such circuit remodeling can be initiated spontaneously, its therapeutic success can be enhanced by manipulations that foster neuronal growth initiation (Lang *et al*, 2013; Yip *et al*, 2010), neutralize plasticity restrictions (García-Alías *et al*, 2009; Lindau *et al*, 2014), and stimulate activity-based rehabilitation (van den Brand *et al*, 2012; Shah *et al*, 2013). An improved understanding of the endogenous signaling networks that enable the reorganization of axonal connections is a key requirement both for the informed advancement of such therapeutic strategies and for the identification of novel targets and approaches. Here, we uncover an integral component of these signaling networks and identify FGF22 as a synaptogenic mediator in the adult nervous system that is required for *de novo* synapse formation and timely synapse maturation during post-injury remodeling of the CNS.

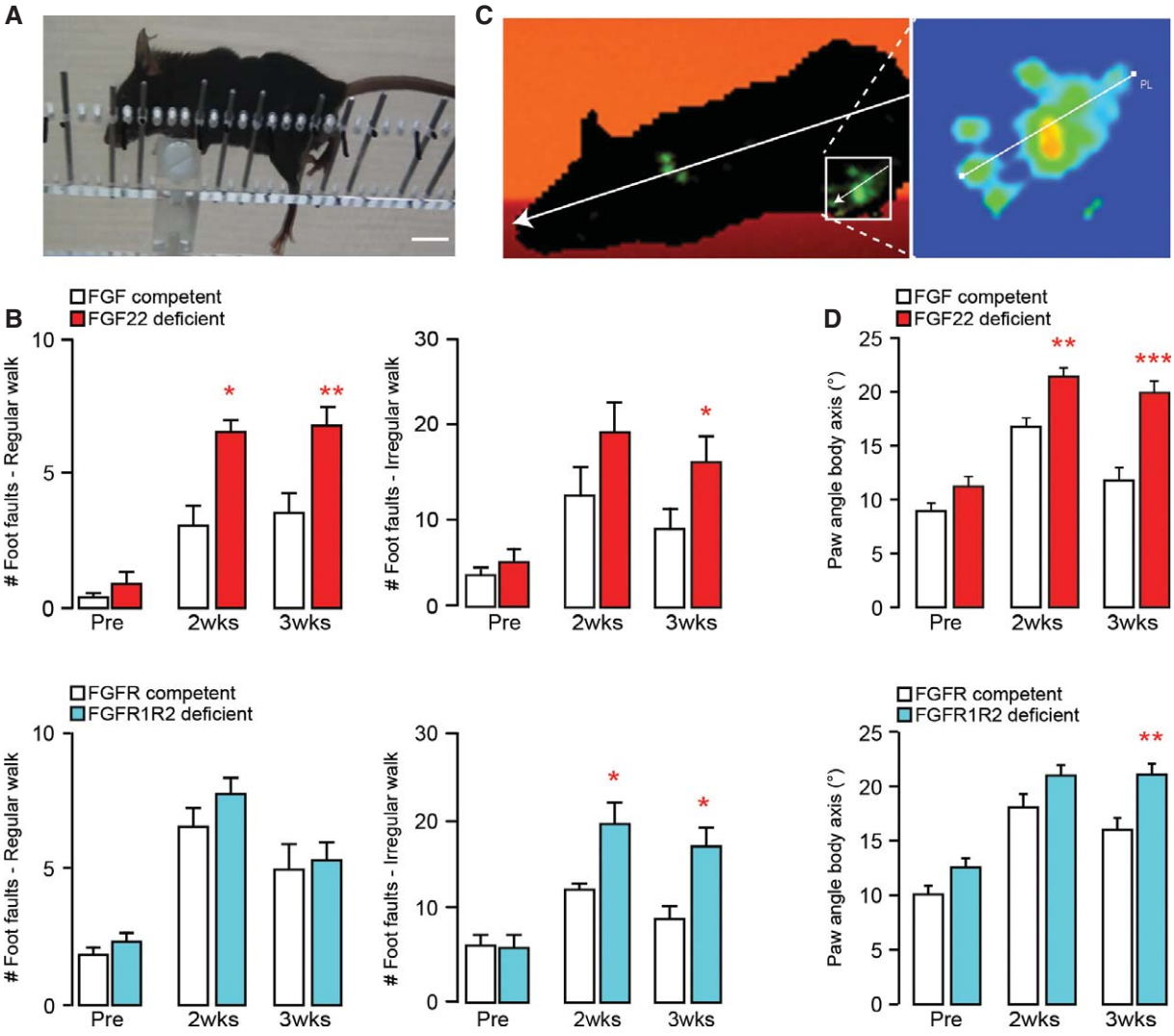

Figure 6. Genetic disruption of FGF22 signaling impedes functional recovery following spinal cord injury.

A Image of a spinal cord injured mouse performing the irregular ladder rung test that assesses recovery of CST function. Scale bar equals 1 cm.

B Quantification of the functional recovery in the ladder rung test (regular walk, left panels; irregular walk, right panels) in FGF22-deficient (top panels, red bars), and hindlimb motor cortex FGFR1/FGFR2 double-deficient (bottom panels, blue bars) mice and the respective FGF22- and FGFR-competent control mice (white bars) before ('Pre') and 2 ('2 wks') and 3 ('3 wks') weeks after a spinal cord injury (n = 7–10 animals per group). *$P < 0.05$, **$P < 0.01$ (repeated-measure ANOVA followed by Bonferroni tests).

C Image of a spinal cord injured mouse walking on the catwalk that assesses locomotor recovery. Illumination of the paws from below allows to determine the paw angle body axis by relating the axis of the paw (line shown magnified in the right panel) to the axis of the body (line shown in left panel).

D Quantification of the paw angle body axis of the hindpaws in FGF22-deficient (top panel, red bars) and hindlimb motor cortex FGFR1/FGFR2 double-deficient (bottom panel, blue bars) mice and respective FGF22- and FGFR-competent control mice (white bars) before ('Pre') and 2 ('2 wks') and 3 ('3 wks') weeks after a spinal cord injury. Between 13 and 40 steps were analyzed per group and timepoint (n = 10–15 animals per group). **$P < 0.01$, ***$P < 0.001$ (two-way ANOVA followed by Bonferroni tests).

Materials and Methods

Animals

Adult mice from 6 to 12 weeks of age were used in the study. To investigate the role of FGF22 during detour circuit formation after injury, we used FGF22 knockout mice (Terauchi *et al*, 2010). Age-matched wild-type C57Bl6j mice (Janvier, France) were used as FGF22-competent controls. To obtain forebrain FGFR1- or FGFR2-deficient mice, we crossed $FGFR1^{fl/fl}$ or $FGFR2^{fl/fl}$ mice (Pirvola *et al*, 2002; Yu *et al*, 2003), in which the FGFR1 or FGFR2 gene is flanked by loxP sites, to EMX1-Cre mice (Gorski *et al*, 2002; Bareyre *et al*, 2005), which express the Cre recombinase in the forebrain starting on embryonic day 10. Cre-negative littermates were used as FGFR-competent controls. For co-deletion of FGFR1 and FGFR2 in cortical projections, we injected a recombinant adeno-associated virus expressing the Cre recombinase (rAAV-GFP-Ires-Cre) in the hindlimb motor cortex of double-floxed $FGFR1^{fl/fl}$/$FGFR2^{fl/fl}$

mice. Littermates injected in the same anatomical location with a rAAV-Ires-GFP served as FGFR-competent controls. All animal procedures were performed according to institutional guidelines and were approved by the local regulatory authorities.

In situ hybridization

Spinal cord tissue (cervical region C3–C5) and brain tissue (bregma −1.06 till −1.70) were sectioned coronally (20 μm thick for the spinal cord, 30 μm thick for the brain) using a cryostat (Leica CM1850) and processed as described previously (Jacobi *et al*, 2014). Briefly, all steps were carried out with DEPC-treated solutions to prevent degradation of target RNAs. Sections were washed in 2× SSC (from 20× stock solution containing 3 M NaCl and 0.3 M Na citrate), and before the pre-hybridization step, the sections were incubated in a 1:1 mixture of 2× SSC and hybridization buffer (50% formamide, 5× SSC, 5× Denhardt's solution, 250 μg/ml yeast tRNA, 500 μg/ml salmon sperm DNA) for 15 min at RT. Sections were then incubated for 1 h in hybridization buffer at the appropriate (pre-) hybridization temperature (65°C). For hybridization, the probe (200–400 ng/ml in hybridization buffer) was heated for 10 min at 80°C, applied to the tissue, and incubated overnight in an oven at 65°C. Sections were then rinsed at RT in 2× SSC and washed in decreasing concentration of SSC (2× to 0.1× SSC at hybridization temperature) before applying an alkaline-phosphatase-conjugated sheep anti-digoxigenin antibody, Fab fragments (1:2,000; Roche Diagnostics), in blocking buffer overnight at 4°C. Alkaline phosphatase activity was detected using nitroblue tetrazolium chloride (337.5 mg/ml) and 5-bromo-4-chloro-3-indolyl phosphate (175 mg/ml). The sections were washed in ddH_2O after the staining procedure. The fluorescent Nissl stain NeuroTrace 435/455 (Life Technologies) was applied for 2 h at RT, and the sections were washed and mounted with Gel Mount (Sigma-Aldrich).

Laser microdissection and single-cell qPCR

Laser microdissection and single-cell qPCR was performed as follows (Hofbauer *et al*, 2003): Total RNA was isolated from LPSN derived from unlesioned animals and from lesioned animals at 3 weeks and 12 weeks post-injury. For this purpose, 20-μm-thick fresh frozen coronal sections of the cervical spinal cord (C3–C5) were collected on Membrane Slides 1.0 PET (Zeiss). Sections were covered with n-propanol to prevent drying and inhibit RNase activity, and transferred to a PALM Microbeam-Z microscope (Zeiss Axiovert 200 M). LPSN retrogradely labeled with dextran TexasRed® and located in the spinal laminae 6–9 at spinal level C4 were marked electronically. After evaporation of the n-propanol, neurons were laser (Crylas FTSS 355-50)-microdissected and pressure-catapulted into a reaction tube (AdhesiveCap 200 clear PCR tubes; Zeiss) and directly transferred on dry ice. For single-cell qPCR, we used the Single cell-to-CT kit (Life Technologies). Primers were as follows: FGF22 forward primer 5′-ACT TTT TCC TGC GTG TGG AC-3′, FGF22 reverse primer 5′-TCA TGG CCA CAT AGA AGC CT-3′; GAPDH forward primer 5′-TCA ACG ACC CCT TCA TTG-3′, GAPDH reverse primer 5′-ATG CAG GGA TGA TGT TCT G-3′. Amplification reaction was performed as follows: 95°C for 3 min, 95°C for 10 s, 56°C for 10 s (39 repeats), and a melting curve with 65–95°C increments.

Generation and production of AAV vectors

pAAV-CMV-GFP-Ires2-Cre (rAAV-GFP-Ires-Cre) was created by inserting an Ires sequence from pIres2-DsRed2 (BD Bioscience) at the HincII site of pAAV-CMV-MCS. The coding sequence for the Cre recombinase was excised from PBS185 (kind gift of Thomas Hughes, Montana State University) and inserted upstream of the Ires sequence. Green fluorescent protein (GFP) was excised from pEGFP-N1 and inserted downstream of the Ires sequence. The control pAAV-CMV-GFP (rAAV- GFP) used was a kind gift of Hildegard Büning (University of Cologne). Recombinant AAV chimeric virions containing a 1:1 ratio of AAV1 and AAV2 capsid proteins and the foreign gene were generated as previously described (Grimm *et al*, 2003; Klugmann *et al*, 2005). Genomic titers were as follows: rAAV-GFP-Ires-Cre, 1.2×10^{12} genome copies/ml; rAAV-GFP, 2.4×10^{12} genome copies/ml.

Surgical procedures

Mid-thoracic dorsal hemisection

Mice were anesthetized with i.p. injections of ketamine/xylazine (ketamine 100 mg/kg, xylazine 13 mg/kg). After a laminectomy to expose the dorsal spinal cord at thoracic level 8 (T8), a thoracic dorsal hemisection, which results in a bilateral transection of the main dorsal and minor dorsolateral CST component but leaves the ventral white matter intact, was performed with fine iridectomy scissors as previously described (Bareyre *et al*, 2004; Lang *et al*, 2013). Prior to and after surgery, animals were kept on a heating pad (38°C) until fully awake and treated with meloxicam (Metacam; Boehringer Ingelheim) twice per day for 48 h.

Stereotactic injection of rAAV into the hindlimb motor cortex

To study the effects of FGFR1 and FGFR2 deletion in cortical projection neurons, we pressure injected 0.7 μl of rAAV-GFP-Ires-Cre or control rAAV-GFP (concentration matched to 0.6×10^{12} genome copies/ml) 4 days prior to the spinal cord injury into the hindlimb motor cortex of double-floxed $FGFR1^{fl/fl}$/$FGFR2^{fl/fl}$ mice using a finely pulled glass micropipette (coordinates from bregma: −1.3 mm, ± 1.0 mm lateral, 0.6 mm depth). The micropipette remained in place for 3 min following the injection. In order to verify that the virus remained confined to the hindlimb motor cortex and did not spread to the forelimb area, we amplified the GFP signal with an anti-GFP antibody (rabbit polyclonal anti-GFP; Life Technologies A11122), cut consecutive 50-μm-thick sections of the entire brain of all mice, and assessed the presence of GFP-labeled cells in layer V of the hindlimb and forelimb motor cortex (Supplementary Fig S7). Mice in which GFP-labeled cells were present in the forelimb motor cortex (coordinate from bregma starting at +0.14 mm) were excluded from further analysis. To control for possible differences related to genetic or viral deletion of FGFRs, we deleted FGFR2 in the hindlimb cortex by injecting 0.7 μl of AAV-GFP-Ires-Cre at the following coordinates (bregma: −1.3 mm caudal, ± 1.0 mm lateral, 0.6 mm depth) in single-floxed $FGFR2^{fl/fl}$ mice. This deletion strategy induced similar changes of CST collateral and bouton formation (Supplementary Fig S8) as the genetic deletion of FGFR2 induced by crossing $FGFR2^{fl/fl}$ mice to EMX1-Cre mice (Fig 4A–F).

Labeling of the hindlimb CST (hCST) fibers

The hindlimb CST of forebrain FGFR1- or FGFR2-deficient mice was traced by pressure injecting 1.5 μl of a 10% (in 0.1 M PB) solution of biotinylated dextran amine (BDA, 10,000 MW; Life Technologies) into the hindlimb motor cortex using a finely pulled glass micropipette 2 weeks prior to sacrifice (coordinates: −1.3 mm to bregma, 1 mm lateral to bregma, 0.6 mm depth). The micropipette remained in place 3 min following the injection.

Labeling of long propriospinal neurons

Long propriospinal neurons were retrogradely labeled by pressure injections of 0.5 μl of 2.5% dextran conjugated with Texas Red® (3,000 MW; Life Technologies D-3328). Briefly, a laminectomy was performed at thoracic level 12 as previously described (Lang *et al*, 2013) and 0.5 μl of 2.5% dextran conjugated with Texas Red® was injected into each side of the spinal cord using a thin glass capillary (coordinates from central vein: ± 0.6 mm, depth: 0.9 mm). The capillary was maintained in place for 3 min following the injection. The number of labeled long propriospinal neurons in the cervical spinal cord (spinal level C4) did not differ significantly between lesioned and unlesioned mice, indicating that the thoracic dorsal bilateral hemisection did not transect the propriospinal projections that run in the ventral white matter (118.6 ± 8.41 labeled propriospinal neurons in lesioned mice versus 111.3 ± 3.8 labeled propriospinal neurons in unlesioned mice; $n = 20$ sections per mouse, 3 mice per group analyzed).

Labeling of cortical projection neurons

Co-localization of the *in situ* hybridization (ISH) signal with the cortical projection neurons of the transected CST was assessed after retrogradely labeling these neurons as shown previously (Lang *et al*, 2013; Jacobi *et al*, 2014). Briefly, 7 days before sacrifice, a laminectomy at thoracic level 8 of the spinal cord was performed and 0.5 μl of dextran conjugated with Texas Red® (5% in 0.1 M PB; Life Technologies) was stereotactically injected rostral to the lesion with a glass capillary into each side of the spinal cord (± 0.2 mm lateral from spinal midline, depth 0.3 mm). The micropipette remained in place for 3 min after completing the injection to avoid backflow. After retrograde labeling, mice were kept on a heating pad (38°C) until fully awake and treated with meloxicam (Metacam; Boehringer Ingelheim) for two more days.

Tissue processing and histological analysis

Mice were deeply anesthetized with isoflurane and perfused transcardially with 4% paraformaldehyde (PFA) in 0.1 M phosphate buffer (PB). Brains and spinal cords were dissected and post-fixed overnight in 4% PFA. The tissue was then cryoprotected in 30% sucrose (Sigma) for at least 3 days. Coronal sections (50 μm thick) were cut on a cryostat. To visualize CST collaterals, BDA detection was performed as follows: Sections were incubated in ABC complex (Vector Laboratories) overnight at 4°C. After a 20-min tyramide amplification (Biotin-XX, TSA Kit #21; Life Technologies), sections were incubated overnight with streptavidin conjugated to FITC (1:500; Life Technologies). To visualize CST collaterals in rAAV-injected mice, an anti-GFP (rabbit polyclonal anti-GFP; Life Technologies A11122) staining was performed to amplify the GFP signal. For this purpose, an anti-GFP antibody (Life Technologies) diluted 1:500 in PBS containing 0.1% Triton X-100 and 2.5% goat serum (Life Technologies) was applied and incubated overnight at 4°C. On day 2, the corresponding secondary antibody was applied for at least 4 h (goat anti-rabbit conjugated with Alexa 488).

For immunohistochemical analysis of synapse maturation, 20-μm-thick sections were cut and blocked for 1 h with 5% goat serum and 0.3% Triton X-100 diluted in 1× PBS. Sections were incubated with ABC (Vector Laboratories) and a rabbit polyclonal antibody reactive against synapsin I (Millipore AB1543; dilution 1:500) or a mouse monoclonal antibody reactive against bassoon (ENZO Life Science SAP7F407, dilution 1:200) in 0.1 M Tris buffer containing 2% horse serum overnight at 4°C. The following day, after a 20-min tyramide amplification (Biotin-XX, TSA Kit #21; Life Technologies) to detect BDA, sections were then incubated together with streptavidin–FITC (1:500; Life Technologies) and the appropriate secondary antibodies for the synaptic markers (donkey anti-rabbit conjugated with Alexa Fluor 647 or goat anti-rabbit conjugated with Alexa Fluor 635) overnight at 4°C. For the analysis of rAAV-injected animals, the sections were first incubated with an anti-GFP antibody (see above) to amplify the GFP signal together with the primary antibodies against synapsin I or bassoon (concentrations as above) in 2.5% goat serum and 0.1% Triton X-100 in 1× PBS overnight at 4°C. On the next day, the appropriate secondary antibodies for the anti-GFP (goat anti-rabbit conjugated with Alexa Flour 488) and anti-synapsin I and anti-bassoon primary antibodies (donkey anti-rabbit conjugated with Alexa Fluor 647 or goat anti-rabbit conjugated with Alexa Fluor 635) were applied overnight at 4°C. For FGFR2 immunohistochemistry, the above-described protocol was used, but sections were pre-treated with trypsin for 10 min at 37°C for antigen retrieval. Then, sections were incubated with an antibody reactive against FGFR2 (1:500, ABCAM ab10648) and a goat anti-rabbit Alexa 488 secondary antibody (1:500). The counterstaining was performed with NeuroTrace 435/455, and sections were mounted in Vectashield (Vector Laboratories).

Quantifications

Quantification of exiting hindlimb CST fibers

To evaluate axonal remodeling following a mid-thoracic dorsal bilateral hemisection of the spinal cord, CST collaterals entering the gray matter at cervical levels C4 were counted on 30 consecutive coronal sections per animal using a light microscope (Olympus IX471) with a ×40/0.65 air objective. To correct for differences in inter-animal tracing efficiency, the number of collaterals was divided by the number of labeled fibers in the main CST tract and expressed as the ratio of exiting collaterals per main CST fiber (Bareyre *et al*, 2004). All quantifications were performed by an observer blinded with respect to injury status and genotype/treatment.

Quantification of contacts onto LPSN

For quantifying the proportion of contacts of LSPN contacted by CST collaterals, a total amount of 30 sections of the cervical spinal cord (level C3–C5) were evaluated using a fluorescent microscope (Olympus IX471) with a ×40/0.65 air objective. Collaterals were visualized as mentioned above (tyramide amplification or GFP amplification); the number of LPSN contacted by CST collaterals and the total number of LPSN labeled were counted. The proportion of LPSN contacted by CST collaterals was then calculated as the

ratio of all LPSN contacted by collaterals over the total number of LPSN. Values were further normalized according to the number of labeled fibers in the main CST tract. All quantifications were performed by an observer blinded with respect to injury status and genotype/treatment.

Quantification of the length of the collaterals and density of boutons

To determine the length of the collaterals and the number of bouton per μm collateral, 10 sections spanning the C3 to C5 area of the cervical spinal cord (50 μm thickness, sections randomly taken) were acquired with an Olympus FV1000 confocal microscope equipped with standard filter sets and a ×60/1.45 oil immersion objective. Image stacks obtained with confocal microscopy were processed using ImageJ software to generate maximum intensity projections. The lengths of all individual collaterals in those sections were measured with the help of the measurement tool of ImageJ and averaged to obtain the average collateral length per section. This value was then further averaged across all (10) sections evaluated for a given animal. All boutons on CST collaterals in the cervical cord were counted in 30 sections under a fluorescent microscope. A bouton was defined as a thick varicosity along a comparably thin CST collateral in the cervical spinal cord. The total number of boutons per animal was divided by the total length in micrometers of collaterals per animal to calculate the density in boutons/μm. All quantifications were performed by an observer blinded with respect to injury status and genotype/treatment.

Quantification of synaptic marker expression

To determine the proportion of boutons that express the active zone protein, bassoon, and the synaptic vesicle-associated protein, synapsin I, about 20 sections spanning the C3 to C5 area of the cervical spinal cord (20 μm thickness, with every 5th section taken) were stained with anti-bassoon and anti-synapsin I antibodies as described above. Image stacks of CST collaterals (labeled as described above) were then acquired with an Olympus FV1000 confocal microscope equipped with standard filter sets and a ×60/1.45 oil immersion objective and processed using ImageJ software. Image stacks were used for analysis, and maximum intensity projections were generated for figure representation. The percentages of synapsin I- or bassoon-positive boutons were determined in confocal image stacks (all single planes from the image stacks were analyzed) upon the following criteria: A bouton was defined as a thick varicosity along a comparably thin CST collateral in the cervical spinal cord. Such a bouton was considered synapsin I or bassoon positive when the respective synapsin I or bassoon immunosignal covered the contour of the bouton but did not extend beyond it. The number of boutons positive for synapsin I or bassoon was expressed as a percentage of all CST boutons evaluated in the cervical spinal cord. A minimum of 300 boutons per group was counted. All quantifications were performed by an observer blinded with respect to injury status and genotype/treatment.

Cortical neuronal density

To determine whether genetic deletion of FGFR1 or FGFR2 at embryonic day 10 or constitutive FGF22 deficiency alters cortical lamination and cortical neuronal density, we cut 50-μm brain sections and performed NeuN immunohistochemistry (using an anti-NeuN antibody, Millipore, dilution 1:500, stained at 4°C overnight). Counterstaining was performed with NeuroTrace 500/525. The density of cells in layer V of the motor cortex and somatosensory cortex was quantified by counting the number of NeuN-positive cells in a defined box of 37.5 mm^2 that was positioned on layer V on a total of 5 sections spanning the cortex at the following coordinates from bregma 1.5, 0.5, −0.22, −1.06, −1.3. Data were expressed as a number of neurons per 37.5 mm^2. All quantifications were performed by an observer blinded with respect to injury status and genotype.

Quantification of retrogradely labeled CST neurons co-labeled with ISH

The co-labeling of retrogradely labeled cortical projection neurons with an ISH signal was assessed under the fluorescent microscope (Olympus IX71) by alternating between fluorescence and bright field illumination. To determine the proportion of cortical projection neurons that express FGFR1 or FGFR2, we counted all retrogradely labeled neurons on every third section of the cortex (n = 3 mice). Sections were assessed from anterior to posterior starting with the first section in which retrogradely labeled CST neurons appeared. Results were expressed as a ratio of the number of double-labeled neurons divided by the total number of retrogradely labeled neurons. All counts were performed by an observer blinded with respect to injury status and genotype/treatment.

Lesion volume

We assessed the extent of the spinal cord lesion in FGF22-deficient and hindlimb motor cortex FGFR1/FGFR2 double-deficient mice as well as the respective FGF22- and FGFR-competent control animals by measuring the lesion volume on longitudinal 50-μm-thick sections of the thoracic spinal cord that spanned the entire lesion extent. Following staining with a fluorescent Nissl dye (NT435; Life Technologies N-21479, dilution 1:500), the sections were imaged using an Olympus IX71 microscope. Images were then processed with ImageJ and the lesion area, including both the cavity and surrounding damaged tissue, was outlined. To calculate the total lesion volume, the measured lesion area of each section was multiplied by the section thickness (50 μm) and the results of all consecutive sections spanning the entire lesion extension were summed up for each animal.

Behavioral analysis

The following behavioral tests were used to assess locomotor recovery after spinal cord injury.

Ladder rung test

For assessment of the CST function following spinal cord injury, we used the ladder rung test (also called grid walk test) as previously described (Metz & Whishaw, 2002). Briefly, mice were scored for their ability to cross a 1-m-long horizontal metal-rung runway with either regular gaps of 1 cm (regular walk) or varying gaps of 1–2 cm (irregular walk) between the rungs. All mice underwent a couple of familiarization sessions with the task prior to preoperative baseline testing. Following familiarization, sessions were videotaped and scored to determine baseline performance. Preoperative scores as well as postoperative performance at 2 and 3 weeks post-injury were assessed. A hindlimb foot error was defined as a complete miss or slip from the rung at the moment of the placement of the

paw onto the rung. Baseline and postoperative testing sessions consisted of 3 runway crossings. The total number of errors of the hindlimbs in each session was counted.

Catwalk analysis

To further evaluate unforced locomotion and gait patterns in FGF22-deficient as well as hindlimb motor cortex FGFR1/FGFR2 double-deficient mice, the Catwalk XT™ (Hamers *et al*, 2006; Noldus) was used. For data collection, all animals were familiarized with the system at least 3 times prior to preoperative baseline acquisition and the system was calibrated each day prior to acquisition. Three valid runs for each timepoint (−2 days, 2 weeks, 3 weeks) and each animal were recorded. A run was considered valid if it fulfilled the requirements pre-set in the system, a minimum run duration of 0.5 s, a maximum run duration of 4.0 s, and a maximum speed variation of 60% to ensure that the animal constantly walks on the runway without pausing. The body axis and paw angle was calculated by the software and the paw angle body axis was calculated as the deviation (in °) of the paw angle from the body axis.

Image processing

Image stacks obtained with confocal microscopy were processed using ImageJ software to generate maximum intensity projections. To obtain final images, these maximum intensity projections were processed in Adobe Photoshop using gamma adjustments to enhance visibility of intermediate gray values and median filtering to suppress noise when necessary. For the 3D rendering of contacts between CST collaterals and LPSN (Fig 2F), Imaris software (Bitplane) was used. For visualizing the co-localization of the FGF22 *in situ* signal with long propriospinal neurons (LPSN) labeling (Fig 1B), the ISH signal was inverted and pseudocolored (red) before being overlaid with the fluorescent LPSN label. For imaging retrogradely labeled CST neurons (Fig 3C), we first imaged the fluorescence signals using a confocal microscope (FV1000; Olympus) using standard filter settings before we unmounted the sections, performed ISH, and re-imaged the sections as previously described (Jacobi *et al*, 2014). Again, the ISH signal was inverted and pseudocolored (red) before being overlaid with the retrogradely labeled CST neurons.

Statistical evaluation

Results are given as mean ± SEM. GraphPad Prism 5.01 for Windows (GraphPad Software) was used to perform statistical analysis. Student's *t*-tests were used for comparisons between two groups. For multiple comparisons, a one-way ANOVA followed by a Tukey test was performed. For behavioral analysis over time, a repeated one-way ANOVA followed by a Bonferroni *post hoc* test was used for the ladder rung test. A two-way ANOVA followed by Bonferroni tests was used for analyzing the catwalk data (as the number of suitable steps for analysis differs for each timepoint). Significance levels are indicated as follows: $*P < 0.05$; $**P < 0.01$; $***P < 0.001$.

Supplementary information for this article is available online: http://emboj.embopress.org

Acknowledgements

We would like to thank Martin Adrian and Geraldine Heitmann, for excellent technical assistance, Dana Matzek for animal husbandry, Klaus Dornmair and Kathrin Held for their help with single-cell laser microdissection and quantitative PCR, and Alexander Gun for his help analyzing CST maturation in mutant mice. We thank Daniel Kerschensteiner for critical reading of the manuscript. Work in F.M.B.'s laboratory is supported by grants from the Deutsche Forschungsgemeinschaft (DFG, SFB 870) and the German Federal Ministry of Education and Research (BMBF). Work in M.K.'s laboratory is financed through grants from the DFG (Transregio 128, SPP1710), the BMBF (Competence Network Multiple Sclerosis), the European Research Council under the European Union's Seventh Framework Program (FP/2007–2013; ERC Grant Agreement n. 310932), the Hertie-Foundation, and the 'Verein Therapieforschung für MS-Kranke e.V.'. F.M.B. and M.K. are further supported by the Munich Center for Systems Neurology (SyNergy; EXC 1010). Work in H.U.'s laboratory is funded by NIH Grant NS070005.

Author contributions

FMB, HU, and MK conceived the experiments. AJ performed and analyzed spinal surgeries and tracing. AJ and AMS performed and analyzed *in situ* hybridizations and single-cell PCR. AJ, KL, MH, and AMS performed anatomical and immunohistochemical analysis. HU characterized mutant mouse strains. AJ, FMB, and KL performed and analyzed behavioral tests. FMB, AJ, and MK wrote the paper.

Conflict of interest

The authors declare that they have no conflict of interest.

References

Bareyre FM, Kerschensteiner M, Raineteau O, Mettenleiter TC, Weinmann O, Schwab ME (2004) The injured spinal cord spontaneously forms a new intraspinal circuit in adult rats. *Nat Neurosci* 7: 269 – 277

Bareyre FM, Kerschensteiner M, Misgeld T, Sanes JR (2005) Transgenic labeling of the corticospinal tract for monitoring axonal responses to spinal cord injury. *Nat Med* 11: 1355 – 1360

van den Brand R, Heutschi J, Barraud Q, DiGiovanna J, Bartholdi K, Huerlimann M, Friedli L, Vollenweider I, Moraud EM, Duis S, Dominici N, Micera S, Musienko P, Courtine G (2012) Restoring voluntary control of locomotion after paralyzing spinal cord injury. *Science* 336: 1182 – 1185

Courtine G, Song B, Roy RR, Zhong H, Herrmann JE, Ao Y, Qi J, Edgerton VR, Sofroniew MV (2008) Recovery of supraspinal control of stepping via indirect propriospinal relay connections after spinal cord injury. *Nat Med* 14: 69 – 74

Fox MA, Sanes JR, Borza DB, Eswarakumar VP, Fassler R, Hudson BG, John SW, Ninomiya Y, Pedchenko V, Pfaff SL, Rheault MN, Sado Y, Segal Y, Werle MJ, Umemori H (2007) Distinct target-derived signals organize formation, maturation, and maintenance of motor nerve terminals. *Cell* 129: 179 – 193

García-Alías G, Barkhuysen S, Buckle M, Fawcett JW (2009) Chondroitinase ABC treatment opens a window of opportunity for task-specific rehabilitation. *Nat Neurosci* 12: 1145 – 1151

Girgis J, Merrett D, Kirkland S, Metz GA, Verge V, Fouad K (2007) Reaching training in rats with spinal cord injury promotes plasticity and task specific recovery. *Brain* 130: 2993 – 3003

Goldshmit Y, Spanevello MD, Tajouri S, Li L, Rogers F, Pearse M, Galea M, Bartlett PF, Boyd AW, Turnley AM (2011) EphA4 blockers promote axonal

regeneration and functional recovery following spinal cord injury in mice. *PLoS One* 6: e24636

Gorski JA, Talley T, Qiu M, Puelles L, Rubenstein JL, Jones KR (2002) Cortical excitatory neurons and glia, but not GABAergic neurons, are produced in the Emx1-expressing lineage. *J Neurosci* 22: 6309 – 6314

Grimm D, Kay MA, Kleinschmidt JA (2003) Helper virus-free, optically controllable, and two-plasmid-based production of adeno-associated virus vectors of serotypes 1 to 6. *Mol Ther* 7: 839 – 850

Hamers FP, Koopmans GC, Joosten EA (2006) CatWalk-assisted gait analysis in the assessment of spinal cord injury. *J Neurotrauma* 23: 537 – 548

Hofbauer M, Wiesener S, Babbe H, Roers A, Wekerle H, Dornmair K, Hohlfeld R, Goebels N (2003) Clonal tracking of autoaggressive T cells in polymyositis by combining laser microdissection, single-cell PCR, and CDR3-spectratype analysis. *Proc Natl Acad Sci USA* 100: 4090 – 4095

Jacobi A, Schmalz A, Bareyre FM (2014) Abundant expression of guidance and synaptogenic molecules in the injured spinal cord. *PLoS One* 9: e88449

Kaneko S, Iwanami A, Nakamura M, Kishino A, Kikuchi K, Shibata S, Okano HJ, Ikegami T, Moriya A, Konishi O, Nakayama C, Kumagai K, Kimura T, Sato Y, Goshima Y, Taniguchi M, Ito M, He Z, Toyama Y, Okano H (2006) A selective Sema3A inhibitor enhances regenerative responses and functional recovery of the injured spinal cord. *Nat Med* 12: 1380 – 1389

Klugmann M, Symes CW, Leichtlein CB, Klaussner BK, Dunning J, Fong D, Young D, During MJ (2005) AAV-mediated hippocampal expression of short and long Homer 1 proteins differentially affect cognition and seizure activity in adult rats. *Mol Cell Neurosci* 28: 347 – 360

Lang C, Guo X, Kerschensteiner M, Bareyre FM (2012) Single collateral reconstructions reveal distinct phases of corticospinal remodeling after spinal cord injury. *PLoS One* 7: e30461

Lang C, Bradley PM, Jacobi A, Kerschensteiner M, Bareyre FM (2013) STAT3 promotes corticospinal remodelling and functional recovery after spinal cord injury. *EMBO Rep* 14: 931 – 937

Lindau NT, Bänninger BJ, Gullo M, Good NA, Bachmann LC, Starkey ML, Schwab ME (2014) Rewiring of the corticospinal tract in the adult rat after unilateral stroke and anti-Nogo-A therapy. *Brain* 137: 739 – 756

Metz GA, Whishaw IQ (2002) Cortical and subcortical lesions impair skilled walking in the ladder rung walking test: a new task to evaluate fore- and hindlimb stepping, placing, and co-ordination. *J Neurosci Methods* 115: 169 – 179

Micheva KD, Busse B, Weiler NC, O'Rourke N, Smith SJ (2010) Single-synapse analysis of a diverse synapse population: proteomic imaging methods and markers. *Neuron* 68: 639 – 653

Piaton G, Aigrot MS, Williams A, Moyon S, Tepavcevic V, Moutkine I, Gras J, Matho KS, Schmitt A, Soellner H, Huber AB, Ravassard P, Lubetzki C (2011) Class 3 semaphorins influence oligodendrocyte precursor recruitment and remyelination in adult central nervous system. *Brain* 134: 1156 – 1167

Pirvola U, Ylikoski J, Trokovic R, Hébert JM, McConnell SK, Partanen J (2002) FGFR1 is required for the development of the auditory sensory epithelium. *Neuron* 35: 671 – 680

Sanes JR, Lichtman JW (2001) Induction, assembly, maturation and maintenance of a postsynaptic apparatus. *Nat Rev Neurosci* 2: 791 – 805

Shah PK, Garcia-Alias G, Choe J, Gad P, Gerasimenko Y, Tillakaratne N, Zhong H, Roy RR, Edgerton VR (2013) Use of quadrupedal step training to re-engage spinal interneuronal networks and improve locomotor function after spinal cord injury. *Brain* 136: 3362 – 3377

Shapira M, Zhai RG, Dresbach T, Bresler T, Torres VI, Gundelfinger E, Ziv N, Garner CC (2003) Unitary assembly of presynaptic active zones from Piccolo-Bassoon transport vesicles. *Neuron* 38: 237 – 252

Shim SO, Cafferty WB, Schmidt EC, Kim BG, Fujisawa H, Strittmatter SM (2012) PlexinA2 limits recovery from corticospinal axotomy by mediating oligodendrocyte-derived Sema6A growth inhibition. *Mol Cell Neurosci* 50: 193 – 200

Siddiqui TJ, Craig AM (2011) Synaptic organizing complexes. *Curr Opin Neurobiol* 21: 132 – 143

Singh R, Su J, Brooks J, Terauchi A, Umemori H, Fox MA (2012) Fibroblast growth factor 22 contributes to the development of retinal nerve terminals in the dorsal lateral geniculate nucleus. *Front Mol Neurosci* 4: 61

Stevens HE, Smith KM, Maragnoli ME, Fagel D, Borok E, Shanabrough M, Horvath TL, Vaccarino FM (2010) Fgfr2 is required for the development of the medial prefrontal cortex and its connections with limbic circuits. *J Neurosci* 30: 5590 – 5602

Terauchi A, Johnson-Venkatesh EM, Toth AB, Javed D, Sutton MA, Umemori H (2010) Distinct FGFs promote differentiation of excitatory and inhibitory synapses. *Nature* 465: 783 – 787

Umemori H, Linhoff MW, Ornitz DM, Sanes JR (2004) FGF22 and its close relatives are presynaptic organizing molecules in the mammalian brain. *Cell* 118: 257 – 270

Weidner N, Ner A, Salimi N, Tuszynski MH (2001) Spontaneous corticospinal axonal plasticity and functional recovery after adult central nervous system injury. *Proc Natl Acad Sci USA* 98: 3513 – 3518

Williams ME, de Wit J, Ghosh A (2010) Molecular mechanisms of synaptic specificity in developing neural circuits. *Neuron* 68: 9 – 18

Yip PK, Wong LF, Sears TA, Yáñez-Muñoz RJ, McMahon SB (2010) Cortical overexpression of neuronal calcium sensor-1 induces functional plasticity in spinal cord following unilateral pyramidal tract injury in rat. *PLoS Biol* 8: e1000399

Yu K, Xu J, Liu Z, Sosic D, Shao J, Olson EN, Towler DA, Ornitz DM (2003) Conditional inactivation of FGF receptor 2 reveals an essential role for FGF signaling in the regulation of osteoblast function and bone growth. *Development* 130: 3063 – 3074

Zhai RG, Vardinon-Friedman H, Cases-Langhoff C, Becker B, Gundelfinger ED, Ziv NE, Garner CC (2001) Assembling the presynaptic active zone: a characterization of an active zone precursor vesicle. *Neuron* 29: 131 – 143

Zhang X, Ibrahimi OA, Olsen SK, Umemori H, Mohammadi M, Ornitz DM (2006) Receptor specificity of the fibroblast growth factor family. The complete mammalian FGF family. *J Biol Chem* 281: 15694 – 15700

Zörner B, Bachmann LC, Filli L, Kapitza S, Gullo M, Bolliger M, Starkey ML, Röthlisberger M, Gonzenbach RR, Schwab ME (2014) Chasing central nervous system plasticity: the brainstem's contribution to locomotor recovery in rats with spinal cord injury. *Brain* 137: 1716 – 1732

FGF22 signaling regulates synapse formation during post-injury remodeling of the spinal cord

Anne Jacobi[1], Kristina Loy[1], Anja M. Schmalz[1], Mikael Hellsten[1], Hisashi Umemori[2,3], Martin Kerschensteiner[1,4] and Florence M. Bareyre[1,4]

Supplementary Figure Legends

Figure S1. Hindlimb CST maturation is not altered in FGF22 deficient mice.

A Confocal images of the cortex of an adult FGF22 competent mouse. Scale bar equals 100 µm.

B Confocal images of the cortex of an adult FGF22 deficient mouse. Scale bar equals 100 µm.

C Quantification of the number of neurons in an area of 37.5mm^2 of layer V of the motor and somatosensory cortex in adult FGF22 competent and FGF22 deficient mice (n=3 animals per group). Mean±SEM. No significant differences between the groups were detected (unpaired two-tailed t-test).

D Quantification of the number of boutons per µm hindlimb CST collateral in the cervical and lumbar spinal cord of adult FGF22 competent and deficient mice (n=6 animals per group). Mean±SEM. No significant differences between the groups were detected (unpaired two-tailed t-test).

E Quantification of the number of branchpoints per µm hindlimb CST collateral in the cervical and lumbar spinal cord of adult FGF22 competent and deficient mice (n=6

animals per group). Mean±SEM. No significant differences between the groups were detected (unpaired two-tailed t-test).

F Quantification of the number of exiting hindlimb CST collaterals in the cervical and lumbar spinal cord of adult FGF22 competent and deficient mice (n=6 animals per group). Mean±SEM. No significant differences between the groups were detected (unpaired two-tailed t-test).

Figure S2. Quantification of the average length of the collaterals in control, FGF22 deficient and FGFR deficient mice.

A Quantification of average collateral length in FGF competent (white bar) and FGF22 deficient (red bar) mice.

B Quantification of average collateral length in FGF competent (white bar) and FGFR1 forebrain deficient (dark blue bar) and forebrain FGFR2 deficient (dark green bar) mice.

C Quantification of average collateral length in FGF competent (white bar) and FGFR1R2 hindlimb motor cortex co-deficient (light blue bar) mice.

Figure S3. Hindlimb CST maturation is not altered in forebrain FGFR1 deficient mice.

A Confocal images of the cortex of an adult FGFR competent mouse. Scale bar equals 100 μm.

B Confocal images of the cortex of an adult, forebrain FGFR1 deficient mouse. Scale bar equals 100 μm.

C Quantification of the number of neurons in an area of 37.5mm^2 of layer V of the motor and somatosensory cortex in adult FGFR competent and FGFR1 deficient mice (n=3 animals per group). Mean±SEM. No significant differences between the groups were detected (unpaired two-tailed t-test).

D Quantification of the number of boutons per μm hindlimb CST collateral in the cervical and lumbar spinal cord of adult FGFR competent and FGFR1 deficient mice (n=4 animals per group). Mean±SEM. No significant differences between the groups were detected (unpaired two-tailed t-test).

E Quantification of the number of branchpoints per μm hindlimb CST collateral in the cervical and lumbar spinal cord of adult FGFR competent and FGFR1 deficient mice (n=4 animals per group). Mean±SEM. No significant differences between the groups were detected (unpaired two-tailed t-test).

F Quantification of the number of exiting hindlimb CST collaterals in the cervical and lumbar spinal cord of adult FGFR competent and FGFR1 deficient mice (n=4 animals per group). Mean±SEM. No significant differences between the groups were detected (unpaired two-tailed t-test).

Figure S4. Hindlimb CST maturation is not altered in forebrain FGFR2 deficient mice.

A Confocal images of the cortex of an adult FGFR competent mouse. Scale bar equals 100 μm.

B Confocal images of the cortex of an adult, forebrain FGFR2 deficient mouse. Scale bar equals 100 μm.

C Quantification of the number of neurons in an area of 37.5mm^2 of layer V of the motor and somatosensory cortex in adult FGFR competent and FGFR2 deficient mice (n=3 animals per group). Mean±SEM. No significant differences between the groups were detected (unpaired two-tailed t-test).

D Quantification of the number of boutons per µm hindlimb CST collateral in the cervical and lumbar spinal cord of adult FGFR competent and FGFR2 deficient mice (n=7-8 animals per group). Mean±SEM. No significant differences between the groups were detected (unpaired two-tailed t-test).

E Quantification of the number of branchpoints per µm hindlimb CST collateral in the cervical and lumbar spinal cord of adult FGFR competent and FGFR2 deficient mice (n=7-8 animals per group). Mean±SEM. No significant differences between the groups were detected (unpaired two-tailed t-test).

F Quantification of the number of exiting hindlimb CST collaterals in the cervical and lumbar spinal cord of adult FGFR competent and FGFR2 deficient mice (n=7-8 animals per group). Mean±SEM. No significant differences between the groups were detected (unpaired two-tailed t-test).

Figure S5. Deletion of either FGFR1 or FGFR2 alone does not affect functional recovery after spinal cord injury.

A Quantification of functional recovery in the ladder rung test (irregular walk) in control (white bars) and forebrain FGFR1 (blue bars) or FGFR2 (green bars) deficient mice (n=8-14 mice per group). Mean±SEM. No significant differences between the groups were detected (repeated-measure ANOVA followed by Bonferroni tests).

B Quantification of functional recovery in the ladder rung test (regular walk) in control (white bars) and forebrain FGFR1 (blue bars) or FGFR2 (green bars) deficient mice (n=8-14 mice per group). Mean±SEM. No significant differences between the groups were detected (repeated-measure ANOVA followed by Bonferroni tests).

Figure S6. FGFR2 is located in CST collaterals and in particular in CST boutons.

A Confocal image of FGFR2 immunoreactivity in the cortex of an FGFR competent (left panel) and an FGFR2 deficient mouse (right panel). The inset on the left panel is a magnification of the boxed area. Scale bar equals 100μm in **A** and 10μm in inset.

B Single confocal image plane of FGFR2 immunoreactivity in the corticospinal tract imaged on a cross section of the cervical spinal cord 3weeks following lesioned in FGFR competent mouse (FGFR2: green; CST: red). The boxed area in B is magnified 2 times in the right panels which show the overlay and the single channels. Scale bar equals 10 μm.

C Single confocal plane of FGFR2 immunoreactivity in and around a CST collateral imaged on a cross section in the cervical gray matter (FGFR2: green; CST collateral: red). The boxed area in C is magnified 2 times in the right panels, which show the overlay and the single channels. Scale bar equals 10 μm.

Figure S7. Stereotactic injection of AAVs allows selective targeting of the hindlimb motor cortex.

A Confocal image of the hindlimb motor cortex 3 weeks following injection of a rAAV-GFP-Ires-Cre illustrating the presence of many transduced neurons (green) in layer V of the cortex (blue, counterstaining with Neurotrace 435/455). Scale bar equals 150 μm.

B No transduced neurons (green) are seen in the forelimb motor cortex of the same animal. Same scale as **A**.

Figure S8. Viral and genetic deletion of FGFR2 have similar effects on post-injury remodeling.

A Confocal images of hindlimb CST collaterals exiting the main CST tract (arrows) in the cervical spinal cord 3 weeks following a T8 dorsal bilateral hemisection in FGFR2 floxed mice after injection of either rAAV-GFP (left panel) or rAAV-GFP-Ires-Cre (right panel) in the hindlimb motor cortex. Scale bar equals in 40 μm.

B Quantification of the number of exiting hindlimb CST collaterals in the cervical spinal cord 3 weeks following spinal cord injury in FGFR2 floxed mice after injection of either rAAV-GFP or rAAV-GFP-Ires-Cre in the hindlimb motor cortex (n=7-8 animals per group). The observed increase of CST sprouting is similar to the one observed after stable genetic deletion of FGFR2 (cf. **Fig 4C**). Mean±SEM. ** P =0.004 (unpaired two-tailed t-test).

C Confocal images showing putative synaptic boutons (arrows) on newly formed cervical hindlimb CST collaterals 3 weeks following spinal cord injury in FGFR2 floxed mice after injection of either rAAV-GFP (left panel) or rAAV-GFP-Ires-Cre (right panel) in the hindlimb motor cortex. Scale bar equals in 15 μm.

D Quantification of the number of boutons on cervical CST collaterals at 3 weeks after injury in FGFR2 floxed mice after injection of either rAAV-GFP or rAAV-GFP-Ires-Cre in the hindlimb motor cortex (n=7-8 animals per group). The changes are similar to those obtained by stable genetic deletion of FGFR2 (cf **Fig 4E**). Mean±SEM. * P =0.04 (unpaired two-tailed t-test).

E Quantification of the percentage of LPSN contacted by cervical CST collaterals at 3 weeks after injury in FGFR2 floxed mice after injection of either rAAV-GFP or rAAV-GFP-Ires-Cre in the hindlimb motor cortex (n=7-8 animals per group). Again the results are similar to those obtained by stable genetic deletion of FGFR2 (cf **Fig 4F**). Mean±SEM. No significant differences were found (unpaired two-tailed t-test).

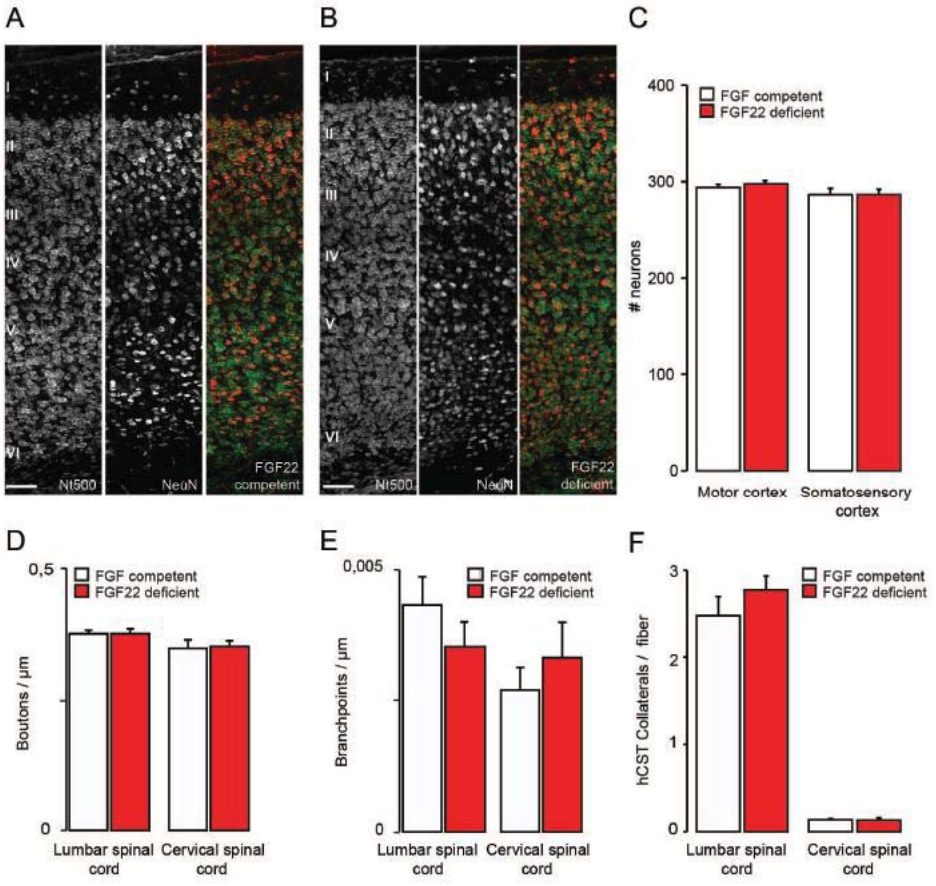

Jacobi et al., Figure S1

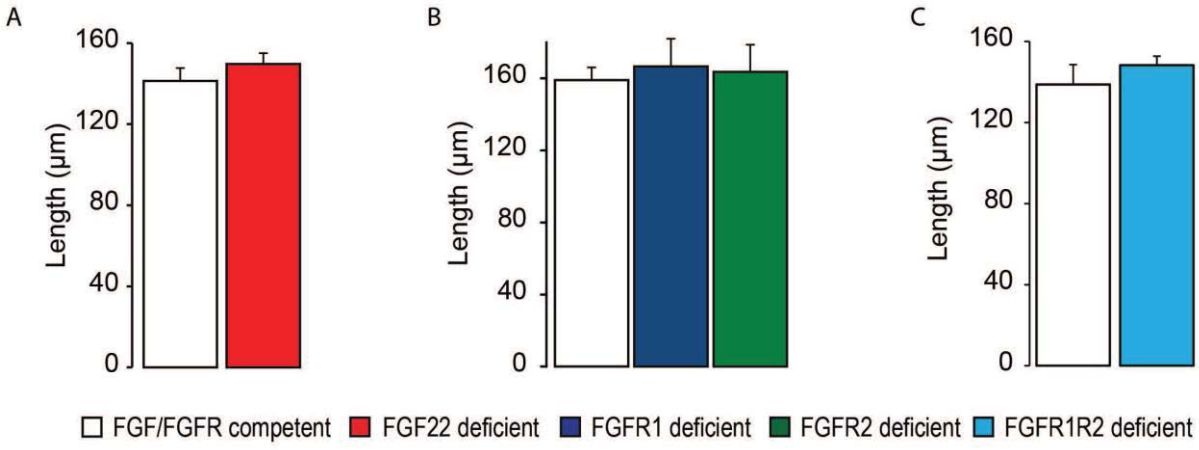

Jacobi et al., Figure S2

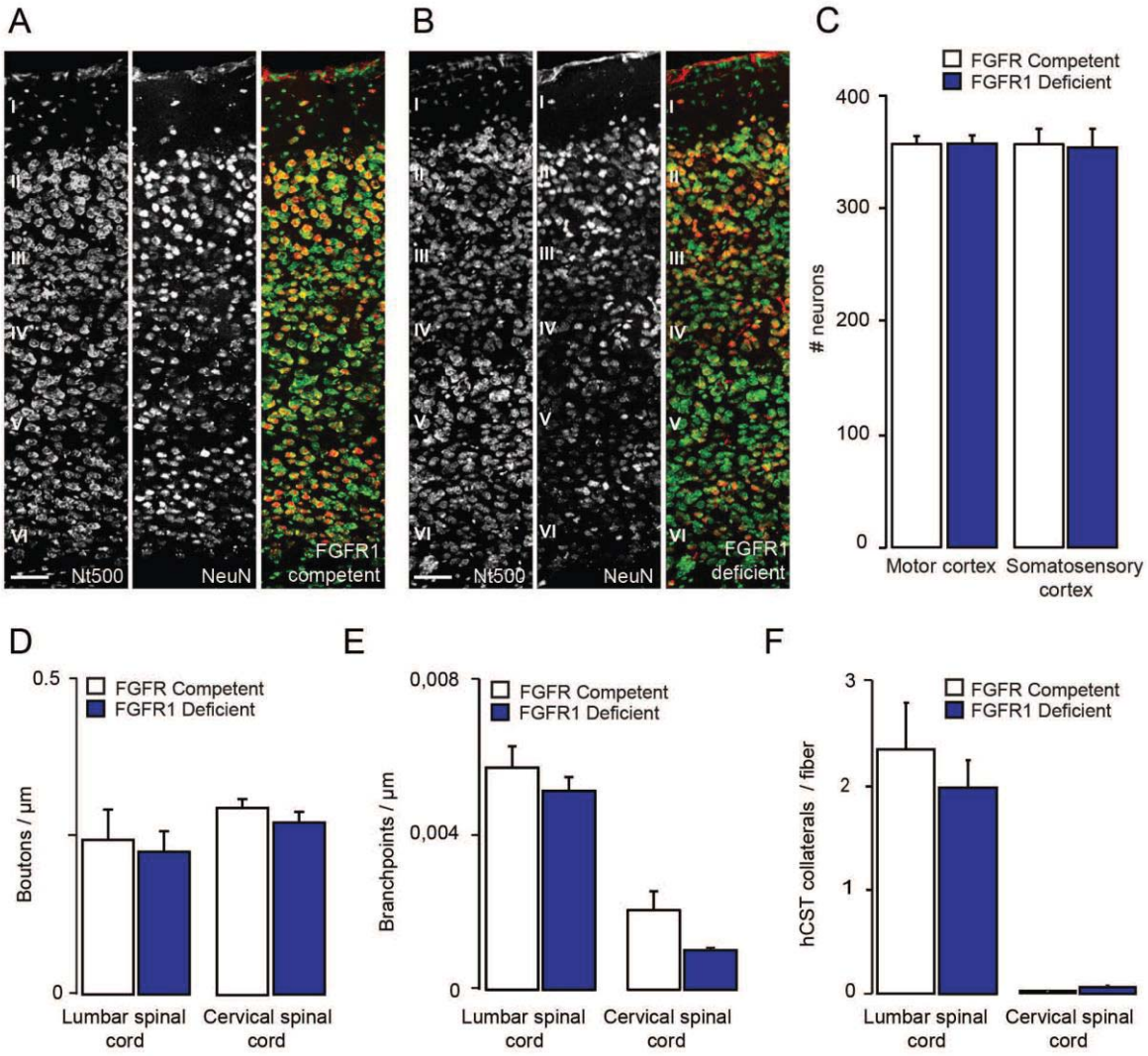

Jacobi et al., Figure S3

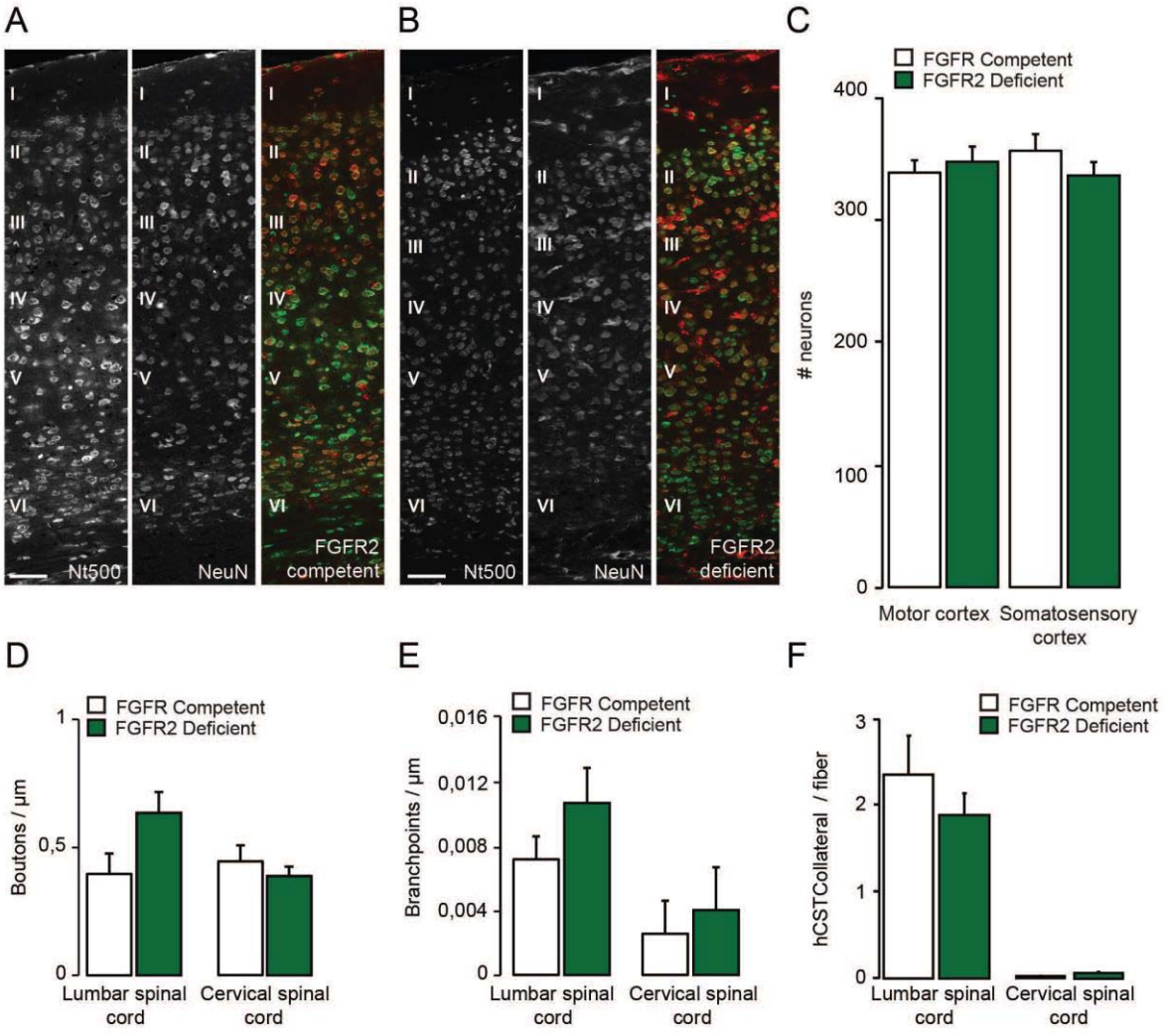

Jacobi et al., Figure S4

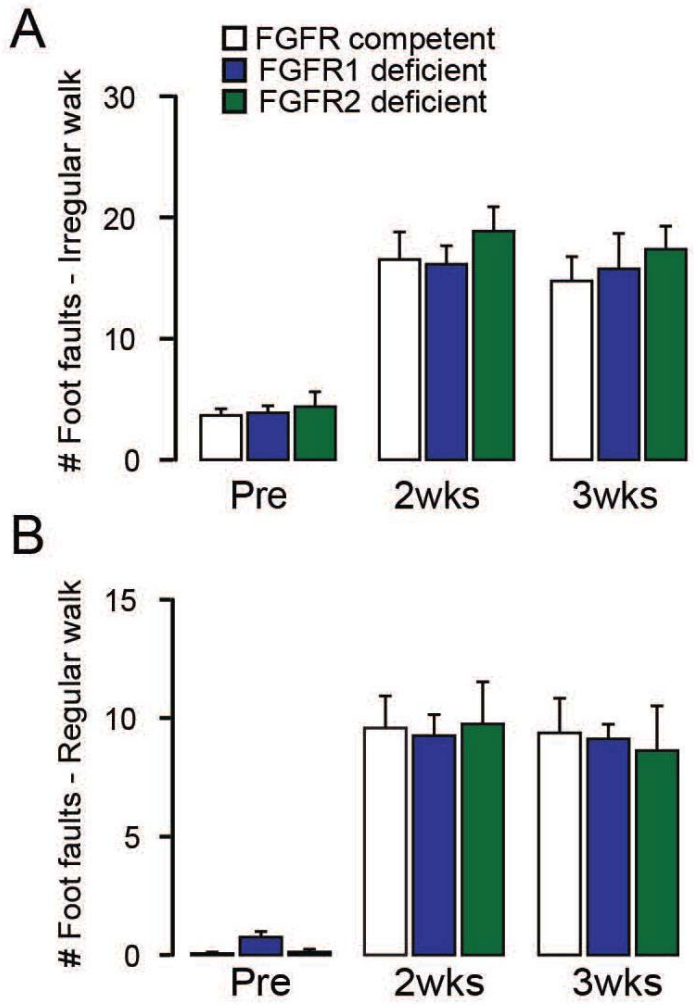

Jacobi et al., Figure S5

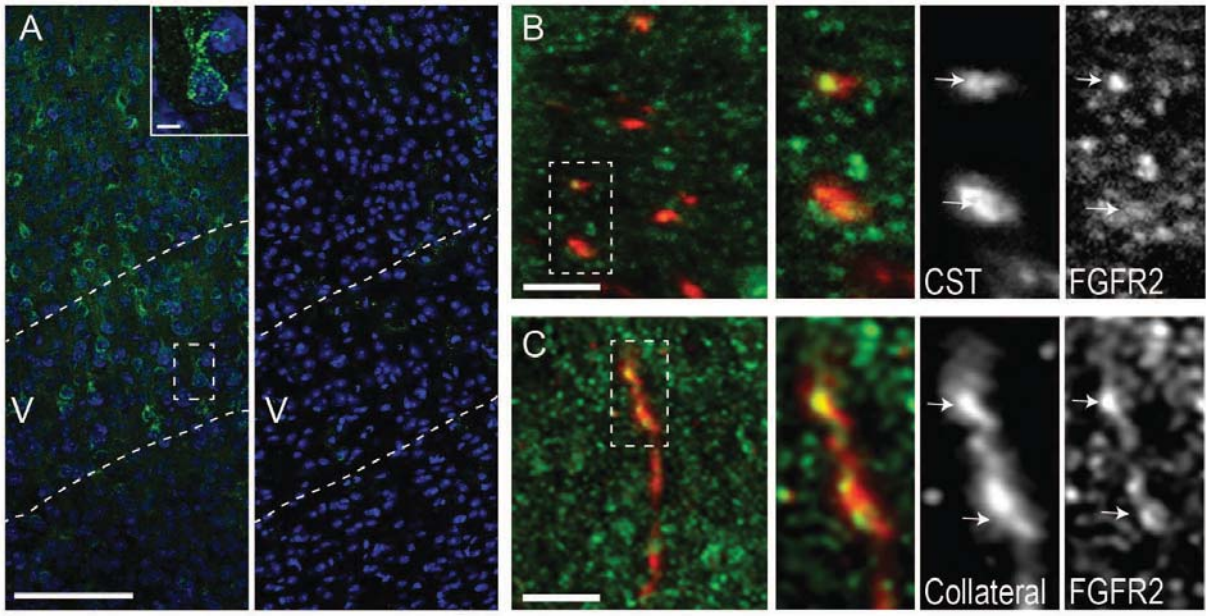

Jacobi et al., Figure S6

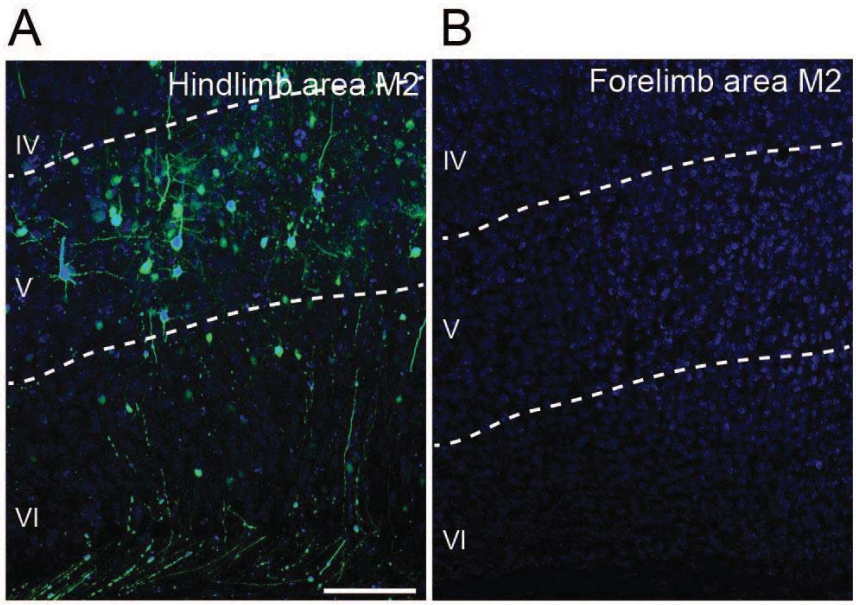

Jacobi et al., Figure S7

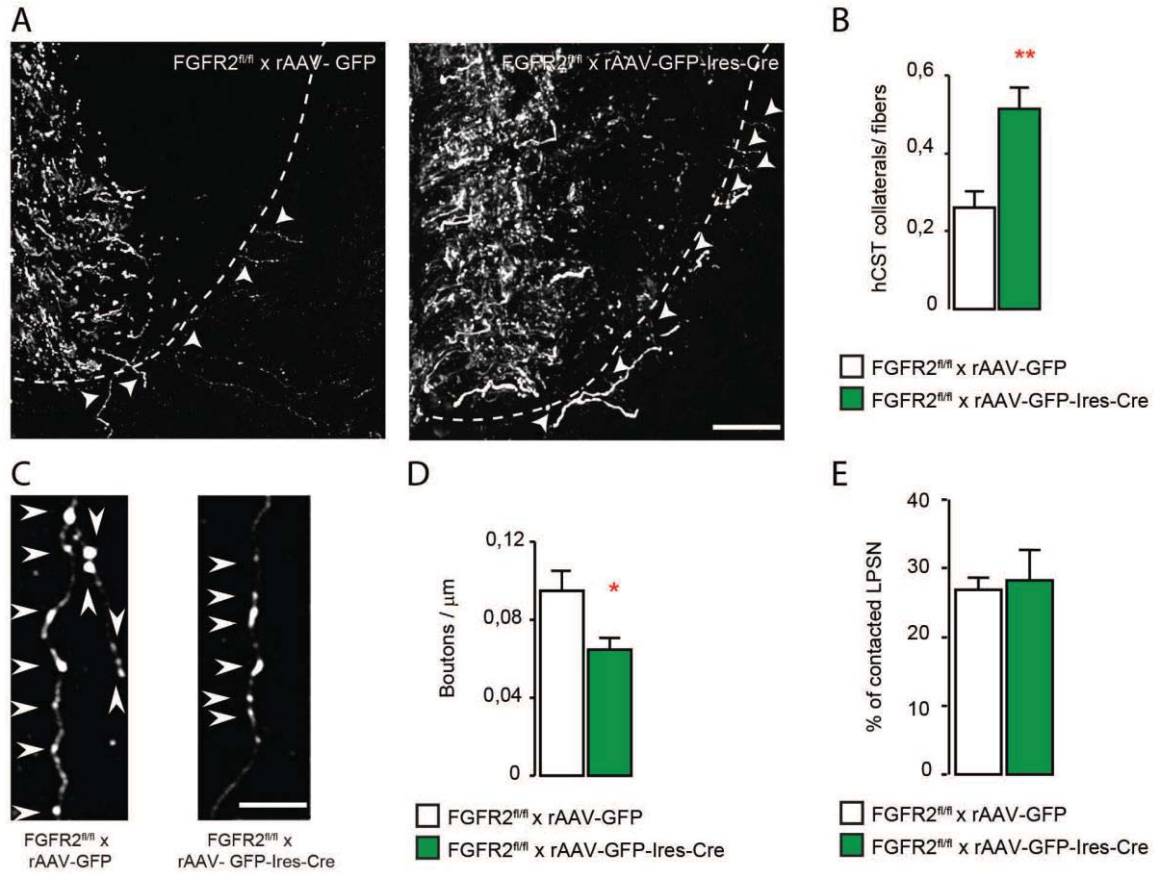

Jacobi et al., Figure S8

4. Discussion

My thesis aimed at better understanding functional recovery in a mouse model of spinal cord injury with a focus on axonal remodelling. I investigated the effect of voluntary exercise as well as two molecular factors and their impact on axonal remodelling and motor recovery after SCI. The discussion will first cover voluntary rehabilitation and its impact on SCI and then Semaphorin 7A, a molecular cue for growth and guidance and FGF22, an inducer of excitatory synapse formation.

4.1. The impact of voluntary rehabilitation on functional recovery following incomplete spinal cord injury in mice

Until today rehabilitation is the 'state of the art' subacute and long-term treatment after spinal cord injury (Nas et al., 2015), but the underlying mechanism of the ensuing functional recovery remains poorly understood. Animal models of rehabilitation and SCI are crucial to gain more insight into the positive effects of exercise on neuronal and glial recovery after injury and to harvest that potential further with the best rehabilitation strategies. I took advantage of the fact that wheel running is an elective voluntary behaviour in mice that can also be triggered in undomesticated animals in their natural habitat (Meijer and Robbers, 2014). If presented with a running wheel, mice run on average 5km per 24 hours which is a considerable amount of exercise for a small rodent. Strikingly, following SCI, mice quickly regained the ability and motivation to run in the wheel first mostly using their unimpaired forelimbs and then over time regained quadrupedal running abilities. Motivation was found to additionally boost recovery after spinal cord injury (Sawada et al., 2015), making voluntary wheel running a suitable model with maximum outcome and minimum time investment of the researcher for spinal cord injury rehabilitation and recovery. I also aimed at presenting the animals with a rehabilitation paradigm at their free disposal which they could choose to use as much as they want at each given timepoint after the injury. In contrast to forced rehabilitative training in rodents that is usually accompanied with a rise in serum corticosteroid levels if the animal is impaired, voluntary wheel running does not impede stress on the animal (Sato, 2017). Corticosteroids are nowadays thought to be non-beneficial to rather detrimental after spinal cord injury which could abolish the positive effect of training to a certain degree. However this rehabilitation paradigm is not suitable for models of severe spinal cord injuries in which animals permanently drag their hind- and/or forelimbs which would confer an inability to run in a wheel. For these studies forced or passive paradigms like treadmill or bicycle models are more suitable (Dominici et al., 2012). Wheel running can only be used in dorsal or lateral hemisection, pyramidotomy or mild contusion injury paradigms. One strong advantage of such training paradigms is that wheel running allows for prolonged training time compared to, for example, treadmill

training which is typically administered 20 minutes per day due to the limited availability of the researcher (Battistuzzo et al., 2016).

Hemisected mice that trained in the wheels showed a significant improvement in overground locomotion and fine paw placement as well as rhythmic stepping. Locomotion and balance were assessed with the constant and accelerated RotaRod on which mice have to walk on a constant or accelerated speed (See paper 1). This recovery relies primarily on the central pattern generator wiring as well as supraspinal serotonergic pathways from the nucleus raphe obscurus whereas the recovery of the irregular Ladder Rung, which evaluates fine paw placement and necessitates supraspinal input, depends more on CST rewiring (Escalona et al., 2017, Marder and Bucher, 2001, Takakusaki et al., 2004). The ability to step rhythmically and hold posture, which is thought to be mediated mostly by intraspinal networks in the spinal cord, also recovers better in wheel trained animals compared to controls after SCI (Takakusaki et al., 2004). This can be seen in the higher performance on the regular RotaRod in which lesioned and wheel trained animals performed better than controls. Moreover non rhythmic stepping was improved by wheel training after SCI, which can especially be seen in the performance in the irregular Ladder Rung in which animals have to cope with irregularly spaced bars and adjust their fine paw placement accordingly. These improvements could be best explained by some extent of recovery of CST-mediated functionality in the trained animals, as the CST coordinates the fine movements of the paws (Han et al., 2015). We aimed at also specifically challenging the CST remodelling by employing the complex wheels with irregular spaced bars. We concluded that motor recovery after SCI can be seen in rhythmic stepping and fine paw placement with running in the irregular wheels, most likely involving intra- and supraspinal pathways, namely the CST and the serotonergic projections onto the lumbar motor neurons.

I further wanted to understand the cellular mechanisms underlying this profound improvement in stepping ability with exercise after SCI. I first analysed lesion volume and local changes at the lesion site. Lesion volume was equal between the trained and untrained groups and did not correlate with behavioural recovery after the 10 weeks study-period. Changes in neuronal collateral formation as well as glial reactivity and myelin preservation at the lesion site were only transient at 2 weeks post lesion and may account for an early contribution to functional improvements but cannot explain the lasting recovery.

We used a dorsal thoracic hemisection model in our mice to mimic a partial transection of the spinal cord that affects the main dCST as an important motor tract. In fact most human spinal cord injuries are incomplete, thus leaving potential for recovery and neurorehabilitation (Friedli et al., 2015). Partial spinal cord transections trigger a rewiring and remodelling process via the spared neuronal tissue

(Zorner et al., 2014) which is why the prognosis of incomplete injuries (ASIA B, C, D) is considerably better than complete injuries. This remodelling can be seen in intra- and supraspinal circuitry and I have chosen to investigate the intraspinal serotonergic wiring and connections from the NRO as well as the dCST. The serotonergic system that mainly modulates and facilitates movement, as well as generates rhythmic stepping patterns has its highest impact in the lumbar spinal cord after thoracic injuries, as this is where the hindlimb motor neurons are located (Engesser-Cesar et al., 2007, Ghosh and Pearse, 2014, Grillner, 2006). Wheel running initiates an early increase in serotonergic contacts on lumbar motor neurons at 2 weeks post lesion which is accompanied with improvements in regular stepping. At later timepoints the control group reaches similar levels of contacts and regular stepping patterns, making the effect of exercise on serotonergic wiring transient. The CPG dependent function recovers in both groups with acceleration if the mice have access to a running wheel.

While the serotonergic system mostly functions in initiation and regulation of rhythmic stepping, the CST is of particular importance in fine and coordinated locomotor movements. In my distinct injury model the dCST re-connects at the cervical level with long propriospinal neurons which then, in turn, connect with lumbar motor neurons, thereby bridging the thoracic lesion site ventrally (Bareyre et al., 2004). As fine stepping ability recovers more quickly and better with voluntary wheel running I analysed the CST in the cervical spinal cord and its contacts onto LPSN. There was a significant increase in CST sprouting into the grey matter as well as contact formation on LPSN early and late after injury. The detour circuit was established faster in runners in comparison to non-runners, in which the circuit usually fully forms after 3 weeks, not 2 (Lang et al., 2012) and this effect is sustained throughout the whole study period making the improved CST remodelling the most likely candidate for the improved behavioural recovery.

Nevertheless there are some critical considerations that have to be made regarding this study. Some of the main open questions in human rehabilitation are the optimal onset and duration of rehabilitation as well as the optimal dose. Early onset is preferred to late onset of rehabilitation, but some reports of improvements with exercise even years after the incident are published (McDonald and Sadowsky, 2002, Nas et al., 2015). In our paradigm the mice start exercising before the injury which is more feasible, because the healthy mouse will more likely start wheel running than the impaired mouse. This of course does not reflect the patient situation, in which rehabilitative training is not administered before the accident. Exercise improves neuroplasticity in the healthy nervous system which could have a ‘priming’ effect on the CNS in injury and disease which is an influence factor we did not exclude from our study (Hotting and Roder, 2013). We nevertheless found changes in the nervous system that are sustained over a long period and seem to reflect a stable new circuit establishment, which is a new insight regardless of onset and duration of treatment. One main unanswered question is whether these

positive effects are sustained after the end of the training sessions as patients also at some point leave the rehabilitative facility and their exercise levels tend to decrease. This would require a follow up study in which mice are trained for several weeks after injury, then the wheel is removed and their recovery and neuronal remodelling is analysed some weeks later following the end of training.

Taken together this part of my thesis shows that voluntary wheel running in mice is a suitable model for human rehabilitation and allows us to study the underlying mechanisms of exercise-driven improvements in humans and animals after SCI. Wheel running after SCI is accompanied by improved hindlimb locomoter recovery in mice. I demonstrated that voluntary exercise leads to transient early changes in glial reactivity and neuronal growth at the lesion site as well as earlier serotonergic circuit refinement and an earlier and 3 fold increased formation of detour circuits of the CST after injury which likely mediates the improved functional recovery.

4.2. Sema7A and its role in the proper targeting of corticospinal and serotonergic fibers following spinal cord injury

As a second topic I wanted to focus on the molecular players that are involved in axonal growth and guidance to uncover a potential molecular target or better understand the regenerative failure after SCI. Therefore I decided to study the effect of Semaphorin 7A in a mouse model of spinal cord injury, as it is known to play a role in axonal growth and guidance during development (Pasterkamp et al., 2003). Sema7A is a molecule involved in many different functions and many different systems. It is expressed throughout all white and gray matter structures in the spinal cord and enriched in LPSN which are the primary relay neurons in detour circuit formation (Fig 14, (Bareyre et al., 2004, Jacobi et al., 2014)).

Table 2. Distribution and intensity of the ligands in the unlesioned cervical spinal cord of adult mice.

Area	Slit-1	Slit-2	Slit-3	Sema6a	Sema7a	SynCam1	SynCam3	SynCam4	NL1	NL4	EphB2	EphrinB1
Gray Matter												
Laminae I – IV	++	+++	+	+	++	++	+	++	+	++	+++	+
Laminae V	++	++++	++	+++	+++	++++	+++	+++	++	++	+++	++
Laminae VI – IX	+++	++++	++	++++	+++	+++	++++	+++	+++	++	+++	++
White Matter												
Dorsal Column	+	+	–	–	+	–	–	+	–	–	+	+
Ventral Funiculus	+	+	–	–	+	–	–	+	–	–	–	+

Relative intensities were estimated by visual comparison with sense probe in situ hybridization slides: +: weak; ++: moderate; +++: strong; ++++: very strong; –: not detected.
doi:10.1371/journal.pone.0088449.t002

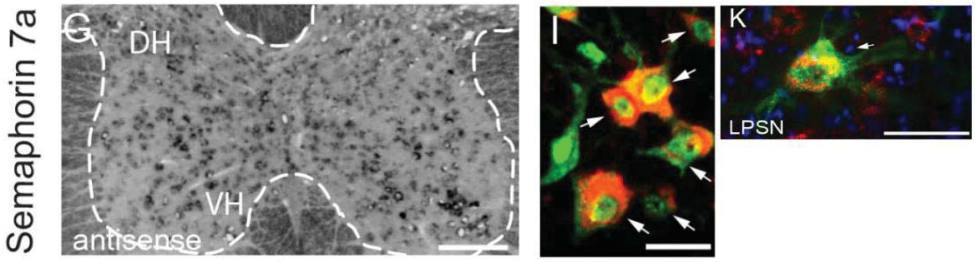

***Figure 14**: Expression of Sema7A and other guidance factors throughout the spinal cord (table top). Bottom: In-Situ staining of Sema7A in the spinal cord and higher magnification of neurons expressing Sema7A (NeuN: green, Sema7A: red) and a LPSN positive for Sema7A (LPSN: green; Sema7A: red) (modified from (Jacobi et al., 2014)).*

Recovery from spinal cord injury involves many mechanisms and signalling cascades and Sema7A is one signalling pathway that sounded interesting to me based on previous work. When we started this work, based on publications in development (Pasterkamp et al., 2003), my working hypothesis was that Sema7A is an attractive molecule, highly expressed on LPSN that stirs newly forming collaterals towards these LPSN in order to establish a functional detour circuit. Therefore I expected to see that without Sema7A signalling, axons would not be attracted anymore to LPSN neurons.

Recovery from spinal cord injury is multifarious and characterized by failure to restore the damage completely. It involves re-vascularization (Figley et al., 2013), a complicated cascade of immune responses that are until today in heavy discussion to determine whether they are beneficial or detrimental for neuronal survival (Schwab et al., 2014).This also holds true for glial cells (Silver et al., 2014). Blood perfusion of CNS tissue is crucial for survival and maintenance. After SCI this blood supply to the spinal cord is lost temporarily and then re-established by neo-vascularization mainly mediated by secretion of VEGF (vascular endothelial growth factor). This process re-establishes the supply of oxygen and nutrients to the injured tissue (Kundi et al., 2013). The positive and negative involvement of different glial cells in the recovery from CNS injury also remains multifarious until today, but a few mechanisms are well studied. Oligodendrocytes and myelin, although providing the encasement of the CNS axon, seem to be hindering axonal growth to a vast extend by secreting soluble inhibitory molecules. First CNS lesion studies in rodents of different ages found that in young neonates robust regeneration after injuries occurs only before the onset of myelination at about 2-3 weeks of age (Keirstead et al., 1992). Later on several growth inhibitory molecules like NogoA and myelin associated

glycoprotein were discovered that are secreted by oligodendrocytes (Chen et al., 2000, Mukhopadhyay et al., 1994). GFAP positive astrocytes also secrete growth inhibiting molecules, such as chondroitin sulphate proteoglycans and constitute a physical barrier at the lesion site hindering axonal growth (Morgenstern et al., 2002). On the other hand glial cell precursors can serve as neuronal progenitor cells, which could replace injured neurons of the CNS (Heins et al., 2002). The role of the immune response after SCI is well understood. The unlesioned spinal cord is, as part of the CNS, immune privileged, meaning that the blood brain barrier (BBB) hinders the free migration of immune cells. This barrier gets disrupted after injury causing migration of immune cells into the CNS, which potentially leads to secondary tissue damage, autoimmunity and a maladaptation of the now unregulated immune system (Schwab et al., 2014).

And of course recovery from spinal cord injury involves regulation of intrinsic and extrinsic programs that promote or hinder neuronal regeneration across the lesion site and remodelling more distant from the lesion (Di Giovanni, 2009, Yiu and He, 2006).

I first explored the functional recovery of animals lacking Sema7A signalling after a dorsal thoracic hemisection and discovered, by comparision it to control mice competent for Sema7A that functional recovery of fine stepping and gross rhythmic motor function is strongly impaired in KO mice in comparision to WT mice. While fine stepping is more CST related, rhythmic stepping can be achieved via the CPG in the spinal cord and serotonergic input (Marder and Bucher, 2001). Therefore, I chose to investigate both motor centres, the brain and CST for fine and higher motor function and the serotonergic wiring in brain and spinal cord. The impaired recovery could also be due to reduced vascularization or an aberrant immune response worsening the cord damage, as Sema7A is expressed widely throughout the nervous system, but also has a very important role in immune activation and growing knowledge suggests the involvement of Sema7A in tumour progression through its pro-angiogenic mode of action (Garcia-Areas et al., 2014, Garcia-Areas et al., 2013, Li et al., 2017, Pasterkamp et al., 2007). After SCI the neuronal tissue must be re-vascularized to ensure proper sustenance of the regenerating tissue, with grey matter vascularization being especially susceptible to damage (Figley et al., 2013). We investigated re-vascularization after spinal cord injury in WT and KO mice and found no differences in the number of vessel branchpoints, which is a measure of vascular network complexity or length of the vasculature after SCI. We then concluded that following spinal cord injury, Sema7A signalling is not necessary for correct vascular remodelling and tissue re-perfusion. This is not completely surprising as the pro-angiogenic activity has thus far only been reported in cancer progression and overexpression, but not in development (Ghanem et al., 2011, Saito et al., 2015). Typically, after injury the developmental programs are re-activated for healing, which also seems to be the case in the vascular system (Jeansson et al., 2011).

De facto our data is in line with these previous observations. Cell proliferation after injury, measured by number of KI67 positive cells, is also not altered in KO mice. We also could not see differences in infiltrating immune cells in the spinal cord after injury. Previous results presented conflicting evidence regarding the effects of Sema7A deletion: it was shown to either increase or decrease the immune responses in the spinal cord by activation and recruitment of T-cells and macrophages (Czopik et al., 2006, Suzuki et al., 2007). In our injury model there was no difference between infiltrating lymphocytes, $CD4^+$ T-cells or macrophages which suggests that differences in immune response do not account for the behavioural phenotype in the KO mice. Spinal cord injury causes a significantly lower immune cell infiltration to the CNS if compared to EAE, an autoimmune disease, which could explain the lack of differences that have been seen in mice with EAE. Our cell numbers in the flow cytometry might have been insufficient to detect subtle differences. To investigate the role of Sema7A in immune cell infiltration and activation after injury more markers for T-cell and macrophage activation, like CD80, CD86 or cytokine secretion, would need to be analysed to see not only recruitment but also activation of immune cells in the spinal cord tissue.

My main interest was to study Sema7A in neuronal outgrowth, guidance and repulsion, in which the molecule was known to play a role as growth promoting molecule in many tracts in development, but to date nothing is known about its role following injury. It was also of particular interest to determine, if Sema7A also plays a role in the adult CNS after injury which resembles in part the developmental situation, because new neuronal fibers have to grow and find the right partners to re-establish a functional circuit. Recent studies found Sema7A growth promoting and involved in repulsive and attractive axon guidance in the LOT and the brain dopaminergic system (Chabrat et al., 2017, Pasterkamp and Kolodkin, 2003, Pasterkamp et al., 2003). We first focussed on the dCST that is known to remodel extensively in the cervical cord after complete transection at T8 and to contact LPSN neurons that express Sema7A (Jacobi et al., 2014). We found that although there was a significant increase in collateral number, length and complexity there was no increase in contacts on LPSN 3 weeks after SCI, indicating that Semaphorin7A signalling per se is not involved in detour circuit formation (Lang et al., 2012). This is in contrast to our assumption that Sema7A might be the guidance/growth promoting cue leading the newly emerging CST collaterals to the LPSN neurons to form contacts. In absence of Sema7A signalling, the increase in collaterals and their length points rather more towards a repulsive action of Sema7A on the CST fibers. This is reminiscent of recent studies that demonstrated this repulsive phenomenon in the dopaminergic tract of the brain, which is mediated by the PlexinC1 receptor (Chabrat et al., 2017). I also ensured proper motor cortex architecture in WT and KO mice to exclude a developmental phenotype in the hindlimb motor cortex.

I observed impairment in regular rhythmic walking recovery in the KO mice compared to the WT mice. Rhythmic walking is dependent on the intraspinal circuitry, prompting me to study the serotonergic wiring in the lumbar spinal cord and the brainstem, in which the major descending serotonergic motor pathways arise (Jacobs and Azmitia, 1992, Marder and Bucher, 2001). Serotonergic neurons can also be found throughout the spinal cord and their number increases after a full spinal cord transection. With loss of the central serotonergic brainstem input, serotonergic spinal interneurons undergo injury induced plasticity in order to compensate for the heavy loss of 5HT caudal to the lesion (Hou et al., 2016). Furthermore, the 5HTR2a receptor is upregulated after lesion in target neurons to render those more sensitive to the decreased serotonin signalling in the spinal cord (Kong et al., 2010).Those are compensatory mechanisms to re-facilitate movement in de-innervated lumbar regions after injury. I first ensured that the nucleus raphe obscurus (NRO), pallidus and magnus have similar serotonergic cell numbers in WT and KO. I then moved on to the lumbar spinal cord, the region of the $ChAT^{+}$ motoneurons that produce hindlimb movements if receiving central or intraspinal input. The number of $ChAT^{+}$ neurons was similar throughout all timepoints and lSPC segments analysed for Sema7A-deficient and competent mice. I then looked at the patterning and intensity of serotoninergic fibers throughout different lumbar spinal cord segments acutely (2d) and sub-acutely (7d and 21d) after injury. Early the Sema7A deficient mice showed a reduced intensity in serotonergic labelling in comparison to wildtype mice with equal patterning and distribution of innervation. The later post-injury adaptation however showed a significant increase in fiber density and intensity in the deficient mice if compared to the wildtype mice. I also found ectopic fiber locations in deficient, but not in competent mice. In these experiments I could not distinguish between the intra- and supraspinal serotonergic system. The supraspinal system sends fibers to all spinal cord segments, which are usually heavily concentrated around spinal motor neurons. Intraspinal serotonergic cells were only studied in the rat, in which there were very few reported, which mostly reside in the sacral spinal cord. Descending supraspinal input from the nucleus raphe obscurus (NRO), pallidus and magnus is reported to descend ventrally as well as dorsally, arguing for a disruption of at least part of the supraspinal descending input to the lumbar spinal cord (Ballion et al., 2002). This evidence from literature points more towards a remodelling of the supraspinal pathways to compensate for lost innervation of the lumbar motor neurons than intraspinal strengthening of circuitry. Furthermore, serotoninergic axons are capable of regeneration, which is rarely seen in for example glutamatergic central axons (Kajstura et al., 2017). To determine the origin of the excess serotonergic fibers in the deficient mice further experiments would be needed. Viral tracing of the central 5HT neurons in the brainstem could shed light on the origin of the newly emerging fibers in the lumbar spinal cord. This finding is in accordance with a very recent publication which reported the Sema7A/PlexinC1 interaction crucial for the correct targeting of the mesodiencephalic dopaminergic tracts (mDA) of the brain. This repulsive interaction is responsible for their correct outgrowth and

topographical organization of mDA neurons. If Sema7A is absent the mDA neurons are no longer repelled from the ventral tegmental area (VTA) and overgrow their target area into the striatum (Chabrat et al., 2017).

Serotoninergic innervation in the spinal cord is responsible for the modulation of sensory, motor and autonomic functions (Jacobs and Azmitia, 1992). The ectopic and extensive serotonergic innervation in the lumbar spinal cord can impair correct motor neuron facilitation, thereby explaining the motor recovery phenotype of the Sema7A KO mice. Contacts onto motor neurons could not be formed, growing neuronal fibers usually stop growing upon finding a synaptic partner. This process could be impaired with the missing repulsive action of Sema7A. Hyperinnervation can also lead to spasticity, as the balance between excitation and inhibition can be disturbed. Spasticity is a problem in incomplete spinal cord injuries and causes many difficulties in movement in the affected individuals as spasticity has a negative impact on otherwise sufficiently innervated motor units and therapeutic approaches to treat that phenomenon improve the quality of life (Duffell et al., 2015, Hofstoetter et al., 2014). Recent research also discovered that constitutively active 5HTR2α facilitate muscle spasms after human spinal cord injury linking the serotonergic system to spasticity (D'Amico et al., 2013). Increases spasticity induced by elevated serotonin levels in the lumbar cord could also explain the impaired motor recovery from spinal cord injury of the Sema7A-deficient mice. Spasticity however is difficult to measure in a mouse model.

Most basic research in spinal cord injury is motivated by either understanding regenerative failure and potential or uncovering possible therapeutic targets that can be delivered pharmaceutically or virally. Viral modulation of the Sema7A – PlexinC1 and – α1β1 Integrin signalling pathway, needs careful consideration as the precise involvement in immunomodulation and cancer progression is still not completely clear (Black et al., 2016, Czopik et al., 2006, Gutierrez-Franco et al., 2016, Scott et al., 2009, Suzuki et al., 2007). We first need to understand the different roles of Sema7A in the nervous and immune system as well as in tumour growth before we aim at a therapeutic approach.

4.3. FGF22 in recovery and synapse formation after injury

Synapse formation is a critical step for neurons during development. It is not only about finding the right partner, but also the right and sufficient connections that need to be established. Likewise, the formation of a pre- and a postsynapse need to be induced by signalling molecules and matching receptors like SynCam, Wnt or FGFs and their receptors (Fox and Umemori, 2006). Once the connections that were established during development are severed by, for example, an injury or inflammation, the neuron usually uses the developmental blue prints again to search for a new meaningful connection. We

identified FGF22 and its receptors FGFR1 and R2 as key regulators in synapse establishment during detour circuit formation after SCI. FGFR1 and R2 are expressed on the outgrowing dCST collateral while FGF22, the postsynaptic partner, is expressed by LPSN. The contact between these dCST fibers and the LPSN establishes the detour circuit for functional recovery (Bareyre et al., 2004). FGF22 or FGFR1 and FGFR2 deficient mice show an impairment in functional recovery which is in accordance with the delayed and reduced detour circuit formation. Whereas a deletion of FGF22 did not alter the sprouting of CST collaterals per se, it impaired the formation of synaptic boutons and contacts onto the relay neurons that mediate functional recovery. Moreover, the boutons that did form were significant less likely to express bassoon, a marker for the presynaptic active zone, or synapsin, a presynaptic vesicle protein. If one of the receptors FGFR1 and R2 was absent from the CST, a significant increase in CST sprouting and a reduction in boutons, but no reduction in contacts on LPSN was observed. The increase in CST sprouting is most likely compensatory. If both receptors were deleted from the CST collateral formation normalized, but synapse formation impairment was comparably to the FGF22 KO. Both the deletion of the two receptors as well as deletion of FGF22 significantly impaired functional recovery after SCI measured by the Ladder Rung and the Catwalk gait analysis. The role of FGF22 in synapse formation during development has been shown before (Terauchi et al., 2016, Terauchi et al., 2010), but our study revealed a role in injury-induced synaptic plasticity and circuit formation of the spinal cord for FGF22 and its receptors. This argues for a ubiquitous function of FGF22 in synapse formation throughout development and adulthood whenever the de novo formation of synapses is required.

As impairment of correct FGF22 and FGFR1 and R2 signalling reduces synapses, sprouting and detour circuit formation as well as functional recovery, we started to be interested in the potential of FGF22 overexpression as potential therapeutic approach to improve not only synapse and detour circuit formation, but also functional recovery following SCI.

To this end, I am now carrying a study in the laboratory that aims at investigating the role of FGF22 delivered via gene therapy in the cervical spinal cord to induce synapse formation between CST and LPSN and functional recovery. Viral gene transfer is an interesting strategy that is already currently used in clinic in the treatment of certain conditions such as hereditary loss of eyesight for example (Pierce and Bennett, 2015). It is relatively selective as expression can be targeted to certain cell populations with either different capsid proteins or selective neuronal promoters like hSyn (human synapsin promotor to specifically target neurons), or Vglut2 (vesicular glutamine transporter 2 to specifically target excitatory neurons) thereby reducing the risk of aberrant growth induction and side effects (Aschauer et al., 2013). Thereby FGF22 overexpression might be a therapeutic intervention to improve functional recovery, circuit rewiring and remodelling after SCI.

FGF22 is a growth factor and thereby bears risks if overexpressed. FGF22 and its receptor has been implicated in the development and progression of skin and breast carcinoma (Jarosz et al., 2012, Katoh, 2008), which could be a severe adverse side effect if the molecule is overexpressed. Nevertheless, viral gene transfer can selectively target certain cell populations with either capsid proteins or selective neuronal promoters like hSyn (human synapsin promoter), thereby reducing the risk of aberrant growth induction (Aschauer et al., 2013). Thereby FGF22 overexpression might be a therapeutic target to improve functional recovery, circuit rewiring and remodelling after SCI.

We used a therapeutic gene delivery strategy using a recombinant AAV2 (adeno associated virus, rAAV) to overexpress FGF22 alongside with GFP (green fluorescent protein) in the cervical spinal cord of mice. We choose an AAV2 system for its neuronal tropism and the CMV for efficient expression (Figure 15). As control vector we used the same AAV expressing GFP without the FGF22 sequence to control for a possible effect of the virus injection and the GFP expression only.

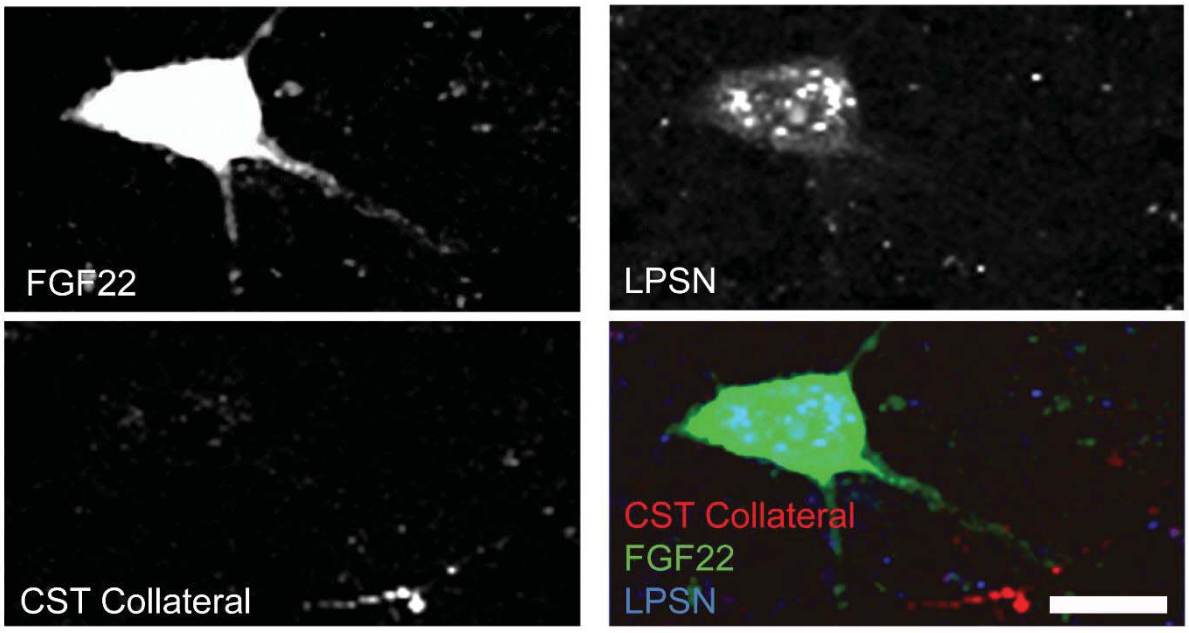

***Figure 15**: Confocal Scan of a LPSN (blue) overexpressing FGF22 and GFP (green). CST collateral in close proximity to the neuron (red).*

We traced the corticospinal tract, the LPSN, performed a T8 dorsal thoracic hemisection and injected the AAV overexpressing FGF22 5 days prior to the lesion in the cervical cord. We then analysed detour circuit formation in the cervical spinal cord of these mice and found an increase in CST collateral boutons and branchpoints, which is in accordance with the role of FGF22 in synapse formation. We then analysed the contacts of the CST collaterals onto interneurons, separating into contacts on LPSN, contacts onto FGF22 or control GFP positive interneurons and GFP/FGF22 positive interneurons regardless of whether they were LPSN or not. We found a significant increase in contacts onto

interneurons that over-expressed FGF22 in comparison to GFP only, regardless of whether they were LPSN or not. There was no significant increase in contacts onto LPSN per se, indicating that the effect on contact formation is FGF22 dependent (Figure 16).

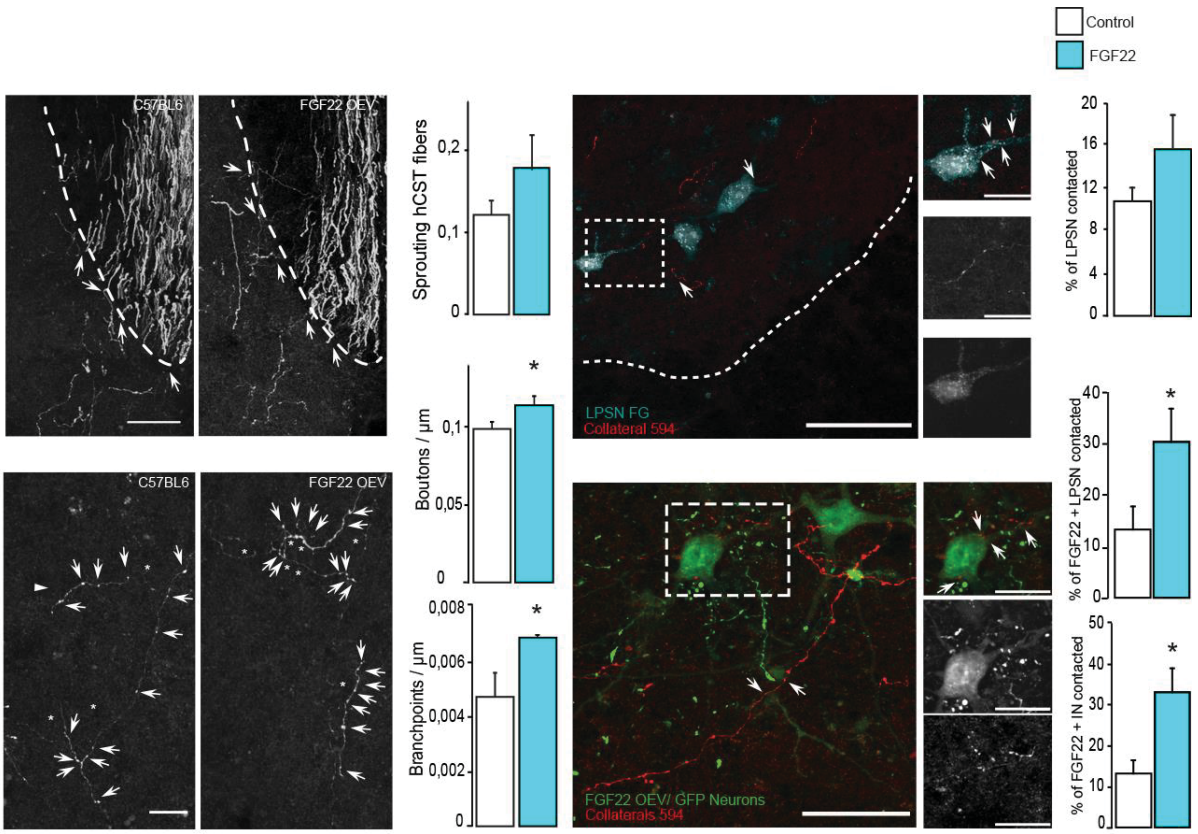

***Figure 16**: Representative pictures and quantification of FGF22 overexpression experiments in the cervical spinal cord. We analyzed sprouting hCST fibers, boutons, branchpoints and contacts onto different interneuron populations (red: CST collateral, green: FGF22 or GFP only, blue: LPSN labelled with fluorogold).*

Pre-treatment 5 days before injury increases the formation of the detour circuit. However, pre-treatment is not feasible clinically as patients do not plan on experiencing spinal cord trauma, which is why we currently aim to test this treatment paradigm at different timepoints after injury. We want to determine whether post-treatment with FGF22 overexpression also has a positive effect on detour circuit formation and functional recovery and determine whether and until when this treatment is beneficial after the injury. As FGF22 is a growth factor treatment with overexpression always bears some risks for tumour induction or other aberrant neuronal and non-neuronal growth that could be detrimental to recovery. So far, we have not seen any adverse side effects of the treatment, which is in part due to the injection into the CNS where the potential for growth and proliferation is generally rather limited.

Combination of exercise to generate more growth and remodelling as well as correct targeting, together with overexpression of the synaptogenic FGF22 and a potent growth factor, like STAT3 (Bareyre et al., 2011, Lang et al., 2013) could provide the injured circuit with a potent therapy to optimize detour circuit formation. These combinatorial therapies are already used with success for example with chondroitinase treatment, which digests the inhibitory extracellular matrix, in combination with exercise. Chondroitinase alone does not improve functional recovery, only with training (Garcia-Alias et al., 2009). We would like to combine our FGF22 overexpression with STAT3 overexpression (Lang et al., 2013) and voluntary wheel running to optimize collateral sprouting, synapse and detour circuit formation. This will hopefully harness the full capacity of the injured CST fibers for remodelling and thus result in greatly improved and accelerated behavioural recovery in comparison to a single therapeutic intervention. Combinatory therapies should be the future in SCI research as one treatment alone has yet to be found that made the transition from bench to bedside and has a potent enough therapeutic effect to reverse the impairments of such a devastating disease as spinal cord injury.

5. Conclusion

In contrast to complete spinal cord transections, incomplete spinal cord injuries have the potential to be followed by functional recovery. It has been extensively shown that axonal remodelling contributes to functional recovery by re-connecting deinnervated regions directly or by relay neurons (Bareyre et al., 2004, van den Brand et al., 2012, Zorner et al., 2014). In this thesis I aimed at understanding the underlying principles that contribute to axonal remodelling and functional recovery as a complete understanding of every step of the plastic abilities of a neuron is a necessary prerequisite for efficient therapy development. I demonstrated that voluntary exercise is a growth promoting intervention that helps forming relevant functional connections, and investigated additional molecular factors that contribute to axonal targeting and synapse formation.

While I could see differences in functional recovery with every intervention, I believe that combining therapies is the only way to achieve functional improvements that resembles the motor capacities before the injury. Therefore, my work paves the way for the development of such combinatorial interventions as we identified here two molecules that respectively modify axon targeting (Sema7A) and synapse formation (FGF22) and we demonstrate that voluntary exercise is key to potentiate the recovery. One avenue to this work is the combination of rehabilitation with gene therapies enhancing meaningful factors, like FGF22, STAT3 or Sema7A in targeted areas of the injured spinal cord. I believe this is the exciting direction spinal cord injury research should take and this might, one day, positively influence the outcome of spinal cord injured patients.

6. References

ABBOTT, A. 2014. Biomedicine: the changing face of primate research. *Nature,* 506**,** 24-6.

ALSTERMARK, B., LUNDBERG, A., PINTER, M. & SASAKI, S. 1987. Subpopulations and functions of long C3-C5 propriospinal neurones. *Brain Res,* 404**,** 395-400.

ARMOUR, B. S., COURTNEY-LONG, E. A., FOX, M. H., FREDINE, H. & CAHILL, A. 2016. Prevalence and Causes of Paralysis-United States, 2013. *Am J Public Health,* 106**,** 1855-7.

ASCHAUER, D. F., KREUZ, S. & RUMPEL, S. 2013. Analysis of transduction efficiency, tropism and axonal transport of AAV serotypes 1, 2, 5, 6, 8 and 9 in the mouse brain. *PLoS One,* 8**,** e76310.

ATKINSON, P. P. & ATKINSON, J. L. D. 1996. Spinal Shock. *Mayo Clinic Proceedings,* 71**,** 384-389.

BALLION, B., BRANCHEREAU, P., CHAPRON, J. & VIALA, D. 2002. Ontogeny of descending serotonergic innervation and evidence for intraspinal 5-HT neurons in the mouse spinal cord. *Brain Res Dev Brain Res,* 137**,** 81-8.

BAREYRE, F. M., GARZORZ, N., LANG, C., MISGELD, T., BUNING, H. & KERSCHENSTEINER, M. 2011. In vivo imaging reveals a phase-specific role of STAT3 during central and peripheral nervous system axon regeneration. *Proc Natl Acad Sci U S A,* 108**,** 6282-7.

BAREYRE, F. M., KERSCHENSTEINER, M., RAINETEAU, O., METTENLEITER, T. C., WEINMANN, O. & SCHWAB, M. E. 2004. The injured spinal cord spontaneously forms a new intraspinal circuit in adult rats. *Nat Neurosci,* 7**,** 269-77.

BATTISTUZZO, C. R., RANK, M. M., FLYNN, J. R., MORGAN, D. L., CALLISTER, R., CALLISTER, R. J. & GALEA, M. P. 2016. Gait recovery following spinal cord injury in mice: Limited effect of treadmill training. *The Journal of Spinal Cord Medicine,* 39**,** 335-343.

BEATTIE, M. S., BRESNAHAN, J. C., KOMON, J., TOVAR, C. A., VAN METER, M., ANDERSON, D. K., FADEN, A. I., HSU, C. Y., NOBLE, L. J., SALZMAN, S. & YOUNG, W. 1997. Endogenous repair after spinal cord contusion injuries in the rat. *Exp Neurol,* 148**,** 453-63.

BECKER, S. 2002. Rehabilitation und lebenslange Nachsorge nach Querschnittlähmung. *Trauma und Berufskrankheit,* 4**,** S32-S36.

BERLLY, M. & SHEM, K. 2007. Respiratory Management During the First Five Days After Spinal Cord Injury. *The Journal of Spinal Cord Medicine,* 30**,** 309-318.

BERTRAND, S. S. & CAZALETS, J. R. 2013. Activity-dependent synaptic plasticity and metaplasticity in spinal motor networks. *Curr Pharm Des,* 19**,** 4498-508.

BLACK, S. A., NELSON, A. C., GURULE, N. J., FUTSCHER, B. W. & LYONS, T. R. 2016. Semaphorin 7a exerts pleiotropic effects to promote breast tumor progression. *Oncogene,* 35**,** 5170-8.

BUNGE, R. P., PUCKETT, W. R., BECERRA, J. L., MARCILLO, A. & QUENCER, R. M. 1993. Observations on the pathology of human spinal cord injury. A review and classification of 22 new cases with details from a case of chronic cord compression with extensive focal demyelination. *Adv Neurol,* 59**,** 75-89.

CABAJ, A. M., MAJCZYNSKI, H., COUTO, E., GARDINER, P. F., STECINA, K., SLAWINSKA, U. & JORDAN, L. M. 2017. Serotonin controls initiation of locomotion and afferent modulation of coordination via 5-HT7 receptors in adult rats. *J Physiol,* 595**,** 301-320.

CAPOGROSSO, M., MILEKOVIC, T., BORTON, D., WAGNER, F., MORAUD, E. M., MIGNARDOT, J. B., BUSE, N., GANDAR, J., BARRAUD, Q., XING, D., REY, E., DUIS, S., JIANZHONG, Y., KO, W. K., LI, Q., DETEMPLE, P., DENISON, T., MICERA, S., BEZARD, E., BLOCH, J. & COURTINE, G. 2016. A brain-spine interface alleviating gait deficits after spinal cord injury in primates. *Nature,* 539**,** 284-288.

CARCEA, I., PATIL, S. B., ROBISON, A. J., MESIAS, R., HUNTSMAN, M. M., FROEMKE, R. C., BUXBAUM, J. D., HUNTLEY, G. W. & BENSON, D. L. 2014. Maturation of cortical circuits requires Semaphorin 7A. *Proc Natl Acad Sci U S A,* 111**,** 13978-83.

CHABRAT, A., BRISSON, G., DOUCET-BEAUPRE, H., SALESSE, C., SCHAAN PROFES, M., DOVONOU, A., AKITEGETSE, C., CHAREST, J., LEMSTRA, S., COTE, D., PASTERKAMP, R. J., ABRUDAN, M. I., METZAKOPIAN, E., ANG, S. L. & LEVESQUE, M. 2017. Transcriptional repression of Plxnc1 by Lmx1a and Lmx1b directs topographic dopaminergic circuit formation. *Nat Commun,* 8**,** 933.

CHEN, M. S., HUBER, A. B., VAN DER HAAR, M. E., FRANK, M., SCHNELL, L., SPILLMANN, A. A., CHRIST, F. & SCHWAB, M. E. 2000. Nogo-A is a myelin-associated neurite outgrowth inhibitor and an antigen for monoclonal antibody IN-1. *Nature,* 403**,** 434-9.

CHERIYAN, T., RYAN, D. J., WEINREB, J. H., CHERIYAN, J., PAUL, J. C., LAFAGE, V., KIRSCH, T. & ERRICO, T. J. 2014. Spinal cord injury models: a review. *Spinal Cord,* 52**,** 588-95.

CHOO, A. M., LIU, J., LIU, Z., DVORAK, M., TETZLAFF, W. & OXLAND, T. R. 2009. Modeling spinal cord contusion, dislocation, and distraction: characterization of vertebral clamps, injury severities, and node of Ranvier deformations. *J Neurosci Methods,* 181**,** 6-17.

CINA, C. & HOCHMAN, S. 2000. Diffuse distribution of sulforhodamine-labeled neurons during serotonin-evoked locomotion in the neonatal rat thoracolumbar spinal cord. *J Comp Neurol,* 423**,** 590-602.

CÔTÉ, M.-P., MURRAY, M. & LEMAY, M. A. 2016. Rehabilitation Strategies after Spinal Cord Injury: Inquiry into the Mechanisms of Success and Failure. *Journal of Neurotrauma,* 34**,** 1841-1857.

COURTINE, G., SONG, B., ROY, R. R., ZHONG, H., HERRMANN, J. E., AO, Y., QI, J., EDGERTON, V. R. & SOFRONIEW, M. V. 2008. Recovery of supraspinal control of stepping via indirect propriospinal relay connections after spinal cord injury. *Nat Med,* 14**,** 69-74.

CZOPIK, A. K., BYNOE, M. S., PALM, N., RAINE, C. S. & MEDZHITOV, R. 2006. Semaphorin 7A is a negative regulator of T cell responses. *Immunity,* 24**,** 591-600.

D'AMICO, J. M., MURRAY, K. C., LI, Y., CHAN, K. M., FINLAY, M. G., BENNETT, D. J. & GORASSINI, M. A. 2013. Constitutively active 5-HT2/alpha1 receptors facilitate muscle spasms after human spinal cord injury. *J Neurophysiol,* 109**,** 1473-84.

DAVID, S. & KRONER, A. 2011. Repertoire of microglial and macrophage responses after spinal cord injury. *Nat Rev Neurosci,* 12**,** 388-99.

DEVIVO, M., CHEN, Y., MENNEMEYER, S. & DEUTSCH, A. 2011. Costs of Care Following Spinal Cord Injury. *Topics in Spinal Cord Injury Rehabilitation,* 16**,** 1-9.

DI GIOVANNI, S. 2009. Molecular targets for axon regeneration: focus on the intrinsic pathways. *Expert Opin Ther Targets,* 13**,** 1387-98.

DOMINICI, N., KELLER, U., VALLERY, H., FRIEDLI, L., VAN DEN BRAND, R., STARKEY, M. L., MUSIENKO, P., RIENER, R. & COURTINE, G. 2012. Versatile robotic interface to evaluate, enable and train locomotion and balance after neuromotor disorders. *Nat Med,* 18**,** 1142-7.

DUFFELL, L. D., BROWN, G. L. & MIRBAGHERI, M. M. 2015. Interventions to Reduce Spasticity and Improve Function in People With Chronic Incomplete Spinal Cord Injury: Distinctions Revealed by Different Analytical Methods. *Neurorehabil Neural Repair,* 29**,** 566-76.

DUMONT, R. J., OKONKWO, D. O., VERMA, S., HURLBERT, R. J., BOULOS, P. T., ELLEGALA, D. B. & DUMONT, A. S. 2001a. Acute spinal cord injury, part I: pathophysiologic mechanisms. *Clin Neuropharmacol,* 24**,** 254-64.

DUMONT, R. J., VERMA, S., OKONKWO, D. O., HURLBERT, R. J., BOULOS, P. T., ELLEGALA, D. B. & DUMONT, A. S. 2001b. Acute spinal cord injury, part II: contemporary pharmacotherapy. *Clin Neuropharmacol,* 24**,** 265-79.

DUPONT-VERSTEEGDEN, E. E., HOULE, J. D., DENNIS, R. A., ZHANG, J., KNOX, M., WAGONER, G. & PETERSON, C. A. 2004. Exercise-induced gene expression in soleus muscle is dependent on time after spinal cord injury in rats. *Muscle Nerve,* 29**,** 73-81.

ENGESSER-CESAR, C., ANDERSON, A. J., BASSO, D. M., EDGERTON, V. R. & COTMAN, C. W. 2005. Voluntary wheel running improves recovery from a moderate spinal cord injury. *J Neurotrauma,* 22**,** 157-71.

ENGESSER-CESAR, C., ICHIYAMA, R. M., NEFAS, A. L., HILL, M. A., EDGERTON, V. R., COTMAN, C. W. & ANDERSON, A. J. 2007. Wheel running following spinal cord injury improves locomotor recovery and stimulates serotonergic fiber growth. *Eur J Neurosci,* 25**,** 1931-9.

ESCALONA, M., DELIVET-MONGRAIN, H., KUNDU, A., GOSSARD, J.-P. & ROSSIGNOL, S. 2017. Ladder Treadmill: A Method to Assess Locomotion in Cats with an Intact or Lesioned Spinal Cord. *The Journal of Neuroscience,* 37**,** 5429-5446.

FIGLEY, S. A., KHOSRAVI, R., LEGASTO, J. M., TSENG, Y.-F. & FEHLINGS, M. G. 2013. Characterization of Vascular Disruption and Blood–Spinal Cord Barrier Permeability following Traumatic Spinal Cord Injury. *Journal of Neurotrauma,* 31**,** 541-552.

FINK, K. B. & GÖTHERT, M. 2007. 5-HT Receptor Regulation of Neurotransmitter Release. *Pharmacological Reviews,* 59**,** 360-417.

FOUAD, K. & TETZLAFF, W. 2012. Rehabilitative training and plasticity following spinal cord injury. *Exp Neurol,* 235**,** 91-9.

FOX, M. A. & UMEMORI, H. 2006. Seeking long-term relationship: axon and target communicate to organize synaptic differentiation. *J Neurochem,* 97**,** 1215-31.

FRIEDLI, L., ROSENZWEIG, E. S., BARRAUD, Q., SCHUBERT, M., DOMINICI, N., AWAI, L., NIELSON, J. L., MUSIENKO, P., NOUT-LOMAS, Y., ZHONG, H., ZDUNOWSKI, S., ROY, R. R., STRAND, S. C., VAN DEN BRAND, R., HAVTON, L. A., BEATTIE, M. S., BRESNAHAN, J. C., BÉZARD, E., BLOCH, J., EDGERTON, V. R., FERGUSON, A. R., CURT, A., TUSZYNSKI, M. H. & COURTINE, G. 2015. Pronounced species divergence in corticospinal tract reorganization and functional recovery after lateralized spinal cord injury favors primates. *Science Translational Medicine,* 7**,** 302ra134-302ra134.

GARCIA-ALIAS, G., BARKHUYSEN, S., BUCKLE, M. & FAWCETT, J. W. 2009. Chondroitinase ABC treatment opens a window of opportunity for task-specific rehabilitation. *Nat Neurosci,* 12**,** 1145-51.

GARCIA-AREAS, R., LIBREROS, S., AMAT, S., KEATING, P., CARRIO, R., ROBINSON, P., BLIEDEN, C. & IRAGAVARAPU-CHARYULU, V. 2014. Semaphorin7A promotes tumor growth and exerts a pro-angiogenic effect in macrophages of mammary tumor-bearing mice. *Front Physiol,* 5**,** 17.

GARCIA-AREAS, R., LIBREROS, S. & IRAGAVARAPU-CHARYULU, V. 2013. Semaphorin7A: branching beyond axonal guidance and into immunity. *Immunol Res,* 57**,** 81-5.

GENSEL, J. C., TOVAR, C. A., HAMERS, F. P., DEIBERT, R. J., BEATTIE, M. S. & BRESNAHAN, J. C. 2006. Behavioral and histological characterization of unilateral cervical spinal cord contusion injury in rats. *J Neurotrauma,* 23**,** 36-54.

GEOFFROY, C. G., LORENZANA, A. O., KWAN, J. P., LIN, K., GHASSEMI, O., MA, A., XU, N., CREGER, D., LIU, K., HE, Z. & ZHENG, B. 2015. Effects of PTEN and Nogo Codeletion on Corticospinal Axon Sprouting and Regeneration in Mice. *J Neurosci,* 35**,** 6413-28.

GHANEM, R. C., HAN, K. Y., ROJAS, J., OZTURK, O., KIM, D. J., JAIN, S., CHANG, J. H. & AZAR, D. T. 2011. Semaphorin 7A promotes angiogenesis in an experimental corneal neovascularization model. *Curr Eye Res,* 36**,** 989-96.

GHOSH, M. & PEARSE, D. D. 2014. The role of the serotonergic system in locomotor recovery after spinal cord injury. *Frontiers in Neural Circuits,* 8**,** 151.

GIRGIS, J., MERRETT, D., KIRKLAND, S., METZ, G. A., VERGE, V. & FOUAD, K. 2007. Reaching training in rats with spinal cord injury promotes plasticity and task specific recovery. *Brain,* 130**,** 2993-3003.

GRILLNER, S. 2006. Biological pattern generation: the cellular and computational logic of networks in motion. *Neuron,* 52**,** 751-66.

GRUNER, J. A. 1992. A monitored contusion model of spinal cord injury in the rat. *J Neurotrauma,* 9**,** 123-6; discussion 126-8.

GUERTIN, P. A. 2009. The mammalian central pattern generator for locomotion. *Brain Res Rev,* 62**,** 45-56.

GUTIERREZ-FRANCO, A., COSTA, C., EIXARCH, H., CASTILLO, M., MEDINA-RODRIGUEZ, E. M., BRIBIAN, A., DE CASTRO, F., MONTALBAN, X. & ESPEJO, C. 2016. Differential expression of sema3A and sema7A in a murine model of multiple sclerosis: Implications for a therapeutic design. *Clin Immunol,* 163**,** 22-33.

HAN, Q., CAO, C., DING, Y., SO, K. F., WU, W., QU, Y. & ZHOU, L. 2015. Plasticity of motor network and function in the absence of corticospinal projection. *Exp Neurol,* 267**,** 194-208.

HANNON, J. & HOYER, D. 2008. Molecular biology of 5-HT receptors. *Behav Brain Res,* 195**,** 198-213.

HARKEMA, S. J., HILLYER, J., SCHMIDT-READ, M., ARDOLINO, E., SISTO, S. A. & BEHRMAN, A. L. 2012. Locomotor training: as a treatment of spinal cord injury and in the progression of neurologic rehabilitation. *Arch Phys Med Rehabil,* 93**,** 1588-97.

HAYES, H. B., CHANG, Y. H. & HOCHMAN, S. 2009. An in vitro spinal cord-hindlimb preparation for studying behaviorally relevant rat locomotor function. *J Neurophysiol,* 101**,** 1114-22.

HEINS, N., MALATESTA, P., CECCONI, F., NAKAFUKU, M., TUCKER, K. L., HACK, M. A., CHAPOUTON, P., BARDE, Y. A. & GOTZ, M. 2002. Glial cells generate neurons: the role of the transcription factor Pax6. *Nat Neurosci,* 5**,** 308-15.

HICKS, A. L., MARTIN, K. A., DITOR, D. S., LATIMER, A. E., CRAVEN, C., BUGARESTI, J. & MCCARTNEY, N. 2003. Long-term exercise training in persons with spinal cord injury: effects on strength, arm ergometry performance and psychological well-being. *Spinal Cord,* 41**,** 34-43.

HOFSTOETTER, U. S., MCKAY, W. B., TANSEY, K. E., MAYR, W., KERN, H. & MINASSIAN, K. 2014. Modification of spasticity by transcutaneous spinal cord stimulation in individuals with incomplete spinal cord injury. *J Spinal Cord Med,* 37**,** 202-11.

HOTTING, K. & RODER, B. 2013. Beneficial effects of physical exercise on neuroplasticity and cognition. *Neurosci Biobehav Rev,* 37**,** 2243-57.

HOU, S., CARSON, D. M., WU, D., KLAW, M. C., HOULE, J. D. & TOM, V. J. 2016. Dopamine is produced in the rat spinal cord and regulates micturition reflex after spinal cord injury. *Exp Neurol,* 285**,** 136-146.

HOULE, J. D. & COTE, M. P. 2013. Axon regeneration and exercise-dependent plasticity after spinal cord injury. *Ann N Y Acad Sci,* 1279**,** 154-63.

HUBLI, M. & DIETZ, V. 2013. The physiological basis of neurorehabilitation - locomotor training after spinal cord injury. *Journal of NeuroEngineering and Rehabilitation,* 10**,** 5.

HURLBERT, R. J. 2000. Methylprednisolone for acute spinal cord injury: an inappropriate standard of care. *J Neurosurg,* 93**,** 1-7.

IWANAMI, A., YAMANE, J., KATOH, H., NAKAMURA, M., MOMOSHIMA, S., ISHII, H., TANIOKA, Y., TAMAOKI, N., NOMURA, T., TOYAMA, Y. & OKANO, H. 2005. Establishment of graded spinal cord injury model in a nonhuman primate: the common marmoset. *J Neurosci Res,* 80**,** 172-81.

JACOBI, A. & BAREYRE, F. M. 2015. Regulation of axonal remodeling following spinal cord injury. *Neural Regen Res,* 10**,** 1555-7.

JACOBI, A., SCHMALZ, A. & BAREYRE, F. M. 2014. Abundant expression of guidance and synaptogenic molecules in the injured spinal cord. *PLoS One,* 9**,** e88449.

JACOBS, B. L. & AZMITIA, E. C. 1992. Structure and function of the brain serotonin system. *Physiol Rev,* 72**,** 165-229.

JACOBS, B. L. & FORNAL, C. A. 1997. Serotonin and motor activity. *Curr Opin Neurobiol,* 7**,** 820-5.

JAKEMAN, L. B., GUAN, Z., WEI, P., PONNAPPAN, R., DZWONCZYK, R., POPOVICH, P. G. & STOKES, B. T. 2000. Traumatic spinal cord injury produced by controlled contusion in mouse. *J Neurotrauma,* 17**,** 299-319.

JAKEMAN, L. B., HOSCHOUER, E. L. & BASSO, D. M. 2011. Injured mice at the gym: review, results and considerations for combining chondroitinase and locomotor exercise to enhance recovery after spinal cord injury. *Brain Res Bull,* 84**,** 317-26.

JAROSZ, M., ROBBEZ-MASSON, L., CHIONI, A. M., CROSS, B., ROSEWELL, I. & GROSE, R. 2012. Fibroblast growth factor 22 is not essential for skin development and repair but plays a role in tumorigenesis. *PLoS One,* 7**,** e39436.

JEANSSON, M., GAWLIK, A., ANDERSON, G., LI, C., KERJASCHKI, D., HENKELMAN, M. & QUAGGIN, S. E. 2011. Angiopoietin-1 is essential in mouse vasculature during development and in response to injury. *J Clin Invest,* 121**,** 2278-89.

JONGBLOETS, B. C., LEMSTRA, S., SCHELLINO, R., BROEKHOVEN, M. H., PARKASH, J., HELLEMONS, A. J., MAO, T., GIACOBINI, P., VAN PRAAG, H., DE MARCHIS, S., RAMAKERS, G. M. & PASTERKAMP, R. J. 2017. Stage-specific functions of Semaphorin7A during adult hippocampal neurogenesis rely on distinct receptors. *Nat Commun,* 8**,** 14666.

KAJSTURA, T. J., DOUGHERTY, S. E. & LINDEN, D. J. 2017. Serotonin axons in the neocortex of the adult female mouse regrow after traumatic brain injury. *J Neurosci Res*.

KAKULAS, B. A. 1999. The applied neuropathology of human spinal cord injury. *Spinal Cord,* 37**,** 79-88.

KATOH, M. 2008. Cancer genomics and genetics of FGFR2 (Review). *Int J Oncol,* 33**,** 233-7.

KE, Z., YIP, S. P., LI, L., ZHENG, X. X. & TONG, K. Y. 2011. The effects of voluntary, involuntary, and forced exercises on brain-derived neurotrophic factor and motor function recovery: a rat brain ischemia model. *PLoS One,* 6**,** e16643.

KEIRSTEAD, H. S., HASAN, S. J., MUIR, G. D. & STEEVES, J. D. 1992. Suppression of the onset of myelination extends the permissive period for the functional repair of embryonic spinal cord. *Proc Natl Acad Sci U S A,* 89**,** 11664-8.

KONG, X. Y., WIENECKE, J., HULTBORN, H. & ZHANG, M. 2010. Robust upregulation of serotonin 2A receptors after chronic spinal transection of rats: an immunohistochemical study. *Brain Res,* 1320**,** 60-8.

KOPP, M. A., BROMMER, B., GATZEMEIER, N., SCHWAB, J. M. & PRUSS, H. 2010. Spinal cord injury induces differential expression of the profibrotic semaphorin 7A in the developing and mature glial scar. *Glia,* 58**,** 1748-56.

KUHN, P. L. & WRATHALL, J. R. 1998. A mouse model of graded contusive spinal cord injury. *J Neurotrauma,* 15**,** 125-40.

KUNDI, S., BICKNELL, R. & AHMED, Z. 2013. The role of angiogenic and wound-healing factors after spinal cord injury in mammals. *Neurosci Res,* 76**,** 1-9.

LANDRY, E. S., LAPOINTE, N. P., ROUILLARD, C., LEVESQUE, D., HEDLUND, P. B. & GUERTIN, P. A. 2006. Contribution of spinal 5-HT1A and 5-HT7 receptors to locomotor-like movement induced by 8-OH-DPAT in spinal cord-transected mice. *Eur J Neurosci,* 24**,** 535-46.

LANG, C., BRADLEY, P. M., JACOBI, A., KERSCHENSTEINER, M. & BAREYRE, F. M. 2013. STAT3 promotes corticospinal remodelling and functional recovery after spinal cord injury. *EMBO Rep,* 14**,** 931-7.

LANG, C., GUO, X., KERSCHENSTEINER, M. & BAREYRE, F. M. 2012. Single collateral reconstructions reveal distinct phases of corticospinal remodeling after spinal cord injury. *PLoS One,* 7**,** e30461.

LEE, B. B., CRIPPS, R. A., FITZHARRIS, M. & WING, P. C. 2014. The global map for traumatic spinal cord injury epidemiology: update 2011, global incidence rate. *Spinal Cord,* 52**,** 110-6.

LEE, J. K., JOHNSON, C. S. & WRATHALL, J. R. 2007. Up-regulation of 5-HT2 receptors is involved in the increased H-reflex amplitude after contusive spinal cord injury. *Exp Neurol,* 203**,** 502-11.

LI, Y., LUCAS-OSMA, A. M., BLACK, S., BANDET, M. V., STEPHENS, M. J., VAVREK, R., SANELLI, L., FENRICH, K. K., DI NARZO, A. F., DRACHEVA, S., WINSHIP, I. R., FOUAD, K. & BENNETT, D. J. 2017. Pericytes impair capillary blood flow and motor function after chronic spinal cord injury. *Nat Med,* 23**,** 733-741.

LIEBETANZ, D. & MERKLER, D. 2006. Effects of commissural de- and remyelination on motor skill behaviour in the cuprizone mouse model of multiple sclerosis. *Exp Neurol,* 202**,** 217-24.

LIU, K., LU, Y., LEE, J. K., SAMARA, R., WILLENBERG, R., SEARS-KRAXBERGER, I., TEDESCHI, A., PARK, K. K., JIN, D., CAI, B., XU, B., CONNOLLY, L., STEWARD, O., ZHENG, B. & HE, Z. 2010. PTEN deletion enhances the regenerative ability of adult corticospinal neurons. *Nat Neurosci,* 13**,** 1075-81.

LU, P., WOODRUFF, G., WANG, Y., GRAHAM, L., HUNT, M., WU, D., BOEHLE, E., AHMAD, R., POPLAWSKI, G., BROCK, J., GOLDSTEIN, L. S. & TUSZYNSKI, M. H. 2014. Long-distance axonal growth from human induced pluripotent stem cells after spinal cord injury. *Neuron,* 83**,** 789-96.

MAGILL-SOLC, C. & MCMAHAN, U. J. 1988. Motor neurons contain agrin-like molecules. *J Cell Biol,* 107**,** 1825-33.

MAGOULAS, P. L. & EL-HATTAB, A. W. 2012. Chromosome 15q24 microdeletion syndrome. *Orphanet Journal of Rare Diseases,* 7**,** 2-2.

MARDER, E. & BUCHER, D. 2001. Central pattern generators and the control of rhythmic movements. *Current Biology,* 11**,** R986-R996.

MARTINEZ, M., DELIVET-MONGRAIN, H. & ROSSIGNOL, S. 2013. Treadmill training promotes spinal changes leading to locomotor recovery after partial spinal cord injury in cats. *J Neurophysiol,* 109**,** 2909-22.

MCDONALD, J. W., BECKER, D., SADOWSKY, C. L., JANE, J. A., SR., CONTURO, T. E. & SCHULTZ, L. M. 2002. Late recovery following spinal cord injury. Case report and review of the literature. *J Neurosurg,* 97**,** 252-65.

MCDONALD, J. W. & SADOWSKY, C. 2002. Spinal-cord injury. *Lancet,* 359**,** 417-25.

MEHRHOLZ, J., KUGLER, J. & POHL, M. 2012. Locomotor training for walking after spinal cord injury. *Cochrane Database Syst Rev,* 11**,** Cd006676.

MEIJER, J. H. & ROBBERS, Y. 2014. Wheel running in the wild. *Proc Biol Sci,* 281.

MESSINA, A., FERRARIS, N., WRAY, S., CAGNONI, G., DONOHUE, D. E., CASONI, F., KRAMER, P. R., DERIJCK, A. A., ADOLFS, Y., FASOLO, A., PASTERKAMP, R. J. & GIACOBINI, P. 2011. Dysregulation of Semaphorin7A/β1-integrin signaling leads to defective GnRH-1 cell migration, abnormal gonadal development and altered fertility. *Human Molecular Genetics,* 20**,** 4759-4774.

METZ, G. A. & WHISHAW, I. Q. 2009. The ladder rung walking task: a scoring system and its practical application. *J Vis Exp*.

MILLER, L. E., ZIMMERMANN, A. K. & HERBERT, W. G. 2016. Clinical effectiveness and safety of powered exoskeleton-assisted walking in patients with spinal cord injury: systematic review with meta-analysis. *Med Devices (Auckl),* 9**,** 455-66.

MORGENSTERN, D. A., ASHER, R. A. & FAWCETT, J. W. 2002. Chondroitin sulphate proteoglycans in the CNS injury response. *Prog Brain Res,* 137**,** 313-32.

MUKHOPADHYAY, G., DOHERTY, P., WALSH, F. S., CROCKER, P. R. & FILBIN, M. T. 1994. A novel role for myelin-associated glycoprotein as an inhibitor of axonal regeneration. *Neuron,* 13**,** 757-67.

MULTON, S., FRANZEN, R., POIRRIER, A. L., SCHOLTES, F. & SCHOENEN, J. 2003. The effect of treadmill training on motor recovery after a partial spinal cord compression-injury in the adult rat. *J Neurotrauma,* 20**,** 699-706.

MURRAY, K. C., NAKAE, A., STEPHENS, M. J., RANK, M., D'AMICO, J., HARVEY, P. J., LI, X., HARRIS, R. L., BALLOU, E. W., ANELLI, R., HECKMAN, C. J., MASHIMO, T., VAVREK, R., SANELLI, L., GORASSINI, M. A., BENNETT, D. J. & FOUAD, K. 2010. Recovery of motoneuron and locomotor function after spinal cord injury depends on constitutive activity in 5-HT2C receptors. *Nat Med,* 16**,** 694-700.

NAS, K., YAZMALAR, L., ŞAH, V., AYDıN, A. & ÖNEŞ, K. 2015. Rehabilitation of spinal cord injuries. *World Journal of Orthopedics,* 6**,** 8-16.

OHNO, Y., SHIMIZU, S., TOKUDOME, K., KUNISAWA, N. & SASA, M. 2015. *New insight into the therapeutic role of the serotonergic system in Parkinson's disease*.

OTOSHI, C. K., WALWYN, W. M., TILLAKARATNE, N. J., ZHONG, H., ROY, R. R. & EDGERTON, V. R. 2009. Distribution and localization of 5-HT(1A) receptors in the rat lumbar spinal cord after transection and deafferentation. *J Neurotrauma,* 26**,** 575-84.

OVERMAN, J. J. & CARMICHAEL, S. T. 2014. Plasticity in the injured brain: more than molecules matter. *Neuroscientist,* 20**,** 15-28.

PASTERKAMP, R. J. 2012. Getting neural circuits into shape with semaphorins. *Nat Rev Neurosci,* 13**,** 605-18.

PASTERKAMP, R. J., KOLK, S. M., HELLEMONS, A. J. & KOLODKIN, A. L. 2007. Expression patterns of semaphorin7A and plexinC1 during rat neural development suggest roles in axon guidance and neuronal migration. *BMC Dev Biol,* 7**,** 98.

PASTERKAMP, R. J. & KOLODKIN, A. L. 2003. Semaphorin junction: making tracks toward neural connectivity. *Curr Opin Neurobiol,* 13**,** 79-89.

PASTERKAMP, R. J., PESCHON, J. J., SPRIGGS, M. K. & KOLODKIN, A. L. 2003. Semaphorin 7A promotes axon outgrowth through integrins and MAPKs. *Nature,* 424**,** 398-405.

PIERCE, E. A. & BENNETT, J. 2015. The Status of RPE65 Gene Therapy Trials: Safety and Efficacy. *Cold Spring Harb Perspect Med,* 5**,** a017285.

PLEMEL, J. R., DUNCAN, G., CHEN, K. W., SHANNON, C., PARK, S., SPARLING, J. S. & TETZLAFF, W. 2008. A graded forceps crush spinal cord injury model in mice. *J Neurotrauma,* 25**,** 350-70.

ROSSIGNOL, S. & BOUYER, L. 2004. Adaptive mechanisms of spinal locomotion in cats. *Integr Comp Biol,* 44**,** 71-9.

SAITO, T., KASAMATSU, A., OGAWARA, K., MIYAMOTO, I., SAITO, K., IYODA, M., SUZUKI, T., ENDO-SAKAMOTO, Y., SHIIBA, M., TANZAWA, H. & UZAWA, K. 2015. Semaphorin7A Promotion of Tumoral Growth and Metastasis in Human Oral Cancer by Regulation of G1 Cell Cycle and Matrix Metalloproteases: Possible Contribution to Tumoral Angiogenesis. *PLoS One,* 10**,** e0137923.

SANES, J. R. & HALL, Z. W. 1979. Antibodies that bind specifically to synaptic sites on muscle fiber basal lamina. *J Cell Biol,* 83**,** 357-70.

SANES, J. R. & LICHTMAN, J. W. 1999. Development of the vertebrate neuromuscular junction. *Annu Rev Neurosci,* 22**,** 389-442.

SASADA, S., KATO, K., KADOWAKI, S., GROISS, S. J., UGAWA, Y., KOMIYAMA, T. & NISHIMURA, Y. 2014. Volitional walking via upper limb muscle-controlled stimulation of the lumbar locomotor center in man. *J Neurosci,* 34**,** 11131-42.

SATO, C., KOEDA S., SUMIGAWA M., MIKAMI M., AKAHIRA K., YAMADA J. 2017. Voluntary rehabilitation for promoting motor paralysis recovery in intracerebral hemorrhage model rats. *2017 Neuroscience Meeting Planner,* Program No. 317.14.

SAWADA, M., KATO, K., KUNIEDA, T., MIKUNI, N., MIYAMOTO, S., ONOE, H., ISA, T. & NISHIMURA, Y. 2015. Function of the nucleus accumbens in motor control during recovery after spinal cord injury. *Science,* 350**,** 98-101.

SCHELLINO, R., TROVA, S., CIMINO, I., FARINETTI, A., JONGBLOETS, B. C., PASTERKAMP, R. J., PANZICA, G., GIACOBINI, P., DE MARCHIS, S. & PERETTO, P. 2016. Opposite-sex attraction in male mice requires testosterone-dependent regulation of adult olfactory bulb neurogenesis. *Sci Rep,* 6**,** 36063.

SCHWAB, J. M., ZHANG, Y., KOPP, M. A., BROMMER, B. & POPOVICH, P. G. 2014. The paradox of chronic neuroinflammation, systemic immune suppression and autoimmunity after traumatic chronic spinal cord injury. *Experimental neurology,* 0**,** 121-129.

SCOTT, G. A., MCCLELLAND, L. A., FRICKE, A. F. & FENDER, A. 2009. Plexin C1, a receptor for semaphorin 7a, inactivates cofilin and is a potential tumor suppressor for melanoma progression. *J Invest Dermatol,* 129**,** 954-63.

SHAH, P. K., GARCIA-ALIAS, G., CHOE, J., GAD, P., GERASIMENKO, Y., TILLAKARATNE, N., ZHONG, H., ROY, R. R. & EDGERTON, V. R. 2013. Use of quadrupedal step training to re-engage spinal interneuronal networks and improve locomotor function after spinal cord injury. *Brain,* 136**,** 3362-77.

SHEN, K. & COWAN, C. W. 2010. Guidance Molecules in Synapse Formation and Plasticity. *Cold Spring Harbor Perspectives in Biology,* 2**,** a001842.

SILVER, J., SCHWAB, M. E. & POPOVICH, P. G. 2014. Central nervous system regenerative failure: role of oligodendrocytes, astrocytes, and microglia. *Cold Spring Harb Perspect Biol,* 7**,** a020602.

SUN, F., PARK, K. K., BELIN, S., WANG, D., LU, T., CHEN, G., ZHANG, K., YEUNG, C., FENG, G., YANKNER, B. A. & HE, Z. 2011. Sustained axon regeneration induced by co-deletion of PTEN and SOCS3. *Nature,* 480**,** 372-5.

SUZUKI, K., OKUNO, T., YAMAMOTO, M., PASTERKAMP, R. J., TAKEGAHARA, N., TAKAMATSU, H., KITAO, T., TAKAGI, J., RENNERT, P. D., KOLODKIN, A. L., KUMANOGOH, A. & KIKUTANI, H. 2007. Semaphorin 7A initiates T-cell-mediated inflammatory responses through alpha1beta1 integrin. *Nature,* 446**,** 680-4.

TAKAKUSAKI, K., OOHINATA-SUGIMOTO, J., SAITOH, K. & HABAGUCHI, T. 2004. Role of basal ganglia-brainstem systems in the control of postural muscle tone and locomotion. *Prog Brain Res,* 143**,** 231-7.

TERAUCHI, A., JOHNSON-VENKATESH, E. M., BULLOCK, B., LEHTINEN, M. K. & UMEMORI, H. 2016. Retrograde fibroblast growth factor 22 (FGF22) signaling regulates insulin-like growth factor 2 (IGF2) expression for activity-dependent synapse stabilization in the mammalian brain. *Elife,* 5.

TERAUCHI, A., JOHNSON-VENKATESH, E. M., TOTH, A. B., JAVED, D., SUTTON, M. A. & UMEMORI, H. 2010. Distinct FGFs promote differentiation of excitatory and inhibitory synapses. *Nature,* 465**,** 783-7.

THURET, S., MOON, L. D. & GAGE, F. H. 2006. Therapeutic interventions after spinal cord injury. *Nat Rev Neurosci,* 7**,** 628-43.

UESAKA, N., UCHIGASHIMA, M., MIKUNI, T., NAKAZAWA, T., NAKAO, H., HIRAI, H., AIBA, A., WATANABE, M. & KANO, M. 2014. Retrograde semaphorin signaling regulates synapse elimination in the developing mouse brain. *Science,* 344**,** 1020-3.

UMEMORI, H., LINHOFF, M. W., ORNITZ, D. M. & SANES, J. R. 2004. FGF22 and its close relatives are presynaptic organizing molecules in the mammalian brain. *Cell,* 118**,** 257-70.

VAN DEN BRAND, R., HEUTSCHI, J., BARRAUD, Q., DIGIOVANNA, J., BARTHOLDI, K., HUERLIMANN, M., FRIEDLI, L., VOLLENWEIDER, I., MORAUD, E. M., DUIS, S., DOMINICI, N., MICERA, S., MUSIENKO, P. & COURTINE, G. 2012. Restoring voluntary control of locomotion after paralyzing spinal cord injury. *Science,* 336**,** 1182-5.

VAYNMAN, S. & GOMEZ-PINILLA, F. 2005. License to run: exercise impacts functional plasticity in the intact and injured central nervous system by using neurotrophins. *Neurorehabil Neural Repair,* 19**,** 283-95.

WEIDNER, N., NER, A., SALIMI, N. & TUSZYNSKI, M. H. 2001. Spontaneous corticospinal axonal plasticity and functional recovery after adult central nervous system injury. *Proc Natl Acad Sci U S A,* 98**,** 3513-8.

WENGER, N., MORAUD, E. M., RASPOPOVIC, S., BONIZZATO, M., DIGIOVANNA, J., MUSIENKO, P., MORARI, M., MICERA, S. & COURTINE, G. 2014. Closed-loop neuromodulation of spinal sensorimotor circuits controls refined locomotion after complete spinal cord injury. *Sci Transl Med,* 6**,** 255ra133.

WESSELS, M., LUCAS, C., ERIKS, I. & DE GROOT, S. 2010. Body weight-supported gait training for restoration of walking in people with an incomplete spinal cord injury: a systematic review. *J Rehabil Med,* 42**,** 513-9.

WILLIAMS, A. J., YEE, P., SMITH, M. C., MURPHY, G. G. & UMEMORI, H. 2016. Deletion of fibroblast growth factor 22 (FGF22) causes a depression-like phenotype in adult mice. *Behav Brain Res,* 307**,** 11-7.

WIRZ, M., ZEMON, D. H., RUPP, R., SCHEEL, A., COLOMBO, G., DIETZ, V. & HORNBY, T. G. 2005. Effectiveness of automated locomotor training in patients with chronic incomplete spinal cord injury: a multicenter trial. *Arch Phys Med Rehabil,* 86**,** 672-80.

YEO, J. D., WALSH, J., RUTKOWSKI, S., SODEN, R., CRAVEN, M. & MIDDLETON, J. 1998. Mortality following spinal cord injury. *Spinal Cord,* 36**,** 329-36.

YIU, G. & HE, Z. 2006. Glial inhibition of CNS axon regeneration. *Nat Rev Neurosci,* 7**,** 617-27.

ZHANG, X., IBRAHIMI, O. A., OLSEN, S. K., UMEMORI, H., MOHAMMADI, M. & ORNITZ, D. M. 2006. Receptor specificity of the fibroblast growth factor family. The complete mammalian FGF family. *J Biol Chem,* 281**,** 15694-700.

ZHOU, Y., GUNPUT, R. A. & PASTERKAMP, R. J. 2008. Semaphorin signaling: progress made and promises ahead. *Trends Biochem Sci,* 33**,** 161-70.

ZORNER, B., BACHMANN, L. C., FILLI, L., KAPITZA, S., GULLO, M., BOLLIGER, M., STARKEY, M. L., ROTHLISBERGER, M., GONZENBACH, R. R. & SCHWAB, M. E. 2014. Chasing central nervous system plasticity: the brainstem's contribution to locomotor recovery in rats with spinal cord injury. *Brain,* 137**,** 1716-32.

IV Acknowledgement

There are a lot of ‚thanks' to be said at the end of my PhD.

First of all: I want to thank PD Dr. Florence Bareyre for giving me the opportunity to work in this amazing field of neuroscience research and for allowing me to work on all these interesting projects. Moreover thank you for your always open door and supporting my scientific as well as my personal development. And thank you for all the good advice and being a steady support throughout the rollercoaster ride that is a PhD.

A big thank you to Prof. Dr. Martin Kerschensteiner for every comment, advise and question regarding my research and for being part of my examination board in the end. I also want to thank all members of my thesis advisory committee: Prof. Dr. Leda Dimou, Prof. Dr. Hans Straka and Prof. Dr. Heidrun Potschka. Thank you for your support and your comments over the years. An extra thank you goes to Leda for also being my thesis reviewer and part of my examination board. Thanks to Dr. Leanne Godinho for being part of my examination board and Dr. Jean Livet for reviewing my thesis.

Then I would also like to thank the big and colorful crowd of the Graduate School of Systemic Neuroscience for providing me with a unique framework for my PhD filled with opportunities and joy. My first thank yous go to Lena Bittl, Renate Herzog and Stefanie Bosse for helping with virtually everything. Then I would like to thank Maj-Catherine Botheroyd-Hobohm for tirelessly managing a crowd of students throughout every social and organizing all of that. My special thanks goes to Birgit Reinbold who was always willing to help with the paperwork and formal questions that come with writing a PhD thesis and for explaining everything in an understandable way. Last of all I wanted to mention all my fellow GSN students for being peers as well as friends on this journey.

My gratitude also goes to all members of the Bareyre and Kerschensteiner Lab for all the good times spent with scientific discussions and lab work as well as late nights out, Wiesnvisits, BBQs or the like. There are some people who need a special mention. My first thanks go to the two master students I got to supervise over the years: Tobias Hoche and Ning Meng, thank you for being a big help. Then I would like to thank Marta for being the best table-mate one could ever wish for, for trips and dinners as well as for listening and always being there to help. Thanks Bep for letting me glimpse in the world of FACS. A big thanks to Ola and Elisa for letting me be part of your scientific and personal life as well as for being good friends. A special thanks to you Anne, for letting me be part of your FGF project right after I joined until the very end and more importantly for being a good friend and advisor over the years. Thank you for teaching me most of the techniques I know, for always helping out if I struggled, for encouraging me when I needed it, for all the good laughs and for all the evenings in Kennedys and the like. And last but most important: Thank you Anja for joining my project in time of need, always listening to all of my problems, sharing countless lunches, jokes and evening beers, ski trips and many other things lab related and not lab related. But most importantly thank you for being my dear friend.

I also would like to thank all my friends, especially Caro, Julian, Philipp, George, the whole original SpVgg Erlangen soccer team and the Munich IT crowd that I was fortunate to meet in my first year in Munich. Thank you for all the distractions, whether it was climbing, mountaineering or lots and lots of beers, you are the best and thank you so much for being there. A special thank you to you Michi, I am fortunate to have met you.

Last but not least I would like to thank my family for all their support over the years. Thanks to my grandparents, to whom I am especially grateful for encouraging me to pursue all my dreams. My special thanks to my parents and brothers for always being there, their constant support and helping me with everything I ever needed help with throughout all the way from school until my PhD.

V List of Publications

Loy K, Meng N, Jacobi A, Locatelli G, Bareyre FM. *Semaphorin 7A controls the proper targeting of corticospinal and serotonergic fibers following spinal cord injury.* (In preparation)

Loy K, Schmalz A, Hoche T, Jacobi A, Kreutzfeld M, Merkler D, Bareyre FM. *Voluntary exercise improves functional recovery and strengthens rewiring of supraspinal circuits following spinal cord injury*. (submitted)

Jacobi A, ***Loy K***, Schmalz AM, Hellsten M, Umemori H, Kerschensteiner M, Bareyre FM. *FGF22 signaling regulates synapse formation during post-injury remodeling of the spinal cord*. EMBO J. 2015

Purohit P, Perez-Branguli F, Prots I, Borger E, Gunn-Moore F, Welzel O, ***Loy K***, Wenzel EM, Grömer TW, Brachs S, Holzer M, Buslei R, Fritsch K, Regensburger M, Böhm KJ, Winner B, Mielenz D. *The Ca2+ sensor protein swiprosin-1/EFhd2 is present in neurites and involved in kinesin-mediated transport in neurons*. PLoS One, 2014

Loy K*, Welzel O*, Kornhuber J, Groemer TW. *Common strength and localization of spontaneous and evoked synaptic vesicle release sites.* Mol Brain 2014 (*cofirst-authors)

Jung J*, ***Loy K****, Schilling EM, Röther M, Brauner JM, Huth T, Schlötzer-Schrehardt U, Alzheimer C, Kornhuber J, Welzel O, Groemer TW. *The Antidepressant Fluoxetine Mobilizes Vesicles to the Recycling Pool of Rat Hippocampal Synapses During High Activity*. Mol Neurobiol. 2013 (*cofirst-authors)

Welzel O, ***Loy K***, Tischbirek CH, Tabor A, Gmeiner P, Kornhuber J, Groemer TW. *The pH probe CypHer^{TM}5E is effectively quenched by FM dyes*. J Fluoresc. 2013

Weider M, Küspert M, Bischof M, Vogl MR, Hornig J, ***Loy K***, Kosian T, Müller J, Hillgärtner S, Tamm ER, Metzger D, Wegner M. *Chromatin-remodeling factor Brg1 is required for Schwann cell differentiation and myelination*. Dev Cell, 2012

VII Eidesstattliche Versicherung/Affidavit

Hiermit versichere ich an Eides statt, dass ich die vorliegende Dissertation **‚Remodelling of Spinal and Supraspinal Axonal Tracts following Spinal Cord Injury: Effects of Rehabilitation and Molecular Factors'** selbstständig angefertigt habe, mich außer der angegebenen keiner weiteren Hilfsmittel bedient und alle Erkenntnisse, die aus dem Schrifttum ganz oder annähernd übernommen sind, als solche kenntlich gemacht und nach ihrer Herkunft unter Bezeichnung der Fundstelle einzeln nachgewiesen habe.

I hereby confirm that the dissertation **‚Remodelling of Spinal and Supraspinal Axonal Tracts following Spinal Cord Injury: Effects of Rehabilitation and Molecular Factors'** is the result of my own work and that I have only used sources or materials listed and specified in the dissertation.

17.01.2018	Kristina Loy
München, den (Munich, date)	Unterschrift (Signature)

VIII Author contributions

Voluntary exercise improves functional recovery and strengthens rewiring of supraspinal circuits following spinal cord injury

Kristina Loy, Anja Schmalz, Tobias Hoche, Anne Jacobi, Mario Kreutzfeldt, Doron Merkler and Florence M. Bareyre

Contributions of KL:

- designed experiments (Fig. 3, 4, 5)
- performed all surgical procedures if not stated otherwise (Fig.1-6)
- collected and analyzed all data if not stated otherwise (Fig. 1D,E,F; Fig.2, Fig.3D, Fig.4, Fig.5B catwalk data, C,D; Fig. 6)
- contributed to the writing of the manuscript

Contributions of AS:

- collected and analyzed data for the 5HT/ChAT dataset (Fig. 5B, excl Catwalk data)

Contributions of TH:

- implemented behavior experiments
- analyzed part of the behavior experiments (Fig.1)
- collected and analyzed data (Fig. 3B,C)

Contributions of AJ:

- performed part of the CST labeling

Contributions of MK and DM:

- implemented quantitative wheel running experiments (Fig. 1B)
- analyzed wheel running parameters (Fig. 1B)

Contributions of FB:

- designed experiments (Fig.1, 2, 5, 6)
- collected and analyzed data (Fig. 3 B,C)
- wrote the main part of the manuscript

Date, place

Signature Kristina Loy

Signature PD Dr. Florence Bareyre (Supervisor)

Mice lacking Semaphorin 7A show adaptations of spinal and supraspinal networks following spinal cord injury

Kristina Loy, Ning Meng, Anne Jacobi, Giuseppe Locatelli and Florence M Bareyre

Contributions of KL:

- designed experiments (Fig. 1, 2, 5, 6, S2)
- performed all surgical procedures if not stated otherwise (Fig. 1-6)
- collected and analyzed data, if not stated otherwise (Fig. 1, Fig.2A,C,D; Fig.3, Fig.4, Fig.S1, Fig. S2)
- contributed to writing the manuscript

Contributions of NM:

- performed all 5HT, 5HTR2a and ChAT immunohistochemistry
- collected and analyzed data for 5HT, 5HTR2a and ChAT experiments (Fig. 5; Fig. 6)

Contributions of AJ:

- performed part of the brain injections for CST tracing

Contributions of GL:

- designed and helped with the implementation of the FACS experiment (Fig. 2B)
- analyzed the FACS data (Fig. 2B)

Contributions of FB:

- designed experiments (Fig. 1, 3, 4, S1)
- wrote the main part of the manuscript

Date, place

Signature Kristina Loy

Signature PD Dr. Florence Bareyre (Supervisor)

FGF22 signaling regulates synapse formation during post-injury remodeling of the spinal cord

Anne Jacobi, Kristina Loy, Anja M Schmalz, Mikael Hellsten, Hisashi Umemori, Martin Kerschensteiner and Florence M Bareyre

Contributions of AJ:

- performed all surgical procedures and collected and analyzed tracing data (Fig. 1-6; S1-S8)
- performed and analyzed in-situ hybridizations and single cell PCR (Fig.1)
- performed all anatomical and immunohistochemical analysis if not stated otherwise (Fig.2, Fig.3, Fig.4, Fig.5; Fig. S2-S8)
- performed and analyzed behavioral tests (Fig.6B)
- wrote the manuscript

Contributions of KL:

- contributed anatomical and immunohistochemical analysis (Fig. S6-S8)
- performed and analyzed behavioral tests (Fig. 6B,C,D; Fig. S5)

Contributions of AS:

- performed and analyzed in-situ hybridizations and single cell PCR data (Fig. 1)
- performed anatomical and immunohistochemical analysis (Fig. S1)

Contributions of MH:

- contributed to anatomical and immunohistochemical analysis (Fig. S2)

Contributions of HU:

- contributed mouse lines

Contributions of MK:

- designed experiments
- wrote the manuscript

Contributions of FB:

- designed experiments
- wrote the manuscript

Date, place

Signature Kristina Loy

Signature PD Dr. Florence Bareyre (Supervisor)